

Université de Montréal

**Utilisation du 9,9'-spirobifluorène comme unité centrale
en génie cristallin et réactions à l'intérieur de cristaux
poreux en tectonique moléculaire.**

par
Eric Demers

Département de Chimie
Faculté des Arts et des Sciences

Thèse présentée à la Faculté des études supérieures
en vue de l'obtention du grade de
Philosophiae Doctor (Ph.D.)
en chimie

Juin 2005



© Eric Demers, 2005

QD

3

054

2005

V.027

AVIS

L'auteur a autorisé l'Université de Montréal à reproduire et diffuser, en totalité ou en partie, par quelque moyen que ce soit et sur quelque support que ce soit, et exclusivement à des fins non lucratives d'enseignement et de recherche, des copies de ce mémoire ou de cette thèse.

L'auteur et les coauteurs le cas échéant conservent la propriété du droit d'auteur et des droits moraux qui protègent ce document. Ni la thèse ou le mémoire, ni des extraits substantiels de ce document, ne doivent être imprimés ou autrement reproduits sans l'autorisation de l'auteur.

Afin de se conformer à la Loi canadienne sur la protection des renseignements personnels, quelques formulaires secondaires, coordonnées ou signatures intégrées au texte ont pu être enlevés de ce document. Bien que cela ait pu affecter la pagination, il n'y a aucun contenu manquant.

NOTICE

The author of this thesis or dissertation has granted a nonexclusive license allowing Université de Montréal to reproduce and publish the document, in part or in whole, and in any format, solely for noncommercial educational and research purposes.

The author and co-authors if applicable retain copyright ownership and moral rights in this document. Neither the whole thesis or dissertation, nor substantial extracts from it, may be printed or otherwise reproduced without the author's permission.

In compliance with the Canadian Privacy Act some supporting forms, contact information or signatures may have been removed from the document. While this may affect the document page count, it does not represent any loss of content from the document.

Université de Montréal
Faculté des études supérieures

Cette thèse intitulée :

Utilisation du 9,9'-spirobifluorène comme unité centrale en génie cristallin et réactions à l'intérieur de cristaux poreux en tectonique moléculaire.

présentée par :

Eric Demers

a été évaluée par un jury composé des personnes suivantes :

Professeur	C. Géraldine Bazuin	président-rapporteur
Professeur	James D. Wuest	directeur de recherche
Professeur	Shawn Collins	membre du jury
Professeur	Yves Dory	examinateur externe
Professeur	Robert Cochrane	représentant du doyen de la FES

Sommaire

Un des aspects les plus prometteurs de la chimie supramoléculaire est la formation de nouveaux matériaux ayant diverses propriétés. Parmi les nombreuses branches de la chimie supramoléculaire, il en existe une, la tectonique moléculaire, qui est une stratégie pour la formation de nouveaux matériaux ordonnés. Elle repose sur l'emploi de petites molécules, appelées tectons, sur lesquelles sont greffés des sites de reconnaissance intermoléculaire. Ces sites procurent aux tectons la capacité de s'auto-assembler afin de former des architectures supramoléculaires ordonnées. Ainsi, en choisissant avec soin la forme moléculaire du tecton, la nature des sites de reconnaissance intermoléculaire ainsi que les groupes fonctionnels désirés, il est possible de réaliser de nouveaux matériaux moléculaires possédant d'intéressantes propriétés. Par exemple, l'association dirigée par la stratégie de la tectonique moléculaire facilite la constitution de réseaux moléculaires poreux.

Les études menées dans le cadre de nos travaux se sont concentrées autour de deux axes principaux : le premier est l'emploi du noyau 9,9'-spirobifluorène dans divers aspects de la tectonique moléculaire. Le second est l'étude de la faisabilité de réaction à l'intérieur de cristaux poreux formés par le biais de la tectonique moléculaire.

Plusieurs tectons basés sur diverses unités centrales ont été étudiés afin de voir l'impact sur la cristallisation. Parmi elles, le 9,9'-spirobifluorène a donné de bons résultats pour l'obtention de réseau avec une forte porosité. En effet, il semble que cette unité possède une prédisposition naturelle à former des réseaux poreux. Pour cette raison, il est au cœur du sujet de cette thèse. La première étude se concentre sur l'effet d'un espaceur phényle placé entre l'unité centrale et l'unité de reconnaissance du tecton sur l'auto-assemblage ainsi que son lien avec la porosité. Les résultats obtenus ont permis de constater que la porosité d'un réseau construit via un tecton ayant quatre groupes diaminotriazinyles en positions-2,2',7,7' du cœur spirobifluorène est de 60%, tandis que celle du tecton analogue avec quatres espaces phényles entre le cœur et les sites triazine

n'est que 53%, montrant que la relation entre la forme du tecton et la porosité n'est pas simple.

Un autre aspect important en tectonique moléculaire est le choix des unités de reconnaissance. On a ainsi réalisé quelques études portant sur l'emploi de diverses unités de reconnaissance greffées sur l'unité centrale 9,9'-spirobifluorène. Ces études permettaient entre autres de vérifier l'efficacité en génie cristallin des interactions faibles de type C-H $\bullet\bullet\bullet$ O provenant d'une fonction nitro et C-H $\bullet\bullet\bullet$ N provenant d'une fonction cyano. Les résultats obtenus ont permis de conclure que les interactions de type C-H $\bullet\bullet\bullet$ O sont suffisamment efficaces pour jouer un rôle important dans la formation du réseau, alors que les interactions de type C-H $\bullet\bullet\bullet$ N semblent trop faibles pour entrer en compétition avec les interactions de type aryle-aryle guidant l'auto-assemblage cristallin.

On a également réalisé des études ciblant l'emploi des arylamines comme unité de reconnaissance par ponts hydrogène en chimie supramoléculaire. Ainsi plusieurs unités centrales ont été utilisées avec cette unité de reconnaissance et les résultats obtenus démontrent une tendance marquée pour une association par pont hydrogène sans motif de reconnaissance particulier, ainsi qu'une prédilection pour la formation de réseaux moléculaires compacts.

En deuxième partie, le côté plus appliqué de la tectonique moléculaire a été abordé. En effet, les réseaux tectoniques sont souvent comparés aux zéolithes avec la visée qu'ils deviendront un outil complémentaire à ces dernières. Pour ce faire, il faut bien entendu explorer leur potentiel, tel que la faisabilité de réactions à l'intérieur de ces réseaux. Les derniers chapitres ont été consacrés à la démonstration de ces concepts ainsi qu'à leurs utilités en tectonique moléculaire. Des études, basées sur l'emploi d'allylamines à la fois comme groupement de reconnaissance et d'unité fonctionnalisable, ont montré comment on peut se servir d'une stratégie de diffusion pour réaliser des réactions topotactiques à l'intérieur de cristaux poreux. Suite à ces résultats, une autre étude a démontré qu'on peut se servir de la même stratégie de diffusion afin d'augmenter la robustesse de nos réseaux

via une réticulation covalente. En terminant, une dernière étude a permis de montré qu'on peut également se servir de cette stratégie de diffusion afin d'augmenter la porosité d'un réseau supramoléculaire.

Mots clés : Chimie supramoléculaire, génie cristallin, ponts hydrogène, interactions faibles, 9,9'-spirobifluorène, auto-assemblage, réseaux, porosité, réactions topotactiques, photochimie.

Summary

One of the goals of supramolecular chemistry is the formation of new materials possessing specific structures and properties. Among the numerous fields of supramolecular chemistry is one referred to as molecular tectonics. Molecular tectonics is a strategy that can be used for the formation of new materials. It is based on the use of small molecules called tectons, which incorporate multiple groups that engage in intermolecular recognition. These groups direct the association of the tectons and program the assembly of ordered supramolecular architectures. By careful choice of the core and peripheral sticky sites of the tectons, it is possible to create new materials possessing interesting properties. For example, association directed by the strategy of molecular tectonics permits the construction of porous networks.

The studies presented herein focus on two separate aspects of molecular tectonics: the first aspect examines the use of 9,9'-spirobifluorene derivatives as tectons, while the second considers the feasibility of conducting reactions inside permeable crystals formed by tectonic networks.

Many tectons based on different central cores have been studied in order to understand the impact on crystallization. Among the cores studied, derivatives of 9,9'-spirobifluorene have led to the formation of particularly porous crystals. Indeed, it appears that this core has a natural predisposition to form porous networks, and it is therefore a central subject of this thesis. The first study focuses on the effect of a phenyl spacer between the central 9,9'-spirobifluorene core and the peripheral recognition groups of the tecton on the self-assembly and porosity. The results show that the porosity of a network built from a tecton bearing four diaminotriazine groups at the 2,2',7,7'-positions of the spirobifluorene core is 60%, whereas the porosity of the analogous tecton with four added phenyl spacers between the core and the triazines is only 53%. These results suggest that the relationship between the shape of the tecton and porosity is not straightforward.

Another important factor in crystallization is the choice of the sites of association. We therefore carried out studies where several different sites were grafted onto the 9,9'-spirobifluorene core. These studies consider the effectiveness of weak interactions such as C-H $\bullet\bullet\bullet$ O interactions of nitro groups and C-H $\bullet\bullet\bullet$ N interactions of cyano groups in crystal engineering. The results demonstrate that C-H $\bullet\bullet\bullet$ O interactions are sufficiently strong enough to play a role in network formation, but C-H $\bullet\bullet\bullet$ N interactions are too weak to compete with arene-arene interactions in directing self-assembly in the crystalline state.

We also carried out studies targeting arylamines as hydrogen-bonding groups in supramolecular chemistry. Several different molecular cores substituted with amino groups were studied. The results demonstrate the tendency of these molecules to associate by hydrogen bonds with no preferred motif and with no special predisposition to form close-packed networks.

The second part of this thesis examines a more practical side of molecular tectonics. Tectonic networks are often compared to zeolites, and we hope that they will become a complementary tool to zeolites for certain applications. To accomplish this, it is necessary to demonstrate the feasibility of certain processes, such as the possibility of conducting reactions inside the crystalline networks. The later chapters of this thesis are dedicated to the demonstration of these concepts, as well as to an exploration of their utility in molecular tectonics. Studies based on the dual use of allylamines as recognition groups and as reactive groups showed that diffusion of reagents can be used to carry out topotactic reactions inside porous crystals. Following these results, a second study demonstrated that the same strategy of diffusion can be used to increase the robustness of the networks by covalent crosslinking. Finally, another study allowed us to demonstrate that this strategy can be used to increase the porosity of a supramolecular network.

Key words: supramolecular chemistry, crystal engineering, hydrogen bonds, weak interactions, 9,9'-spirobifluorene, self-assembly, molecular networks, porosity, topotactic reactions, photochemistry.

Table des matières

Sommaire	I
Summary	IV
Table des matières.....	VI
Liste des tableaux.....	IX
Liste des schémas.....	X
Liste des figures	XI
Liste des abréviations.....	XXIII
Remerciements.....	XXV
Notes	XXVIII

Chapitre 1 : Introduction

1.1 De la nature vers la chimie supramoléculaire	2
1.2 Historique de la tectonique moléculaire	7
1.4 Objectifs de cette thèse	19

Chapitre 2 : Introduction du 9,9'-spirobifluorène comme unité centrale dans la conception de tectons

2.1 Introduction.....	23
2.2 Le 9,9-spirobifluorène.....	27
2.3 Utilisation de l'unité 9,9'-spirobifluorène dans la conception de tectons	31

Chapitre 3 : Effet d'un espaceur phényle dans la formation de réseaux par le 9,9'spirobifluorène-DAT

3.1 Introduction.....	33
3.2 Stratégie visant le contrôle et l'augmentation de la porosité.....	36
3.3 Étude sur l'effet de l'espacement entre l'unité centrale et le site de reconnaissance	37
3.4 Article 1 : Molecular Tectonics. Porous Hydrogen-Bonded Networks Built from Derivatives of 2,2',7,7'-Tetraphenyl-9,9'-spirobi[9H-fluorene].....	39
3.5 Conclusion	76

Chapitre 4 : Étude de l'utilisation d'interactions faibles dans la formation de réseaux poreux

4.1 La liaison hydrogène.....	78
4.2 Les interactions faibles abordées dans le chapitre	83
4.3 Les interactions CH···X _(O,N)	84
4.4 Les interactions aryle - aryle	87
4.5 Article 2 : Weakly Bonded Molecular Networks Built from Tetranitro- and Tetracyanospirobifluorenes.....	90
4.6 Conclusion	127

Chapitre 5 : Utilisation de ponts hydrogène provenant de l'aniline en génie cristallin

5.1 La tectonique moléculaire et le pont hydrogène	129
5.2 Article 3 : Molecular Tectonics. Hydrogen-Bonded Networks Built from Tetra- and Hexaanilines	134
5.3 Conclusion : la tectonique moléculaire et le pont hydrogène	162

Chapitre 6 : Réactions à l'intérieur de cristaux poreux

6.1 Introduction.....	164
6.2 La tectonique moléculaire et les réactions à l'état cristallin	168
6.3 Article 4 : Topotactic Reactions in Networks: Designing Permeable Molecular Crystals that React with External Agents To Give Crystalline Products.....	170
6.4 Conclusions et perspectives	185

Chapitre 7 : Excavation de cristaux moléculaires

7.1 Introduction.....	187
7.2 Article 5 : Excavations in Molecular Crystals	189
7.3 Conclusions et perspectives	200

Chapitre 8 : Conclusions et perspectives

8.1 Conclusions.....	203
8.2 Perspectives et voies futures	206

Annexe 1 : Supporting Information article 1A1-1

Annexe 2 : Supporting Information article 2A2-1

Annexe 3 : Supporting Information article 3A3-1

Annexe 4 : Supporting Information article 4A4-1

Annexe 5 : Supporting Information article 5A5-1

Liste des tableaux

Tableau 4.1 Caractéristiques des liaisons hydrogène «fortes», «modérées» ou «faibles» selon la classification de Jeffrey.....	80
---	----

Liste des Schémas

Schéma 2.1	Synthèse du 9,9'-spirobifluorène	28
Schéma 2.2	Bromation régiosélective du 9,9'-spirobifluorène en position 2,2' et 7,7'	30
Schéma 4.1	Liaison hydrogène formée entre un atome d'hydrogène acide (lié à un atome donneur D de liaison hydrogène) et un accepteur approprié (A)	78

Article 4: Topotactic Reactions in Networks: Designing Permeable Molecular Crystals that React with External Agents To Give Crystalline Products.

Scheme 1	Tecton 1 and the synthesis of tectons 2 and 5a in solution	173
----------	--	-----

Fin de l'article 4

Article 5: Excavations in Molecular Crystals.

Scheme 1	Tecton 1 and the synthesis of tecton 2	192
----------	--	-----

Fin de l'article 5

Liste des figures

Figure 1.1 Leonardo Da Vinci et son rêve de voler.	2
Figure 1.2 Jules Verne et son livre : De la terre à la lune.	3
Figure 1.3 Représentation schématique de la réPLICATION d'un brin d'ADN et de la transcription de l'ARN jusqu'à sa traduction en protéine.....	5
Figure 1.4 Représentation de l'acide adamantane- 1,3,5,7-tetracarboxylique et d'un motif de reconnaissance entre deux unités d'acides carboxyliques.	7
Figure 1.5 Représentation schématique de la tendance naturelle des molécules à former un empilement compact. Les molécules, symbolisées sous la forme de cubes, formeront préférentiellement un arrangement compact qui maximise les forces de van der Waals et minimise la présence d'espaces vides, défavorisée énergétiquement.	9
Figure 1.6 Formation d'un réseau supramoléculaire par la stratégie de la tectonique moléculaire.	9
Figure 1.7 Utilisation d'un tecton tétraédrique lors de la formation d'un réseau diamantoïde incorporant des molécules de solvant invitées.	10
Figure 1.8 La Figure A représente une vue selon l'axe c en rayon de van der Waals du réseau formé par la cristallisation du tecton 1.1 (la tétrapyridonesilane) dans l'acide propionique. Les tectons sont en bleu et les molécules invitées ($\text{CH}_3\text{CH}_2\text{COOH}$) sont en rouge. Dans la Figure B, les molécules de solvant ont été omises afin de visualiser la dimension des canaux. Finalement, la Figure C représente l'espace occupé par les molécules de solvant. Cette dernière a été réalisée en visualisant le volume parcouru par le centre d'une sphère d'un rayon de 2,5Å sur la surface de van der Waals du réseau.....	12
Figure 1.9 Vue en rayons de van der Waals du réseau formé par la cristallisation du tecton 1.2 dans HCOOH/dioxane. Les cavités forment des canaux parallèles à l'axe c. Les molécules de solvant ont été omises pour plus de clarté	13

Figure 1.10 Quelques exemples d'unités de reconnaissance utilisant le pont hydrogène, incluant la diaminotriazine A , la pyridone B , les phénols C , les acides carboxyliques D et boroniques E	15
Figure 1.11 Les tectons 1.3 , 1.4 , 1.5 représentent quelques exemples de tectons réalisés dans le groupe Wuest dans le cadre d'études sur l'impact des différences entre les formes et la rigidité de l'unité centrale d'un tecton.....	15
Figure 1.12 Représentation d'un processus d'échange de molécules de solvant invitées (rouges) à l'intérieur d'un réseau cristallin par d'autres petites molécules (bleus) organiques sans perte de la cristallinité du réseau	16
Figure 1.13 A) Représentation de la chromatographie d'exclusion où les molécules de dimension inférieure aux canaux (cubes rouges) diffusent à l'intérieur du réseau, mais où les molécules de dimension supérieure (cubes gris) sont exclues du réseau. B) Représentation de la catalyse hétérogène où des substrats (triangles rouges) sont transformés par les sites catalytiques incorporés au réseau (polygones bleus) en produits désirés (cubes jaunes).....	17
Figure 1.14 Représentation en rayons de van der Waals du réseau formé par la cristallisation du tecton 1.3 (A) et l'image de l'espace occupé par les molécules de solvant et les contre-ions (B). Cette dernière a été réalisée en roulant une sphère de 2,5 Å de rayon sur la surface de van der Waals du réseau	18
Figure 2.1 Unités centrales favorisant la formation de réseaux en forme de couches.....	23
Figure 2.2 Unités centrales favorisant une reconnaissance tridimensionnelle.....	24
Figure 2.3 Utilisation d'unités centrales tétraédriques favorisant l'obtention de réseaux diamantoïdes	25
Figure 2.4 Représentation des tectons 2.1 , 2.2 et 2.3 basés sur le tétraphénylméthane comme unité centrale et conduisant à la formation de réseaux diamantoïdes poreux	26
Figure 2.5 Réactivité du tétraphénylméthane envers les électrophiles	28
Figure 2.6 Stabilisation des intermédiaires réactionnels lors de réactions de substitution électrophile aromatique sur le 9,9'-spirobifluorène	29

Figure 3.1	Structure du tecton 3.1 et vue selon l'axe <i>c</i> du réseau formé par sa cristallisation dans DMSO/benzène. Les molécules invitées sont omises pour plus de clarté. Le réseau est retenu via 12 ponts hydrogène par tecton et définit des canaux parallèles à l'axe <i>c</i>	33
Figure 3.2	Structure du sel tétraphénylphosphonium du tecton 3.2 et vue selon l'axe <i>c</i> du réseau formé par sa cristallisation dans DMSO/toluène. Les molécules de solvant et les cations désordonnés sont omis. Le réseau définit des canaux parallèles à l'axe <i>c</i> et est retenu par 16 ponts hydrogène par tecton	34
Figure 3.3	Vue selon l'axe <i>c</i> du réseau formé par la cristallisation du tecton 3.3 (A) dans DMSO/dioxane ainsi que les canaux formés qui sont parallèles à l'axe <i>c</i> du réseau (B)	35
Figure 3.4	Représentations des effets attendus par l'ajout d'un espaceur entre l'unité centrale et les sites de reconnaissance.....	36
Figure 3.5	Représentations des principaux motifs d'association de la diaminotriazine.	37
Figure 3.6	Représentation du tecton 3.4 et du réseau découlant de sa cristallisation dans DMSO/dioxane (vue selon l'axe <i>a</i> avec les molécules invitées omises).	38

Article 1: Molecular Tectonics. Porous Hydrogen-Bonded Networks Built from Derivatives of 2,2',7,7'-Tetraphenyl-9,9'-spirobi[9H-fluorene].

Figure 1	Cyclic hydrogen-bonding motifs characteristic of aminotriazines.	61
Figure 2	Representation of the structure of crystals of simple spirobifluorene 4 grown from DMSO/dioxane, showing a tecton (white) surrounded by three of a total of six hydrogen-bonded neighboring tectons. The other three neighbors are equivalent by symmetry and are omitted for clarity, as are all guests. Hydrogen bonds appear as broken lines. Two of the six neighbors (one shown in green, with a second equivalent by symmetry and omitted) each form two hydrogen bonds with the central tecton (white), creating motifs of type I . Two other neighbors (blue) each form four hydrogen bonds with the central tecton, creating distorted motifs of type II , and the remaining two neighbors	

(red) each form two hydrogen bonds with the central tecton according to motif III	62
Figure 3 View along the <i>a</i> axis of the network constructed from tecton 4 showing a $2 \times 3 \times 3$ array of unit cells. Guests are omitted, and atoms are shown as spheres of van der Waals radii in order to reveal the cross sections of the channels. Atoms of hydrogen appear in white, atoms of carbon in gray, and atoms of nitrogen in blue.....	63
Figure 4 View of the structure of crystals of extended spirobifluorene 2 grown from DMSO/acetone, showing a central tecton (tecton A , white) and its five hydrogen-bonded neighbors. Guests are omitted for clarity, and hydrogen bonds are represented by broken lines. Two of the neighbors (red) are each linked to tecton A (white) by two hydrogen bonds of type III , two others (blue) each form four hydrogen bonds with tecton A according to motif II , and the remaining neighbor (tecton B , dark gray) forms a single distorted hydrogen bond. Tecton A (white) and its four multiply hydrogen-bonded neighbors (red and blue) are all equivalent by symmetry, and together they define a square-planar network. Tectons A (white) and B (dark gray) are symmetry-independent.....	64
Figure 5 View of the structure of crystals of extended spirobifluorene 2 grown from DMSO/acetone, showing a central tecton (tecton B , dark gray) and its five hydrogen-bonded neighbors. Guests are omitted for clarity, and hydrogen bonds are represented by broken lines. Two of the neighbors (red) are each linked to tecton B (dark gray) by two hydrogen bonds of type III , two others (blue) each form three hydrogen bonds with tecton B (two according to motif II), and the remaining neighbor (tecton A , white) forms a single hydrogen bond. Tecton B (dark gray) and its four multiply hydrogen-bonded neighbors (red and blue) are all equivalent by symmetry, and together they define a square-planar network. Tectons A (white) and B (dark gray) are symmetry-independent.	65
Figure 6 Representation of the network formed by crystallizing extended spirobifluorene 2 from DMSO/acetone. Each sheet composed uniquely of tecton A (white) is paired with one sheet built uniquely from tecton B (dark gray) to form a bilayer held together by single	

hydrogen bonds between neighboring tectons A and B in the two adjacent layers (Figures 4-5). In this representation, solid lines correspond to hydrogen bonds of types II-III between tectons A (white) or B (dark gray), and the intersections show the position of the central spirocyclic carbon atom of each tecton.....	66
Figure 7 View along the <i>a</i> axis of the network constructed from extended spirobifluorene 2 showing a $4 \times 4 \times 4$ array of unit cells. Guests are omitted, and atoms are shown as spheres of van der Waals radii in order to reveal the cross sections of the channels. Atoms of hydrogen appear in white, atoms of carbon in gray, and atoms of nitrogen in blue.....	67
Figure 8 Stereoscopic representation of interconnected channels within the network constructed from extended spirobifluorene 2 . The image shows a $3 \times 3 \times 2$ array of unit cells viewed along the <i>a</i> axis. The outsides of the channels appear in light gray, and dark gray is used to show where the channels are cut by the boundaries of the array. The surface of the channels is defined by the possible loci of the center of a sphere of diameter 3.0 Å as it rolls over the surface of the ordered network	68
Figure 9 Representation of the interactions between symmetry-independent molecules C (white) and D (black) in the structure of crystals of extended spirobifluorene 3 grown from DMSO/CH ₃ OH. a) Four distorted hydrogen bonds of type III . b) Aromatic interactions.....	69-70
Figure 10 View of the structure of crystals of extended spirobifluorene 3 grown from DMSO/CH ₃ OH, showing symmetry-independent tectons C (white) and D (dark gray) and the five neighbors (blue) that form hydrogen bonds according to motifs I-II . Guests are omitted for clarity, and hydrogen bonds are represented by broken lines.....	71
Figure 11 View of the structure of crystals of extended spirobifluorene 3 grown from DMSO/CH ₃ OH, showing symmetry-independent tectons C (white) and D (dark gray) and the five neighbors (red) that form distorted single hydrogen bonds. Guests are omitted for clarity, and hydrogen bonds are represented by broken lines.....	72

Figure 12 View along the α axis of the network constructed from extended spirobifluorene 3 showing a $4 \times 4 \times 4$ array of unit cells. Guests are omitted, and atoms are shown as spheres of van der Waals radii in order to reveal the cross sections of the channels. Atoms of hydrogen appear in white, atoms of carbon in gray, and atoms of nitrogen in blue.....	73
Figure 13 Stereoscopic representation of interconnected channels within the network constructed from extended spirobifluorene 3. The image shows a $3 \times 2 \times 2$ array of unit cells viewed along the α axis. The outsides of the channels appear in light gray, and dark gray is used to show where the channels are cut by the boundaries of the array. The surface of the channels is defined by the possible loci of the center of a sphere of diameter 3 Å as it rolls over the surface of the ordered network	74

Fin de l'article 1

Figure 4.1 Représentation des tectons 4.1 à 4.6 étudiés dans ce chapitre.....	83
Figure 4.2 Représentation des principaux donneurs C-H dans les ponts hydrogène faibles	84
Figure 4.3 Représentation des principaux motifs de reconnaissance possibles pour les interactions entre les atomes d'hydrogène aromatiques et la fonction nitro.....	85
Figure 4.4 Représentation des principales configurations possibles pour les interactions entre les atomes d'hydrogène aromatique et la fonction cyano	86
Figure 4.5 Représentation des principales interactions entre des groupements aryles	87
Figure 4.6 Représentation d'empilements π complémentaires	89

Article 2: Weakly Bonded Molecular Networks Built from Tetranitro- and Tetracyanospirobifluorenes.		
Figure 1	Selected C-H···O and C-H···N interactions in nitroarenes and benzonitriles.....	116
Figure 2	View of the structure of crystals of 2,2',7,7'-tetranitro-9,9'-spirobi[9H-fluorene] (4) grown from dioxane/toluene, showing a central molecule (gray) and the four neighbors linked by C-H···O interactions involving nitro groups. Included molecules of dioxane are omitted for clarity. The central molecule 1) forms a cyclic pair of C-H···O interactions of type I (Figure 1) with one neighbor (blue); 2) serves as both donor and acceptor in single C-H···O interactions of type II (Figure 1) with two other neighbors (red); and 3) acts as both donor and acceptor in C-H···O interactions of type II (Figure 1) with a fourth neighbor (green). C-H···O interactions are represented by broken lines.....	117
Figure 3	View along the <i>c</i> axis of the network formed by 2,2',7,7'-tetranitro-9,9'-spirobi[9H-fluorene] (4), showing a 4 × 4 × 3 array of unit cells. Guests are omitted, and atoms are represented by spheres of van der Waals radii to show the cross sections of the channels. Atoms of carbon appear in gray, hydrogen in white, nitrogen in blue, and oxygen in red.	118
Figure 4	View along the <i>c</i> axis of the network formed by crystallizing 2,2',7,7'-tetracyano-9,9'-spirobi[9H-fluorene] (5) from CHCl ₃ /hexane, showing a 3 × 3 × 3 array of unit cells. Guests are omitted, and atoms are represented by spheres of van der Waals radii to show the cross sections of the channels. Atoms of carbon appear in gray, hydrogen in white, and nitrogen in blue.	119
Figure 5	(a) Representation of π -stacking of a central molecule of 2,2',7,7'-tetracyano-9,9'-spirobi[9H-fluorene] (5) (shown in red) with two neighbors. (b) Representation of the resulting network, with π -stacking shown as straight red lines intersecting at the centers of neighboring molecules.....	120
Figure 6	Views of the structure of crystals of 2,2',7,7'-tetrakis(4-nitrophenyl)-9,9'-spirobi[9H-fluorene] (6) grown from ethyl acetate/hexane,	

showing the two symmetry-independent molecules **A** (red) and **B** (blue) in the unit cell. Included molecules of ethyl acetate are omitted for clarity. **(a)** Aryl-aryl interactions between molecule **A** (red) and four neighbors (green) satisfying the condition that the centroids of the interacting phenyl rings are separated by less than 4.5 Å. **(b)** Molecule **B** (blue) and the five neighbors (green) that satisfy the same condition. Note that one of the neighbors is hidden behind molecule **B** and is not visible. **(c)** C-H···O interactions (largely type **III**) between molecule **A** (red) and four neighbors (green) with H···O distances less than or equal to 2.65 Å. The C-H···O interactions are represented by broken lines. **(d)** Similar view of C-H···O interactions (types **II** and **III**) involving molecule **B** (blue) and four neighbors (green).....121

Figure 7 View along the *b* axis of the network formed by crystallizing 2,2',7,7'-tetrakis(4-cyanophenyl)-9,9'-spirobi[9*H*-fluorene] (**7**) from dioxane/hexane, showing a 4 × 2 × 3 array of unit cells. Guests are omitted, and atoms are represented by spheres of van der Waals radii to show the cross sections of the channels. Atoms of carbon appear in gray, hydrogen in white, and nitrogen in blue.122

Figure 8 Representation of the principal aryl-aryl interactions between a central molecule of 2,2',7,7'-tetrakis(4-cyanophenyl)-9,9'-spirobi[9*H*-fluorene] (**7**) (shown in red) and three neighbors (green) satisfying the condition that the centroids of the interacting phenyl rings are separated by less than 4.5 Å.....123

Figure 9 Views of the closely related structures of crystals of 2,2',7,7'-tetrakis(3-nitrophenyl)-9,9'-spirobi[9*H*-fluorene] (**8**) and 2,2',7,7'-tetrakis(3-cyanophenyl)-9,9'-spirobi[9*H*-fluorene] (**9**), grown from CHCl₃/acetone and toluene/hexane, respectively. **(a)** Aryl-aryl interactions involving a central molecule of compound **8** (red) with four neighbors (green) satisfying the condition that the centroids of the interacting phenyl rings are separated by less than 4.5 Å. **(b)** C-H···O interactions (types **III-IV**) between a central molecule of compound **8** (red) and the set of four neighbors that also have aryl-aryl interactions (green), as well as those involving a second set of four neighbors (blue). C-H···O interactions are represented by broken

lines. Together, the red and green molecules define a non-interpenetrated diamondoid network, and the red and blue molecules describe a diamond network with five-fold interpenetration. **(c)** Similar view of aryl-aryl interactions involving a central molecule of extended tetracyanospirobifluorene **9** (red) and its four neighbors (green). **(d)** Non-interpenetrated diamondoid network defined by connecting the centers of molecules of compound **9** linked by aryl-aryl interactions.....124

Fin de l'article 2

Figure 5.1	Motifs de reconnaissance couramment observés pour les interactions entre les acides carboxyliques.....	130
Figure 5.2	Reconnaissance dimérique directionnelle de la pyridone.....	131
Figure 5.3	Les trois principaux motifs de reconnaissance de la diaminotriazine.....	131
Figure 5.4	Exemple de motifs d'association connus pour les acides boroniques et les phénols.....	132

Article 3: Molecular Tectonics. Hydrogen-Bonded Networks Built from Tetra- and Hexaanilines.

Figure 1	Representation of the structure of crystals of 2,2',7,7'-tetraamino-9,9'-spirobi[9H-fluorene] (1c) grown from DMF/H ₂ O. Three molecules of tetraaniline 1c (red) each donate a single hydrogen bond to a hydrogen-bonded pair of H ₂ O molecules (blue), and a fourth molecule of compound 1c (green) donates a single hydrogen bond to the oxygen atom of a molecule of DMF (yellow), which accepts an additional hydrogen bond from the H ₂ O dimer. Hydrogen bonds appear as broken lines, and hydrogen atoms of the spirobifluorene cores are omitted for clarity.....	155
Figure 2	View along the <i>c</i> axis of the structure of crystals of tetrakis(4-aminophenyl)methane (2c) grown from DMF/CHCl ₃ showing a	

central molecule (red) and its four hydrogen-bonded neighbors (blue). Hydrogen bonds appear as broken lines, and hydrogen atoms of the tetraphenylmethyl cores are omitted for clarity.....	156
Figure 3 View along the <i>c</i> axis of the structure of crystals of tetrakis[(4-aminophenoxy)methyl]methane (3c) grown from THF showing the characteristic cyclic hydrogen-bonded motif formed by four molecules of tetraaniline 3c . Hydrogen bonds appear as broken lines, and hydrogen atoms of the pentaerythrityl tetraphenyl ether cores are omitted for clarity.	157
Figure 4 View of the structure of crystals of 1,1'-oxybis[3-(4-aminophenoxy)-2,2-bis[(4-aminophenoxy)methyl]]propane (4c) grown from benzene/CH ₃ OH/hexane showing a central tecton (red) surrounded by its six hydrogen-bonded neighbors. Two neighbors (yellow) each share two N-H···N hydrogen bonds with the central tecton, two other neighbors (green) each accept one hydrogen bond (one N-H···N and one N-H···O), and the remaining two neighbors (blue) each donate one hydrogen bond (one N-H···N and one N-H···O). Hydrogen bonds appear as broken lines, and hydrogen atoms of the dipentaerythrityl hexaphenyl ether cores are omitted for clarity.....	158
Figure 5 View of the layered structure of crystals of tetrakis(4-aminophenyl)ethylene (5) grown from DMF/H ₂ O. Hydrogen bonds appear as broken lines, and hydrogen atoms of the tetraphenylethenyl cores and H ₂ O are omitted for clarity. a) In one type of layer (red = R), each tecton shares a total of four N-H···N hydrogen bonds with four neighbors. b) In the other type of layer (blue = B), each tecton forms a total of three N-H···N hydrogen bonds with three neighbors, and one of the neighbors also accepts a hydrogen bond from H ₂ O. c) The layers then stack along the <i>a</i> axis according to the repeating pattern RBBRBB.	159

Fin de l'article 3

Figure 6.1 Illustration de l'azurite se transformant graduellement en son pseudomorphe, la malachite.....	164
--	-----

Figure 6.2	Représentation de l'acide cinnamique et de son agencement cristallin menant aux acides truxiniques	165
Figure 6.3	Polymérisation topochimique.....	166
Figure 6.4	Photoréarrangement à l'état cristallin du 1,2-bis(2-méthyl-5-p-méthoxyphényl-3-thiènyle)perfluorocyclopentène.....	167
Figure 6.5	Représentation selon l'axe c, en rayons de van der Waals, du réseau formé par la cristallisation du tecton 6.1	169
Article 4:	Topotactic Reactions in Networks: Designing Permeable Molecular Crystals that React with External Agents To Give Crystalline Products.	
Figure 1	View along the c axis of the crystal structure of tecton 2 showing a single tecton (blue) and the four neighbors (red) with which it forms hydrogen bonds (- - - -).....	174
Figure 2	View along the b axis of the crystal structure of tecton 2 showing the cross sections of helical channels. Hydrogen atoms and some allyl groups (upper channels) have been removed for clarity.....	175
Figure 3	Stereoscopic representation of the channels in the structure of tecton 2.[13] The image shows a 1 x 1 x 2 array of unit cells with the c axis vertical. The outsides of the channels appear in light gray, and dark gray is used to show where the channels are cut by the boundaries of the array. The surface is defined by the possible loci of the center of a sphere of diameter 3 as it rolls over the surface of the ordered tectonic network.....	176
Figure 4	Structure of the macromolecule obtained by cross-linking crystals of tecton 2 with HSCH ₂ CH ₂ SH, as viewed approximately along the c axis. The image shows a central unit derived from tecton 2 (blue), four neighboring units (red) joined by hydrogen bonds (- - - -), and one of the farther units (also in blue) to which the central unit has been linked covalently.	179

Fin de l'article 4

Figure 6.6 Représentation schématique de l'encapsulation de molécules invitées (cube rouge) à l'intérieur d'un cristal (cube gris) par une réaction de surface à l'aide d'un gros dithiol (jaune). 185

Article 5: Excavations in Molecular Crystals.

Figure 1 View along the *c* axis of the crystal structure of tecton **2** showing a central tecton (red) and the 4 neighbors (green) with which it interacts by hydrogen bonds (blue) involving triaminotriazine groups.... 193

Figure 2 View along the *a* axis of the crystal structure of tecton **2** showing a central tecton (red) and the 4 neighbors (blue) with which it interacts by hydrogen bonds (blue) involving $-\text{NH}(\text{CH}_2)_2\text{OCOCH}_3$ groups..... 194

Fin de l'article 5

Figure 7.1 Le groupement phosphate est comparable à l'état de transition de l'hydrolyse d'une fonction ester 201

Liste des abréviations

A	: accepteur
Å	: Ångström
ADN	: Acide désoxyribonucléique
ARN	: Acide ribonucléique
Anal.	: analyse
Ar	: aryle
bs	: broad signal (en IR et en RMN)
°C	: degré Celsius
calcd	: calculated
CCD	: Charged Coupled Device
cm	: centimètre
δ	: déplacement chimique
◦	: degré
d	: doublet (en RMN)
D	: donneur
DAT	: 2,4-diamino-1,3,5-triazine
dd	: doublet de doublets (en RMN)
Deg	: degré
DMF	: N,N-diméthylformamide
DMSO	: diméthyl sulfoxyde
e	: électron
E ⁺	: électrophile
FAB	: fast atom bombardment
g	: gramme
GoF	: Goodness-of-fit
h	: heure
HRMS	: high resolution mass spectrometry
hν	: sous irradiation
Hz	: hertz
i-Pr	: iso-propyle
IR	: infrarouge
J	: constante de couplage
K	: Kelvin

kcal	: kilocalorie
M	: molaire
m	: masse ou multiplet (en RMN)
Me	: méthyle
mg	: milligramme
MHz	: mégahertz
mL	: millilitre
mm	: millimètre
mmol	: millimole
mol	: mole
mp	: melting point
MS	: mass spectrometry
N	: normal
NMR	: nuclear magnetic resonance
ORTEP	: Oak Ridge Thermal Ellipsoid Program
<i>P</i>	: porosity
π	: électron π
R ₁	: Facteur d'accord sur les réflexions observées
wR ₂	: Facteur d'accord pondéré
RMN	: résonance magnétique nucléaire
s	: singulet (en RMN)
t	: triplet (en RMN)
THF	: tétrahydrofurane
UV	: ultraviolet
<i>V</i>	: volume
<i>V_g</i>	: guest-accessible volume
Vis	: visible
Z	: nombre d'unités formulaires par maille

Remerciements

En premier lieu, j'aimerais remercier mon directeur de recherche, le professeur James D. Wuest. Il m'a d'abord permis de faire un stage d'été dans son groupe où j'ai développé mon intérêt pour la chimie supramoléculaire. Par la suite, il m'a accepté au sein de son équipe afin que j'y fasse des études graduées. Sa passion pour la chimie en général et sa grande culture furent pour moi une source d'inspiration tout au long de mon passage dans ce groupe. Je tiens particulièrement à le remercier pour la liberté qu'il m'a laissée dans le cheminement de mes recherches. Je garderai toujours une grande admiration pour cet homme tant au plan professionnel que personnel.

Je voudrais également remercier le Dr. Philippe Brunet, un ancien membre du groupe avec qui j'ai appris à travailler en laboratoire. Il m'a enseigné les rudiments du métier et m'a encouragé à développer mon sens critique ainsi qu'une rigueur scientifique essentielle afin de bien travailler. Philippe fut pour moi un mentor, mais aussi un ami avec qui j'ai aimé travailler.

Un autre grand chimiste que je tiens à remercier est le Dr. Thierry Maris. Thierry est l'exemple même du chimiste que tout employeur voudrait dans son entreprise. Il est un homme très travaillant, méthodique et rigoureux. Sans exagérer, sa compétence et sa culture en général en font un homme à part et je m'imagine très mal le groupe sans lui. Thierry, je tiens à te remercier non seulement pour tous les immenses services que tu nous rends au labo, mais aussi pour ton amitié.

Je tiens également à remercier tous les membres du groupe passés et présents. Ce sont ces personnes qui ont rendu très agréable mon passage dans le groupe. Avec eux, j'ai eu à la fois des conseils et des échanges scientifiques très enrichissants, mais également des moments de loisirs inoubliables. Le sport, les "party", les congrès, le camping et j'en passe, resteront gravés à jamais dans ma mémoire. Merci à tous, mais plus particulièrement à ceux que j'ai côtoyé plusieurs années, soient Dom, Jean-Hugues,

Erwan, Gerson, Lionel, Philippe, Joël, Marie-Éve, Jean-Seb, Greg, Ken, Hugues, Thierry, Francis.

Je ne veux pas non plus oublier tous les amis que je me suis fait durant mon passage à l'université et qui ont toujours été présents à mes côtés, merci à vous tous.

Je remercie également les professeurs de l'Université de Montréal, les gens qui travaillent au laboratoire de résonance magnétique nucléaire, au laboratoire d'analyse élémentaire, à la bibliothèque, au Centre de spectrométrie de masse, à l'atelier mécanique ainsi que tous les gens du secrétariat.

Je veux également faire un remerciement bien spécial à Marjolaine. Elle a toujours été là pour moi, elle a cru en moi et m'a fait grandir. Les mots n'exprimeront jamais toute ma gratitude, merci Marjo.

Je tiens à remercier mes amis de longue date, Ariel, Jaclin, Sig, Christian et spécialement Justin. Un passage dans la vie n'aurait pas autant de couleur sans des amis comme vous.

En terminant, je remercie ma douce Janie qui inspire chacune de mes journées, ma famille pour son éternel support et plus particulièrement mes parents Michel et Lucette. Sans vous, rien n'aurait été possible.

Merci à tous.



À mes parents



Notes

La liste suivante démontre la contribution personnelle de Eric Demers et de ses co-auteurs dans les articles présentés dans cette thèse:

Premier article

Eric Demers a réalisé toute la partie synthétique et la partie caractérisation de cet article. De plus, il a participé à la rédaction de ce dernier.

Thierry Maris est le cristallographe du groupe. À ce titre, il a résolu les structures et collaboré à la rédaction de l'article.

Deuxième article

Eric Demers a réalisé 5/6 de la partie synthétique et de la partie caractérisation de cet article. De plus, il a participé à la rédaction de ce dernier.

Thierry Maris est le cristallographe du groupe. À ce titre, il a résolu les structures et collaboré à la rédaction de l'article.

Jean-Hugues Fournier a contribué à 1/6 de la partie synthétique et de la partie caractérisation de cet article.

Janie Cabana, à titre d'étudiante d'été, a contribué à la partie recherche de cet article sous la supervision d'Eric Demers.

Troisième article

Eric Demers a réalisé 2/5 de la partie synthétique et de la partie caractérisation de cet article.

Thierry Maris est le cristallographe du groupe. À ce titre, il a résolu les structures et collaboré à la rédaction de l'article.

Dominic Laliberté a participé à 2/5 dans la partie synthétique et dans la partie caractérisation de cet article. Il a participé à la rédaction.

Mathieu Arseneault, à titre d'étudiant d'été, a contribué à la partie recherche de cet article sous la supervision d'Eric Demers.

Fatima Helzy a participé à 1/5 dans la partie synthétique et dans la partie caractérisation de cet article.

Quatrième article

Eric Demers a réalisé la partie traitant des réactions de polymérisation à l'intérieur de cristaux poreux ainsi qu'à l'étude sur l'effet de la grosseur des réactifs lors de la diffusion dans les cristaux. De plus, il a participé à la rédaction de cet article.

Thierry Maris est le cristallographe du groupe. À ce titre, il a résolu les structures et collaboré à la rédaction de l'article.

Gary D. Enright est cristallographe et a participé à la collecte des données de certaines structures.

Philippe Brunet a développé la méthode pour la réalisation de réactions à l'intérieur des cristaux.

Cinquième article

Eric Demers a réalisé toute la partie sur les réactions à l'intérieur des cristaux et il a participé à la rédaction de cet article.

Thierry Maris est le cristallographe du groupe. À ce titre, il a résolu les structures et collaboré à la rédaction de l'article.

Erwan Le Fur a participé au développement et à la cristallisation du tecton.

Chapitre 1

Introduction

1.1 De la nature vers la chimie supramoléculaire

L'homme, depuis le début de son existence, démontre qu'il est un être doté d'une curiosité et d'une volonté d'apprendre sans bornes. Il n'a cessé d'observer ce qui l'entoure pour mieux comprendre et acquérir une connaissance n'ayant d'égale que son imagination. Il suffit de penser au nombre d'inventions qu'il a réalisées sous l'inspiration de ce qui l'entoure. Après tout, le rêve de Léonardo Da Vinci n'était-il pas de voler comme un oiseau (Figure 1.1)?

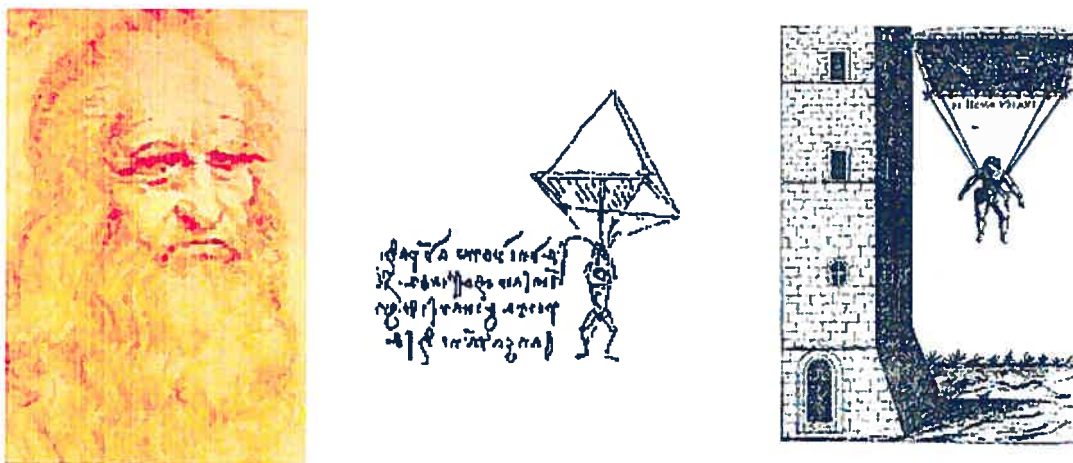


Figure 1.1 Leonardo Da Vinci et son rêve de voler.¹

Aujourd'hui ce rêve, qui autrefois paraissait de la pure folie, est devenu une banalité que notre société réalise tous les jours. Outre son sens de l'observation et sa logique rationnelle, l'homme possède aussi une imagination débordante lui permettant de pousser davantage et de réaliser des rêves encore plus fous. Le sous-marin du capitaine Nemo n'a plus grand chose de mystérieux pour l'homme moderne, mais mieux encore, le rêve de Jules Verne d'envoyer un homme dans l'espace est depuis peu accessible non seulement aux astronautes, mais aussi aux touristes fortunés (Figure 1.2). L'homme d'aujourd'hui n'a

¹ a) www.bordeaux.ensam.fr/elevessam/elam/questce.html
b) http://digilander.libero.it/debiblioteca/Arte/Leonardofly_file/page_01.htm
c) www.skydivecairns.com.au/history.htm

toutefois pas changé. Il s'inspire toujours de ses observations, mais il n'est plus limité par ses yeux. En effet, il peut maintenant voir des objets invisibles à l'œil nu grâce à des appareils lui permettant d'observer plus ou moins directement la matière. La muse de l'homme demeure toujours la nature, mais cette fois-ci à l'échelle de l'atome. Ainsi, l'homme étudie maintenant l'agencement des atomes afin de comprendre les interactions de ces derniers pour former des objets de plus grande taille.

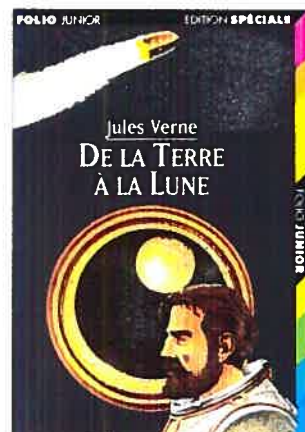


Figure 1.2 Jules Verne et son livre : De la terre à la lune.²

La chimie est la science qui étudie la façon dont les atomes sont rattachés directement les uns aux autres par des liens covalents ainsi que la réalisation de ces liens par diverses réactions. C'est ce qu'on appelle la chimie de synthèse. Cette science donne la possibilité à celui qui la pratique de créer de nombreuses molécules ayant diverses propriétés désirées. Ce processus logique et rationnel permet au chimiste de former des produits qui sont indispensables à notre mode de vie. À titre d'exemple, on peut penser aux larges domaines que couvrent la chimie médicinale et la chimie des matériaux.

Alors que la chimie de synthèse moléculaire traditionnelle s'intéresse à la formation, par des réactions, de liens covalents pour former et déterminer les propriétés des

² a) <http://www.a360.org/CB/VERNE.htm>
b) <http://jv.gilead.org.il/store/fr/by.html>

molécules, il existe une autre branche de la chimie qui s'intéresse aux interactions non-covalentes entre des molécules. Cette branche de la chimie a émergé ces dernières années sous l'appellation de chimie supramoléculaire. C'est encore une fois son désir de comprendre qui poussa l'homme à concevoir des structures moléculaires très complexes, débutant ainsi son exploration de la chimie supramoléculaire. Cette quête le mena vers ce qui est devenu l'un des domaines les plus fascinants et diversifiés de la chimie moderne.³ C'est Jean-Marie Lehn, prix Nobel de chimie en 1987 (co-récipiendaire avec Donald J. Cram et Charles J. Pedersen), qui donna ses titres de noblesses ainsi qu'une définition concrète de la chimie supramoléculaire :

"Supramolecular chemistry is the chemistry of the intermolecular bond, covering the structures and functions of the entities formed by association of two or more chemical species."⁴

En d'autres termes, la chimie supramoléculaire peut être définie comme la chimie "par-delà la molécule" portant sur les entités organisées, de complexités supérieures, qui résultent de l'association de deux ou plusieurs espèces chimiques maintenues ensemble par des forces intermoléculaires.

Cet auto-assemblage est gouverné par des interactions non-covalentes entre les molécules. Les principales interactions non-covalentes retrouvées dans ces architectures sont les ponts hydrogène, les liaisons de coordination, les liens électrostatiques, les interactions $\pi \cdots \pi$, les interactions dipôle-dipôle, les interactions de van der Waals et les interactions hydrophobes.

Comparativement aux liaisons covalentes, la plupart des interactions non-covalentes sont relativement faibles, mais par le fait même, elles ont l'avantage d'être réversibles.

³ Lehn, J.-M. *Supramolecular Chemistry*; VCH Publishers : Weinheim, 1995.

⁴ Lehn, J.-M. *Angew. Chem. Int. Ed.* **1988**, 27, 89.

Cette réversibilité est grandement exploitée dans la nature. Il suffit de penser aux deux brins d'ADN formés par des liaisons covalentes entre les bases azotées, mais dont la reconnaissance entre les brins est basée sur le pont hydrogène. La réversibilité d'association entre les deux brins permet leur réPLICATION. Plus impressionnant encore, cette réversibilité du pont hydrogène permet de minimiser les erreurs lors de la duplication du brin. Ce même phénomène est constaté lors de la transcription de l'ARN en protéine (Figure 1.3). On peut donc dire que cette réversibilité donne l'avantage de tendre vers une perfection en terme d'association moléculaire. De plus, la faiblesse en terme d'association est souvent compensée par la force du nombre, car les liaisons, une fois cumulées, peuvent former des superstructures relativement solides.

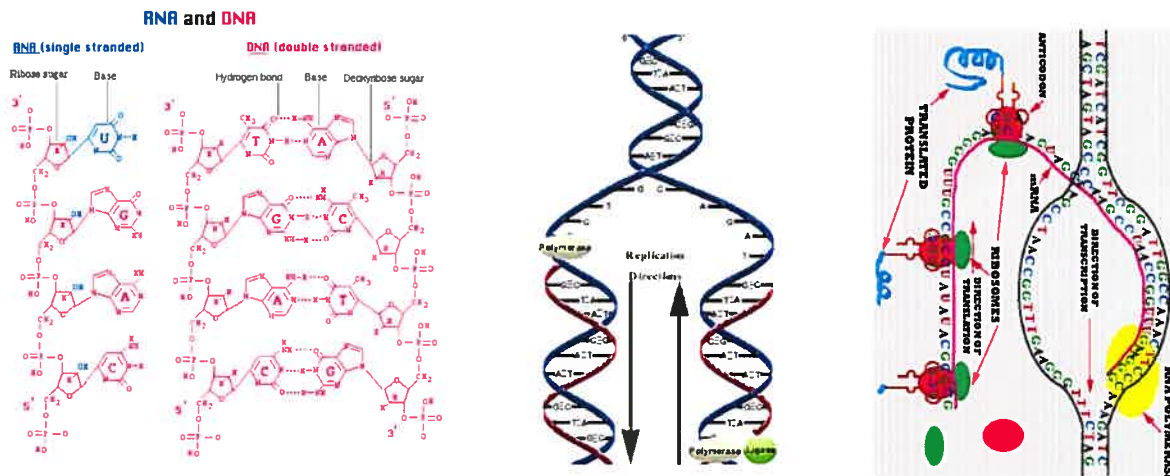


Figure 1.3 Représentation schématique de la réPLICATION d'un brin d'ADN et de la transcription de l'ARN jusqu'à sa traduction en protéine.⁵

Plusieurs domaines de recherche découlent de l'observation des prouesses que la nature nous offre et l'utilisation des interactions non-covalentes en chimie supramoléculaire n'échappe pas à cette règle. La chimie supramoléculaire comprend d'ores et déjà plusieurs

⁵ a) <http://ntri.tamuk.edu/cell/nucleic.html>
 b) <http://www.swbic.org/products/clipart/images/replication.jpg>
 c) http://www.netschool.de/pp/bio_gbs/transk.htm

sous disciplines telle que le champ des récepteurs artificiels, l'auto-assemblage programmé, le génie cristallin, la tectonique moléculaire, l'assemblage de couches, de membranes ou de fibres, la synthèse de polymères assemblés par des ponts hydrogène et bien d'autres encore.^{1,6} Malgré la jeunesse de ces domaines comparativement à la chimie de synthèse conventionnelle, ils n'en demeurent pas moins des sujets de recherche occupant une grande place dans la chimie moderne. Les applications présentes et futures découlant de ces domaines leurs confèrent un potentiel n'ayant pour limite que l'imagination de leur concepteur.

⁶ Pour des revues récentes sur la chimie supramoléculaire, le lecteur est invité à consulter :
a) Menger, F.M. *Proc. Nat. Acad. Sci.* **2002**, *99*, 4818.
b) Nguyen, S.T.; Gin, D.L.; Hupp, J.T.; Zhang, X. *Proc. Nat. Acad. Sci.* **2001**, *98*, 11849.

1.2 Historique de la tectonique moléculaire

Un des défis les plus excitants de la science contemporaine est le développement de méthodes permettant la formation de matériaux ordonnés avec des structures et des propriétés prédéterminées. L'obtention spontanée de matériaux moléculaires ordonnés par des processus d'auto-assemblage, comme dans la cristallisation, revêt un intérêt tout particulier.

Les premières recherches visant l'application des principes de la reconnaissance supramoléculaire au problème de contrôler l'organisation des molécules dans un cristal ont été effectuées par Ermer en 1988.⁷ Pour ce faire, il utilisa une molécule d'adamantane à laquelle il a greffé des acides carboxyliques. Les acides carboxyliques agissent à titre d'unités de reconnaissance et le réseau résultant de la cristallisation de cette molécule repose sur les ponts hydrogène intermoléculaires formés par ces derniers. La Figure 1.4 montre la molécule d'acide adamantane- 1,3,5,7-tetracarboxylique utilisée ainsi qu'un motif de reconnaissance intermoléculaire par pont hydrogène observé entre les acides carboxyliques.

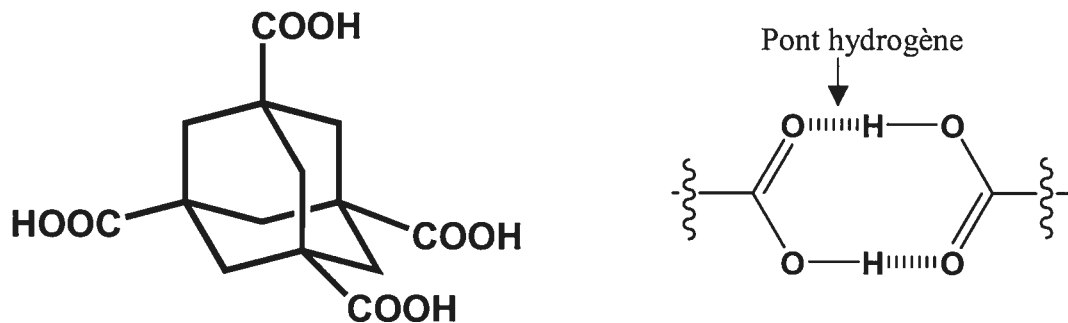


Figure 1.4 Représentation de l'acide adamantane- 1,3,5,7-tetracarboxylique et d'un motif de reconnaissance entre deux unités d'acides carboxyliques.

⁷ Ermer, O. *J. Am. Chem. Soc.* **1988**, *110*, 3747.

De nos jours, la prédition détaillée de la structure d'un cristal moléculaire à partir de ses composantes reste impossible.⁸ L'ingénierie du cristal procure toutefois une variété de stratégies de plus en plus efficaces pour la création de molécules prédisposées à s'assembler de manières particulières.⁹ L'une de ses stratégies se nomme la tectonique moléculaire.^{10,11,12} Elle a été introduite dans la littérature pour la première fois en 1991 par le groupe de recherche du professeur James D. Wuest de l'Université de Montréal.¹²

Lorsqu'on regarde l'association normale entre plusieurs molécules, on remarque que ces dernières ont une tendance naturelle à s'associer de manière compacte afin de minimiser l'énergie et de favoriser les interactions de van der Waals (Figure 1.5). La tectonique moléculaire, pour sa part, repose plutôt sur l'emploi de petites molécules de géométrie bien définie et possédant plusieurs sites périphériques leurs permettant d'interagir de manière intermoléculaire selon des motifs de reconnaissance efficaces. Ces petites molécules, que l'on nomme *tecton*, du mot grec signifiant constructeur, sont prédisposées à s'auto-assembler pour former des architectures dans lesquelles leurs voisins sont positionnés de façon prévisible (Figure 1.6).

⁸ a) Dunitz, J. D. *Chem. Commun.* **2003**, 545.
b) Desiraju, G. R. *Nature Materials* **2002**, 1, 77.
c) Gavezzotti, A. *Acc. Chem. Res.* **1994**, 27, 309.
d) Maddox, J. *Nature* **1988**, 335, 201.

⁹ Braga, D. *Chem. Commun.* **2003**, 2751. Biradha, K. *CrystEngComm* **2003**, 5, 374. Hollingsworth, M. D. *Science* **2002**, 295, 2410. *Crystal Engineering: From Molecules and Crystals to Materials*; Braga, D.; Grepioni, F.; Orpen, A. G., Eds.; Kluwer: Dordrecht, Netherlands, 1999. Desiraju, G. R. *Crystal Engineering: The Design of Organic Solids*; Elsevier: Amsterdam, 1989.

¹⁰ Mann, S. *Nature* **1993**, 365, 499.

¹¹ Hosseini, M. W. *CrystEngComm* **2004**, 6, 318.

¹² Simard, M.; Su, D.; Wuest, J. D. *J. Am. Chem. Soc.* **1991**, 113, 4696.

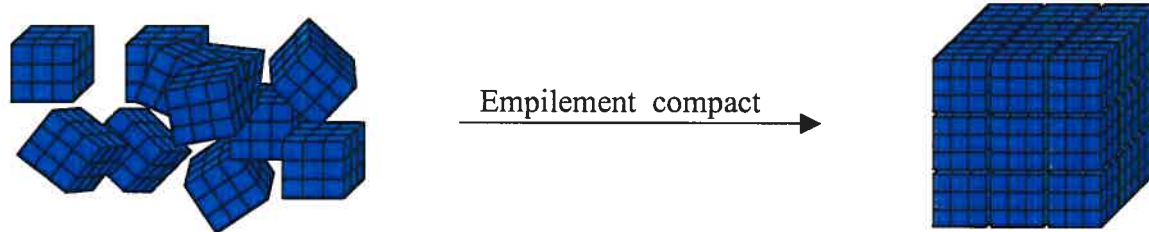


Figure 1.5 Représentation schématique de la tendance naturelle des molécules à former un empilement compact. Les molécules, symbolisées sous la forme de cubes, formeront préférentiellement un arrangement compact qui maximise les forces de van der Waals et minimise la présence d'espaces vides, défavorisée énergétiquement.¹²

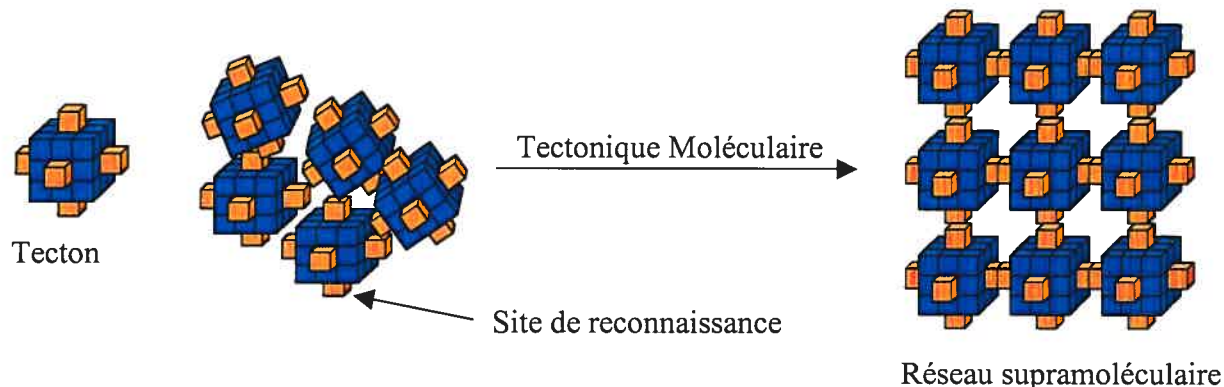


Figure 1.6 Formation d'un réseau supramoléculaire par la stratégie de la tectonique moléculaire.

Les tectons, lors de l'auto-assemblage, favorisent généralement les interactions entre leurs sites de reconnaissance plutôt que l'empilement compact. Pour ce processus de cristallisation, les sites de reconnaissance de l'unité tectonique sont donc la principale force directrice de l'assemblage. Implicitement, la forme de l'unité centrale portant ces groupes de reconnaissance aura un impact direct sur le réseau formé. Par conséquent, l'emploi d'unités centrales rigides et directionnelles combiné à l'utilisation de sites de reconnaissance forts limitera la possibilité de créer un empilement compact respectant la reconnaissance entre les sites. Il en résulte ainsi la possibilité de former des réseaux supramoléculaires poreux. La Figure 1.7 représente un exemple où l'on utilise une unité

centrale de forme tétraédrique favorisant la formation d'un réseau diamantoïde poreux. Lorsqu'on parle du réseau, on implique bien entendu l'architecture formée par l'association des tectons entre eux par les interactions non-covalentes. La porosité, pour sa part, représente l'espace occupé par les molécules n'appartenant pas au réseau. Ces molécules sont nommées "molécules invitées".

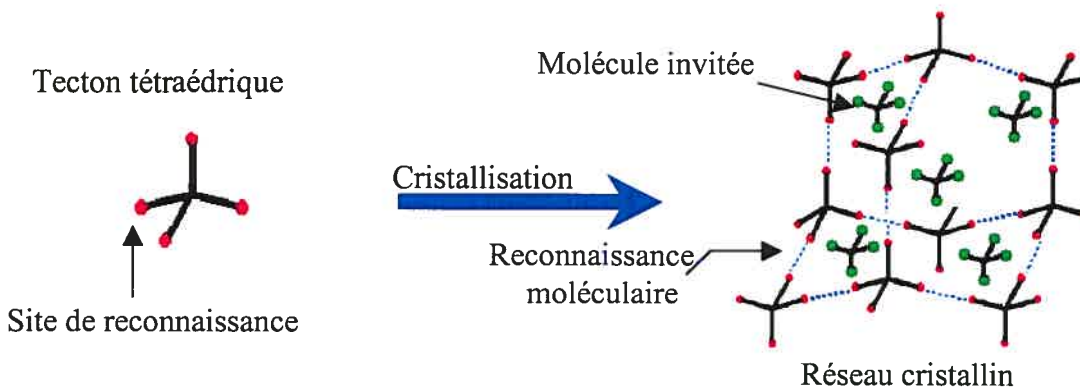


Figure 1.7 Utilisation d'un tecton tétraédrique lors de la formation d'un réseau diamantoïde incorporant des molécules de solvant invitées.

Historiquement, c'est en 1994 que le groupe du professeur Wuest a démontré l'efficacité de cette stratégie dans la formation de réseaux supramoléculaires poreux.¹³ Pour ce faire, il utilisa la tétrapyridoresilane comme unité tectonique (tecton 1.1 de la Figure 1.8). Les fonctions pyridone agissent comme groupements de reconnaissance et la géométrie tétraédrique de ce tecton conduit à la formation d'un réseau cristallin de type diamantoïde. De plus, l'utilisation de l'acide propionique comme solvant de cristallisation a permis de former un réseau poreux où les molécules de solvant invitées occupent jusqu'à 53% du volume total du cristal.

L'arrivée de cette stratégie dans le domaine de la chimie supramoléculaire s'est accompagnée d'une multitude de concepts et d'une terminologie bien spécifique à cette branche de la chimie. La Figure 1.8 illustre certains de ces concepts et permet ainsi leur clarification. Le tecton 1.1 (dont on a discuté plus haut) cristallise avec l'acide propionique

¹³ Wang, X.; Simard, M.; Wuest, J.D. *J. Am. Chem. Soc.* 1994, 116, 12119.

pour former un réseau d'une porosité de 53%. On a d'ores et déjà défini le réseau comme étant l'architecture formée par la reconnaissance intermoléculaire des tectons et la porosité comme étant l'espace disponible pour les molécules invitées. Le pourcentage de porosité représente donc le volume (espace) pouvant être occupé par les molécules invitées par rapport au volume total du cristal.¹⁴ On utilise le terme cavité lorsque ces volumes (espaces) sont ponctuels, mais lorsque ces espaces sont interconnectés et qu'ils traversent entièrement le cristal, on parle plutôt de canaux. Lorsque le réseau forme de tels canaux et qu'il est suffisamment robuste, il est possible de remplacer les molécules invitées présentes par de nouvelles molécules. Ce processus de remplacement, par exposition du cristal à un nouveau solvant, se nomme un "échange". La robustesse du réseau est importante dans le cas des échanges, car s'il n'est pas suffisamment solide, il s'effondre et perd sa cristallinité.

Regardons maintenant la Figure 1.8. La Figure **A** représente le réseau formé par la cristallisation du tecton **1.1** dans l'acide propionique. Les tectons y sont représentés en bleu et les molécules invitées, d'acide propionique, y sont représentées en rouge. La Figure **B** représente une vue de ce même réseau dans laquelle on a retiré les molécules invitées. Ce type de vue nous permet de voir la dimension et l'orientation des canaux. Finalement, la Figure **C** représente un relief négatif du réseau. Ce type d'image est l'équivalent de verser du ciment à l'intérieur du réseau et d'ensuite retirer les molécules constituant ce dernier. Elle permet de voir l'espace occupé par les molécules invitées, la forme des canaux créés ainsi que leurs connexions.

¹⁴ Le pourcentage de volume accessible pour les molécules invitées est estimé par le programme PLATON. PLATON calcule le volume accessible en faisant rouler une sphère de rayon variable sur la surface de van der Waals du réseau.

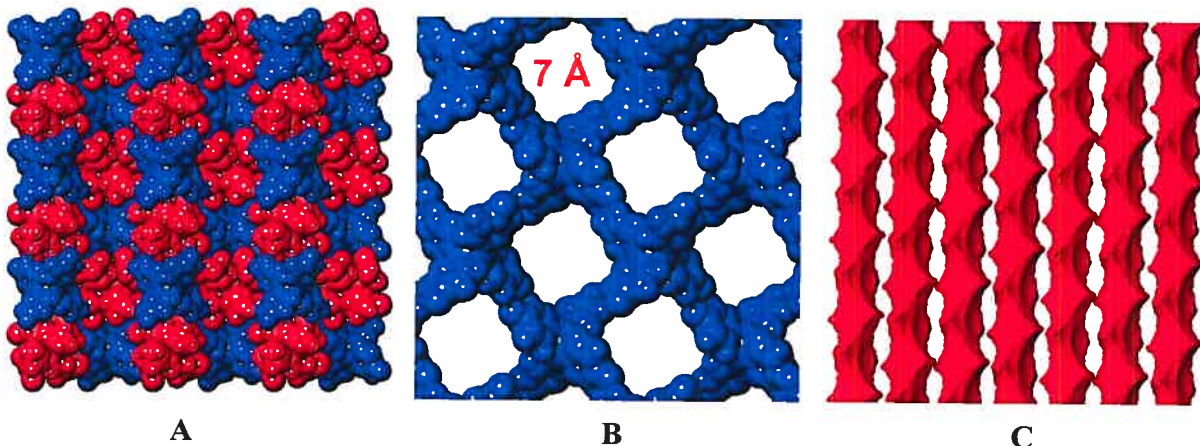
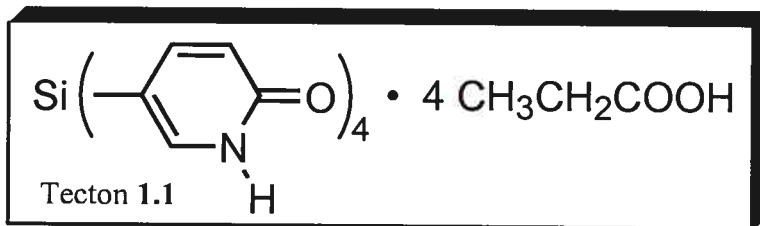


Figure 1.8 La Figure A représente une vue selon l'axe c en rayon de van der Waals du réseau formé par la cristallisation du tecton 1.1 (la tétrapyridonesilane) dans l'acide propionique. Les tectons sont en bleu et les molécules invitées ($\text{CH}_3\text{CH}_2\text{COOH}$) sont en rouge. Dans la Figure B, les molécules de solvant ont été omises afin de visualiser la dimension des canaux. Finalement, la Figure C représente l'espace occupé par les molécules de solvant. Cette dernière a été réalisée en visualisant le volume parcouru par le centre d'une sphère d'un rayon de $2,5\text{\AA}$ sur la surface de van der Waals du réseau.

Par la suite, le groupe du professeur Wuest a été très prolifique dans le domaine et a publié plusieurs articles au sujet de la tectonique moléculaire.¹⁵ Il a couvert ainsi plusieurs aspects fondamentaux dans le domaine de la cristallisation. Il étudia d'abord la formation de réseau à partir d'unité centrale simple et rigide tel le tétraphénylméthane. La Figure 1.9 illustre un de ces tectons simple et rigide.

¹⁵ Laliberté, D.; Maris, T.; Wuest, J. D. *J. Org. Chem.* **2004**, *69*, 1776. Laliberté, D.; Maris, T.; Wuest, J. D. *Can. J. Chem.* **2004**, *82*, 386. Fournier, J.-H.; Maris, T.; Wuest, J. D.; Guo, W.; Galoppini, E. *J. Am. Chem. Soc.* **2003**, *125*, 1002. Laliberté, D.; Maris, T.; Sirois, A.; Wuest, J. D. *Org. Lett.* **2003**, *5*, 4787. Sauriat-Dorizon, H.; Maris, T.; Wuest, J. D.; Enright, G. D. *J. Org. Chem.* **2003**, *68*, 240. Saied, O.; Maris, T.; Wuest, J. D. *J. Am. Chem. Soc.* **2003**, *125*, 14956.

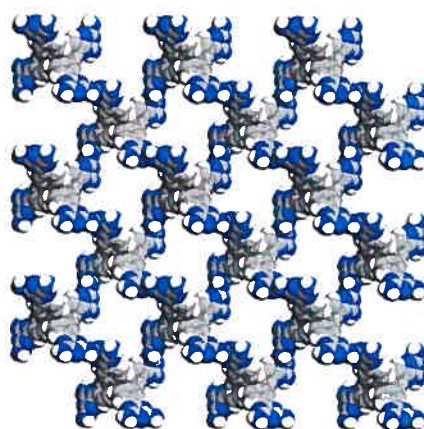
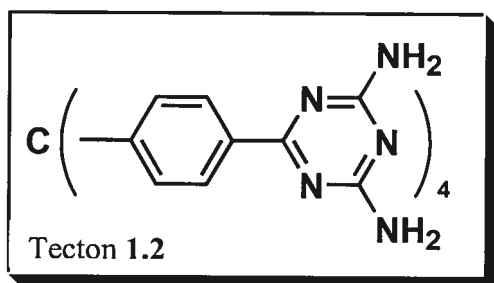


Figure 1.9 Vue en rayons de van der Waals du réseau formé par la cristallisation du tecton 1.2 dans HCOOH/dioxane. Les cavités forment des canaux parallèles à l'axe c . Les molécules de solvant ont été omises pour plus de clarté.

Le tecton 1.2, qui est basé sur un motif de reconnaissance dérivé de la 2,4-diamino-1,3,5-triazine, cristallise dans un mélange d'acide formique et de dioxane pour former un réseau poreux pouvant perdre jusqu'à 63% de ses molécules invitées tout en gardant l'intégralité de la structure du réseau hôte (Figure 1.9).¹⁶ La cristallisation de ce nouveau tecton apportait ainsi la preuve que les réseaux formés par la tectonique moléculaire peuvent atteindre une grande robustesse, malgré le fait qu'ils ne reposent que sur des interactions non-covalentes.

¹⁶ Brunet, P.; Simard, M.; Wuest, J.D. *J. Am. Chem. Soc.* **1997**, *119*, 2737.

Comme on le verra plus loin dans cette thèse, la robustesse du réseau est d'une importance capitale pour les applications potentielles de la tectonique moléculaire. Le développement du génie cristallin en général s'est arrêté sur l'emploi de différentes unités de reconnaissance.¹⁷ Parmi elles, on en retrouve plusieurs basées sur le pont hydrogène. En effet, le pont hydrogène est parmi les interactions plus employées pour diriger l'auto-assemblage, car il est à la fois directionnel et robuste pour une interaction non-covalente.¹⁸ C'est pour ces raisons que le groupe Wuest, comme bien d'autres groupes, s'attarda plus particulièrement sur le développement de ce type d'unité de reconnaissance. Parmi les unités employées pour diriger l'auto-assemblage reposant sur le

¹⁷ Jagadish, B.; Carducci, M. D.; Bosshard, C.; Günter, P.; Margolis, J. I.; Williams, L. J.; Mash, E. A. *Cryst. Growth Des.* **2003**, *3*, 811. George, S.; Nangia, A.; Bagieu-Beucher, M.; Masse, R.; Nicoud, J.-F. *New J. Chem.* **2003**, *27*, 568. Zyss, J.; Brasselet, S.; Thalladi, V. R.; Desiraju, G. R. *J. Chem. Phys.* **1998**, *109*, 658. Nangia, A.; Desiraju, G. R. *Top. Curr. Chem.* **1998**, *198*, 57. Desiraju, G. R. *Angew. Chem., Int. Ed.* **1995**, *34*, 2311.

¹⁸ Uemura, K.; Kitagawa, S.; Fukui, K.; Saito, K. *J. Am. Chem. Soc.* **2004**, *126*, 3817. Sada, K.; Inoue, K.; Tanaka, T.; Tanaka, A.; Eperges, A.; Nagahama, S.; Matsumoto, A.; Miyata, M. *J. Am. Chem. Soc.* **2004**, *126*, 1764. Maspoch, D.; Domingo, N.; Ruiz-Molina, D.; Wurst, K.; Tejada, J.; Rovira, C.; Veciana, J. *J. Am. Chem. Soc.* **2004**, *126*, 730. Baudron, S. A.; Avarvari, N.; Canadell, E.; Auban-Senzier, P.; Batail, P. *Chem. Eur. J.* **2004**, *10*, 4498. Angeloni, A.; Crawford, P. C.; Orpen, A. G.; Podesta, T. J.; Shore, B. *J. Chem. Eur. J.* **2004**, *10*, 3783. Murata, T.; Morita, Y.; Fukui, K.; Sato, K.; Shiomi, D.; Takui, T.; Maesato, M.; Yamochi, H.; Saito, G.; Nakasuji, K. *Angew. Chem., Int. Ed.* **2004**, *43*, 6343. Soldatov, D. V.; Moudrakovski, I. L.; Ripmeester, J. A. *Angew. Chem., Int. Ed.* **2004**, *43*, 6308. Du, Y.; Creighton, C. J.; Toung, B. A.; Reitz, A. B. *Org. Lett.* **2004**, *6*, 309. Bhogala, B. R.; Vangala, V. R.; Smith, P. S.; Howard, J. A. K.; Desiraju, G. R. *Cryst. Growth Des.* **2004**, *4*, 647. Balasubramaniam, V.; Wong, L. G. J.; Vittal, J. J.; Valiyaveettil, S. *Cryst. Growth Des.* **2004**, *4*, 553. Dale, S. H.; Elsegood, M. R. J.; Coombs, A. E. L. *CrystEngComm* **2004**, *6*, 328. Vinod, M.; Goldberg, I. *CrystEngComm* **2004**, *6*, 215. Aakeröy, C. B.; Desper, J.; Helfrich, B. A. *CrystEngComm* **2004**, *6*, 19. Alshahateet, S. F.; Nakano, K.; Bishop, R.; Craig, D. C.; Harris, K. D. M.; Scudder, M. L. *CrystEngComm* **2004**, *6*, 5. Brown, R. J.; Camarasa, G.; Griffiths, J.-P.; Day, P.; Wallis, J. D. *Tetrahedron Lett.* **2004**, *45*, 5103. Pedireddi, V. R.; SeethaLekshmi, N. *Tetrahedron Lett.* **2004**, *45*, 1903. Martin, S. M.; Yonezawa, J.; Horner, M. J.; Macosko, C. W.; Ward, M. D. *Chem. Mater.* **2004**, *16*, 3045. Kumar, D. K.; Jose, D. A.; Dastidar, P.; Das, A. *Chem. Mater.* **2004**, *16*, 2332. Barton, O. G.; Schmidtmann, M.; Müller, A.; Mattay, J. *New J. Chem.* **2004**, *28*, 1335.

pont hydrogène, on retrouve la diaminotriazine, la pyridone, les fonctions phénols, les acides carboxyliques et les acides boroniques (Figure 1.10).

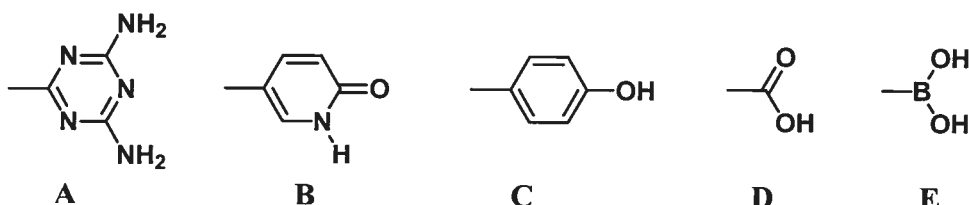


Figure 1.10 Quelques exemples d'unités de reconnaissance utilisant le pont hydrogène, incluant la diaminotriazine **A**, la pyridone **B**, les phénols **C**, les acides carboxyliques **D** et boroniques **E**.

On a aussi mentionné précédemment l'importance de l'unité centrale en tectonique moléculaire. En effet, cette dernière détermine la rigidité ainsi que le point de départ et la direction des unités de reconnaissance du tecton. Pour ces raisons, en plus d'explorer les unités de reconnaissance, la communauté scientifique s'est penchée sur l'impact des unités centrales en génie cristallin. Le groupe Wuest n'a pas fait exception à cette règle et plusieurs de leurs études ont porté sur la diversification de la géométrie de l'unité centrale ainsi que sur les effets reliés à la rigidité de cette dernière. Par conséquent, des tectons basés sur le carbone, le silicium, le bore, l'azote, le phosphore, le benzène, le pentaérythritol et bien d'autres, ont fait l'objet de plusieurs études. La Figure 1.11 montre quelques exemples de tectons étudiés.

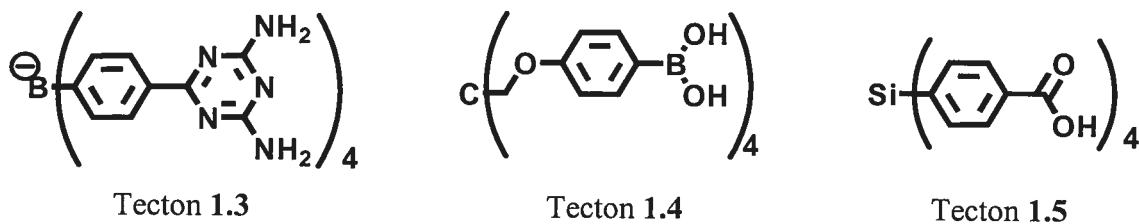


Figure 1.11 Les tectons **1.3**,¹⁹ **1.4**,²⁰ **1.5**²¹ représentent quelques exemples de tectons réalisés dans le groupe Wuest dans le cadre d'études sur l'impact des différences entre les formes et la rigidité de l'unité centrale d'un tecton.

¹⁹ Malek, N.; Maris, T.; Simard, M.; Wuest, J. D., *J. Am. Chem. Soc.* **2005**, *129*, 5910.

²⁰ Laliberté, D.; Maris, T.; Wuest, J. D., résultats non publiés.

²¹ Raymond, M.; Maris, T.; Wuest, J. D., résultats non publiés.

La tectonique moléculaire a donc fait ses preuves comme étant une stratégie efficace dans la formation de réseaux tridimensionnels poreux ayant une certaine robustesse. On se demande maintenant à quoi peuvent bien servir ces matériaux. Il est évident que selon le tecton employé, plusieurs types de réseaux peuvent être obtenus. Ce type de matériau devient d'avantage intéressant lorsque les espaces « libres » sont reliés entre eux de façon à former des canaux traversant le solide cristallin. Ces canaux, qui peuvent être parallèles ou interconnectés, donnent la possibilité d'échanger les molécules qui y sont initialement présentes par d'autres molécules. Ce concept est illustré à la Figure 1.12 où l'on voit les molécules invitées, en rouges, provenant de la cristallisation, se faire remplacer graduellement par des molécules, en bleus, provenant d'un solvant externe auquel on a exposé le cristal. Comme mentionné précédemment, les réseaux cristallins retenus par de multiples ponts hydrogène peuvent souvent suffisamment robustes pour que ce processus d'échange se produise sans perte de la cristallinité du matériau.

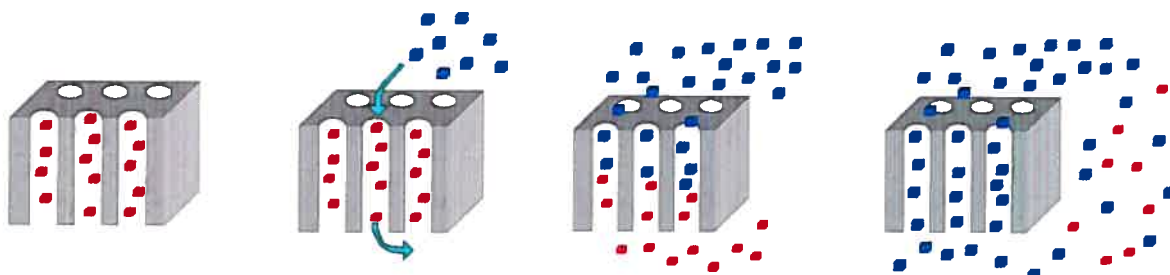


Figure 1.12 Représentation d'un processus d'échange de molécules de solvant invitées (rouges) à l'intérieur d'un réseau cristallin par d'autres petites molécules (bleus) organiques sans perte de la cristallinité du réseau.

Plusieurs applications de ce principe sont donc envisageables. On peut ainsi penser à la chromatographie d'exclusion illustrée à la Figure 1.13. On voit très bien le concept d'exclusion de grosses molécules, en gris, ne pouvant pénétrer à l'intérieur du réseau tectonique alors que les plus petites, en rouge, y diffusent sans problème.

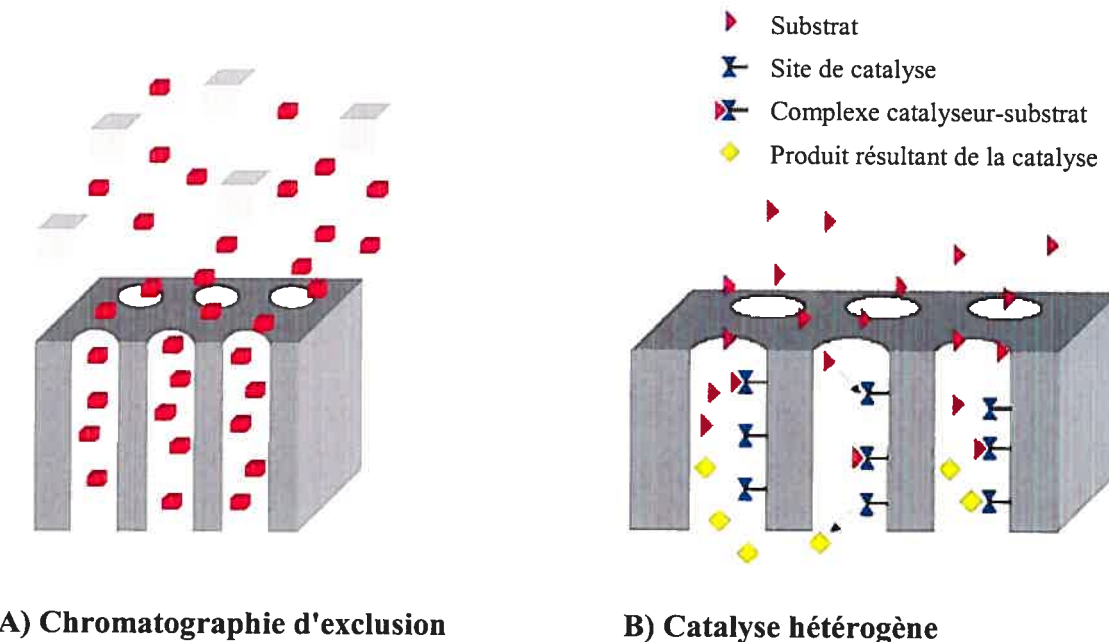


Figure 1.13 A) Représentation de la chromatographie d'exclusion où les molécules de dimension inférieure aux canaux (cubes rouges) diffusent à l'intérieur du réseau, mais où les molécules de dimension supérieure (cubes gris) sont exclues du réseau. B) Représentation de la catalyse hétérogène où des substrats (triangles rouges) sont transformés par les sites catalytiques incorporés au réseau (polygones bleus) en produits désirés (cubes jaunes).

Une autre application de ces réseaux poreux est la catalyse hétérogène. Ce concept, aussi illustré à la Figure 1.13, semble un objectif réalisable à court terme. C'est pour cette dernière application que l'on compare souvent ces nouveaux matériaux moléculaires aux zéolithes inorganiques en disant que la tectonique moléculaire offrira bientôt des composés complémentaires aux zéolithes actuelles. En effet, bien que les matériaux obtenus par le biais de la tectonique moléculaire soient moins résistants, ils ont l'avantage d'être beaucoup plus versatiles. Cette versatilité leurs vient du fait que la stratégie permettant leur conception est basée sur une synthèse rationnelle permettant aisément la modification de l'unité de base (tecton) et par conséquent, l'obtention rapide et facile en théorie d'une multitude de réseaux cristallins aux propriétés diverses.

La Figure 1.14, représentant le tecton 1.3, montre un bon exemple de réseau pour lesquel il est facile d'imaginer des applications à plus ou moins court terme. En effet, il s'agit d'un réseau anionique où plus de 74% du volume est occupé par le solvant et les contre-ions. Étant donné que dans cet exemple, les contre-ions sont mobiles et peuvent être échangés, ce matériau devient prometteur pour des applications comme la chromatographie d'échange d'ions (Figure 1.14).¹⁸ En effet, un réseau chargé négativement constitue un support solide ayant la possibilité de discriminer différentes molécules à la fois par leur grosseur et par leur charge.

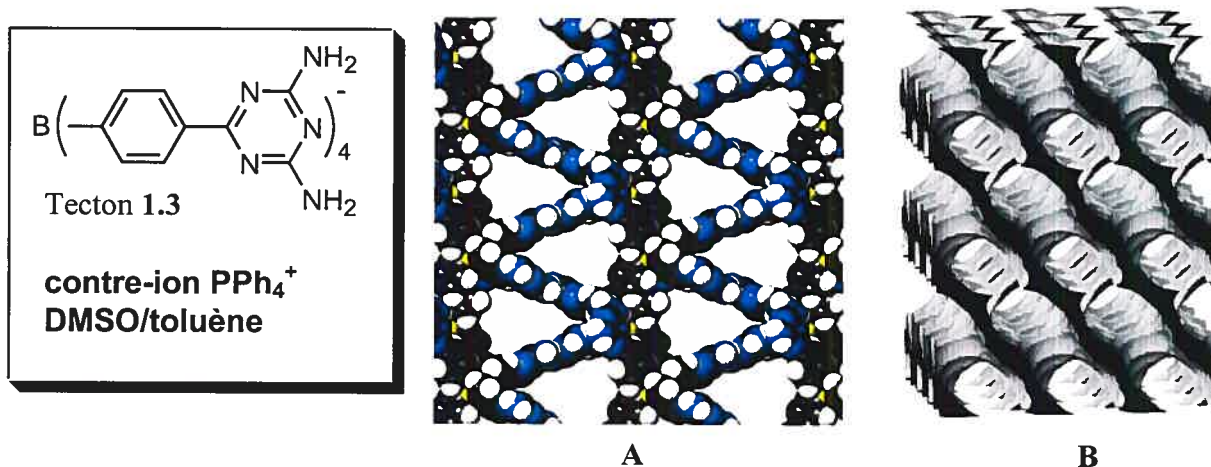


Figure 1.14 Représentation en rayons de van der Waals du réseau formé par la cristallisation du tecton 1.3 (A) et l'image de l'espace occupé par les molécules de solvant et les contre-ions (B). Cette dernière a été réalisée en roulant une sphère de 2,5 Å de rayon sur la surface de van der Waals du réseau.

La compréhension des mécanismes d'association supramoléculaire, l'étude de la mobilité des molécules incluses dans des réseaux poreux et l'obtention de nouvelles architectures cristallines demeurent des sujets d'une importance fondamentale dans le domaine de la tectonique moléculaire. En même temps, cette stratégie permet l'obtention de propriétés physiques inexistantes à l'échelle moléculaire mais présentes dans la structure supramoléculaire. Plusieurs applications très captivantes sont envisageables pour cette nouvelle famille de matériaux et méritent donc d'être explorées.

1.4 Objectifs de cette thèse

La tectonique moléculaire en tant que stratégie de formation de matériaux ordonnés permet entre autre l'obtention de réseaux tridimensionnels poreux. Ce fait est bien connu et accepté dans le domaine de la chimie supramoléculaire. Par contre, les applications de cette dernière dans des domaines plus concrets et pratiques restent à réaliser. En effet, depuis quelques années, on compare les réseaux tectoniques à ceux des zéolithes en disant que par sa versatilité synthétique, la tectonique moléculaire sera un atout complémentaire à ces derniers. Ainsi, les attentes envers la tectonique moléculaire sont immenses, mais ce domaine est encore jeune et il reste beaucoup à explorer avant que ce dernier ne soit reconnu comme un outil essentiel et efficace en chimie supramoléculaire. L'objectif de cette thèse, qui se divisera en trois parties majeures, est de tenter de nous rapprocher de notre objectif ultime, soit de mener la tectonique moléculaire vers des applications concrètes et utiles dans la chimie moderne.

En premier lieu, nous savons qu'il reste beaucoup à faire et à comprendre dans le domaine de la chimie supramoléculaire. Une des énigmes, auxquelles plusieurs scientifiques aimeraient répondre, est la compréhension de la cristallisation dans son ensemble. En effet, en 1988 Maddox déclare: "*L'un des scandales continuels dans les sciences physiques est qu'il demeure en général impossible de prédire la structure des plus élémentaires solides cristallins à partir de la connaissance de leur composition chimique.*".^{8d} Quinze ans plus tard, il semble que le problème de compréhension au sujet de la cristallisation ne soit toujours pas résolu. En effet, c'est au tour de Dunitz de déclarer: "...*Computational methods for predicting crystal structures cannot yet be regarded as reliable. From a more qualitative and descriptive viewpoint has come the notion that certain groupings in organic molecules exercise attractive intermolecular interactions and so guide the molecules into distinctive patterns in their crystal structures. This has become one of the tenets of crystal engineering. The prime example of a structure directing interaction is, of course, the hydrogen bond.*"^{8a} Pour ces raisons, il est évident que la compréhension des phénomènes de la cristallisation rendrait d'immenses services à la

chimie en général, mais aussi faciliterait la transition de la théorie à la pratique pour les applications de la chimie supramoléculaire.

Le travail à accomplir pour mener à une compréhension totale de la cristallisation est immense et cette thèse n'a pas la prétention de toucher à tous les aspects imaginables dans ce domaine. Nous avons ainsi concentré nos études sur une unité centrale avec laquelle on a récemment obtenu de grands succès, soit le 9,9'-spirobifluorène.²² Le Chapitre 2 sera ainsi consacré à l'histoire du développement du 9,9'-spirobifluorène ainsi qu'à son introduction en tectonique moléculaire. Les trois chapitres suivants traiteront de l'utilisation de cette unité centrale en tectonique moléculaire et en génie cristallin.

Le Chapitre 3 sera dédié à l'emploi du spirobifluorène comme unité centrale à laquelle sont rattachées les unités de reconnaissance. On étudiera l'effet que peut avoir un espaceur phényle entre l'unité centrale et les sites de reconnaissance. Cet effet sera étudié pour le cas d'unités de reconnaissance assez fortes comme les ponts hydrogène de la diaminotriazine. Le Chapitre 4 portera sur le même genre d'étude, mais dans le cas d'interactions plus faibles de type C-H···O et C-H···N impliquant des groupements nitro et cyano. Le Chapitre 5 sera consacré à l'utilisation d'arylamine comme donneur et accepteur de ponts hydrogène dans la formation de réseaux supramoléculaires. On étudiera ainsi plusieurs unités centrales, dont le 9,9'-spirobifluorène, afin de comparer les réseaux formés par l'association de ces arylamines. Ceci complètera la première partie de la thèse portant sur l'emploi du 9,9'-spirobifluorène en génie cristallin.

Une grande partie des applications potentielles de la tectonique moléculaire nécessite des réactions à l'intérieur du réseau cristallin formé par les tectons. Il est donc essentiel de démontrer la faisabilité de ce concept. La seconde partie de la thèse, le Chapitre 6, consistera à montrer qu'il est effectivement possible de faire des réactions à l'intérieur de cristaux poreux obtenus par la stratégie de la tectonique moléculaire. En

²² Fournier, J.-H.; Maris, T.; Wuest, J. D. *J. Org. Chem.* 2004, 69, 1762.

effet, on verra que la diffusion de réactifs à l'intérieur des canaux permet l'obtention de réactions sur le réseau tout en conservant l'intégralité de ce dernier. On verra également qu'il est aussi possible, avec cette même stratégie de diffusion, d'augmenter la rigidité du réseau cristallin poreux par polymérisation covalente du cristal afin de former une seule macromolécule. On démontra donc que cette stratégie permet de combiner la quasi-perfection de l'auto-assemblage cristallin, par le biais d'interactions non-covalentes, à la robustesse des interactions covalentes.

Le contrôle de la porosité d'un réseau est d'une importance majeure pour différentes applications potentielles de la tectonique moléculaire. En effet, si on veut réaliser une certaine sélection lors d'applications telle que la chromatographie d'exclusion, il est nécessaire de pouvoir contrôler la grosseur des canaux formés. La réalisation de réactions à l'état cristallin nécessite également un contrôle de la porosité des réseaux visés, car si l'on veut faire de telles réactions, il est impératif que les molécules puissent pénétrer dans le réseau. Il peut aussi être nécessaire d'introduire des groupes fonctionnels pour catalyser certaines réactions. Il est donc incontournable de démontrer la faisabilité de cette incorporation. Enfin, si on veut faire la mimique d'un état de transition afin de catalyser une réaction comme le font les enzymes, il faut également montrer la possibilité de retirer certains groupements fonctionnels appartenant au réseau sans briser la cristallinité de ce dernier. La troisième partie de la thèse, le Chapitre 7, poussera plus loin le principe démontré au Chapitre 6 en utilisant le principe des réactions à l'état cristallin, par la stratégie de diffusion de réactif, afin de montrer que celle-ci peut être utile à la fois dans le contrôle de la porosité et dans le retrait de groupes fonctionnels préalablement incorporés au réseau.

Le dernier chapitre, le huitième, fera une rétrospective de cette thèse où on y discutera des conclusions générales ainsi que des perspectives des projets.

Chapitre 2

*Introduction du
9,9'-spirobifluorène en génie
cristallin*

2.1 Introduction

La forme de l'unité centrale tectonique, comme mentionné au chapitre précédent, revêt une importance capitale dans le type de réseaux obtenus. En effet, le choix de la géométrie de l'unité centrale tectonique se répercute directement sur la forme du réseau qui en résultera. À titre d'exemple, la Figure 2.1 montre quelques dérivés qui orientent les groupements de reconnaissance dans un même plan, favorisant ainsi la formation de réseaux en forme de couches.¹ Bien entendu, une unité centrale planaire permet d'orienter la reconnaissance dans un plan, mais ne permet pas la prédiction de l'empilement qu'auront les molécules hors de ce plan.

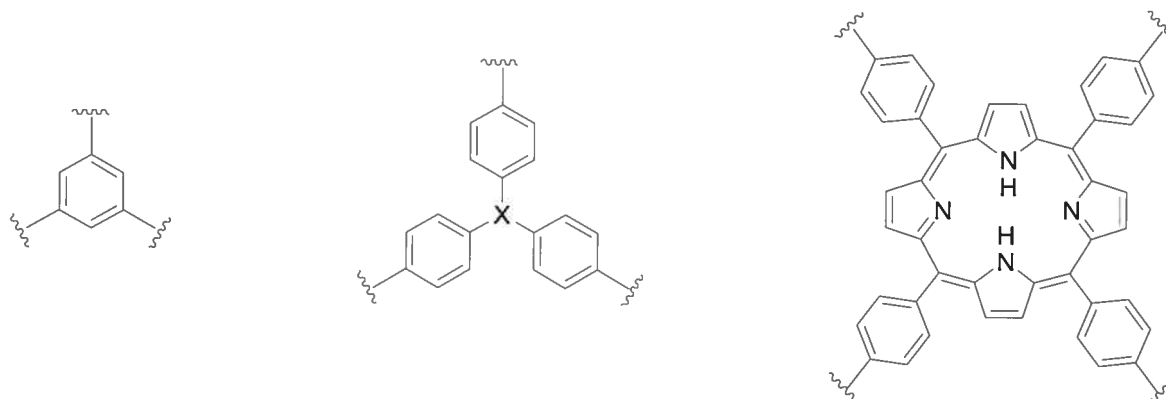


Figure 2.1 Unités centrales favorisant la formation de réseaux en forme de couches.

Pour cette raison, il est encore plus intéressant d'utiliser des unités centrales orientant ces unités de reconnaissance dans les trois dimensions dans l'espace. Plusieurs

¹ Desharnais, J. *Thèse de doctorat*, Université de Montréal, 2001. Dumas, L. *Mémoire de maîtrise*, Université de Montréal, 2002. Gonzalez Gonzalez, G.; *Mémoire de maîtrise*, Université de Montréal, 2002. Gonzalez Gonzalez, G.; Simard, M.; Maris, T.; Wuest, J. D., résultats non publiés. Helzy, F.; Simard, M.; Maris, T.; Wuest, J. D., résultats non publiés. Lautman, M.; Maris, T.; Wuest, J. D., résultats non publiés.

unités centrales tridimensionnelles sont représentées à la Figure 2.2. Ces dernières dirigent les groupes de reconnaissance de façon tétraédrique et prédisposent ainsi à la formation de réseaux dont la reconnaissance se fait de façon tridimensionnelle.²

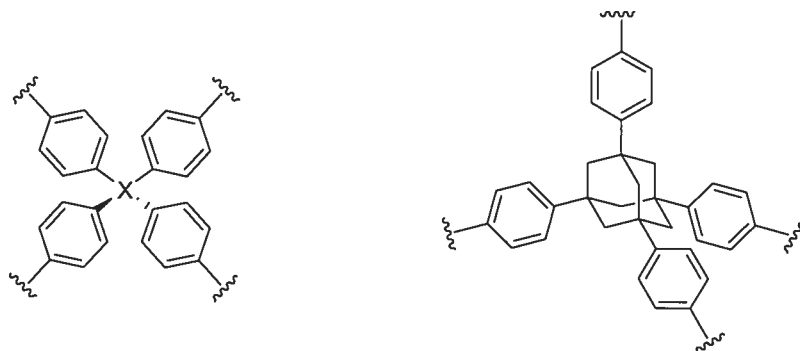


Figure 2.2 Unités centrales favorisant une reconnaissance tridimensionnelle.

Par conséquent, l'utilisation d'unités centrales tétraédriques conduit souvent vers l'obtention de réseaux diamantoïdes tels qu'illustrés à la Figure 2.3. L'utilisation d'unités dirigeant la reconnaissance en trois dimensions possède aussi l'avantage de prédisposer la formation de réseaux poreux. En effet, afin de répondre à la contrainte tétraédrique résultant de l'unité centrale, l'association se fait en laissant des espaces libres qui sont comblés par les molécules invitées.

² Simard, M.; Su, D.; Wuest, J. D. *J. Am. Chem. Soc.* **1991**, *113*, 4696. Brunet, P.; Simard, M.; Wuest, J. D. *J. Am. Chem. Soc.* **1997**, *119*, 2737. Su, D.; Wang, X.; Simard, M.; Wuest, J. D. *Supramolecular Chem.* **1995**, *6*, 171. Wuest, J. D. *Mesomolecules: From Molecules to Materials*; Mendenhall, G. D., Greenberg, A., Liebman, J. F.; Chapman & Hall: New York, 1995; p 107. Wang, X.; Simard, M.; Wuest, J. D. *J. Am. Chem. Soc.* **1994**, *116*, 12119. Le Fur, E. *Mémoire de maîtrise*, Université de Montréal, 2000. Malek, N. *Thèse de doctorat*, Université de Montréal, 2001.

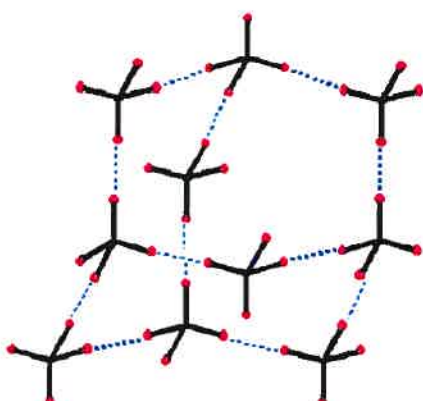
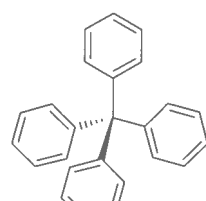


Figure 2.3 Utilisation d'unités centrales tétraédriques favorisant l'obtention de réseaux diamantoïdes.

Un autre facteur important pour l'obtention de réseaux poreux est la rigidité du tecton créé. En effet, même si on utilise une géométrie prédisposant une reconnaissance dans les trois dimensions, si le tecton formé n'est pas suffisamment rigide, il facilitera une déformation de l'orientation de départ pouvant conduire jusqu'à un empilement compact.

L'une des unités centrales les plus utilisées en génie cristallin est le téraphénylméthane (**1**). La synthèse de cette molécule fut réalisée pour la première fois en 1897.³ À cette époque, ce composé suscitait déjà l'intérêt des scientifiques tant du point de vue structural que pour l'accomplissement synthétique. L'intérêt était notamment dû à l'intrigante possibilité de lier quatre cycles aromatiques à un même atome central. Ce composé, qui fut synthétisé pour la première fois par M. Gomberg,³ constitue effectivement un excellent candidat pour des applications en reconnaissance moléculaire. En effet, il a d'abord l'avantage d'être directionnel, mais il implique également une grande rigidité structurelle. De plus l'incorporation de groupes fonctionnels sur les sites aromatiques est facile à réaliser.

³ Gomberg, M. *Ber. Dtsch. Chem. Ges.* **1897**, *30*, 2043. Gomberg, M. *J. Am. Chem. Soc.* **1898**, *20*, 773.



1

Pour ces multiples raisons, le tetraphénylméthane, à titre d'unité centrale, fit l'objet de nombreuses études en reconnaissance moléculaire.⁴ Parmi ces études, on retrouve les trois molécules illustrées à la Figure 2.4. Tous ces tectons ont conduit à la formation de réseaux à la fois poreux et diamantoïdes.

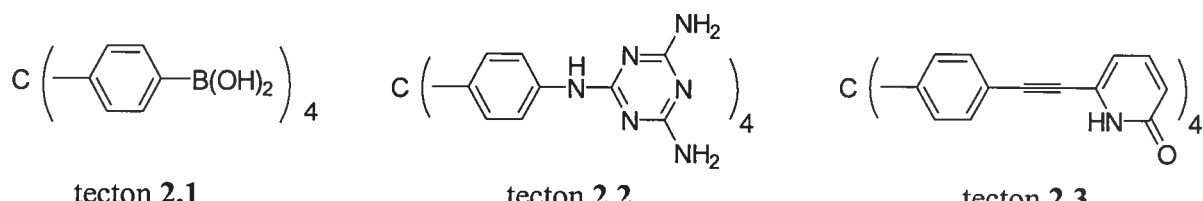


Figure 2.4 Représentation des tectons 2.1,⁵ 2.2⁶, et 2.3⁷ basés sur le tetraphénylméthane comme unité centrale et conduisant à la formation de réseaux diamantoïdes poreux.

⁴ Basavouju, S.; Aitipamula, S.; Desiraju, G. R. *CrystEngComm.* **2004**, *6*, 120.

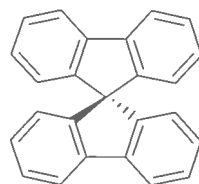
⁵ Fournier, J.-H.; Maris, T.; Wuest, J. D.; Guo, W.; Galoppini, E. *J. Am. Chem. Soc.* **2003**, *125*, 1002.

⁶ S. Hetzel, T. Maris, M. Simard, J. D. Wuest, résultats non publiés.

⁷ M. Simard, D. Su, J. D. Wuest, *J. Am. Chem. Soc.* **1991**, *113*, 4696.

2.2 Le 9,9'-spirobifluorène

Dans la section 2.1, on a montré l'importance de la géométrie et de la rigidité de l'unité centrale employée pour l'obtention de réseaux prévisibles et poreux. On a aussi montré l'efficacité du téraphénylméthane dans ce domaine et les raisons de son succès. Le téraphénylméthane n'est toutefois pas la seule unité centrale possédant ce caractère rigide et directionnel. Dans notre recherche de nouvelles unités centrales en tectonique moléculaire, l'emploi du 9,9'-spirobifluorène (**2**) se révéla une unité très prometteuse pour la formation de tectons conduisant à la formation de réseaux supramoléculaires poreux.⁸



2

La première synthèse du 9,9'-spirobifluorène fut encore une fois réalisée par Gomberg vers les années 1930.⁹ Aujourd'hui la synthèse la plus couramment utilisée est celle développée par J. M. Tour et collaborateurs,¹⁰ qui est essentiellement la même que celle initialement développée par Gomberg. Elle consiste en une réaction d'addition du dérivé lithié du 2-iodobiphényl sur la fonction carbonyle de la 9-fluorénone, suivie par une alkylation interne de Friedel-Crafts catalysée en milieu acide (Schéma 2.1).

⁸ Fournier, J.-H.; Maris, T.; Wuest, J. D. *J. Org. Chem.* **2004**, *69*, 1762.

⁹ Clarkson, R. G.; Gomberg, M. *J. Am. Chem. Soc.* **1930**, *52*, 2881.

¹⁰ Wu, R.; Schumm, J. S.; Pearson, D. L.; Tour, J. M. *J. Org. Chem.* **1996**, *61*, 6906.

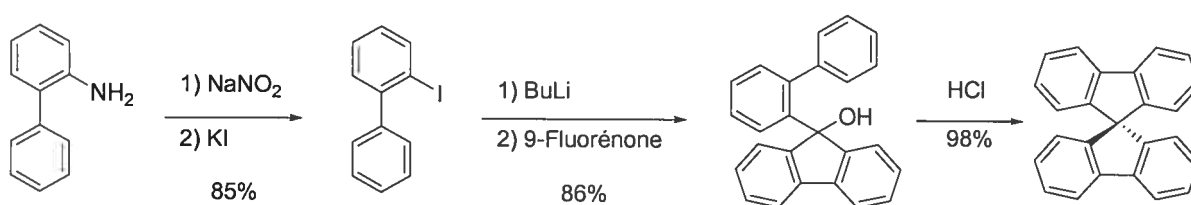


Schéma 2.1 Synthèse du 9,9'-spirobifluorène.¹⁰

En regardant attentivement la géométrie du 9,9'-spirobifluorène, on remarque plusieurs similitudes avec le tétraphénylméthane. Il est, lui aussi, constitué de quatre cycles aromatiques liés à un atome central de carbone, mais cette fois, la liberté de rotation des groupements phényle n'y est plus permise. La rigidité de son squelette en fait donc un candidat idéal pour des études en génie cristallin.

Le 9,9'-spirobifluorène diffère toutefois grandement du tétraphénylméthane dans sa régiosélectivité envers les électrophiles. En effet, la substitution électrophile aromatique sur le tétraphénylméthane donne des dérivés para-substitués. Ces substitutions sont d'une très grande régiosélectivité qui est associée non seulement au caractère électronique relativement plus riche de la position 4, mais également à l'inaccessibilité des positions 2 et 6 pour des raisons d'encombrement stérique (Figure 2.5).

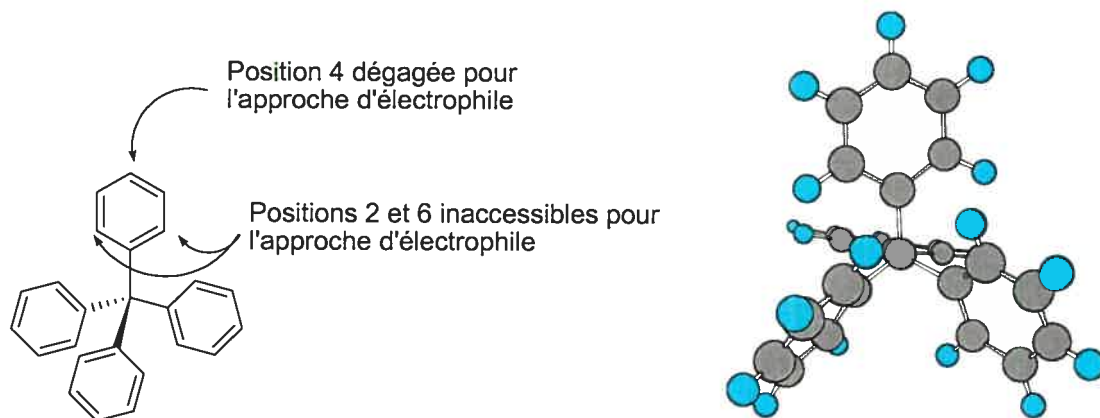
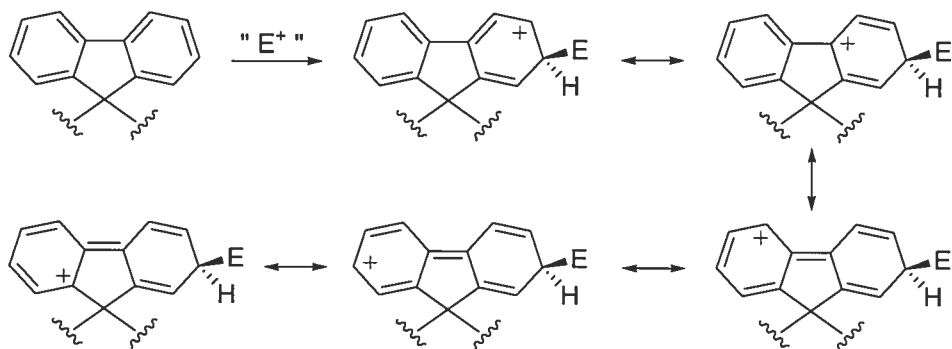


Figure 2.5 Réactivité du tétraphénylméthane envers les électrophiles.

Dans le cas des dérivés du 9,9'-spirobifluorène, la régiosélectivité envers les substitutions électrophiles aromatiques se fait dans les positions 2 et 7, soit en méta du carbone central. Cette régiosélectivité peut être rationalisée en invoquant la plus grande stabilité du carbocation généré lors de l'addition de l'électrophile à ces positions.¹⁰ L'addition d'électrophiles à la position 2 ou 7 profite d'une plus grande délocalisation de charge que lors d'une attaque aux positions 3 et 6 comme illustré à la Figure 2.6.

Attaque aux positions 2 et 7



Attaque aux positions 3 et 6

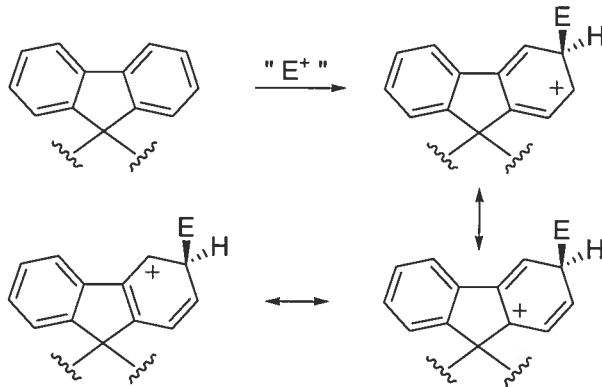


Figure 2.6 Stabilisation des intermédiaires réactionnels lors de réactions de substitution électrophile aromatique sur le 9,9'-spirobifluorène.

La bromation du spirobifluorène est un bon exemple illustrant cette régiosélectivité. En effet, l'ajout de brome en présence d'une quantité catalytique de FeCl_3 conduit à la formation exclusive et quantitative du 2,2',7,7'-tétrabromo-9,9'-spirobi[9H-fluorène].¹⁰

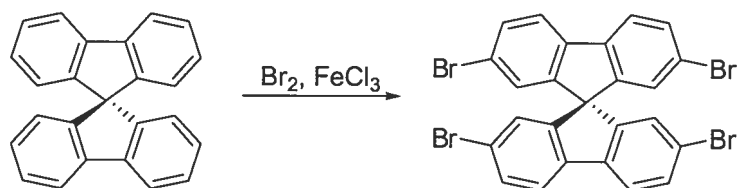


Schéma 2.2 Bromation régiosélective du 9,9'-spirobifluorène en position 2,2' et 7,7'.¹⁰

2.3 Utilisation de l'unité 9,9'-spirobifluorène dans la conception de tectons.

Depuis plusieurs années, la communauté scientifique se spécialisant dans la reconnaissance moléculaire tente de comprendre les phénomènes d'association en chimie supramoléculaire. Le groupe Wuest ne fait pas exception. Pour étudier et comprendre comment prédire la formation de réseaux supramoléculaires, la synthèse d'une variété de tectons a été réalisée. Pour ce faire, plusieurs unités centrales ont été élaborées afin de diriger efficacement et de manière prévisible les sites de reconnaissance intermoléculaire dans une orientation fixe.

Le 9,9'-spirobifluorène comme unité centrale en tectonique moléculaire a été introduit par le Dr. Jean-Hugues Fournier en 2000. Cette molécule était très attrayante, d'abord pour sa rigidité structurale, mais également pour sa tendance vers la formation de produits d'inclusion. Cette unité nous intéresse encore aujourd'hui pour d'autres raisons, notamment la facilité d'obtention de produits substitués en position 2 et 7 permettant de larges études sur ce genre de composés. Les trois prochains chapitres décrivent l'utilisation du 9,9'-spirobifluorène dans divers domaines de la tectonique moléculaire.

Chapitre 3

*Effet d'un espaceur phényle
dans la formation de réseaux
par le 9,9'-spirobifluorène-DAT*

3.1 Introduction

Un des objectifs des chercheurs dans le domaine du génie cristallin est de développer des nouvelles stratégies pour augmenter la porosité. En effet, comme énoncé précédemment, plusieurs applications potentielles découlent de la porosité cristalline. La tectonique moléculaire a fait ses preuves en tant que stratégie efficace pour l'obtention de cristaux poreux. On veut maintenant découvrir jusqu'à quel point un solide moléculaire peut être occupé par des molécules invitées. Jusqu'à maintenant, les «records» de porosité pour de petites molécules organiques tournent autour 70%.

À l'intérieur du groupe Wuest, plusieurs chercheurs ont récemment réussi à cristalliser des tectons pour former des réseaux de très grande porosité. À titre d'exemple, le Dr. Kenneth Maly et son collaborateur Eric Gagnon ont synthétisé le tecton **3.1** basé sur l'hexaphénylbenzène comme unité centrale.¹ Ce composé peut être cristallisé dans le DMSO par une diffusion de benzène pour former un réseau très poreux où les molécules incluses occupent 72% du volume total du cristal (Figure 3.1).

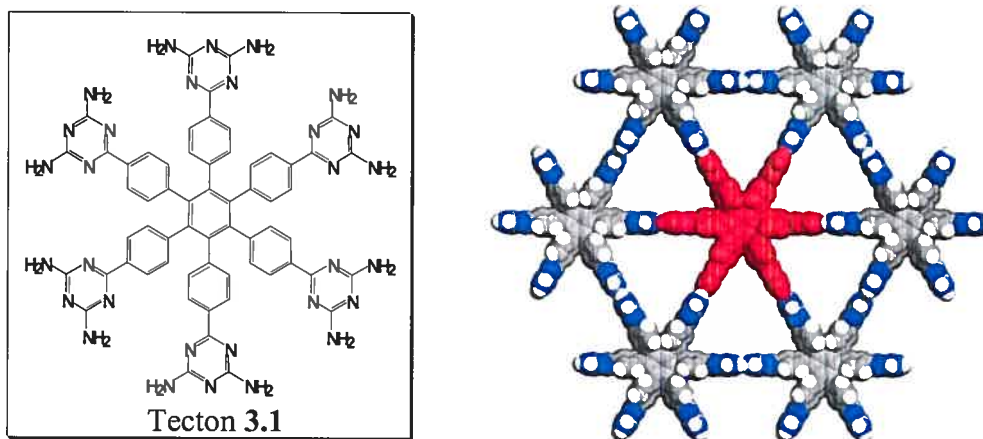


Figure 3.1 Structure du tecton **3.1** et vue selon l'axe *c* du réseau formé par sa cristallisation dans DMSO/benzène. Les molécules invitées sont omises pour plus de clarté. Le réseau est retenu via 12 ponts hydrogène par tecton et définit des canaux parallèles à l'axe *c*.

¹ Maly, K.; Gagnon, E.; Maris, T.; Wuest, J. D., résultats non publiés.

Parmi les réseaux les plus poreux jamais obtenus, il est difficile de passer à côté de celui réalisé par le Dr. Nadia Malek à partir du tecton 3.2.² Ce tecton est anionique et, lorsque cristallisé par diffusion de toluène dans une solution du tecton dans le DMSO, génère un réseau tridimensionnel très poreux (Figure 3.2). Le réseau inclus plusieurs molécules de DMSO ainsi que les contre-ions nécessaires ($^+PPh_4$) afin de maintenir l'équilibre des charges. L'espace libre du réseau atteint ainsi près de 74%, ce qui constituait alors le record en terme de porosité obtenue pour une petite molécule organique. De plus, ce cristal constitue un réseau anionique immobile dans lequel des charges cationiques mobiles sont incluses. Il a aussi été montré que les cations de ce réseau peuvent être librement échangés avec d'autres types de molécules chargées positivement. Ainsi, puisque la dimension des cavités est fixe ($8 \times 12 \text{ \AA}$), le réseau ne laisse passer que les cations d'une taille inférieure aux dimensions des canaux. Ce type de réseau semble donc prometteur pour l'élaboration de matériaux chargés pouvant reconnaître et piéger sélectivement selon la taille des molécules de charge opposée.

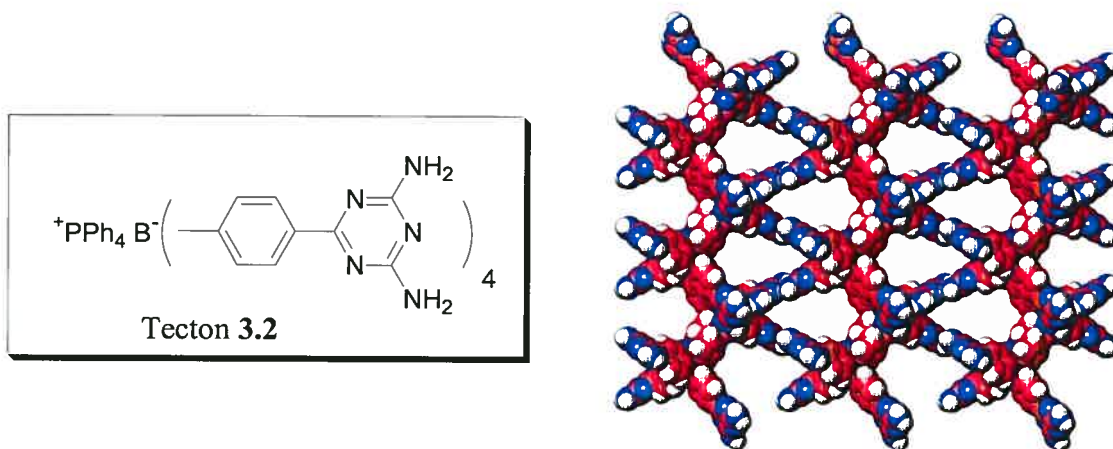


Figure 3.2 Structure du sel tétraphénylphosphonium du tecton 3.2 et vue selon l'axe *c* du réseau formé par sa cristallisation dans DMSO/toluène. Les molécules de solvant et les cations désordonnés sont omis. Le réseau définit des canaux parallèles à l'axe *c* et est retenu par 16 ponts hydrogène par tecton.

² Malek, N.; Maris, T.; Simard, M.; Wuest, J. D. *J. Am. Chem. Soc.* **2005**, *127*, 5910.

Ce « record » en terme de porosité a toutefois été récemment brisé par le Dr Jean-Hugues Fournier,³ qui a préparé le tecton 3.3 (Figure 3.3). Sa cristallisation, par diffusion de dioxane dans une solution du tecton 3.3 dans le DMSO, génère un réseau tridimensionnel d'une porosité de 75%. Les canaux obtenus ont une dimension de 9.1 par 15.3 Å. Ceci représente le plus haut niveau de porosité obtenu à partir d'une petite molécule organique. La Figure 3.3 représente les canaux dans le réseau obtenu ainsi que l'espace occupé par les molécules invitées.

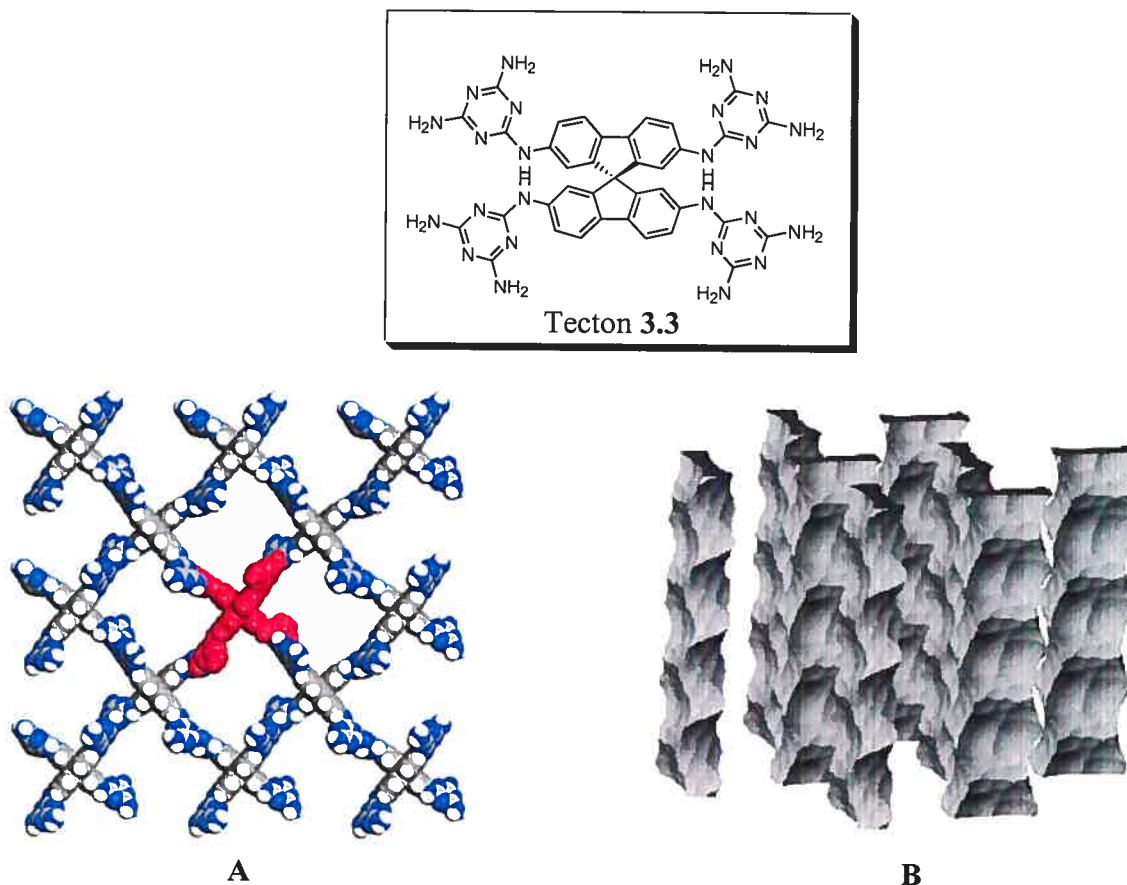


Figure 3.3 Vue selon l'axe *c* du réseau formé par la cristallisation du tecton 3.3 (A) dans DMSO/dioxane ainsi que les canaux formés qui sont parallèles à l'axe *c* du réseau (B).

³ Fournier, J.-H.; Maris, T.; Wuest, J. D. *J. Org. Chem.* 2004, 69, 1762.

3.2 Stratégie visant le contrôle et l'augmentation de la porosité

Les scientifiques travaillant sur la tectonique moléculaire se fient sur leur instinct et leur logique pour identifier des nouvelles molécules capables de former des réseaux poreux. Ils ont considéré systématiquement plusieurs groupes de reconnaissance et ont étudié une grande variété d'unités centrales. Afin de comprendre les subtilités de la cristallisation, on réalise des études sur un même tecton auquel on apporte de légères modifications afin de voir l'effet qu'elles auront sur le réseau. L'étude qui suit explore l'effet qu'aura un espaceur entre l'unité centrale et les groupements de reconnaissance. La Figure 3.4 conceptualise cette idée. En théorie, un tel ajout devrait augmenter la distance entre le centre de chaque tecton et ses voisins. Par le fait même, il est permis d'espérer une augmentation de la porosité.

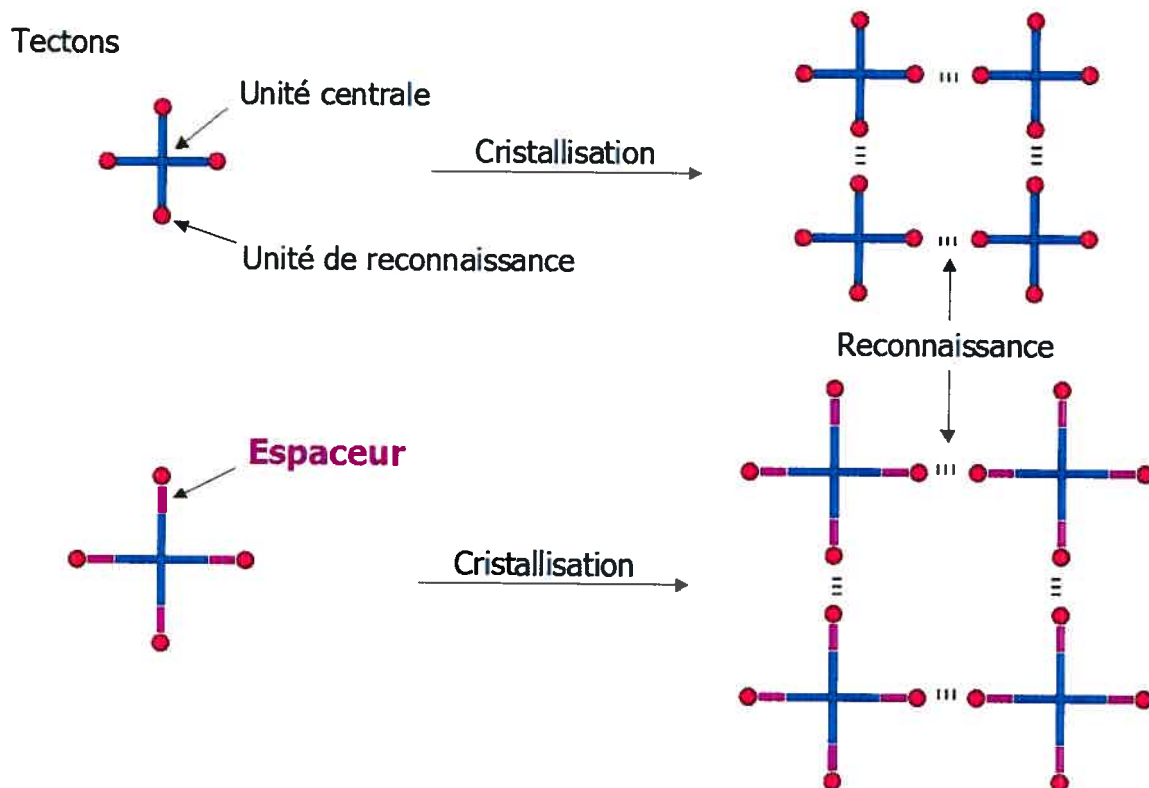


Figure 3.4 Représentations des effets attendus par l'ajout d'un espaceur entre l'unité centrale et les sites de reconnaissance.

3.3 Étude sur l'effet de l'espacement entre l'unité centrale et le site de reconnaissance

Étant donné la tendance marquée du 9,9'-spirobifluorène à former des réseaux tridimensionnels très poreux, on a décidé de faire une étude de l'effet qu'aurait l'ajout d'un espaceur entre l'unité centrale (le 9,9'-spirobifluorène) et les groupements de reconnaissance. Le groupement de reconnaissance choisi est la diaminotriazine, car sa manière de s'associer est généralement prévisible et suit habituellement un des trois motifs illustrés à la Figure 3.5.

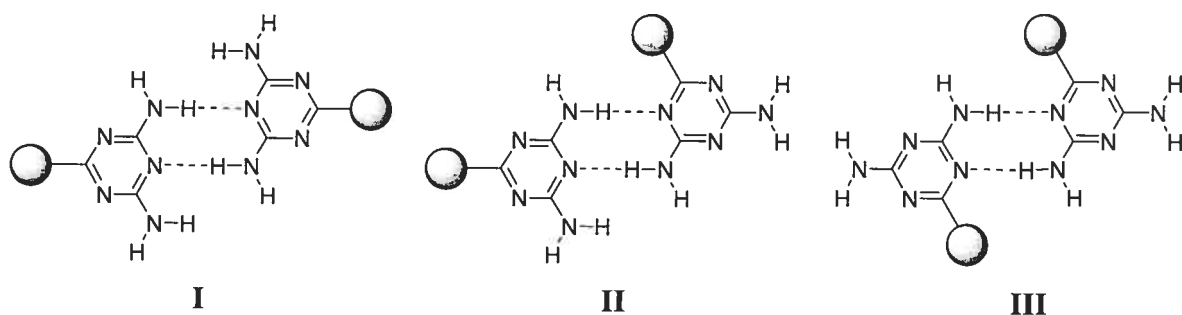


Figure 3.5 Représentations des principaux motifs d'association de la diaminotriazine.

Le tecton de base choisi pour nos études est le tecton 3.4 représenté à la Figure 3.6. Ce dernier a été synthétisé par le Dr. Fournier et semblait être un candidat idéal pour nos études.³ Il est d'abord facile d'accès au plan synthétique et donne une bonne porosité lors de sa cristallisation. En effet, la cristallisation par diffusion de dioxane dans une solution du tecton dans le DMSO génère le réseau tridimensionnel d'une porosité de l'ordre de 60% et dont les canaux obtenus ont une dimension de 5.3 par 5.3 Å. Un autre avantage est sa grande rigidité et le fait qu'il possède moins de degrés de liberté que le tecton 3.3. Cette flexibilité réduite laisse ainsi moins de possibilités d'agencement dans l'espace, rendant l'interprétation de la cristallisation généralement plus facile et prévisible.

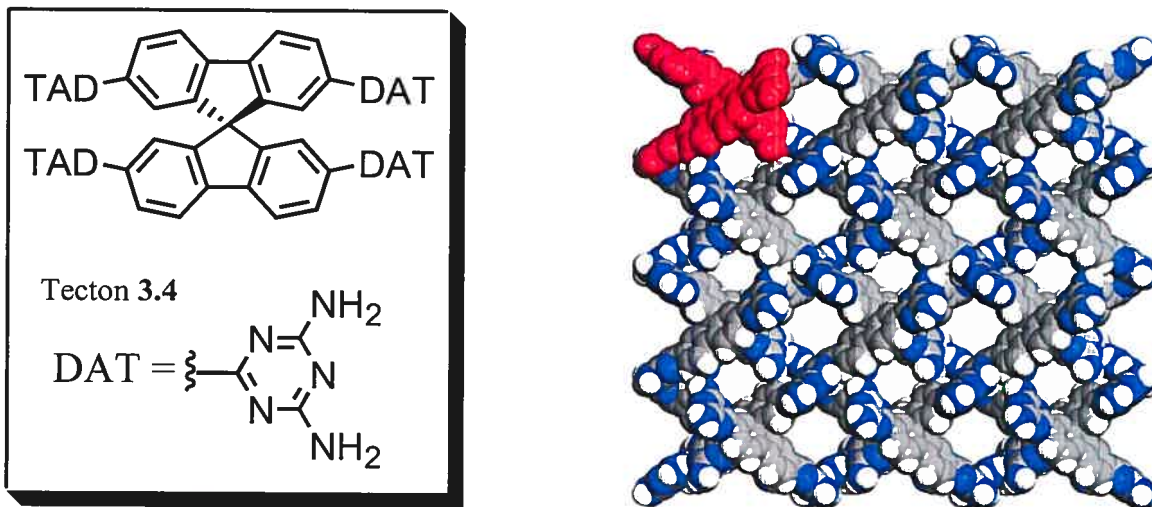


Figure 3.6 Représentation du tecton 3.4 et du réseau découlant de sa cristallisation dans DMSO/dioxane (vue selon l'axe α avec les molécules invitées omises).

L'article qui suit décrit les modifications apportées au tecton 3.4 par l'addition d'un espaceur phényle entre l'unité centrale spirobifluorène et l'unité de reconnaissance diaminotriazine. On y discute de l'efficacité de la méthode dans l'augmentation de la distance entre le centre de chaque tecton et ses voisins ainsi que des répercussions sur la porosité.

3.4 Article 1

Molecular Tectonics. Porous Hydrogen-Bonded Networks Built from Derivatives of 2,2',7,7'-Tetr phenyl-9,9'- spirobi[9H-fluorene]

Eric Demers, Thierry Maris and James D. Wuest

Crystal Growth & Design, 2005, 5, 1227

Molecular Tectonics. Porous Hydrogen-Bonded Networks

Built from Derivatives of 2,2',7,7'-Tetraphenyl-9,9'-spirobi[9H-fluorene]

Eric Demers,¹ Thierry Maris, and James D. Wuest*

Département de Chimie, Université de Montréal

Montréal, Québec H3C 3J7 Canada

*Author to whom correspondence may be addressed:



Abstract

The cruciform shape of spirobifluorene disfavors close molecular packing, and more complex derivatives with multiple sites of hydrogen bonding are known to associate to form highly porous networks with significant space for the inclusion of guests. In principle, the porosity can be increased by introducing spacers between the spirobifluorene core and the peripheral sites of association. To test this strategy, compounds **2-3** with multiple diaminotriazine groups attached to a tetraphenylspirobifluorene core were synthesized, and their behavior was compared with that of a model (**4**) lacking the phenyl spacers. As expected, extended spirobifluorenes **2-3** crystallized to produce open networks held together by hydrogen bonding of diaminotriazine groups; however, the porosities of these networks were lower (53% and 44%, respectively) than that of the network built from model **4** (60%). The decreased porosity arises largely because the added phenyl spacers change the relative contributions of hydrogen bonding and aromatic interactions to the overall lattice energy of the crystals. It becomes advantageous to optimize aromatic interactions at the expense of hydrogen bonds, and crystallization therefore favors networks that permit closer molecular packing.

Introduction

Microporous and mesoporous structures have fascinated materials scientists for many decades, and significant energy continues to be devoted to the effort to discover, characterize, and exploit new porous materials.² This effort is amply justified by the unique utility of micro- and mesoporous materials,³ which includes 1) separations based on the ability of guests to enter the pores and channels of the host; 2) temporary storage of selected gases and reactive guests; 3) heterogeneous catalysis of a wide range of reactions, using sites accessible only to particular substrates; and 4) casting microscopic and nanoscopic replicas within the pores and channels of the host. Of special value are highly ordered micro- and mesoporous materials that have well-defined compositions and structures, thereby ensuring strict uniformity of pores and channels, as well as providing a clear basis for understanding and predicting behavior.

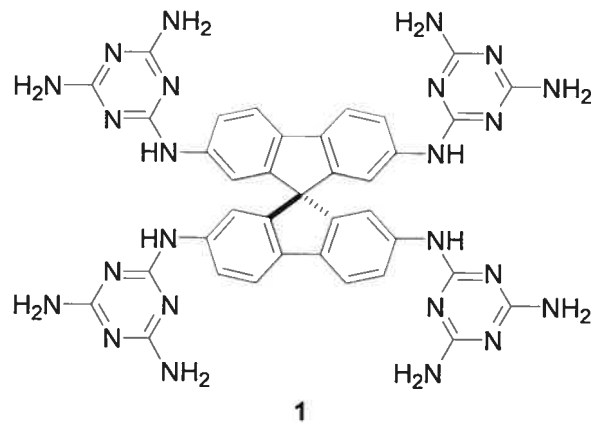
In the field of porous ordered materials, the archetypes are zeolites and related inorganic substances with open frameworks, which have numerous commercial applications and continue to be studied actively.⁴ An exciting advance in recent years has been the development of hybrid organic-inorganic analogues in which open frameworks are created by the coordination of metals with multidentate ligands.^{5,6} These hybrids offer many attractive features, including high porosity, robust crystalline structures, and the possibility of designing materials for particular applications by varying both metals and ligands logically. At the same time, a similar effort has been made to devise analogues of zeolites that are purely molecular, with porous networks maintained only by suitable non-covalent interactions such as hydrogen bonds.⁶⁻⁸ Although inherently less robust than zeolites and organic-inorganic hybrids, purely molecular analogues have uniquely attractive properties of their own, including easy structural deformation and disassembly.⁹

A strategy that has been called molecular tectonics offers a reliable way to make porous molecular networks with predictable structural features.⁸⁻¹⁴ This strategy is based on the use

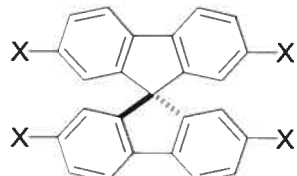
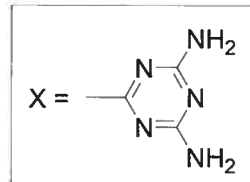
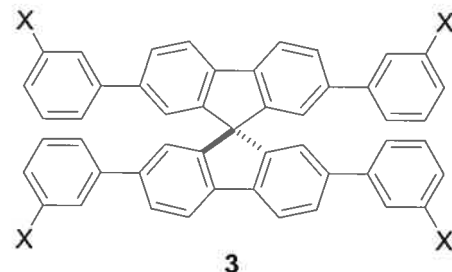
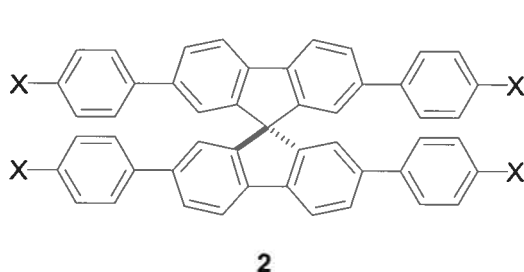
of special molecules, called tectons from the Greek word for builder,¹⁰ which can be considered to consist of 1) structurally well-defined cores and 2) multiple peripheral substituents that participate reliably in strong directional intermolecular interactions. Such molecules are programmed to associate and to form specific networks in which each molecule is positioned relative to its neighbors in a predetermined way. Hydrogen bonds have proven to be especially effective in directing tectonic association.¹⁵

Tectonic association differs from normal molecular association because directional interactions play a more important role in determining how neighbors are positioned. In general, these directional interactions severely constrain molecular packing, because they cannot normally be optimized at the same time that normal close packing is achieved. As a result, tectonic association tends to produce open molecular networks with substantial space for the inclusion of guests. When maintained by multiple interactions, such networks can display high structural integrity, and guests can be exchanged in single crystals without loss of crystallinity. In favorable cases, guests can even be partially removed from intact crystals.¹³ Such observations underscore the close relationship that exists between classical zeolites and purely molecular analogues built by the strategy of molecular tectonics.

Recent work has established that exceptionally porous molecular networks can be built from tectons in which multiple hydrogen-bonding sites are attached to cores with shapes intrinsically resistant to close packing.⁸ Among the most attractive cores for this purpose are rigid cruciform structures with the geometry of an Onsager cross, which are impossible to pack closely in periodic arrays.¹⁶ For example, spirobifluorenes can be considered to be Onsager crosses, and they are known to pack with low efficiency.⁸ These concepts led to the design of tecton 1, which proved to crystallize to form the most porous network yet constructed from small molecules.⁸ Fully 75% of the volume of crystals of spirobifluorene 1 is available for including guests, an amount that far exceeds the porosity of conventional zeolites and approaches the values observed for the most open hybrid organic-inorganic framework structures.^{5,6}

**1**

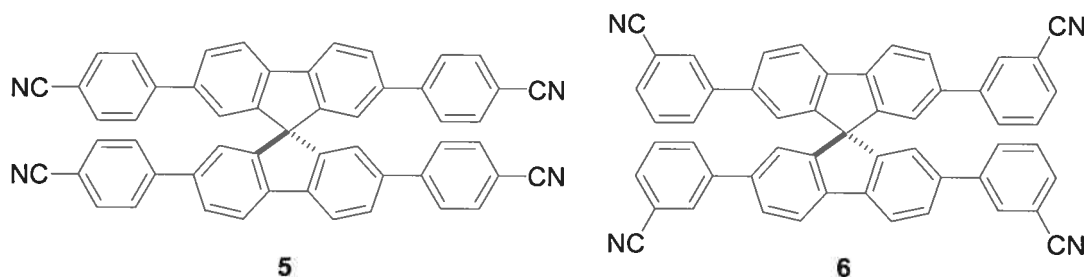
The unusual properties of tecton **1** and closely related compounds encouraged us to study the behavior of analogues with similar hydrogen-bonding sites separated from the spirobifluorene core by the addition of spacers, thereby leading to extended tectons designed to form networks of even higher porosity. In this paper, we report the synthesis and structure of two new tectons of this type, tetraphenylspirobifluorenes **2-3**, and we compare their behavior with that of known model **4**,⁸ which lacks the phenyl spacers.



Results and Discussion

Porous Hydrogen-Bonded Network Constructed from Tecton 4. As previously demonstrated, crystallization of simple spirobifluorene **4** from DMSO/dioxane is directed by hydrogen bonding of diaminotriazine groups to give a three-dimensional interpenetrated network.^{8,17} The observed network has a porosity of 60%,¹⁸ and the crystals have the approximate composition **4** • 4 DMSO • 7 dioxane.²⁰ Each tecton participates in a total of sixteen hydrogen bonds with six neighbors according to characteristic cyclic motifs **I-III** (Figures 1-2).⁸ Motif **I** involves the more accessible N-3/N-3' nitrogen atoms and is therefore considered to be stronger than the alternative N-1/N-3' and N-1/N-1' motifs **II-III**. In the network built from tecton **4**, two of the six neighbors each form two hydrogen bonds with the central tecton according to motif **I**; two other neighbors each form four hydrogen bonds with the central tecton, creating distorted motifs of type **II**; and the remaining two neighbors each form two hydrogen bonds with the central tecton according to motif **III**. Together, the tectons that interact by motif **I** define stacked square grids, whereas those that interact according to motifs **II** and **III** define a diamondoid network with two-fold interpenetration.^{17,21} Guests included in the network are highly disordered and lie in two types of channels aligned with the α axis (Figure 3). The cross sections of these channels measure approximately $4.2 \times 4.2 \text{ \AA}^2$ and $3.9 \times 3.9 \text{ \AA}^2$ at the narrowest points.²²

Porous Hydrogen-Bonded Network Constructed from Extended Tecton 2. Extended spirobifluorene **2** was synthesized in 60% yield by treating the known tetranitrile **5**²³ with



dicyandiamide and KOH under standard conditions.²⁴ Tecton **2** crystallized from DMSO/acetone in the triclinic space group P1 as an inclusion compound of approximate composition **2** • 7 DMSO • 1.5 H₂O.²⁰ Views of the structure are shown in Figures 4-9. As expected, extended tecton **2** behaves like simple analogue **4** and self-associates by hydrogen bonding of its diaminotriazine groups, thereby forming an open network with significant space for including guests. Two symmetry-independent tectons **A** and **B** are present in the structure. Tecton **A** forms a total of thirteen hydrogen bonds with five neighbors as shown in Figure 4. Four of the neighbors are equivalent to tecton **A** by translation, and the fifth is symmetry-independent tecton **B**. Two of the equivalent neighbors (red) are each linked to tecton **A** (white) by two hydrogen bonds of type **III**, and the spirocyclic centers of tecton **A** and the two neighbors are separated by 20.7 Å. Two other equivalent neighbors (blue) each form four hydrogen bonds with tecton **A** (white) according to motif **II**, and the spirocyclic centers are separated by 17.8 Å. The remaining neighbor, symmetry-independent tecton **B** (dark gray), is linked to tecton **A** by only a single distorted hydrogen bond, and the spirocyclic centers are separated by 21.9 Å. Together, each tecton **A** (white) and its four equivalent neighbors (red and blue) form an approximately square-planar unit, and the resulting network is a four-connected sheet.

Symmetry-independent tecton **B** forms a total of eleven hydrogen bonds with five neighbors as shown in Figure 5. Four of the neighbors are equivalent to tecton **B** by translation, and the fifth is symmetry-independent tecton **A**. Two of the equivalent neighbors (red) are each linked to tecton **B** (dark gray) by two hydrogen bonds of type **III**, and the spirocyclic centers of tecton **B** and the two neighbors are separated by 20.7 Å. Two other equivalent neighbors (blue) each form three hydrogen bonds with tecton **B** (two according to motif **II**), and the spirocyclic centers are separated by 17.8 Å. As in the case of tecton **A**, tecton **B** and its four equivalent neighbors define an approximately square-planar grid. In the overall structure of tecton **2**, each sheet composed uniquely of tecton **A** is paired with one sheet built uniquely from tecton **B** to form a bilayer held together by single hydrogen bonds between neighboring tectons **A** and **B** in the two adjacent layers (Figure 6). Stacking of the bilayers then generates the full structure of tecton **2**.

Approximately 53% of the volume of crystals of extended spirobifluorene **2** remains available for including guests,¹⁸ which occupy two types of channels parallel to the *a* axis (Figure 7). The cross sections of the larger channels measure approximately $4.5 \times 4.9 \text{ \AA}^2$ and those of the smaller channels are $4.5 \times 2.4 \text{ \AA}^2$.²² The connectivity of the channels is represented by the surface shown in Figure 8.²⁵

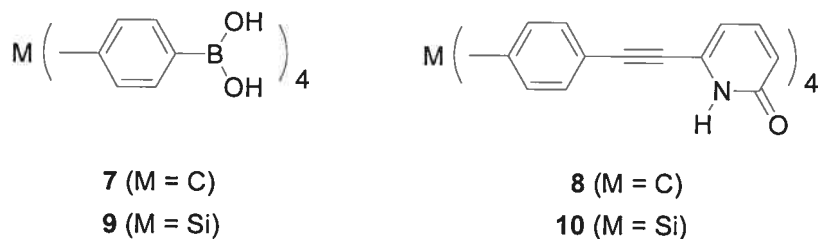
Porous Hydrogen-Bonded Network Constructed from Extended Tecton 3. Extended meta-substituted spirobifluorene **3** was synthesized in 71% yield from the known tetranitrile **6**²³ by the same method used to make para-substituted analogue **2**. Tecton **3** crystallized from DMSO/CH₃OH in the triclinic space group P-1 as an inclusion compound of approximate composition **3** • 5 DMSO • 2.5 CH₃OH.²⁰ Views of the structure are shown in Figures 9-13. As expected, extended tecton **3** behaves like simple analogue **4** and self-associates by hydrogen bonding of its diaminotriazine groups, thereby forming an open network with significant space for including guests. As in the case of para-substituted analogue **2**, two symmetry-independent tectons (**C** and **D**) are present in the unit cell. Tectons **C** and **D** are held in close proximity by a total of four distorted hydrogen bonds of type **III**, as well as by aromatic interactions, and their spirocyclic centers are separated by only 9.2 Å (Figure 9). Together, paired tectons **C** and **D** participate in a total of nineteen additional hydrogen bonds with ten neighbors. Five of these neighbors are linked by standard motifs **I-III** (Figure 10), whereas the other five form distorted single hydrogen bonds (Figure 11).

Approximately 44% of the volume of crystals of extended spirobifluorene **3** remains available for including guests,¹⁸ which occupy two types of channels parallel to the *a* axis (Figure 12). The cross sections measure approximately $7.7 \times 2.0 \text{ \AA}^2$ and $14.0 \times 1.6 \text{ \AA}^2$.²² The connectivity of the channels is represented by the surface shown in Figure 13.²⁵

Conclusions

As planned, crystals constructed from simple spirobifluorene **4** and its extended analogues **2-3** have certain elementary features in common. All three tectons form open networks held together by multiple hydrogen bonds involving aminotriazine groups. In all cases, large numbers of hydrogen bonds are formed per tecton (10-16), the porosity of the networks is substantial (44-60%), and large numbers of guests are included. The consistent behavior of compounds **2-4**, despite their evident differences in size and shape, underscores the reliability of molecular tectonics as a strategy for helping determine the structure and properties of ordered materials.

However, our results also show that porosity cannot always be enhanced simply by increasing the distance from the core of a tecton to its peripheral sticky sites, thereby favoring a larger intertectonic separation and a more open network. This straightforward strategy can be very effective, as demonstrated by the rational geometric expansions engineered by replacing tetraphenylmethanes **7-8** with the analogous tetraphenylsilanes **9-10**.^{12,26} In contrast, the networks built from extended spirobifluorenes **2-3** are *less* porous than the one derived from simple model **4**. Moreover, the architectures of the resulting networks are completely different.



Detailed comparison of the structures suggests that porosity is decreased in the case of tectons **2-3** partly because the four added phenyl spacers perturb significantly the relative contributions of hydrogen bonding and aromatic interactions to the overall lattice energy of the crystals. In effect, the spacers create an energetic incentive to stabilize emerging

crystals by optimizing aromatic interactions at the expense of hydrogen bonds. Clear evidence that aromatic interactions play a larger role in the structures of extended spirobifluorenes **2-3** than in that of model **4** is provided by the following observations: 1) Fewer hydrogen bonds are formed per tecton **2-3** (10-13) than per tecton **4** (16); and 2) a larger fraction of the hydrogen bonds in the structures of extended tectons **2-3** are distorted or single, rather than the classic motifs of Figure 1. Together, these observations suggest that hydrogen bonds between extended tectons **2-3** can no longer play a dominant role in determining how the molecules are positioned in the crystalline state, so they cannot enforce the creation of expanded versions of the already highly open architecture favored by simple model **4**. Instead, crystallization favors the formation of networks with alternative geometries that permit closer molecular packing, thereby optimizing aromatic interactions.

Experimental Section

Extended Para-Substituted Spirobifluorene 2. A mixture of 2,2',7,7'-tetrakis(4-cyanophenyl)-9,9'-spirobi[9H-fluorene] (**5**; 0.116 g, 0.161 mmol),²³ dicyandiamide (0.138 g, 1.64 mmol), and powdered KOH (0.100 g, 1.78 mmol) in 2-methoxyethanol (35 mL) was heated at reflux overnight. The mixture was then cooled to 25 °C, and water (50 mL) was added to induce precipitation. The resulting solid was separated by filtration and washed thoroughly with hot water and hot methanol to give extended para-substituted spirobifluorene **2** (0.103 g, 0.0974 mmol, 60%) as a yellow solid. A sample of analytical purity was obtained by crystallization from DMSO/acetone: mp >300 °C; IR (KBr) 3326, 3197, 1606, 1539, 1385, 801 cm⁻¹; ¹H NMR (400 MHz, DMSO-*d*₆, 100 °C) δ 8.23 (d, 8H, ³J = 8.5 Hz), 8.20 (d, 4H, ³J = 8.1 Hz), 7.85 (dd, 4H, ³J = 8.1 Hz, ⁴J = 1.5 Hz), 7.56 (d, 8H, ³J = 8.5 Hz), 7.06 (d, 4H, ³J = 1.5 Hz), 6.23 (bs, 16H); ¹³C NMR (75.4 MHz, DMSO-*d*₆, 25 °C) δ 65.7, 120.7, 125.5, 126.6, 127.8, 135.7, 139.2, 140.2, 141.6, 148.9, 167.0, 169.6; MS (FAB, 3-nitrobenzyl alcohol) *m/e* 1057. Anal. Calcd for C₆₁H₄₄N₂₀ • 1 DMSO: C, 66.65; H, 4.44; N, 24.68. Found: C, 67.17; H, 4.14; N, 24.35.

Extended Meta-Substituted Spirobifluorene 3. A mixture of 2,2',7,7'-tetrakis(3-cyanophenyl)-9,9'-spirobi[9H-fluorene] (**6**; 0.184 g, 0.255 mmol),²³ dicyandiamide (0.183 g, 2.18 mmol), and powdered KOH (0.140 g, 2.50 mmol) in 2-methoxyethanol (40 mL) was heated at reflux overnight. The mixture was then cooled to 25 °C, and water (50 mL) was added to induce precipitation. The resulting solid was separated by filtration and washed thoroughly with hot water and hot methanol to give extended meta-substituted spirobifluorene **3** (0.190 g, 0.180 mmol, 71%) as a beige solid. A sample of analytical purity was obtained by crystallization from DMSO/CH₃OH: mp >300 °C; IR (KBr) 3469, 3325, 3193, 1606, 1542, 1384, 1246, 827, 799 cm⁻¹; ¹H NMR (400 MHz, DMSO-*d*₆, 25 °C) δ 8.30 (s, 4H), 8.26 (d, 4H, ³J = 8.0 Hz), 8.13 (d, 4H, ³J = 7.8 Hz), 7.82 (d, 4H, ³J = 8.0 Hz), 7.60 (d, 4H, ³J = 7.8 Hz), 7.42 (t, 4H, ³J = 7.8 Hz), 6.98 (s, 4H), 6.76 (bs, 16H); ¹³C NMR (75.4 MHz, DMSO-*d*₆, 25 °C) δ 66.8, 122.2, 122.7, 126.3, 127.8, 128.2, 129.7,

130.5, 138.7, 140.4, 140.9, 141.4, 150.2, 168.2, 170.9; MS (FAB, 3-nitrobenzyl alcohol) *m/e* 1057. Anal. Calcd for C₆₁H₄₄N₂₀ • 1.5 DMSO: C, 65.46; H, 4.55; N, 23.85. Found: C, 65.24; H, 4.14; N, 24.36.

X-ray Crystallographic Studies. X-ray diffraction data were collected with Cu K α radiation using Bruker SMART 2K and 4K CCD diffractometers. The structures were solved by direct methods using SIR2000²⁷ and refined with SHELXH, which is part of the SHELXL suite of programs.²⁸ All non-hydrogen atoms of tectons **2-3** were refined anisotropically, whereas those of the located guests were refined with isotropic thermal parameters. Hydrogen atoms were placed in ideal positions and refined as riding atoms. In the structures of both tectons **2-3**, only part of the guests could be located, and the contribution of the remaining unresolved guests was treated using the procedure SQUEEZE implemented in PLATON.¹⁹ Further description of the solution and refinement of the structures is provided in the Supporting Information.

Structure of Extended Para-Substituted Spirobifluorene **2.** Crystals of tecton **2** grown from DMSO/acetone proved to belong to the triclinic space group P1 with $a = 13.458(2)$ Å, $b = 17.788(2)$ Å, $c = 20.721(3)$ Å, $\alpha = 81.076(8)^\circ$, $\beta = 74.960(8)^\circ$, $\gamma = 70.755(8)^\circ$, $V = 4509.6(11)$ Å³, $D_{\text{calcd}} = 1.201$ g/cm³, and $Z = 1$ at 100 K. Full-matrix least-squares refinements on F^2 of 1731 parameters using 729 restraints led to final residuals $R_1 = 0.0957$ and $wR_2 = 0.2236$ for 15187 observed reflections with $I > 2\sigma(I)$.

Structure of Extended Meta-Substituted Spirobifluorene **3.** Tecton **3** crystallized from DMSO/CH₃OH in the triclinic space group P-1 with $a = 12.2162(10)$ Å, $b = 21.2975(17)$ Å, $c = 30.884(2)$ Å, $\alpha = 93.026(3)^\circ$, $\beta = 94.690(4)^\circ$, $\gamma = 96.419(3)^\circ$, $V = 7942.6(10)$ Å³, $D_{\text{calcd}} = 1.081$ g/cm³, and $Z = 2$ at 223 K. Full-matrix least-squares refinements on F^2 of 1533 parameters using 147 restraints led to final residuals $R_1 = 0.0929$ and $wR_2 = 0.2332$ for 8975 observed reflections with $I > 2\sigma(I)$.

Acknowledgment. We are grateful to the Natural Sciences and Engineering Research Council of Canada, the Ministère de l'Éducation du Québec, the Canada Foundation for Innovation, the Canada Research Chairs Program, and Merck Frosst for financial support. In addition, we thank Prof. Jurgen Sygusch for providing access to a Bruker SMART 6000 CCD diffractometer equipped with a rotating anode.

Supplementary Material Available: ORTEP drawings and tables of crystallographic data, atomic coordinates, anisotropic thermal parameters, and bond lengths and angles for tectons 2-3. This material is available free of charge via the Internet at <http://pubs.acs.org>.

Notes and References

1. Fellow of the Ministère de l'Éducation du Québec, 2002-2004. Fellow of the Natural Sciences and Engineering Research Council of Canada, 2000-2002.
2. For recent reviews, see: Stein, A. *Adv. Mater.* **2003**, *15*, 763. Schüth, F.; Schmidt, W. *Adv. Mater.* **2002**, *14*, 629. Soler-Illia, G. J. d. A. A.; Sanchez, C.; Lebeau, B.; Patarin, J. *Chem. Rev.* **2002**, *102*, 4093.
3. For representative recent references, see: Janiak, C. *J. Chem. Soc., Dalton Trans.* **2003**, 2781. Spange, S. *Angew. Chem., Int. Ed.* **2003**, *42*, 4430. Yang, H.; Shi, Q.; Tian, B.; Lu, Q.; Gao, F.; Xie, S.; Fan, J.; Yu, C.; Tu, B.; Zhao, D. *J. Am. Chem. Soc.* **2003**, *125*, 4724. Davis, M. E. *Nature* **2002**, *417*, 813. De Vos, D. E.; Dams, M.; Sels, B. F.; Jacobs, P. A. *Chem. Rev.* **2002**, *102*, 3615. Corma, A. *Chem. Rev.* **1997**, *97*, 2373.
4. Breck, D. W. *Zeolite Molecular Sieves*; Wiley-Interscience: New York, 1974.
5. For recent reviews, see: Kickelbick, G. *Angew. Chem., Int. Ed.* **2004**, *43*, 3102. Yaghi, O. M.; O'Keeffe, M.; Ockwig, N. W.; Chae, H. K.; Eddaoudi, M.; Kim, J. *Nature* **2003**, *423*, 705. James, S. L. *Chem. Soc. Rev.* **2003**, *32*, 276. Papaefstathiou, G. S.; MacGillivray, L. R. *Coord. Chem. Rev.* **2003**, *246*, 169. Robson, R. *J. Chem. Soc., Dalton Trans.* **2000**, 3735.
6. Moulton, B.; Zaworotko, M. *J. Chem. Rev.* **2001**, *101*, 1629.
7. Nangia, A. *Curr. Opin. Solid State Mater. Sci.* **2001**, *5*, 115. Langley, P. J.; Hulliger, J. *Chem. Soc. Rev.* **1999**, *28*, 279.
8. Fournier, J.-H.; Maris, T.; Wuest, J. D. *J. Org. Chem.* **2004**, *69*, 1762.
9. Saied, O.; Maris, T.; Wuest, J. D. *J. Am. Chem. Soc.* **2003**, *125*, 14956.
10. Simard, M.; Su, D.; Wuest, J. D. *J. Am. Chem. Soc.* **1991**, *113*, 4696.
11. For recent related work, see: Laliberté, D.; Maris, T.; Wuest, J. D. *J. Org. Chem.* **2004**, *69*, 1776. Laliberté, D.; Maris, T.; Wuest, J. D. *Can. J. Chem.* **2004**, *82*, 386. Le Fur, E.; Demers, E.; Maris, T.; Wuest, J. D. *Chem. Commun.* **2003**, 2966. Laliberté, D.; Maris, T.; Sirois, A.; Wuest, J. D. *Org. Lett.* **2003**, *5*, 4787. Sauriat-Dorizon, H.; Maris, T.; Wuest, J. D.; Enright, G. D. *J. Org. Chem.* **2003**, *68*, 240. Brunet, P.; Demers, E.;

- Maris, T.; Enright, G. D.; Wuest, J. D. *Angew. Chem., Int. Ed.* **2003**, *42*, 5303.
- Fournier, J.-H.; Maris, T.; Simard, M.; Wuest, J. D. *Cryst. Growth Des.* **2003**, *3*, 535.
12. Fournier, J.-H.; Maris, T.; Wuest, J. D.; Guo, W.; Galoppini, E. *J. Am. Chem. Soc.* **2003**, *125*, 1002.
13. Brunet, P.; Simard, M.; Wuest, J. D. *J. Am. Chem. Soc.* **1997**, *119*, 2737.
14. For other recent related work, see: Uemura, K.; Kitagawa, S.; Fukui, K.; Saito, K. *J. Am. Chem. Soc.* **2004**, *126*, 3817. Sada, K.; Inoue, K.; Tanaka, T.; Tanaka, A.; Epergyes, A.; Nagahama, S.; Matsumoto, A.; Miyata, M. *J. Am. Chem. Soc.* **2004**, *126*, 1764. Maspoch, D.; Domingo, N.; Ruiz-Molina, D.; Wurst, K.; Tejada, J.; Rovira, C.; Veciana, J. *J. Am. Chem. Soc.* **2004**, *126*, 730. Baudron, S. A.; Avarvari, N.; Canadell, E.; Auban-Senzier, P.; Batail, P. *Chem. Eur. J.* **2004**, *10*, 4498. Angeloni, A.; Crawford, P. C.; Orpen, A. G.; Podesta, T. J.; Shore, B. J. *Chem. Eur. J.* **2004**, *10*, 3783. Murata, T.; Morita, Y.; Fukui, K.; Sato, K.; Shiomi, D.; Takui, T.; Maesato, M.; Yamochi, H.; Saito, G.; Nakasaji, K. *Angew. Chem., Int. Ed.* **2004**, *43*, 6343. Soldatov, D. V.; Moudrakovski, I. L.; Ripmeester, J. A. *Angew. Chem., Int. Ed.* **2004**, *43*, 6308. Du, Y.; Creighton, C. J.; Toung, B. A.; Reitz, A. B. *Org. Lett.* **2004**, *6*, 309. Bhogala, B. R.; Vangala, V. R.; Smith, P. S.; Howard, J. A. K.; Desiraju, G. R. *Cryst. Growth Des.* **2004**, *4*, 647. Balasubramaniam, V.; Wong, L. G. J.; Vittal, J. J.; Valiyaveettill, S. *Cryst. Growth Des.* **2004**, *4*, 553. Dale, S. H.; Elsegood, M. R. J.; Coombs, A. E. L. *CrystEngComm* **2004**, *6*, 328. Hosseini, M. W. *CrystEngComm* **2004**, *6*, 318. Vinodu, M.; Goldberg, I. *CrystEngComm* **2004**, *6*, 215. Aakeröy, C. B.; Desper, J.; Helfrich, B. A. *CrystEngComm* **2004**, *6*, 19. Alshahateet, S. F.; Nakano, K.; Bishop, R.; Craig, D. C.; Harris, K. D. M.; Scudder, M. L. *CrystEngComm* **2004**, *6*, 5. Brown, R. J.; Camarasa, G.; Griffiths, J.-P.; Day, P.; Wallis, J. D. *Tetrahedron Lett.* **2004**, *45*, 5103. Pedireddi, V. R.; SeethaLekshmi, N. *Tetrahedron Lett.* **2004**, *45*, 1903. Martin, S. M.; Yonezawa, J.; Horner, M. J.; Macosko, C. W.; Ward, M. D. *Chem. Mater.* **2004**, *16*, 3045. Shimizu, L. S.; Hughes, A. D.; Smith, M. D.; Davis, M. J.; Zhang, B. P.; zur Loye, H.-C.; Shimizu, K. D. *J. Am. Chem. Soc.* **2003**, *125*, 14972. Ouyang, X.; Fowler, F. W.; Lauher, J. W. *J. Am. Chem. Soc.* **2003**, *125*, 12400. Kobayashi, K.; Sato, A.; Sakamoto, S.; Yamaguchi, K. *J. Am. Chem. Soc.* **2003**, *125*, 3035. Rakotondradany, F.;

- Whitehead, M. A.; Lebuis, A.-M.; Sleiman, H. F. *Chem. Eur. J.* **2003**, *9*, 4771. Jagadish, B.; Carducci, M. D.; Bosshard, C.; Günter, P.; Margolis, J. I.; Williams, L. J.; Mash, E. A. *Cryst. Growth Des.* **2003**, *3*, 811. Bhogala, B. R.; Nangia, A. *Cryst. Growth Des.* **2003**, *3*, 547. Olenik, B.; Smolka, T.; Boese, R.; Sustmann, R. *Cryst. Growth Des.* **2003**, *3*, 183. Kitamura, M.; Nakano, K. *Cryst. Growth Des.* **2003**, *3*, 25. Ma, B.-Q.; Coppens, P. *Chem. Commun.* **2003**, 2290. Yagai, S.; Karatsu, T.; Kitamura, A. *Chem. Commun.* **2003**, 1844. Walsh, R. D. B.; Bradner, M. W.; Fleischman, S.; Morales, L. A.; Moulton, B.; Rodríguez-Hornedo, R.; Zaworotko, M. J. *Chem. Commun.* **2003**, 186. Blay, G.; Fernández, I.; Pedro, J. R.; Ruiz-García, R.; Muñoz, M. C.; Cano, J.; Carrasco, R. *Eur. J. Org. Chem.* **2003**, 1627. Braga, D.; Polito, M.; Bracaccini, M.; D'Addario, D.; Tagliavini, E.; Sturba, L. *Organometallics* **2003**, *22*, 2142. Roesky, H. W.; Andruh, M. *Coord. Chem. Rev.* **2003**, *236*, 91. Ermer, O.; Kusch, A.; Röbke, C. *Helv. Chim. Acta* **2003**, *86*, 922. Arora, K. K.; Pedireddi, V. R. *J. Org. Chem.* **2003**, *68*, 9177. Wen, J.-F.; Hong, W.; Yuan, K.; Mak, T. C. W.; Wong, H. N. C. *J. Org. Chem.* **2003**, *68*, 8918. Moon, K.; Chen, W.-Z.; Ren, T.; Kaifer, A. E. *CrystEngComm* **2003**, *5*, 451. Trivedi, D. R.; Ballabh, A.; Dastidar, P. *CrystEngComm* **2003**, *5*, 358. Burke, N. J.; Burrows, A. D.; Mahon, M. F.; Pritchard, L. S. *CrystEngComm* **2003**, *5*, 355. Pérez, C.; Rodríguez, M. L.; Foces-Foces, C.; Pérez-Hernández, N.; Pérez, R.; Martín, J. D. *Org. Lett.* **2003**, *5*, 641. Shan, N.; Bond, A. D.; Jones, W. *New J. Chem.* **2003**, *27*, 365. Kobayashi, N.; Naito, T.; Inabe, T. *Bull. Chem. Soc. Jpn.* **2003**, *76*, 1351. Görbitz, C. H. *Acta Crystallogr.* **2002**, *B58*, 849. Tanaka, T.; Tasaki, T.; Aoyama, Y. *J. Am. Chem. Soc.* **2002**, *124*, 12453. Moorthy, J. N.; Natarajan, R.; Mal, P.; Venugopalan, P. *J. Am. Chem. Soc.* **2002**, *124*, 6530. Archer, E. A.; Krische, M. J. *J. Am. Chem. Soc.* **2002**, *124*, 5074. Kim, S.; Bishop, R.; Craig, D. C.; Dance, I. G.; Scudder, M. L. *J. Org. Chem.* **2002**, *67*, 3221. Lyssenko, K. A.; Lenev, D. A.; Kostyanovsky, R. G. *Tetrahedron* **2002**, *58*, 8525. Beatty, A. M.; Schneider, C. M.; Simpson, A. E.; Zaher, J. L. *CrystEngComm* **2002**, *4*, 282. Field, J. E.; Combariza, M. Y.; Vachet, R. W.; Venkataraman, D. *Chem. Commun.*, **2002**, 2260. Gauthier, D.; Baillargeon, P.; Drouin, M.; Dory, Y. L. *Angew. Chem., Int. Ed.* **2001**, *40*, 4635. Hong, B. H.; Lee, J. Y.; Lee, C.-W.; Kim, J. C.; Bae, S. C.; Kim, K. S. *J. Am.*

- Chem. Soc.* **2001**, *123*, 10748. Papaefstathiou, G. S.; MacGillivray, L. R. *Org. Lett.* **2001**, *3*, 3835. Zaman, M. B.; Tomura, M.; Yamashita, Y. *J. Org. Chem.* **2001**, *66*, 5987. Dapporto, P.; Paoli, P.; Roelens, S. *J. Org. Chem.* **2001**, *66*, 4930. Vaid, T. P.; Sydora, O. L.; Douthwaite, R. E.; Wolczanski, P. T.; Lobkovsky, E. B. *Chem. Commun.* **2001**, 1300. Sharma, C. V. K.; Clearfield, A. *J. Am. Chem. Soc.* **2000**, *122*, 4394. Corbin, P. S.; Zimmerman, S. C. *J. Am. Chem. Soc.* **2000**, *122*, 3779. Cantrill, S. J.; Pease, A. R.; Stoddart, J. F. *J. Chem. Soc., Dalton Trans.* **2000**, 3715. Videnova-Adrabińska, V.; Janeczko, E. *J. Mater. Chem.* **2000**, *10*, 555. Akazome, M.; Suzuki, S.; Shimizu, Y.; Henmi, K.; Ogura, K. *J. Org. Chem.* **2000**, *65*, 6917. Baumeister, B.; Matile, S. *Chem. Commun.* **2000**, 913. Chowdhry, M. M.; Mingos, D. M. P.; White, A. J. P.; Williams, D. J. *J. Chem. Soc., Perkin Trans. 1* **2000**, 3495. Gong, B.; Zheng, C.; Skrzypczak-Jankun, E.; Zhu, J. *J. Org. Lett.* **2000**, *2*, 3273. Krische, M. J.; Lehn, J.-M.; Kyritsakas, N.; Fischer, J.; Wegelius, E. K.; Rissanen, K. *Tetrahedron* **2000**, *56*, 6701. Fuchs, K.; Bauer, T.; Thomann, R.; Wang, C.; Friedrich, C.; Mülhaupt, R. *Macromolecules* **1999**, *32*, 8404. Holý, P.; Závada, J.; Císařová, I.; Podlaha, J. *Angew. Chem., Int. Ed.* **1999**, *38*, 381. Karle, I. L.; Ranganathan, D.; Kurur, S. *J. Am. Chem. Soc.* **1999**, *121*, 7156. Chin, D. N.; Palmore, G. T. R.; Whitesides, G. M. *J. Am. Chem. Soc.* **1999**, *121*, 2115. Hanessian, S.; Saladino, R.; Margarita, R.; Simard, M. *Chem. Eur. J.* **1999**, *5*, 2169.
15. For recent reviews of hydrogen bonding, see: Steiner, T. *Angew. Chem., Int. Ed.* **2002**, *41*, 48. Prins, L. J.; Reinhoudt, D. N.; Timmerman, P. *Angew. Chem., Int. Ed.* **2001**, *40*, 2382.
16. Aujard, I.; Baltaze, J.-P.; Baudin, J.-B.; Cogné, E.; Ferrage, F.; Jullien, L.; Perez, É.; Prévost, V.; Qian, L. M.; Ruel, O. *J. Am. Chem. Soc.* **2001**, *123*, 8177. Wang, S.; Oldham, W. J., Jr.; Hudack, R. A., Jr.; Bazan, G. C. *J. Am. Chem. Soc.* **2000**, *122*, 5695. Yao, Y.; Tour, J. M. *J. Org. Chem.* **1999**, *64*, 1968. Johansson, N.; Salbeck, J.; Bauer, J.; Weissörtel, F.; Bröms, P.; Andersson, A.; Salaneck, W. R. *Adv. Mater.* **1998**, *10*, 1136.
17. For discussions of interpenetration in networks, see: Batten, S. R. *CrystEngComm* **2001**, *18*, 1. Batten, S. R.; Robson, R. *Angew. Chem., Int. Ed.* **1998**, *37*, 1460.

18. The percentage of volume accessible to guests was estimated by the PLATON program.¹⁹ PLATON calculates the accessible volume by allowing a spherical probe of variable radius to roll over the van der Waals surface of the network. PLATON uses a default value of 1.20 Å for the radius of the probe, which is an appropriate model for small guests such as water. The van der Waals radii used to define surfaces for these calculations are as follows: C: 1.70 Å, H: 1.20 Å, and N: 1.55 Å. If V is the volume of the unit cell and V_g is the guest-accessible volume as calculated by PLATON, then the porosity P in % is given by $100V_g/V$.
19. Spek, A. L. *PLATON, A Multipurpose Crystallographic Tool*; Utrecht University: Utrecht, The Netherlands, 2001. van der Sluis, P.; Spek, A. L. *Acta Crystallogr.* **1990**, *A46*, 194.
20. The composition was estimated by X-ray crystallography and by ¹H NMR spectroscopy of dissolved samples.
21. For a review of diamondoid hydrogen-bonded networks, see: Zaworotko, M. J. *Chem. Soc. Rev.* **1994**, *23*, 283.
22. The dimensions of a channel in a particular direction correspond to those of an imaginary cylinder that could be passed through the hypothetical open network in the given direction in contact with the van der Waals surface. Such values are inherently conservative because 1) they measure the cross section at the most narrow constriction, and 2) they systematically underestimate the sizes of channels that are not uniform and linear.
23. Demers, E.; Maris, T.; Cabana, J.; Fournier, J-H.; Wuest, J. D., submitted for publication.
24. Simons, J. K.; Saxton, M. R. *Organic Syntheses*; Wiley: New York, 1963; Collect. Vol. IV, p 78.
25. Representations of channels were generated by the Cavities option in the program ATOMS (*ATOMS*, Version 5.1; Shape Software: 521 Hidden Valley Road, Kingsport, TN 37663; www.shapesoftware.com).

26. Su, D.; Wang, X.; Simard, M.; Wuest, J. D. *Supramolecular Chem.* **1995**, *6*, 171.
Wuest, J. D. In *Mesomolecules: From Molecules to Materials*; Mendenhall, G. D., Greenberg, A., Liebman, J. F.; Chapman & Hall: New York, 1995; p 107.
27. Burla, M. C.; Camalli, M.; Carrozzini, B.; Cascarano, G. L.; Giacovazzo, C.; Polidori, G.; Spagna, R. *Acta Crystallogr.* **2000**, *A56*, 451.
28. Sheldrick, G. M. *SHELXS-97, Program for the Solution of Crystal Structures* and *SHELXL-97, Program for the Refinement of Crystal Structures*; Universität Göttingen: Germany, 1997.

Figure 1. Cyclic hydrogen-bonding motifs characteristic of aminotriazines.

Figure 2. Representation of the structure of crystals of simple spirobifluorene **4** grown from DMSO/dioxane, showing a tecton (white) surrounded by three of a total of six hydrogen-bonded neighboring tectons. The other three neighbors are equivalent by symmetry and are omitted for clarity, as are all guests. Hydrogen bonds appear as broken lines. Two of the six neighbors (one shown in green, with a second equivalent by symmetry and omitted) each form two hydrogen bonds with the central tecton (white), creating motifs of type **I**. Two other neighbors (blue) each form four hydrogen bonds with the central tecton, creating distorted motifs of type **II**, and the remaining two neighbors (red) each form two hydrogen bonds with the central tecton according to motif **III**.

Figure 3. View along the α axis of the network constructed from tecton **4** showing a $2 \times 3 \times 3$ array of unit cells. Guests are omitted, and atoms are shown as spheres of van der Waals radii in order to reveal the cross sections of the channels. Atoms of hydrogen appear in white, atoms of carbon in gray, and atoms of nitrogen in blue.

Figure 4. View of the structure of crystals of extended spirobifluorene **2** grown from DMSO/acetone, showing a central tecton (tecton **A**, white) and its five hydrogen-bonded neighbors. Guests are omitted for clarity, and hydrogen bonds are represented by broken lines. Two of the neighbors (red) are each linked to tecton **A** (white) by two hydrogen bonds of type **III**, two others (blue) each form four hydrogen bonds with tecton **A** according to motif **II**, and the remaining neighbor (tecton **B**, dark gray) forms a single distorted hydrogen bond. Tecton **A** (white) and its four multiply hydrogen-bonded neighbors (red and blue) are all equivalent by symmetry, and together they define a square-planar network. Tectons **A** (white) and **B** (dark gray) are symmetry-independent.

Figure 5. View of the structure of crystals of extended spirobifluorene **2** grown from DMSO/acetone, showing a central tecton (tecton **B**, dark gray) and its five hydrogen-bonded neighbors. Guests are omitted for clarity, and hydrogen bonds are represented by broken lines. Two of the neighbors (red) are each linked to tecton **B** (dark gray) by two hydrogen bonds of type **III**, two others (blue) each form three hydrogen bonds with tecton **B** (two according to motif **II**), and the remaining neighbor (tecton **A**, white) forms a single hydrogen bond. Tecton **B** (dark gray) and its four multiply hydrogen-bonded neighbors (red and blue) are all equivalent by symmetry, and together they define a square-planar network. Tectons **A** (white) and **B** (dark gray) are symmetry-independent.

Figure 6. Representation of the network formed by crystallizing extended spirobifluorene **2** from DMSO/acetone. Each sheet composed uniquely of tecton **A** (white) is paired with one sheet built uniquely from tecton **B** (dark gray) to form a bilayer held together by single hydrogen bonds between neighboring tectons **A** and **B** in the two adjacent layers (Figures 4-5). In this representation, solid lines correspond to hydrogen bonds of types **II-III** between tectons **A** (white) or **B** (dark gray), and the intersections show the position of the central spirocyclic carbon atom of each tecton.

Figure 7. View along the α axis of the network constructed from extended spirobifluorene **2** showing a $4 \times 4 \times 4$ array of unit cells. Guests are omitted, and atoms are shown as spheres of van der Waals radii in order to reveal the cross sections of the channels. Atoms of hydrogen appear in white, atoms of carbon in gray, and atoms of nitrogen in blue.

Figure 8. Stereoscopic representation of interconnected channels within the network constructed from extended spirobifluorene **2**. The image shows a $3 \times 3 \times 2$ array of unit cells viewed along the α axis. The outsides of the channels appear in light gray, and dark gray is used to show where the channels are cut by the boundaries of the array. The surface of the channels is defined by the possible loci of the center of a sphere of diameter 3.0 Å as it rolls over the surface of the ordered network.²⁵

Figure 9. Representation of the interactions between symmetry-independent molecules **C** (white) and **D** (black) in the structure of crystals of extended spirobifluorene **3** grown from DMSO/CH₃OH. a) Four distorted hydrogen bonds of type **III**. b) Aromatic interactions.

Figure 10. View of the structure of crystals of extended spirobifluorene **3** grown from DMSO/CH₃OH, showing symmetry-independent tectons **C** (white) and **D** (dark gray) and the five neighbors (blue) that form hydrogen bonds according to motifs I-II. Guests are omitted for clarity, and hydrogen bonds are represented by broken lines.

Figure 11. View of the structure of crystals of extended spirobifluorene **3** grown from DMSO/CH₃OH, showing symmetry-independent tectons **C** (white) and **D** (dark gray) and the five neighbors (red) that form distorted single hydrogen bonds. Guests are omitted for clarity, and hydrogen bonds are represented by broken lines.

Figure 12. View along the α axis of the network constructed from extended spirobifluorene **3** showing a $4 \times 4 \times 4$ array of unit cells. Guests are omitted, and atoms are shown as spheres of van der Waals radii in order to reveal the cross sections of the channels. Atoms of hydrogen appear in white, atoms of carbon in gray, and atoms of nitrogen in blue.

Figure 13. Stereoscopic representation of interconnected channels within the network constructed from extended spirobifluorene **3**. The image shows a $3 \times 2 \times 2$ array of unit cells viewed along the α axis. The outsides of the channels appear in light gray, and dark gray is used to show where the channels are cut by the boundaries of the array. The surface of the channels is defined by the possible loci of the center of a sphere of diameter 3 Å as it rolls over the surface of the ordered network.²⁵

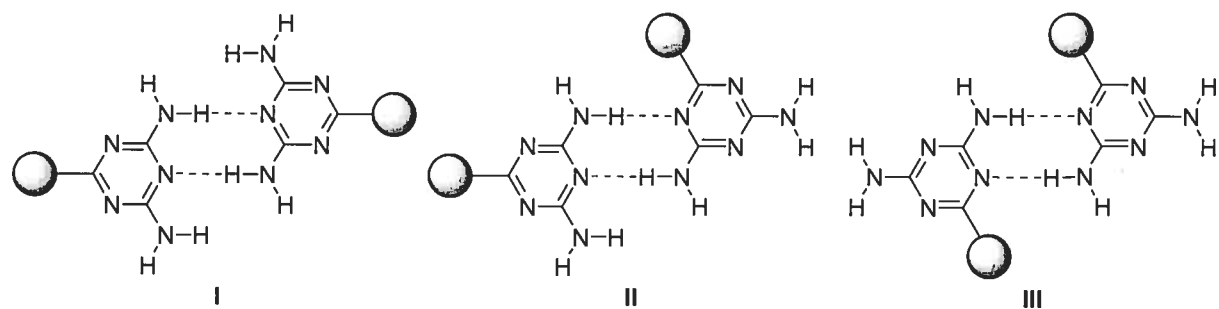


Figure 1. Cyclic hydrogen-bonding motifs characteristic of aminotriazines.

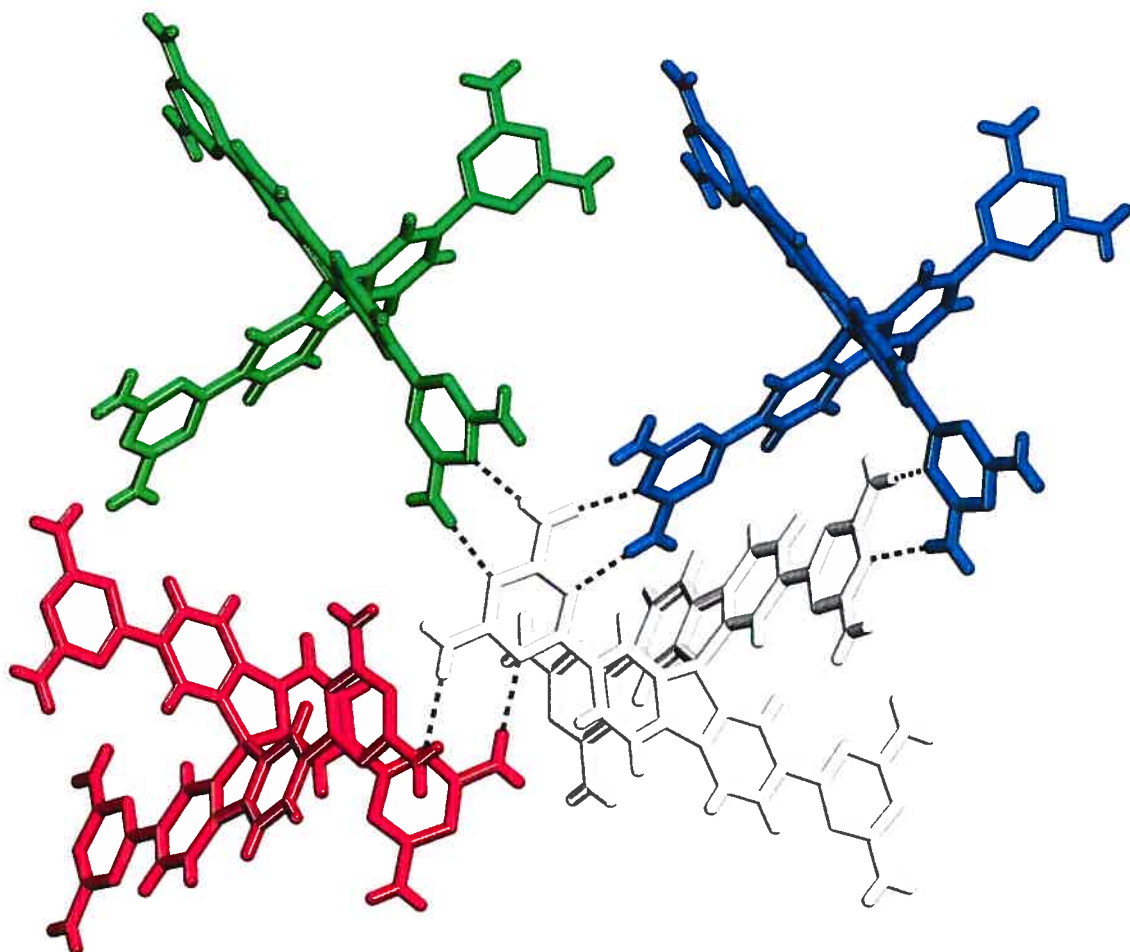


Figure 2. Representation of the structure of crystals of simple spirobifluorene **4** grown from DMSO/dioxane, showing a tecton (white) surrounded by three of a total of six hydrogen-bonded neighboring tectons. The other three neighbors are equivalent by symmetry and are omitted for clarity, as are all guests. Hydrogen bonds appear as broken lines. Two of the six neighbors (one shown in green, with a second equivalent by symmetry and omitted) each form two hydrogen bonds with the central tecton (white), creating motifs of type **I**. Two other neighbors (blue) each form four hydrogen bonds with the central tecton, creating distorted motifs of type **II**, and the remaining two neighbors (red) each form two hydrogen bonds with the central tecton according to motif **III**.

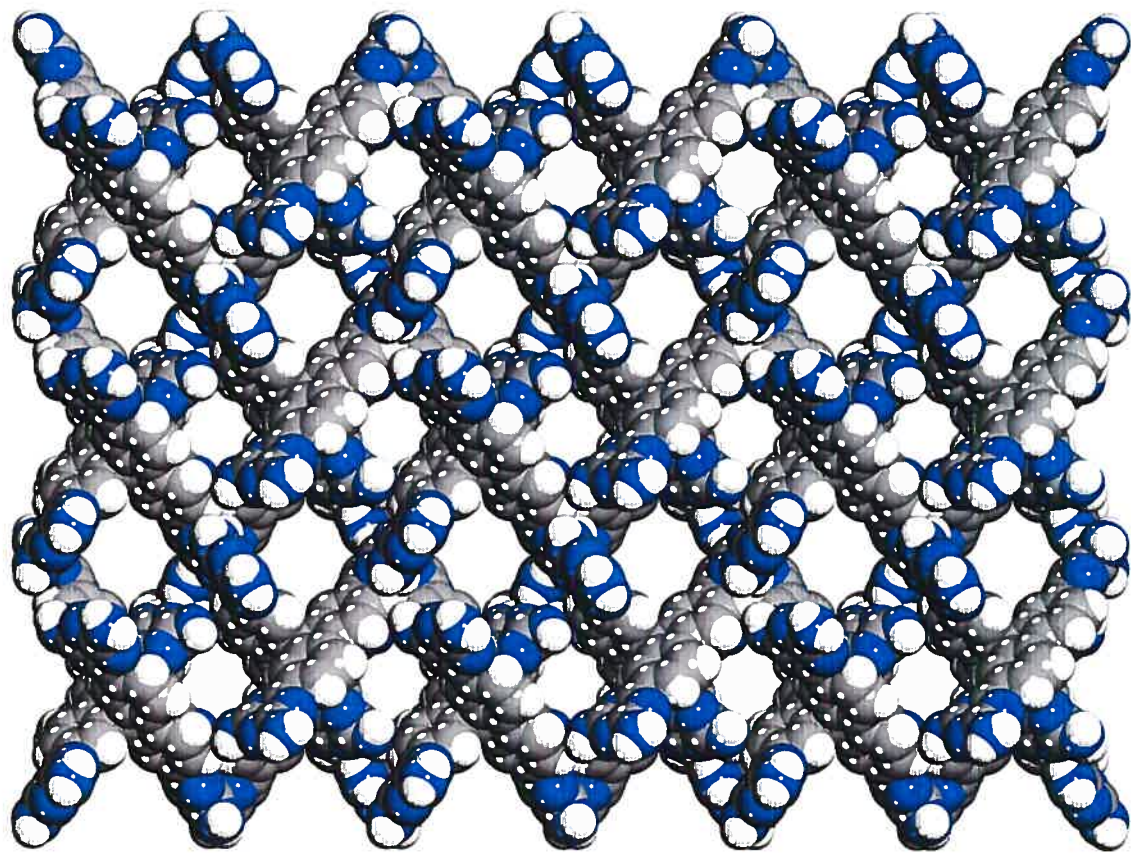


Figure 3. View along the a axis of the network constructed from tecton 4 showing a 2×3 $\times 3$ array of unit cells. Guests are omitted, and atoms are shown as spheres of van der Waals radii in order to reveal the cross sections of the channels. Atoms of hydrogen appear in white, atoms of carbon in gray, and atoms of nitrogen in blue.

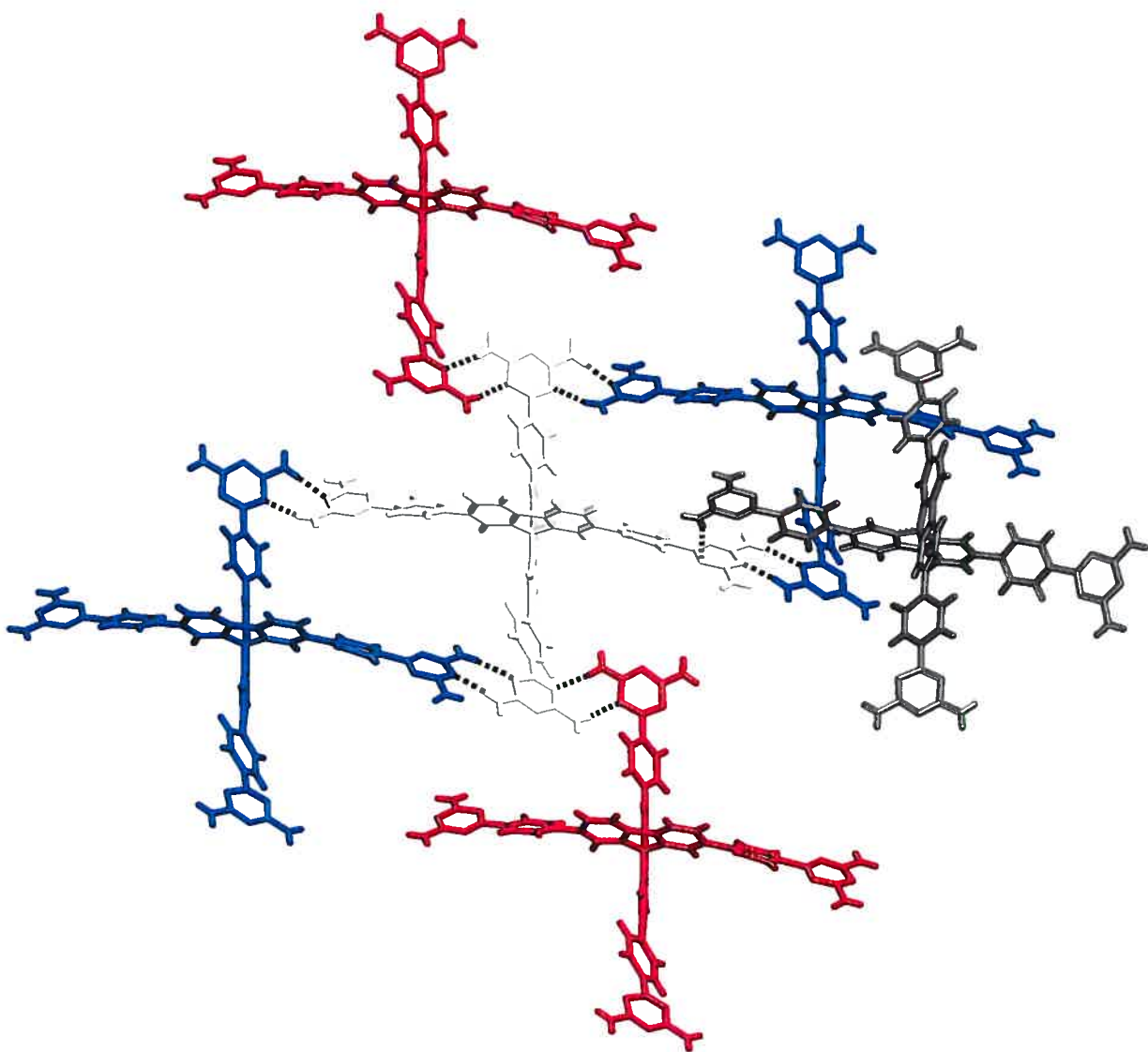


Figure 4. View of the structure of crystals of extended spirobifluorene **2** grown from DMSO/acetone, showing a central tecton (tecton **A**, white) and its five hydrogen-bonded neighbors. Guests are omitted for clarity, and hydrogen bonds are represented by broken lines. Two of the neighbors (red) are each linked to tecton **A** (white) by two hydrogen bonds of type **III**, two others (blue) each form four hydrogen bonds with tecton **A** according to motif **II**, and the remaining neighbor (tecton **B**, dark gray) forms a single distorted hydrogen bond. Tectons **A** (white) and its four multiply hydrogen-bonded neighbors (red and blue) are all equivalent by symmetry, and together they define a square-planar network. Tectons **A** (white) and **B** (dark gray) are symmetry-independent.

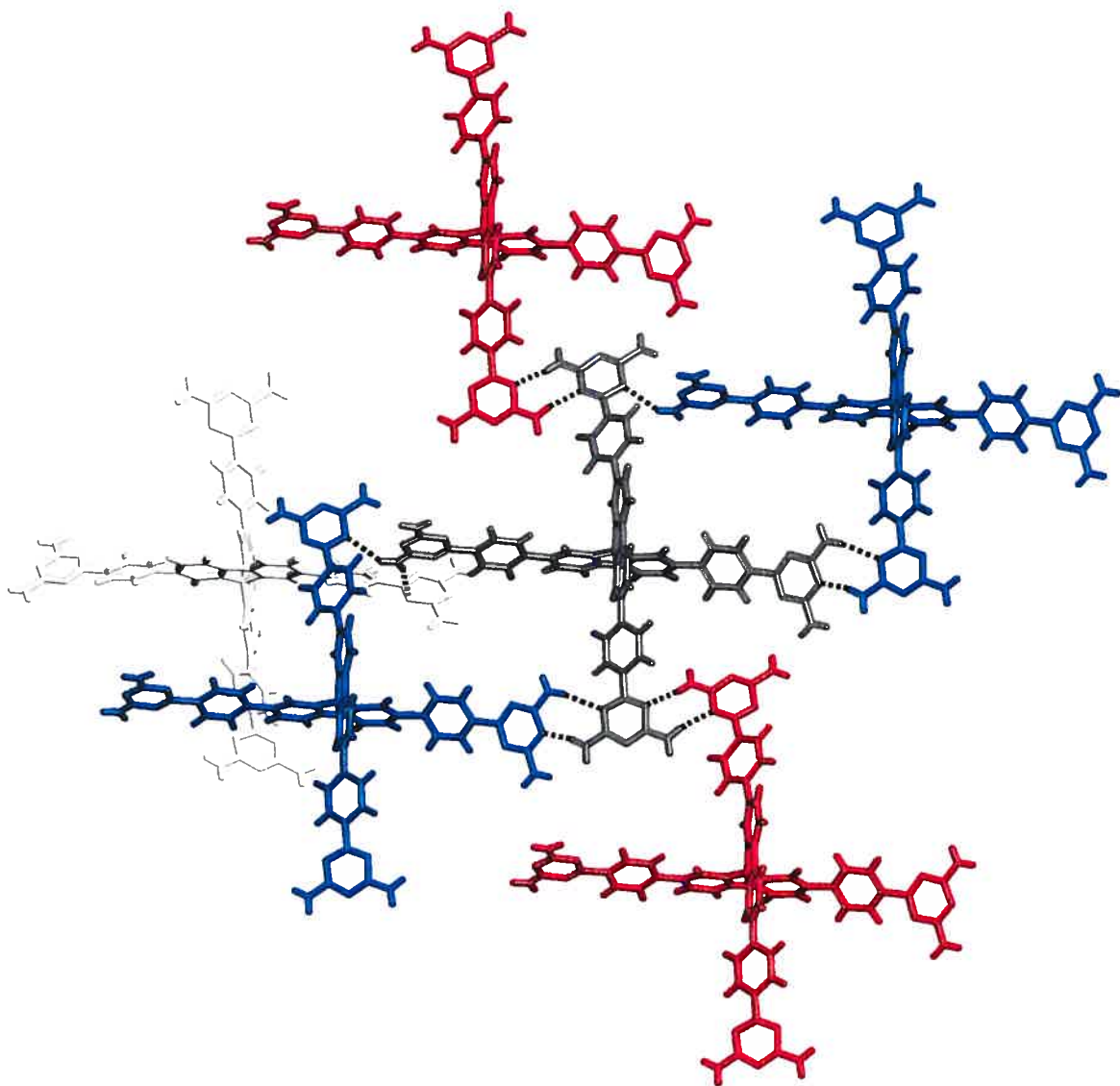


Figure 5. View of the structure of crystals of extended spirobifluorene **2** grown from DMSO/acetone, showing a central tecton (**tector B**, dark gray) and its five hydrogen-bonded neighbors. Guests are omitted for clarity, and hydrogen bonds are represented by broken lines. Two of the neighbors (red) are each linked to tector **B** (dark gray) by two hydrogen bonds of type **III**, two others (blue) each form three hydrogen bonds with tector **B** (two according to motif **II**), and the remaining neighbor (tector **A**, white) forms a single hydrogen bond. Tectors **B** (dark gray) and its four multiply hydrogen-bonded neighbors (red and blue) are all equivalent by symmetry, and together they define a square-planar network. Tectors **A** (white) and **B** (dark gray) are symmetry-independent.

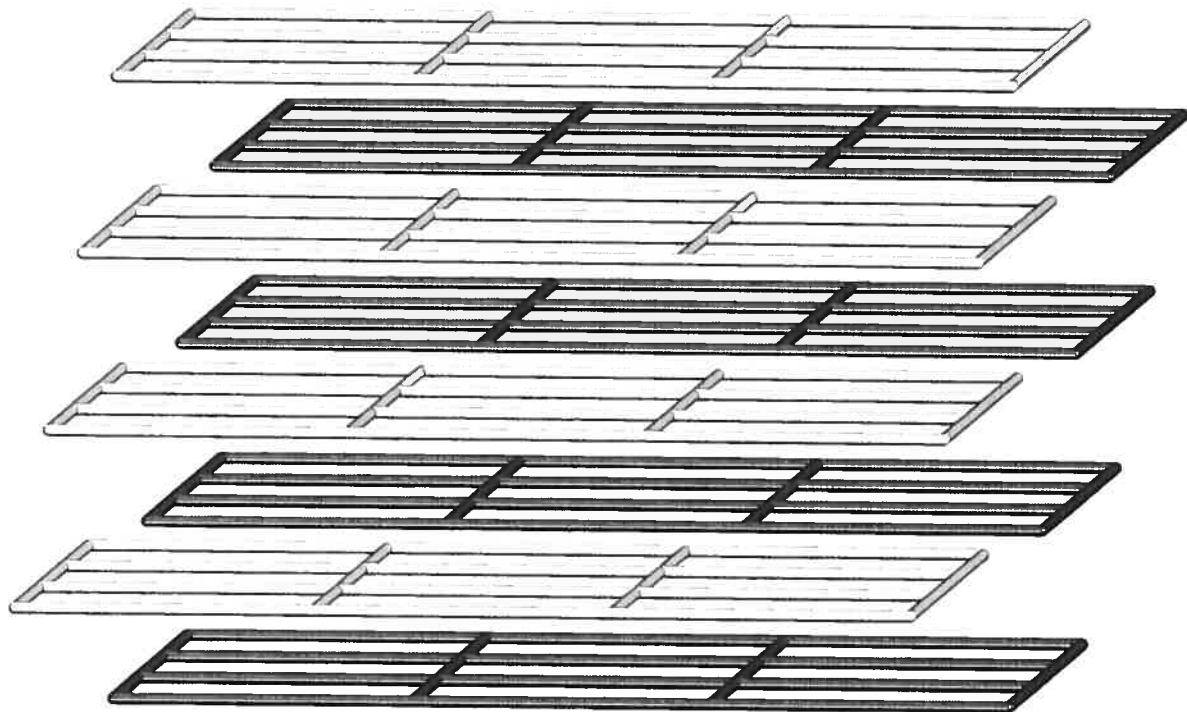


Figure 6. Representation of the network formed by crystallizing extended spirobifluorene **2** from DMSO/acetone. Each sheet composed uniquely of tecton **A** (white) is paired with one sheet built uniquely from tecton **B** (dark gray) to form a bilayer held together by single hydrogen bonds between neighboring tectons **A** and **B** in the two adjacent layers (Figures 4-5). In this representation, solid lines correspond to hydrogen bonds of types **II-III** between tectons **A** (white) or **B** (dark gray), and the intersections show the position of the central spirocyclic carbon atom of each tecton.

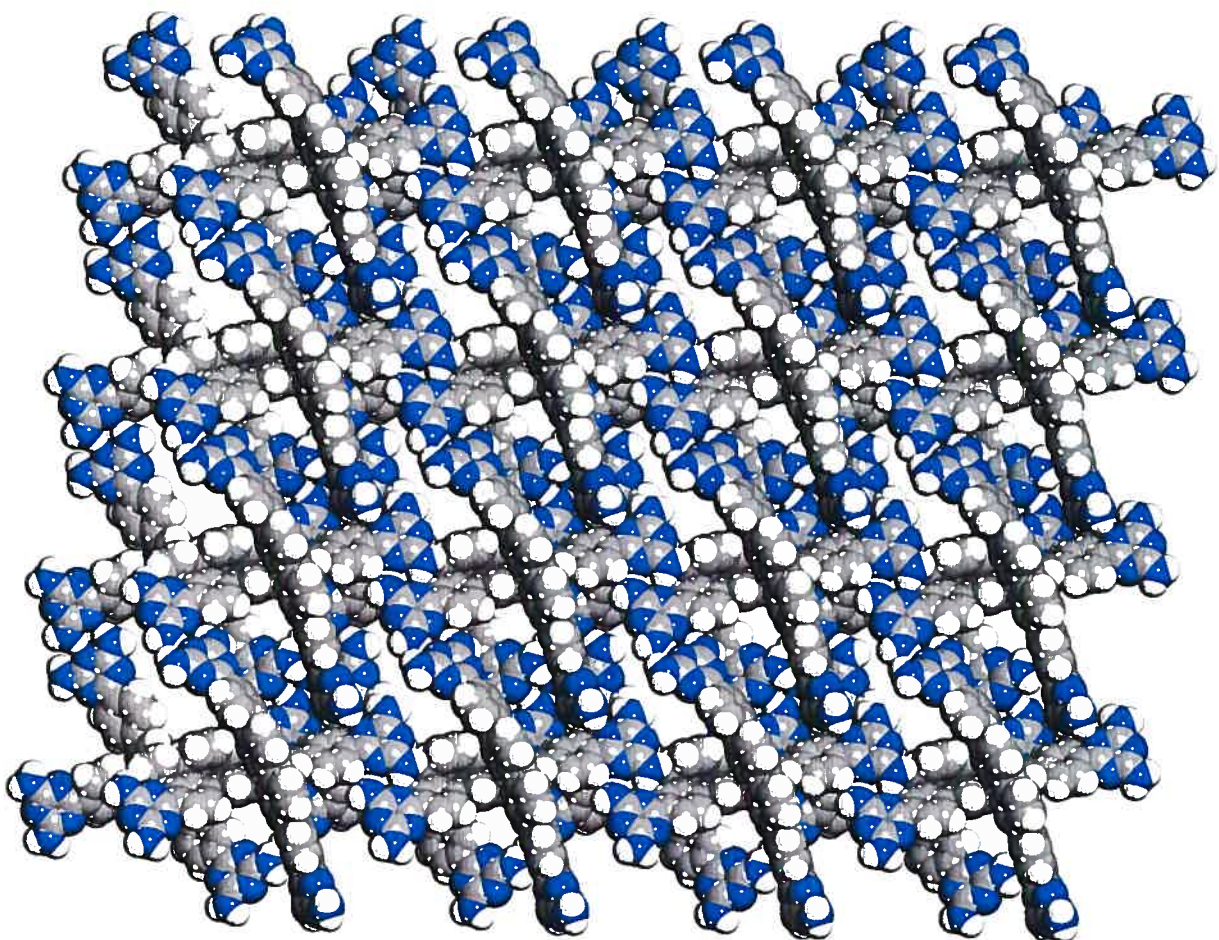


Figure 7. View along the α axis of the network constructed from extended spirobifluorene 2 showing a $4 \times 4 \times 4$ array of unit cells. Guests are omitted, and atoms are shown as spheres of van der Waals radii in order to reveal the cross sections of the channels. Atoms of hydrogen appear in white, atoms of carbon in gray, and atoms of nitrogen in blue.

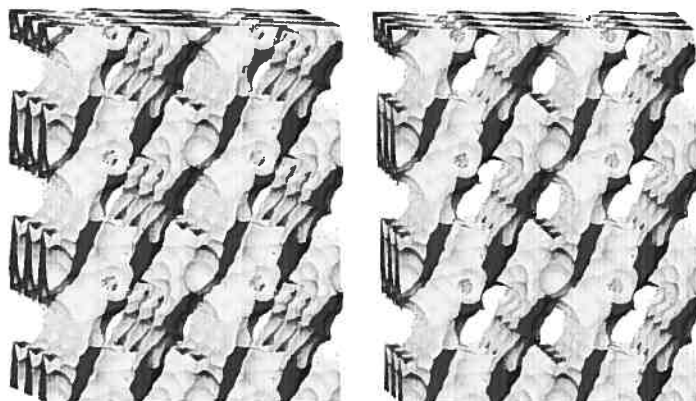
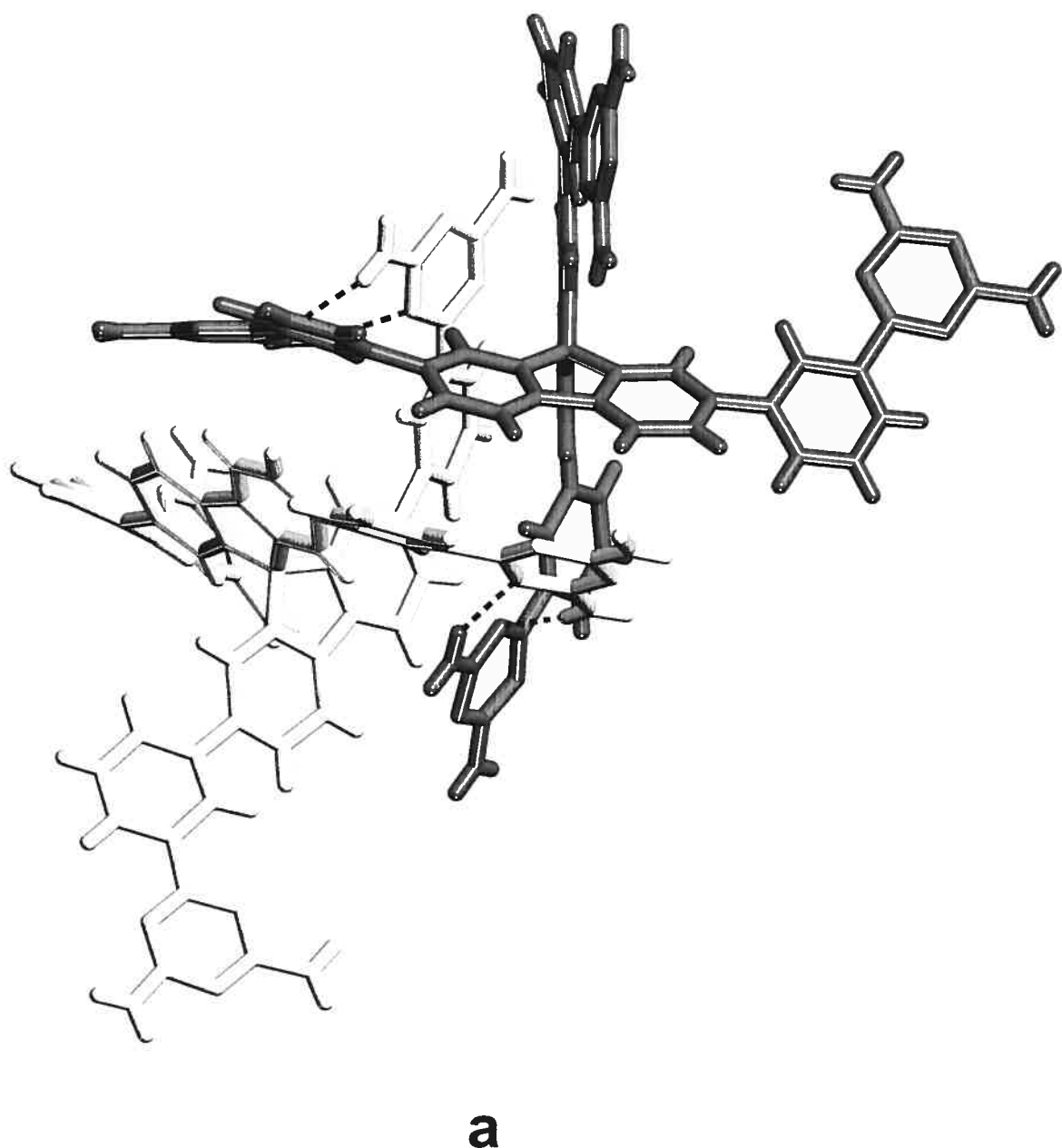


Figure 8. Stereoscopic representation of interconnected channels within the network constructed from extended spirobifluorene **2**. The image shows a $3 \times 3 \times 2$ array of unit cells viewed along the *a* axis. The outsides of the channels appear in light gray, and dark gray is used to show where the channels are cut by the boundaries of the array. The surface of the channels is defined by the possible loci of the center of a sphere of diameter 3.0 Å as it rolls over the surface of the ordered network.²⁵



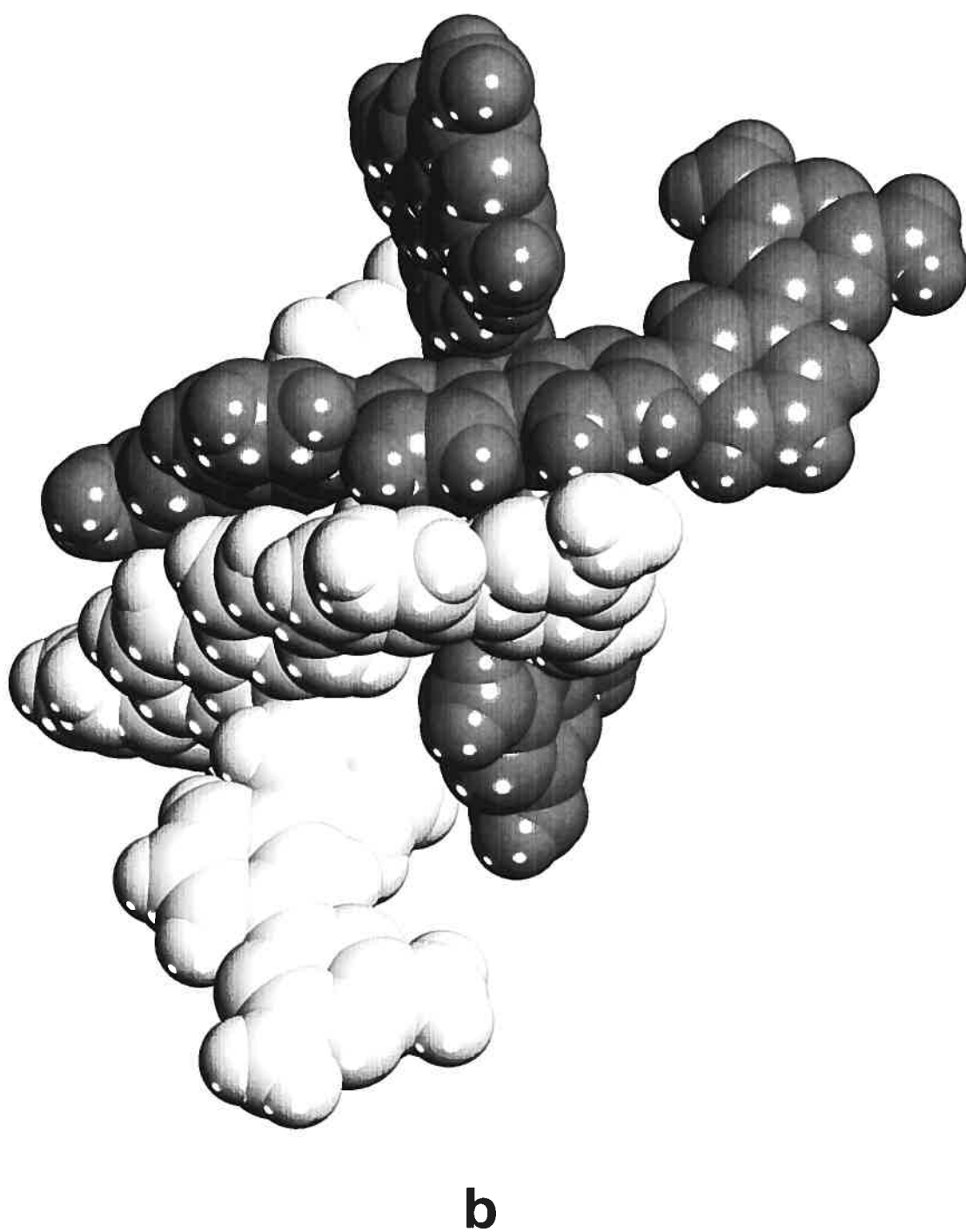


Figure 9. Representation of the interactions between symmetry-independent molecules **C** (white) and **D** (black) in the structure of crystals of extended spirobifluorene **3** grown from DMSO/CH₃OH. a) Four distorted hydrogen bonds of type III. b) Aromatic interactions.

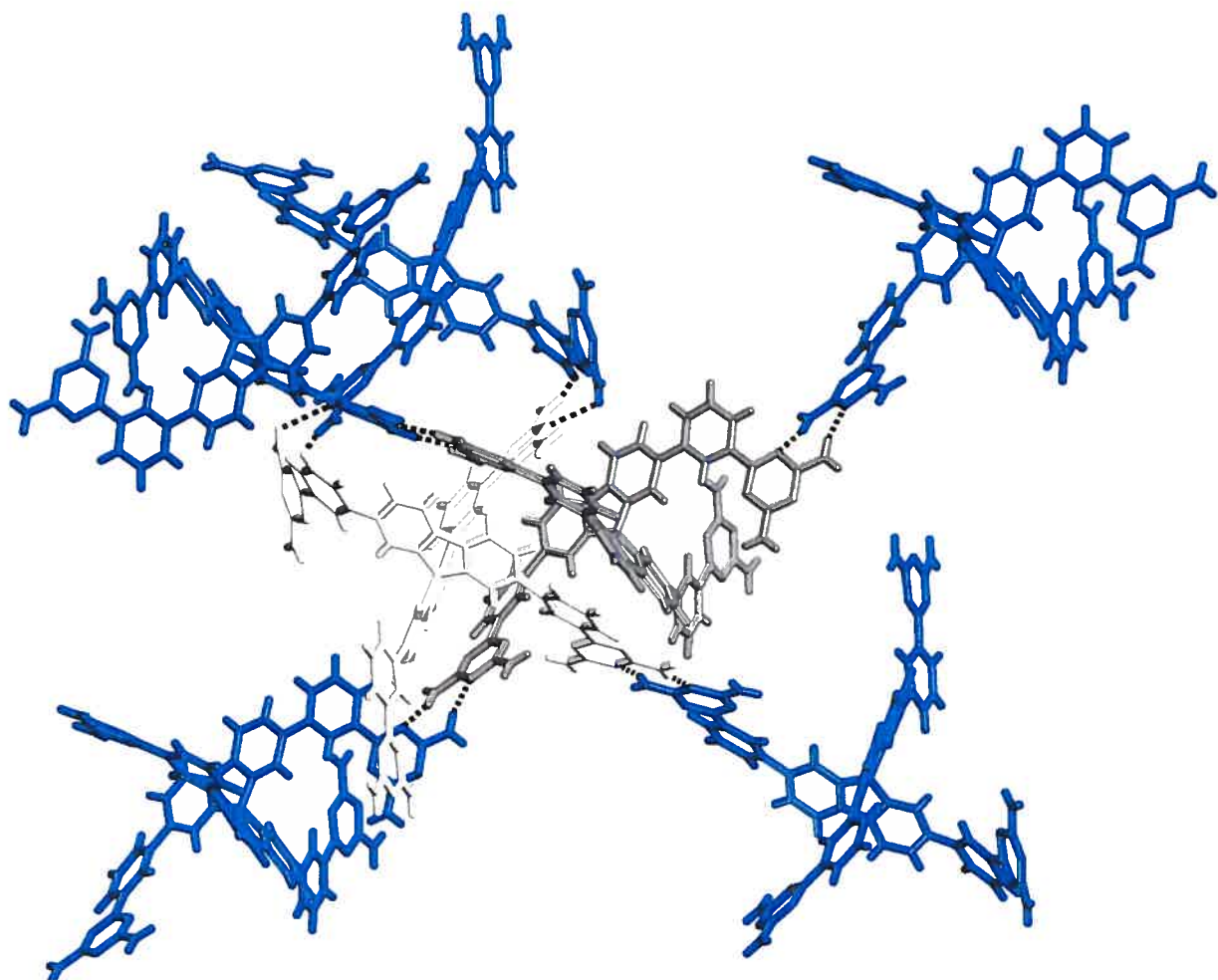


Figure 10. View of the structure of crystals of extended spirobifluorene **3** grown from DMSO/CH₃OH, showing symmetry-independent tectons **C** (white) and **D** (dark gray) and the five neighbors (blue) that form hydrogen bonds according to motifs **I-II**. Guests are omitted for clarity, and hydrogen bonds are represented by broken lines.

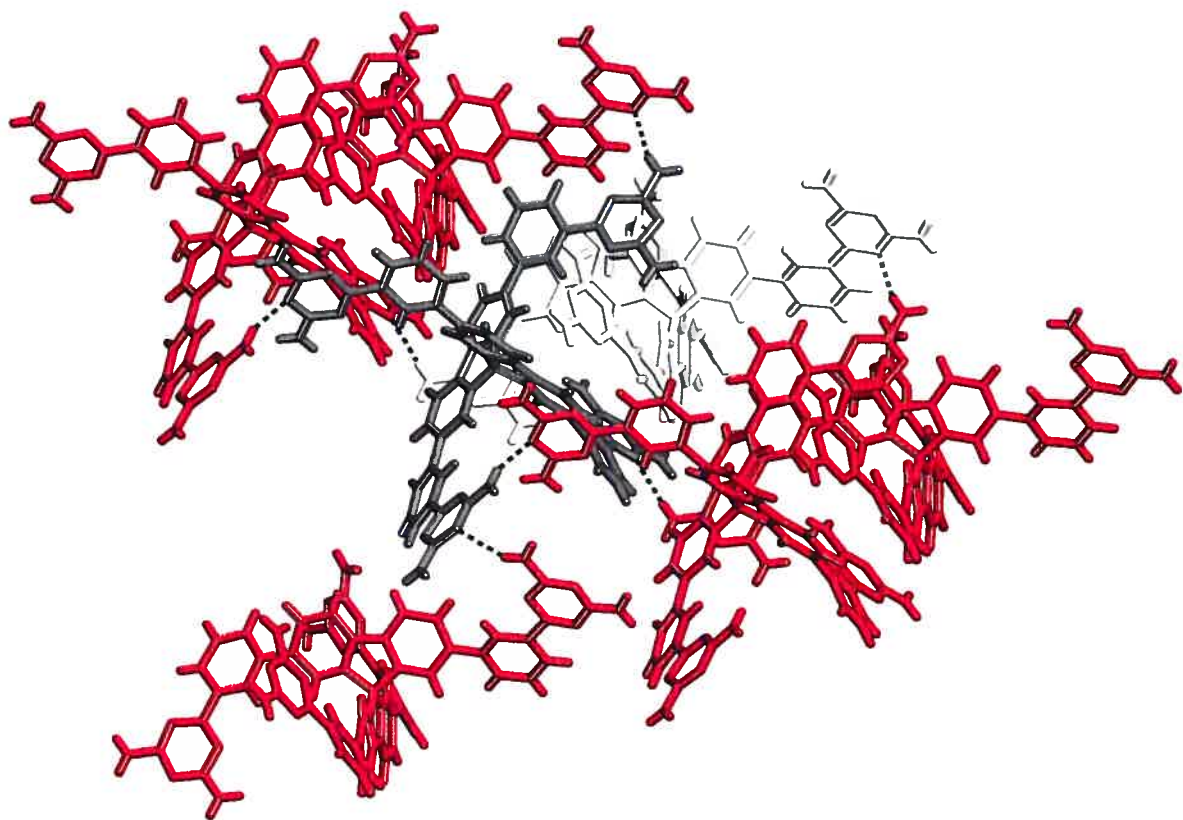


Figure 11. View of the structure of crystals of extended spirobifluorene **3** grown from DMSO/CH₃OH, showing symmetry-independent tectons **C** (white) and **D** (dark gray) and the five neighbors (red) that form distorted single hydrogen bonds. Guests are omitted for clarity, and hydrogen bonds are represented by broken lines.

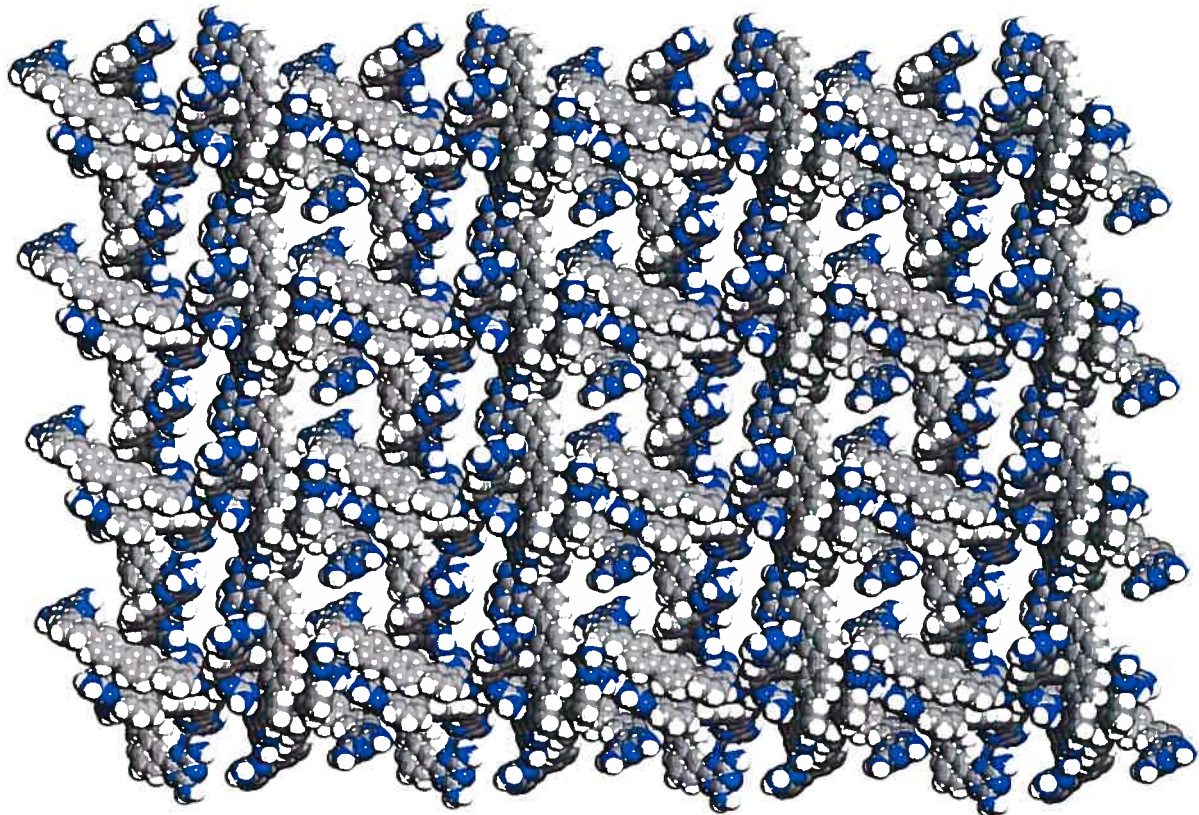


Figure 12. View along the a axis of the network constructed from extended spirobifluorene 3 showing a $4 \times 4 \times 4$ array of unit cells. Guests are omitted, and atoms are shown as spheres of van der Waals radii in order to reveal the cross sections of the channels. Atoms of hydrogen appear in white, atoms of carbon in gray, and atoms of nitrogen in blue.

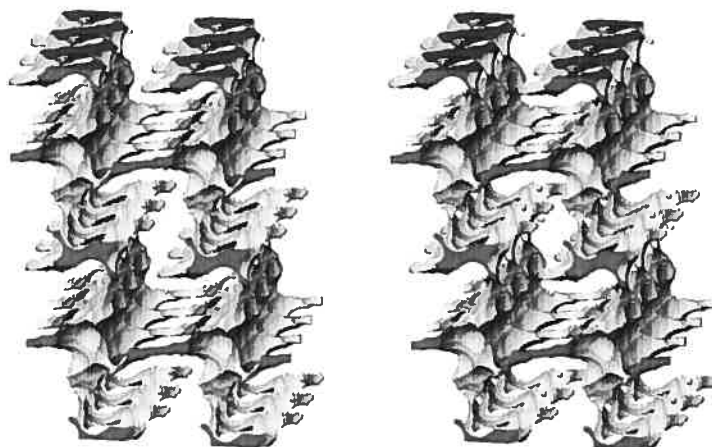
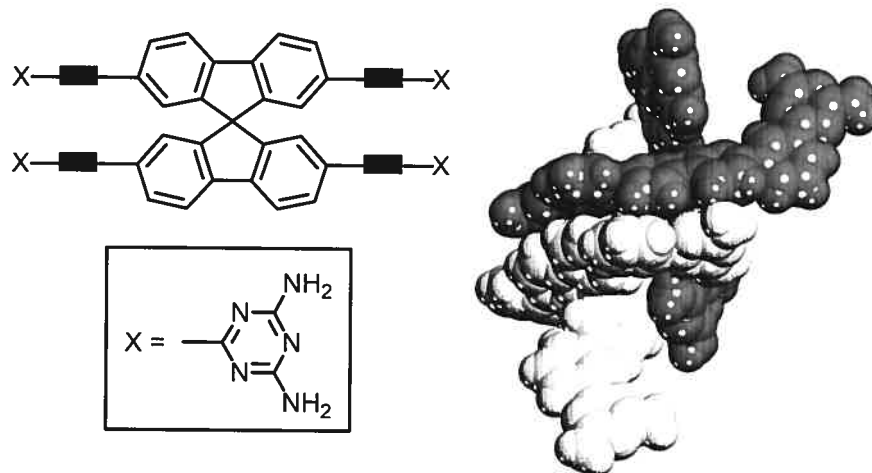


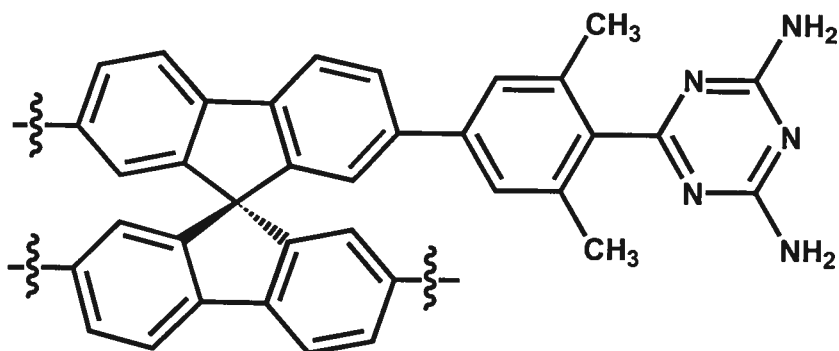
Figure 13. Stereoscopic representation of interconnected channels within the network constructed from extended spirobifluorene **3**. The image shows a $3 \times 2 \times 2$ array of unit cells viewed along the a axis. The outsides of the channels appear in light gray, and dark gray is used to show where the channels are cut by the boundaries of the array. The surface of the channels is defined by the possible loci of the center of a sphere of diameter 3 Å as it rolls over the surface of the ordered network.²⁵

Table of Contents Graphic



3.5 Conclusion

En terminant, nous pouvons faire ressortir quelques faits marquant de cette étude. D'abord, l'ajout d'un espaceur phényle a atteint son premier objectif, soit d'éloigner les unités centrales les unes des autres. Malencontreusement, l'objectif ultime qui consistait en l'augmentation contrôlée de la porosité du réseau s'est avéré un échec. En effet, il semble que l'éloignement des unités centrales ne soit pas suffisant pour induire une augmentation de porosité. On en déduit ainsi que la topologie du réseau cristallin a un impact direct et majeur sur la variation de porosité. Cette observation conduit conséquemment à des questions sur la manière dont la topologie affecte la porosité et sur les stratégies pour pouvoir la contrôler.



Tecton 3.5

Une étude importante qui pourrait être faite afin de poursuivre ce projet serait la cristallisation du tecton 3.5. En effet, l'encombrement dû à la présence des groupements méthyle ferait en sorte de défavoriser les reconnaissances de type II et III de la diaminotriazine pour favoriser celle de type I, soit face à face. Comme cette dernière reconnaissance tend à éloigner les unités centrales, il serait alors intéressant de voir l'effet qu'aurait une telle modification sur le réseau cristallin et conséquemment sur la porosité.

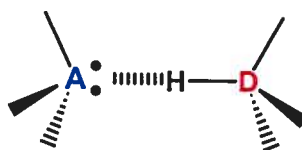
Chapitre 4

***Étude de l'utilisation
d'interactions faibles dans la
formation de réseaux poreux***

4.1 La liaison hydrogène

Depuis le début de cette thèse, tous les composés formant des réseaux poreux ayant été présentés sont basés sur l'auto-assemblage dicté par des liaisons hydrogène. Ces dernières années, la définition du pont hydrogène s'est élargie et on y inclut désormais des subdivisions. On peut, pour simplifier, définir la liaison hydrogène comme suit :¹

La liaison hydrogène est formée quand un donneur (**D**) portant un hydrogène acide et disponible est dans le voisinage proche d'un accepteur (**A**) portant une paire d'électrons disponibles non liée (Schéma 4.1). La distance requise est généralement décrite telle que la distance H···A doit être inférieure à la somme des rayons de van der Waals de H et de A. Steiner^{1b} ajoute qu'une interaction **D**-H···**A** est appelée une «liaison hydrogène» si 1) elle constitue un lien localisé et 2) si **D** agit comme un donneur de proton à **A**. Cette interaction comprend trois centres où quatre électrons sont partagés entre un lien **D**-H donneur et un centre **A** électro-déficient.



A = F, Cl, O, S, N, système- π

D = F, Cl, O, S, N, C

Schéma 4.1 : Liaison hydrogène formée entre un atome d'hydrogène acide (lié à un atome donneur **D** de liaison hydrogène) et un accepteur approprié (**A**).

¹ a) Philp, D.; Stoddart, J. F. *Angew. Chem., Int. Ed. Engl.* 1996, 35, 1154.

b) Steiner, T. *Angew. Chem., Int. Ed. Engl.* 2002, 41, 48.

c) Beijer, F. H. *Cooperative Multiple Hydrogen Bonding in Supramolecular Chemistry*, Proefschrift, Eindhoven, , Chap.1.2, 1.3 et 1.4.

L'énergie d'une liaison hydrogène est généralement comprise entre 4 et 15 kcal/mol.^{1b,} ² Selon la classification décrite par Jeffrey,^{2a} cet intervalle correspond à une liaison hydrogène «modérée» que l'on dit «normale». Cependant, il existe des interactions décrites comme des liaisons hydrogène et qui possèdent des énergies de liaison beaucoup plus fortes et d'autres beaucoup plus faibles. Elles sont alors respectivement classées comme des liaisons hydrogène «fortes» ou «faibles». Leurs caractéristiques générales sont décrites dans le Tableau 4.1. Des exemples extrêmes montrent que l'énergie d'une liaison hydrogène peut varier de 0.2 kcal/mol pour l'interaction faible comme $\text{CH}_4\cdots\text{F}-\text{CH}_3$ ³ et jusqu'à 39 kcal/mol pour un lien fort tel que $\text{F}-\text{H}\cdots\text{F}^-$.⁴

Il est impossible, simplement en regardant une structure obtenue par diffraction des rayons-X, de mesurer la force d'une liaison hydrogène, mais on possède toutefois quelques indices pouvant permettre de savoir à quel type de ponts hydrogène nous avons affaire. En effet, la distance entre le donneur et l'accepteur de ponts hydrogène, la géométrie de la liaison et l'acidité du proton donnent de bons indices à ce sujet. Le Tableau 4.1 représente un résumé des tendances générales applicables aux ponts hydrogène.

² a) Jeffrey, G. A. *An Introduction to Hydrogen Bonding*, Oxford University Press, Oxford, 1997.

b) Joeston, M. D. *J. Chem. Ed.* **1982**, 79, 362. (c) Aakeröy, C. B.; Seddon, K. R. *Chem. Soc. Rev.* **1993**, 22, 397.

³ Howard, J. A. K.; Hoy, V. J.; O'Hagan, D.; Smith, G. T. *Tetrahedron* **1996**, 52, 12613.

⁴ Gronert, A. *J. Am. Chem. Soc.* **1993**, 115, 10258.

Tableau 4.1 : Caractéristiques des liaisons hydrogène «fortes», «modérées» ou «faibles» selon la classification de Jeffrey.^{2a}

	Forte	Modérée	Faible
Type d'interaction	à caractère covalente	principalement électrostatique	électrostatique/ dispersée
Longueur de liaison (Å)			
H···A	~ 1.2-1.5	~ 1.5-2.2	~ 2.2-3,2
D-H	D-H \approx H···A	D-H < H···A	D-H << H···A
D···A	2.2-2.5	2.5-3.2	> 3.2
Directionalité	forte	modérée	faible
Angles de liaisons (deg)	175-180	~ 130-180	~ 90-150
Énergie de liaison (kcal.mole⁻¹)	15-40	4-15	< 4

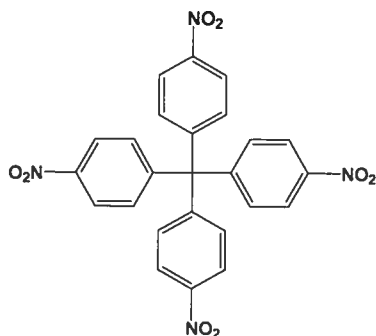
A : Atome accepteur de liaison hydrogène.

D : Atome donneur de liaison hydrogène.

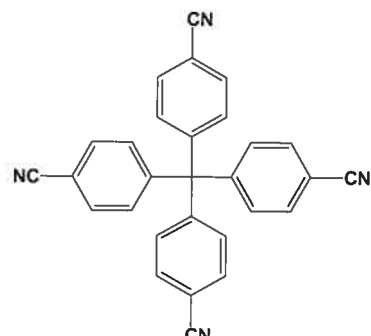
Comme énoncé précédemment, dans la plupart des réseaux poreux organiques obtenus en tectonique moléculaire, la cohésion structurale est assurée par des ponts hydrogène "normaux". Cependant, il existe plusieurs autres exemples où ce sont des interactions faibles qui peuvent être considérées comme maintenant le réseau. Desiraju et collaborateurs ont fait de nombreuses études où la cohésion de réseaux supramoléculaires est assurée par des interactions faibles. À titre d'exemple, ils ont montré que la cristallisation du tétrakis(4-nitrophényl)méthane **1** conduit à la formation de plusieurs réseaux poreux différents selon les solvants de recristallisation utilisés.⁵ Or, dans ces structures, seuls des ponts hydrogène faibles de type C-H ··· O et des interactions de type C-H ··· π retiennent l'architecture supramoléculaire. Cet exemple illustre comment les

⁵ Thaimattam, R.; Xue, F.; Sarma, J.A.R.P.; Mak, T.C.W.; Desiraju, G.R. *J. Am. Chem. Soc.* 2001, 123, 4432.

interactions faibles peuvent être mises à profit pour l'obtention de réseaux supramoléculaires similaires à ceux obtenus avec des ponts hydrogène classiques.



Structure du
tétrakis(4-nitrophényl)méthane 1



Structure du
tétrakis(4-cyanophényl)méthane 2

Le téraphénylméthane a été l'objet de plusieurs études en génie cristallin car c'est une molécule tétraédrique simple et rigide. Dernièrement, le groupe de Desiraju s'est arrêté à faire une autre étude similaire à celle effectuée pour le tétrakis(4-nitrophényl)méthane, avec cette fois le tétrakis(4-cyanophényl)méthane **2**.⁶ Il faut ici noter que l'emploi des dérivés du téraphénylméthane se concentre sur des substitutions en position para.

Le groupe du professeur Wuest a montré depuis quelques années l'efficacité des liaisons hydrogène "normales" en tectonique moléculaire afin de diriger l'auto-assemblage de réseaux supramoléculaires poreux. Dernièrement, le Dr Dominic Laliberté s'est attardé sur ce qu'on pouvait obtenir en utilisant les interactions faibles.⁷ En effet, il a fait plusieurs études impliquant différentes interactions faibles dont celles énumérées plus haut. Ses études portaient sur une unité centrale basée sur le pentaérythritol, soit une unité permettant un bon degré de flexibilité pour optimiser la reconnaissance moléculaire.

⁶ Basavoju, S.; Aitipamula, S.; Desiraju, G. R. *CrystEngComm*, **2004**, 6(25), 120.

⁷ Laliberté, D.; Maris, T.; Wuest, J. D. *CrystEngComm*, **2005**, 7, 158.

Ce chapitre, pour sa part, sera aussi consacré à l'étude des interactions faibles, mais cette fois sur une unité centrale beaucoup plus rigide, soit le 9,9'-spirobifluorène. On débutera avec une brève introduction sur l'historique des interactions faibles qui seront abordées dans ce chapitre puis on discutera des résultats obtenus sur les dérivés du 9,9'-spirobifluorène.

4.2 Les interactions faibles abordées dans ce chapitre

Dans ce chapitre, on abordera la cristallisation de dérivés du 9,9'-spirobifluorène. Les dérivés en question sont illustrés à la Figure 4.1. Comme on peut le constater, il s'agit de dérivés soit nitrés, soit cyanés. De plus, on étudiera, comme au chapitre précédent, l'effet d'un espaceur phényle sur la formation du réseau. Les interactions faibles pouvant intervenir lors du processus de cristallisation sont les ponts hydrogène faibles formés par les fonctions nitro ou cyano ainsi que des interactions de type aryle-aryle.

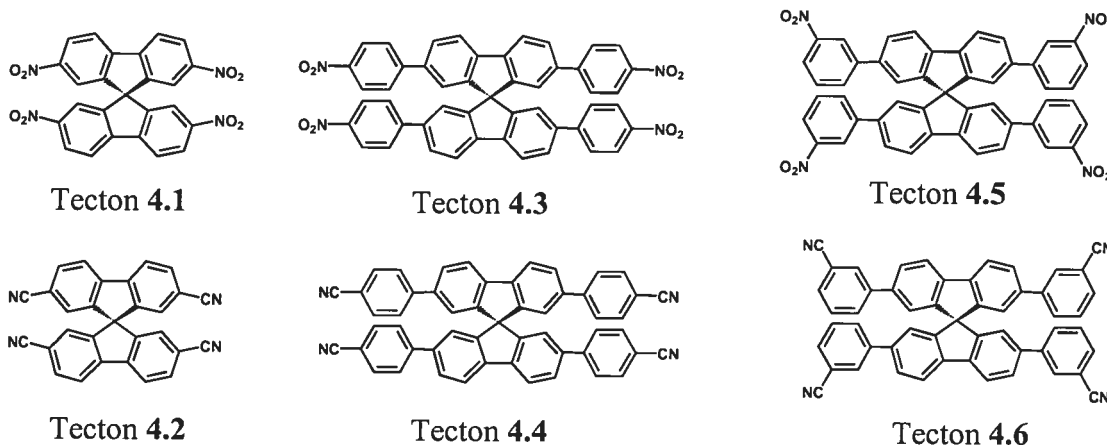


Figure 4.1 Représentation des tectons 4.1 à 4.6 étudiés dans ce chapitre.

4.3 Les interactions CH \cdots X_(O, N)

Les liaisons C-H sont des donneurs de ponts hydrogène faibles non totalement reconnus. La plupart des atomes qui contiennent des électrons de valence disponibles sont aptes à recevoir des ponts hydrogène faibles. Il est toutefois évident que plus l'atome accepteur est gros et polarisable, moins le pont sera fort. C'est la raison pour laquelle l'oxygène et l'azote sont de bons candidats pour ce type d'étude. Quelques exemples de donneurs de ponts hydrogène faibles sont illustrés à la Figure 4.2.

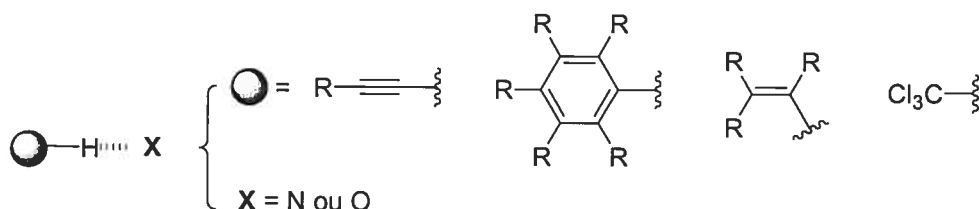


Figure 4.2 Représentation des principaux donneurs C-H dans les ponts hydrogène faibles.

C'est en 1982 que Taylor et Kennard⁸ ont démontré l'évidence des liaisons CH \cdots N et CH \cdots O par une analyse exhaustive de plus de 113 structures cristallines obtenues par diffraction des neutrons. Ils en vinrent à la conclusion que la nature de la liaison est plus attractive que répulsive. Les principales différences entre le pont hydrogène normal et le pont hydrogène faible sont bien entendu la force, mais aussi leur caractère géométrique. En effet, le pont hydrogène "normal" étant plus fort, les distances D_{(donneur)H} \cdots A_(accepteur) sont plus courtes, mais les liaisons sont aussi plus linéaires.^{2a} La géométrie pour les ponts hydrogène faibles est beaucoup plus étendue comme illustré au Tableau 4.1, avec des angles tournant souvent autour de 110-120° et des distances D_{(donneur)H} \cdots A_(accepteur) parfois plus longues que la somme de leurs rayons de van der Waals.⁹ Des énergies de stabilisation variant entre 1 et 2.5 kcal/mol sont généralement attribuées pour ces ponts hydrogène faibles.

⁸ Taylor, R.; Kennard, O. *J. Am. Chem. Soc.* **1982**, *104*, 5063.

⁹ van den Berg, J.-A.; Seddon, K.R. *Cryst. Growth Des.* **2003**, *3*, 643.

Il est difficile de faire la nuance entre les interactions de van der Waals et la présence de ponts hydrogène faibles seulement par leurs énergies. La principale différence intervient essentiellement dans l'orientation des molécules. En effet, contrairement aux interactions de van der Waals qui n'ont aucune préférence d'empilement, les ponts hydrogène faibles adoptent des conformations plus précises où le comportement est comparable à celui observé pour les ponts hydrogène "normaux". Même si jusqu'à présent les ponts hydrogène faibles sont plus un constat pour expliquer certains agencements structuraux, ils doivent être considérés pour la prévision des assemblages moléculaires.¹⁰

Parmi les groupes fonctionnels pouvant participer en tant qu'accepteur de ponts hydrogène faibles, la fonction nitro est la plus versatile. En effet, plusieurs dispositions sont possibles pour les interactions avec les atomes d'hydrogène tel qu'illustre à la Figure 4.3.¹¹

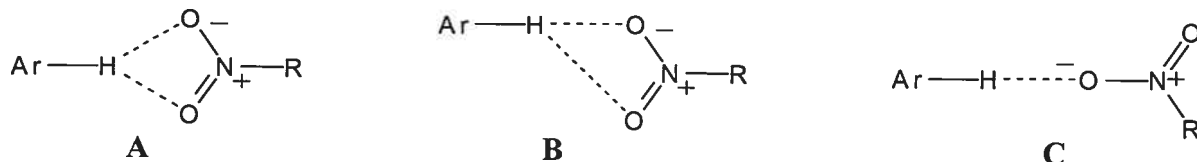


Figure 4.3 Représentation des principaux motifs de reconnaissance possibles pour les interactions entre les atomes d'hydrogène aromatique et la fonction nitro.¹¹

Les interactions de type C-H···N du groupe cyano suivent approximativement les mêmes règles à l'exception que le doublet d'électrons de l'azote ne pointe que dans une

¹⁰ Sharma, C.V.K. in *Crystal Engineering: From Molecules and Crystals to Materials*, Kluwer Academic Publishers, The Netherlands, 1999, p. 481-500. Desiraju, G.R. *Acc. Chem. Res.* **2002**, *35*, 565.

¹¹ Allen, F.H.; Lommerse, J.P.M.; Hoy, V.J.; Howard, J.A.K.; Desiraju, G.R. *Acta Crystallogr.* **1997**, *B53*, 1006.

direction et, par conséquent, rend la fonction cyano moins accessible par rapport à la fonction nitro. Il arrive cependant que le pont hydrogène se forme avec le doublet d'électrons π disponible dans la triple liaison CN, concédant ainsi une autre possibilité d'interaction à la fonction cyano (Figure 4.4).

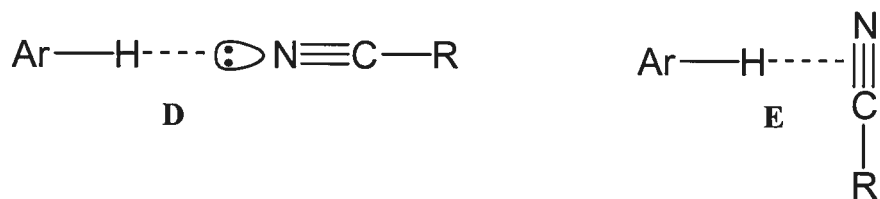


Figure 4.4 Représentation des principales configurations possibles pour les interactions entre les atomes d'hydrogène aromatique et la fonction cyano.

4.4 Les interactions aryle - aryle

Les dérivés du 9,9'-spirobifluorène qui font l'objet de notre étude possèdent des groupements aromatiques. Nous proposons également l'emploi de groupements phényles comme espaceur. Il est donc nécessaire d'aborder le sujet des interactions aryle-aryle plus connues sur leur nom anglais de "π-stacking". L'empilement π a été la première interaction faible à être reconnue et demeure la plus étudiée encore de nos jours. Malgré l'observation fréquente de ces interactions, on n'arrive toujours pas à expliquer leur stabilité avec certitude.^{12,13}

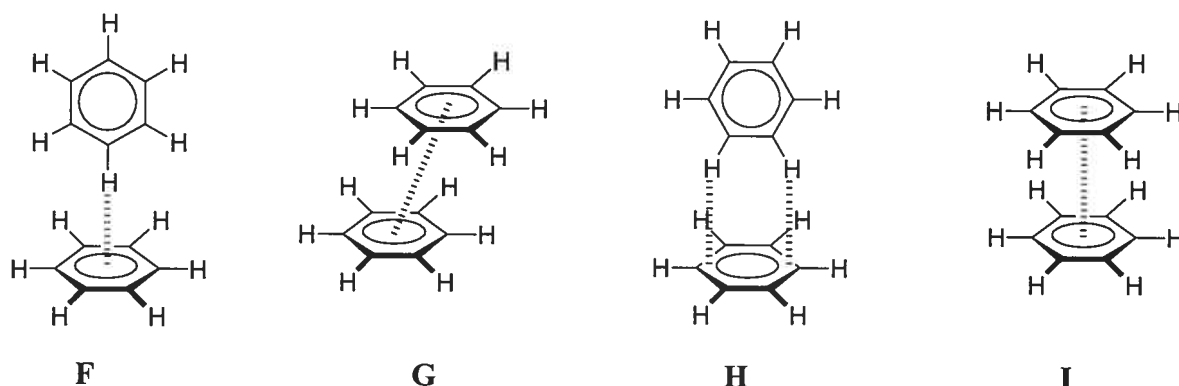


Figure 4.5 Représentation des principales interactions entre des groupements aryles.

Les groupements aryles se reconnaissent de quatre manières préférentielles qui sont illustrées à la Figure 4.5. Ces quatre motifs sont le type face-à-côté **F**, le type face-à-face décalée **G**, le type **H** et finalement le type face-à-face **I**. Les études les plus récentes tendent à démontrer que les formes **F** et **G** sont favorisées, avec des énergies de

¹² Landauer, J.; McConnell, H. *J. Am. Chem. Soc.* **1952**, *74*, 1221.

¹³ Hunter, C.A.; Lawson, K.R.; Perkins, J.; Urch, C.J. *J. Chem. Soc., Perkin Trans. 2*, **2001**, 651.

stabilisation de 2.46 et de 2.48 kcal/mol, respectivement, suivi par l'interaction **H**¹⁴ et finalement par le motif **I** avec une stabilisation de 1.48 kcal/mol.¹⁵ Cette dernière est la moins stable à cause d'une répulsion plus grande entre les nuages électroniques π . En effet, il a été montré que si on diminue le nuage électronique en ajoutant des groupements électroattracteurs, on augmente la force de l'empilement π .^{16, 17} L'effet inverse se produit avec l'incorporation de groupements électrodonneurs.

En plus de ces paramètres, il faut tenir compte d'interactions supplémentaires pouvant intervenir, comme par exemple les interactions quadrupolaires. Ainsi, dans la structure du complexe **J** (Figure 4.6) entre le benzène et l'hexafluorobenzène, une interaction de type **I** est observée avec une énergie de stabilisation de 3.7 kcal/mol.¹⁸ Ce mode d'interaction est suffisamment stable pour donner au complexe cristallin un point de fusion supérieur à ceux des composés purs.¹⁹ Cette stabilité s'expliquerait par des interactions quadrupolaires que l'on retrouve également dans l'empilement face-à-côté des molécules de benzène **K** (Figure 4.6).²⁰ Il est souvent remarqué que l'empilement π entre molécules complémentaires (électron-pauvres et électron-riches) est favorisé et, comme on verra au Chapitre 6, a déjà été utilisé en génie cristallin.

¹⁴ Lorenzo, S.; Lewis, G.R.; Dance, I. *New. J. Chem.* **2000**, *24*, 295.

¹⁵ Tsuzuki, S.; Honda, K.; Uchimaru, T.; Mikami, M.; Tanabe, K. *J. Am. Chem. Soc.* **2002**, *124*, 104.

¹⁶ Hunter, C.A.; Sanders, J.K.M. *J. Am. Chem. Soc.* **1990**, *112*, 5525.

¹⁷ Rashkin, M.J.; Waters, M.L. *J. Am. Chem. Soc.* **2002**, *124*, 1860.

¹⁸ West, A.P. Jr.; Mecozzi, S.; Dougherty, D.A. *J. Phys. Org. Chem.* **1997**, *10*, 347.

¹⁹ Williams, J.H. *Acc. Chem. Res.* **1993**, *26*, 593.

²⁰ a) Jorgensen, W.L.; Severance, D.L. *J. Am. Chem. Soc.* **1990**, *112*, 4768.

b) Hobza, P.; Selzle, H.L.; Schlag, E.W. *J. Am. Chem. Soc.* **1994**, *116*, 3500.

c) Cozzy, F.; Cinquini, M.; Annunziata, R.; Dwyer, T.; Siegel, J.S. *J. Am. Chem. Soc.* **1992**, *114*, 5729.

d) Cozzy, F.; Ponzini, F.; Annunziata, R.; Cinquini, M.; Siegel, J.S. *Angew. Chem. Int. Ed.* **1995**, *34*, 1019. e) Adams, H.; Carver, F.J.; Hunter, C.A.; Morales, J.C.; Seward, E.M. *Angew. Chem. Int. Ed.* **1996**, *35*, 1542.

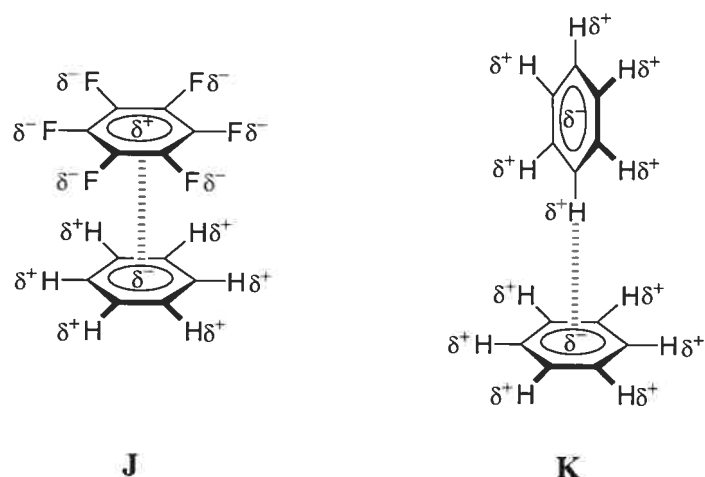


Figure 4.6 Représentation d'empilements π complémentaires.

4.5 Article 2

Weakly Bonded Molecular Networks Built from Tetranitro- and Tetracyanospirobifluorenes

Eric Demers, Thierry Maris, Janie Cabana, Jean-Hugues Fournier, and James D. Wuest

Crystal Growth & Design 2005, 5, 1237

Weakly Bonded Molecular Networks

Built from Tetranitro- and Tetracyanospirobifluorenes

Eric Demers,¹ Thierry Maris, Janie Cabana,²

Jean-Hugues Fournier,³ and James D. Wuest*

Département de Chimie, Université de Montréal

Montréal, Québec H3C 3J7 Canada

*Author to whom correspondence may be addressed:



Abstract

Three tetranitro and three tetracyano derivatives of 9,9'-spirobifluorene were synthesized and crystallized, and their structures were determined by X-ray crystallography. 2,2',7,7'-Tetranitro-9,9'-spirobi[9H-fluorene] (**4**) self-associates via C-H···O interactions to give an open supramolecular network, with 31% of the total volume of the crystal available for including guests. Tetracyano analogue **5** also crystallizes to give a porous network, but no significant C-H···N interactions are present; instead, molecular association is directed primarily by π -stacking. An extended tetranitro analogue, 2,2',7,7'-tetrakis(4-nitrophenyl)-9,9'-spirobi[9H-fluorene] (**6**), crystallizes as a nearly close-packed structure held together by a combination of C-H···O interactions and π -stacking. Tetracyano analogue **7** crystallizes to form an open structure maintained by π -stacking, without significant C-H···N contacts. Extended meta-substituted analogues, 2,2',7,7'-tetrakis(3-nitrophenyl)-9,9'-spirobi[9H-fluorene] (**8**) and 2,2',7,7'-tetrakis(3-cyanophenyl)-9,9'-spirobi[9H-fluorene] (**9**), were also synthesized and crystallized. The two structures are closely similar and show close-packed architectures involving mainly π -stacking. Together, these observations suggest that cyano groups are not effective acceptors for the formation of C-H···N interactions strong enough to direct molecular association in competition with aryl-aryl interactions, at least in the spirobifluorene system. In contrast, nitro groups can be used to help direct association via C-H···O interactions, either in competition with or in cooperation with other weak interactions.

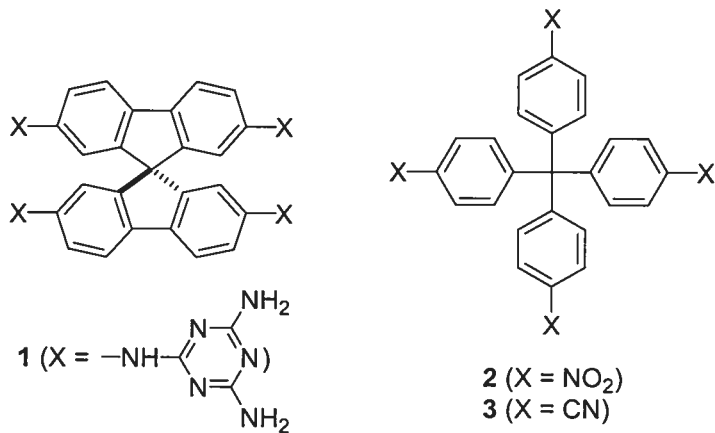
Introduction

Theory provides increasingly useful tools for predicting the structure of molecular crystals.⁴ At present, however, such predictions remain unreliable, in part because our knowledge of intermolecular potentials is not always accurate enough to establish which structure is the most stable. Furthermore, subtle kinetic effects can also determine how molecules crystallize, leading to the existence of multiple less-stable polymorphic forms. For such reasons, predicting the structures of molecular crystals with confidence is a goal that is still far from our reach, particularly for molecules with any significant degree of complexity and flexibility.⁵

As a result, current efforts to engineer molecular crystals are dominated by empirical approaches. A particularly effective strategy emphasizes the importance of a sound qualitative understanding of how molecules in a crystal will be positioned relative to their neighbors. This understanding can be most easily achieved when the molecules have well-defined core structures with multiple peripheral sites that favor strong directional associations according to reliable motifs. Such sticky sites, when oriented by a suitable core, can play a key role in determining how neighboring molecules are positioned. Molecules of this type, which have been called tectons from the Greek word for builder,⁶ have been shown to provide the basic elements of a rational construction set for building molecular networks with predictable architectures.⁷⁻⁹

So far, efforts to develop and exploit this strategy have featured the use of tectons that associate by forming classical hydrogen bonds,¹⁰ and related work has focused on assembly controlled by coordination to metals.¹¹ Such directional interactions are strong enough to play a dominant role in determining the pattern of molecular association, and they typically program the assembly of open networks with significant space for including guests.¹² Particularly porous networks result when the tectons have cores with topologies that are

intrinsically resistant to close packing. For example, spirobifluorenes pack with especially low efficiency, and the most porous network yet constructed from small molecules has been produced by crystallizing tecton 1, in which hydrogen-bonding aminotriazine groups are grafted to a rigid spirobifluorene core.⁸



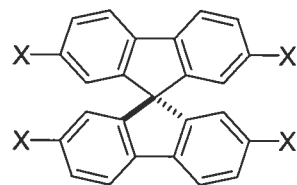
In many cases, porous tectonic networks are robust enough to withstand stresses induced by the exchange of guests or by their partial removal, even when the network is held together largely by hydrogen bonds. In such cases, exposure of single crystals to suitable new guests leads to exchange without loss of crystallinity. These materials are noteworthy because they are molecular analogues of zeolites, with potential applications in the areas of separation, catalysis, sensing, and other areas. In other ways as well, the strategy of molecular tectonics has been able to produce materials with properties not observed in normal molecular crystals.

Recently, the range of non-covalent interactions used by crystal engineers has been extended from classical strong hydrogen bonds, such as $\text{O-H}\cdots\text{O}$, $\text{N-H}\cdots\text{N}$, and $\text{O-H}\cdots\text{N}$ bonds, to include much weaker attractions, such as $\text{C-H}\cdots\text{O}$, $\pi\cdots\pi$, halogen-halogen, and $\text{C-H}\cdots\pi$ interactions.^{13,14} Some of these weaker interactions can display geometrical, structural, and spectroscopic features not unlike those of conventional hydrogen bonds. In particular, nitro and cyano groups have been recognized as hydrogen-bond acceptors that

can take part in a variety of C-H···O and C-H···N interactions, including representative motifs **I–V** shown in Figure 1.^{15–17}

Undeniably, these interactions are promising tools for helping direct molecular association. For example, crystallization of tetrakis(4-nitrophenyl)methane (**2**) is controlled in part by the formation of C-H···O interactions involving nitro groups, leading to the construction of open networks that can include a variety of guests.¹⁵ Similarly, C-H···N interactions involving cyano groups are present in the structure of tetrakis(4-cyanophenyl)methane (**3**), which crystallizes both as an inclusion compound and as a close-packed structure.¹⁶ In general, however, C-H···O and C-H···N interactions are not sufficiently strong and specific to allow them to be used confidently to create robust molecular networks by design. The shortcomings of these interactions, relative to classical strong hydrogen bonds, are revealed clearly by detailed examination of the structures of compounds **2–3**: 1) Highly diverse C-H···O and C-H···N interactions are observed in crystals of compounds **2–3**, suggesting that no single motifs of these types are strongly preferred and can therefore be used reliably to build structures by design; 2) in each case, crystallization does not favor a unique architecture but instead yields widely different types of structures that depend critically on the solvent of crystallization; and 3) the resulting networks have only modest porosity and do not appear to be robust enough to permit the exchange of guests in single crystals without loss of crystallinity.

These observations show that C-H···O and C-H···N interactions are inherently more difficult to use in crystal engineering than strong hydrogen bonds. Nevertheless, we decided to examine their potential further by studying compounds **4–9**, which have nitro and cyano groups attached to cores derived from spirobifluorene. Our expectation, based on previous studies of spirobifluorene **1**, was that crystallization would produce networks more porous than those derived from analogous nitro- and cyano-substituted tetraphenylmethanes.

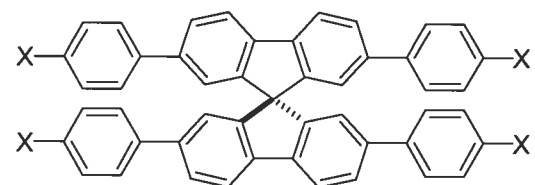


4 ($X = \text{NO}_2$)

5 ($X = \text{CN}$)

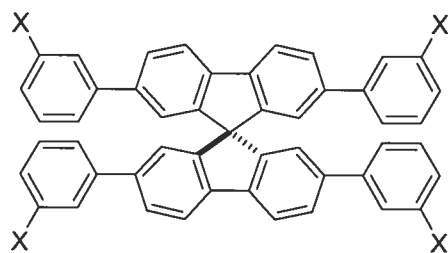
10 ($X = \text{Br}$)

11 ($X = \text{B}(\text{OH})_2$)



6 ($X = \text{NO}_2$)

7 ($X = \text{CN}$)



8 ($X = \text{NO}_2$)

9 ($X = \text{CN}$)

Results and Discussion

Structures of 2,2',7,7'-Tetranitro-9,9'-spirobi[9H-fluorene] (4) and 2,2',7,7'-Tetracyano-9,9'-spirobi[9H-fluorene] (5). Slow diffusion of toluene into a solution of tetranitrospirobifluorene **4**⁸ in dioxane afforded single crystals suitable for analysis by X-ray diffraction. Under these conditions, compound **4** crystallizes in the triclinic space group $P\bar{1}$ as an inclusion compound of composition **4** • 1.5 dioxane.^{18a} As shown in Figure 2, the structure incorporates multiple C-H···O interactions involving nitro groups (H···O distances are considered significant if they are less than or equal to 2.66 Å). Interactions of types I and II (Figure 1) are both observed. Each molecule is linked to a total of four neighbors by a total of six C-H···O interactions, and no significant aryl-aryl interactions are observed. Each central molecule and its four neighbors lie approximately in a plane, thereby defining corrugated sheets held together by C-H···O interactions, which then stack to form the observed structure (see Supporting Information). The included molecules of dioxane are ordered and occupy channels that run parallel to the *c* axis, with cross sections of approximately $3.6 \times 3.2 \text{ \AA}^2$ at the narrowest points (Figure 3).¹⁹ The guests occupy 31% of the total volume of the crystals.²⁰

Slow diffusion of hexane into a solution of tetracyanospirobifluorene **5**⁸ in CHCl₃ yielded crystals suitable for analysis by X-ray diffraction. The crystals were found to belong to the monoclinic space group C2/c and to have the composition **5** • 2 CHCl₃.^{18b} The guests are partially disordered, occupy channels parallel to the *c* axis (Figure 4), and occupy 42 % of the total volume of the crystals.²⁰ In the structure of cyano-substituted spirobifluorene **5**, no significant C-H···N interactions are present,²² and instead π -stacking is the principal source of cohesion (Figure 5a). These interactions define chains, which in turn form parallel sheets (Figure 5b).

Direct comparison of the structures of tetranitro- and tetracyanospirobifluorenes **4-5** with their para-substituted tetraphenylmethane analogues **2-3** is inappropriate, because the tetraphenylmethane core incorporated within the structure of compounds **4-5** is meta-

substituted. Nevertheless, in none of these structures do clear preferences emerge for particular C-H···O or C-H···N motifs, and the porosities of the resulting networks are modest even though the awkward and rigid topology of spirobifluorene cores must be accommodated in the crystal lattice.

Synthesis of Extended Tetranitro- and Tetracyanospirobifluorenes 6-9. We reasoned that increased porosity might be attained by using long spacers to link nitro and cyano groups to spirobifluorene cores, thereby producing extended derivatives of compounds **4-5** and further separating the centers of neighboring molecules in the resulting networks. To test this notion, we made 2,2',7,7'-tetrakis(4-nitrophenyl)-9,9'-spirobi[9H-fluorene] (**6**) and its tetracyano analogue, 2,2',7,7'-tetrakis(4-cyanophenyl)-9,9'-spirobi[9H-fluorene] (**7**), as well as their 3-substituted derivatives **8-9**. Tetralithiation of 2,2',7,7'-tetrabromo-9,9'-spirobi[9H-fluorene] (**10**),²³ followed by addition of B(O-iPr)₃ and hydrolysis, provided tetraboronic acid **11** in 90% yield. Subsequent Suzuki coupling with 4-iodo-1-nitrobenzene, 4-bromobenzonitrile, 3-iodo-1-nitrobenzene, and 3-bromobenzonitrile gave phenyl-extended spirobifluorenes **6-9**, respectively, in yields of 49%, 56%, 44%, and 61%.

Structures of 2,2',7,7'-Tetrakis(4-nitrophenyl)-9,9'-spirobi[9H-fluorene] (6) and its Tetracyano Analogue, 2,2',7,7'-Tetrakis(4-cyanophenyl)-9,9'-spirobi[9H-fluorene] (7). Diffusion of hexane into a solution of extended tetranitrospirobifluorene **6** in ethyl acetate afforded crystals that belong to the triclinic space group $P\bar{1}$ and have the composition **6** • 0.5 ethyl acetate.^{18b} Only 9% of the total volume of the crystal is used to include guests,²⁰ which are partially disordered, and no significant channels are present. The overall structure results from a complex interplay of C-H···O interactions and π -stacking. Two symmetry-independent molecules with slightly different conformations are present. Molecule **A** interacts with four neighbors by π -stacking with distances between the centroids of the phenyl rings less than 4.5 Å (Figure 6a), whereas molecule **B** is linked to five neighbors through similar interactions (Figure 6b). Simultaneously, molecules **A** and **B** are each linked to four neighbors by C-H···O interactions, mainly of type III (Figure 1), with H···O distances not greater than 2.66 Å (Figures 6c-d).²⁴ Overall, molecule **A** interacts

with a total of six neighbors, of which two both π -stack and form C-H \cdots O interactions with molecule **A**. Molecule **B** interacts with a total of seven neighbors, of which two both π -stack and form C-H \cdots O interactions with molecule **B**, four form C-H \cdots O interactions only, and one π -stacks only.

Diffusion of hexane into a solution of the corresponding extended tetracyanospirobifluorene **7** in dioxane gave crystals that proved to belong to the triclinic space group $P\bar{1}$ and to have the approximate composition **7** • 3 dioxane.^{18b} Approximately 36% of the total volume of the crystals is accessible to the guests,²⁰ which are disordered and occupy channels parallel to the *b* axis (Figure 7). Crystals of the analogous tetranitro compound **6** are held together by a combination of different interactions, whereas in the case of tetracyano analogue **7** cohesion results almost exclusively from π -stacking. In the structure of extended tetracyanospirobifluorene **7**, each molecule has three neighbors within 4.5 Å, measured by the distance between the centroids of the aromatic rings (Figure 8). As in the case of simple tetracyanospirobifluorene **5**, C-H \cdots N interactions do not play an important role in determining the structure, and only one such interaction is present (type V, Figure 1), with an H \cdots N distance of 2.52 Å.

Structures of 2,2',7,7'-Tetrakis(3-nitrophenyl)-9,9'-spirobi[9H-fluorene] (8) and its Tetracyano Analogue, 2,2',7,7'-Tetrakis(3-cyanophenyl)-9,9'-spirobi[9H-fluorene] (9). Crystals of meta-substituted extended tetranitrospirobifluorene **8** were obtained by diffusion of acetone into a solution in CHCl₃. Under these conditions, compound **8** crystallizes as a close-packed structure in the tetragonal space group I4₁/a. In this structure, each molecule is linked symmetrically to two sets of four neighbors. One set of neighbors is linked by a combination of π -stacking and C-H \cdots O interactions of type IV (Figure 1), with H \cdots O distances less than or equal to 2.66 Å. Together, these interactions define a non-interpenetrated diamondoid network in which the centers of neighboring molecules are separated by 8.65 Å (Figures 9a-b). Simultaneously, the nitro groups of compound **8** also form symmetric C-H \cdots O interactions of type III (Figure 1) with a second set of four neighbors (Figure 9b). These additional C-H \cdots O interactions are slightly longer and define

a second diamondoid network, in which the centers of neighbors are separated by 15.11 Å. This distance is large enough to permit 5-fold interpenetration,²⁵ giving a close-packed structure.

The analogous meta-substituted extended tetracyanospirobifluorene **9** was crystallized by allowing hexane to diffuse into a solution in toluene. Under these conditions, compound **9** crystallizes in the tetragonal space group I4₁/a as a close-packed structure very similar to the one formed by tetranitro analogue **8**. As noted in the structures of tetracyanospirobifluorenes **5** and **7**, molecular association in the structure of compound **9** involves primarily aryl-aryl interactions (Figure 9c). The resulting network has a diamondoid architecture with no interpenetration (Figure 9d), and the centers of neighboring molecules are separated by 8.522 Å.

Conclusions

Classical hydrogen bonds are strong and directional, and they can be used confidently in crystal engineering to produce molecular networks with predetermined structural features. Particularly impressive control can be achieved when multiple groups that hydrogen bond reliably are attached to rigid molecular cores. Emboldened by this success, crystal engineers have now begun to explore the potential of weaker and less directional interactions, including C-H \cdots O and C-H \cdots N interactions involving nitro- and cyano-substituted aromatic rings. This potential can be probed instructively by crystallizing compounds in which relevant groups are attached to rigid frameworks, such as the tetraphenylmethane cores of compounds **2-3** and the spirobifluorene cores of compounds **4-9**.

The behavior of all these compounds underscores the challenge of using C-H \cdots O and C-H \cdots N interactions to direct molecular crystallization. Compounds **4-5** both form networks with significant porosity, which presumably reflects the inherent difficulty of incorporating spirobifluorene units in periodic close-packed structures. However, the interactions observed in these two structures are highly diverse, and no significant C-H \cdots N interactions of cyano groups are present, suggesting that such interactions cannot compete effectively with aryl-aryl interactions. No other clear guidelines of general utility emerge from analysis of the two structures, thereby underlining the obstacles faced by crystal engineers attempting to exploit C-H \cdots O and C-H \cdots N interactions in rational ways.

The structures of extended derivatives **6-9**, which use phenyl spacers to separate nitro and cyano groups from the spirobifluorene core, are even more complex. Addition of the spacers increases the number of aryl-aryl interactions, which appear to be optimized at the expense of C-H \cdots O or C-H \cdots N interactions. It is noteworthy that π -stacking involving the added phenyl spacers improves the overall molecular packing, thereby reducing the porosity of the resulting networks to very modest levels relative to those observed in the

case of simpler spirobifluorenes. Analysis of the structures of extended spirobifluorenes **6-9** indicates that the cyano derivatives prefer to associate by π -stacking rather than by engaging in C-H \cdots N interactions. In contrast, the nitro derivatives participate in both π -stacking and C-H \cdots O interactions. In part, this tendency presumably reflects the higher strength of C-H \cdots O interactions relative to C-H \cdots N interactions. In addition, π -stacking in the nitro derivatives may be less stabilizing for electronic reasons than it is in the cyano derivatives. Specifically, nitro groups are more electron-withdrawing than cyano groups, so the ability of nitro derivatives **6** and **8** to participate in multiple aryl-aryl interactions may be reduced. Indeed, π -stacking in nitro derivatives **6** and **8** is largely confined to the central spirobifluorene cores, whereas this constraint is not observed in cyano derivatives **7** and **9**. However, even if a few helpful trends can be discerned in the structures of nitro- and cyano-substituted spirobifluorenes **4-9**, our observations confirm that the use of weak interactions to direct molecular crystallization remains a far more complex task than engineering crystals held together by strong hydrogen bonds.

Experimental Section

Ether was dried by distillation from the sodium ketyl of benzophenone. All other reagents were commercial products that were used without further purification.

Tetraboronic Acid 11. A solution of 2,2',7,7'-tetrabromo-9,9'-spirobi[9H-fluorene] (10; 0.50 g, 0.79 mmol)²³ in ether (100 mL) was stirred vigorously with a mechanical stirrer at -78 °C under dry N₂ and treated dropwise with a solution of butyllithium (3.0 mL, 2.5 M in hexane, 7.5 mmol). The resulting mixture was warmed to 25 °C and after 1 h was recooled to -78 °C. B(O-iPr)₃ (2.5 mL, 11 mmol) was added dropwise to the stirred mixture, and the temperature was allowed to rise to 25 °C overnight. Aqueous HCl (25 mL, 1 N) was then added, and the mixture was concentrated by partial evaporation of volatiles under reduced pressure. The concentrate was mixed with aqueous NaOH (1 N), and insoluble material was separated by filtration. Aqueous HCl (1 N) was then added to the filtrate until the pH was reduced to 2. The resulting precipitate was separated by filtration and dried to afford tetraboronic acid 11 (0.35 g, 0.71 mmol, 90%) as a colorless solid. A sample of analytical purity was obtained by crystallization from acetone/hexane: mp >300 °C; IR (KBr) 3400, 2956, 2870, 1606, 1576, 1330 (b), 1252, 824, 717, 675, 627 cm⁻¹; ¹H NMR (400 MHz, DMSO-d₆) δ 7.99 (d, 4H, ³J = 7.6 Hz), 7.89 (s, 8H) 7.86 (d, 4H, ³J = 7.6 Hz), 7.03 (s, 4H); ¹³C NMR (100.1 MHz, DMSO-d₆) δ 64.4, 119.3, 128.8, 133.4, 133.6, 142.7, 147.6. Anal. Calcd for C₂₅H₂₀B₄O₈ • 1.5 H₂O: C, 57.89; H, 4.47. Found: C, 58.28; H, 4.86.

2,2',7,7'-Tetrakis(4-nitrophenyl)-9,9'-spirobi[9H-fluorene] (6). Under N₂, deoxygenated water (30 mL) and DMF (100 mL) were added to a mixture of tetraboronic acid 11 (1.00 g, 2.03 mmol), 4-iodo-1-nitrobenzene (3.10 g, 12.4 mmol), Pd(PPh₃)₄ (0.25 g, 0.22 mmol), and Na₂CO₃ (2.70 g, 25.5 mmol). The mixture was stirred at 80 °C for 7 days and was then extracted thoroughly with CHCl₃. The combined extracts were washed with brine and dried over Na₂SO₄. Volatiles were removed by evaporation under reduced pressure, and the residue was purified by flash chromatography (silica, CHCl₃/hexane) to give 2,2',7,7'-

tetrakis(4-nitrophenyl)-9,9'-spirobi[9H-fluorene] (**6**; 0.801 g, 1.00 mmol, 49%) as an orange solid. A sample of analytical purity was obtained by crystallization from ethyl acetate/hexane: mp > 300 °C; IR (KBr) 3077, 2933, 1725, 1595, 1516, 1463, 1341, 1246, 1108, 1042, 853, 818, 753, 697 cm⁻¹; ¹H NMR (400 MHz, CDCl₃) δ 8.19 (d, 8H, ³J = 8.5 Hz), 8.09 (d, 4H, ³J = 8.0 Hz), 7.77 (d, 4H, ³J = 8.0 Hz), 7.61 (d, 8H, ³J = 8.5 Hz), 7.07 (s, 4H); ¹³C NMR (100.1 MHz, CDCl₃) δ 66.0, 121.3, 122.7, 123.9, 127.6, 127.9, 139.1, 141.6, 146.6, 146.9, 149.4; MS (FAB, 3-nitrobenzyl alcohol) *m/e* 801 (M+1); HRMS (FAB, 3-nitrobenzyl alcohol) calcd for C₄₉H₂₈N₄O₈ + H *m/e* 801.1985, found 801.1939. Anal. Calcd for C₄₉H₂₈N₄O₈ • 6 H₂O: C, 64.75; H, 4.44; N, 6.16. Found: C, 64.43; H, 3.75; N, 6.30.

2,2',7,7'-Tetrakis(4-cyanophenyl)-9,9'-spirobi[9H-fluorene] (7). A similar procedure converted tetraboronic acid **11** (0.300 g, 0.610 mmol) and 4-bromobenzonitrile (0.680 g, 3.74 mmol) into 2,2',7,7'-tetrakis(4-cyanophenyl)-9,9'-spirobi[9H-fluorene] (**7**; 0.247 g, 0.343 mmol, 56%), which was obtained as a beige solid. A sample of analytical purity was obtained by crystallization from dioxane/hexane: mp 157 °C; IR (KBr) 3036, 2927, 2226, 1603, 1464, 1402, 1247, 848, 816, 753, 737 cm⁻¹; ¹H NMR (400 MHz, CDCl₃) δ 8.05 (d, 4H, ³J = 7.8 Hz), 7.72 (d, 4H, ³J = 7.8 Hz), 7.62 (d, 8H, ³J = 7.7 Hz), 7.55 (d, 8H, ³J = 7.7 Hz), 7.01 (s, 4H); ¹³C NMR (100.1 MHz, CDCl₃) δ 66.5, 111.4, 119.2, 121.7, 123.1, 128.0, 128.2, 132.9, 139.9, 141.9, 145.3, 149.9; MS (FAB, 3-nitrobenzyl alcohol) *m/e* 721 (M+1). Anal. Calcd for C₅₃H₂₈N₄ • 0.5 H₂O: C, 87.22; H, 4.01; N, 7.68. Found: C, 87.67; H, 4.14; N, 7.52.

2,2',7,7'-Tetrakis(3-nitrophenyl)-9,9'-spirobi[9H-fluorene] (8). A similar procedure converted tetraboronic acid **11** (1.00 g, 2.03 mmol) and 3-iodo-1-nitrobenzene (3.10 g, 12.4 mmol) into 2,2',7,7'-tetrakis(3-nitrophenyl)-9,9'-spirobi[9H-fluorene] (**8**; 0.711 g, 0.888 mmol, 44%), which was obtained as a yellow solid. A sample of analytical purity was obtained by crystallization from CHCl₃/acetone: mp >300 °C; IR (KBr) 3087, 1525, 1461, 1346, 804, 736 cm⁻¹; ¹H NMR (400 MHz, CDCl₃) δ 8.32 (s, 4H) 8.12-8.08 (m, 8H), 7.81

(d, 4H, $^3J = 7.9$ Hz), 7.77 (d, 4H, $^3J = 7.9$ Hz), 7.51 (t, 4H, $^3J = 8.0$ Hz), 7.06 (s, 4H); ^{13}C NMR (100.1 MHz, CDCl_3) δ 66.1, 121.4, 121.7, 122.0, 122.5, 127.6, 129.5, 133.0, 138.8, 141.3, 142.1, 148.5, 149.4; MS (FAB, 3-nitrobenzyl alcohol) m/e 800; HRMS (FAB, 3-nitrobenzyl alcohol) calcd for $\text{C}_{49}\text{H}_{28}\text{N}_4\text{O}_8$ m/e 800.1907, found 800.1907. Anal. Calcd for $\text{C}_{49}\text{H}_{28}\text{N}_4\text{O}_8 \bullet 1 \text{ H}_2\text{O}$: C, 71.88; H, 3.69; N, 6.84. Found: C, 72.13; H, 3.48; N, 6.76.

2,2',7,7'-Tetrakis(3-cyanophenyl)-9,9'-spirobi[9H-fluorene] (9). A similar procedure converted tetraboronic acid **11** (0.300 g, 0.610 mmol) and 3-bromobenzonitrile (0.680 g, 3.74 mmol) into 2,2',7,7'-tetrakis(3-cyanophenyl)-9,9'-spirobi[9H-fluorene] (**9**; 0.268 g, 0.372 mmol, 61%), which was obtained as a beige solid. A sample of analytical purity was obtained by crystallization from toluene/hexane: mp 150 °C; IR (KBr) 3033, 2926, 2228, 1599, 1581, 1464, 1431, 1406, 1250, 887, 825, 795, 738, 689 cm^{-1} ; ^1H NMR (400 MHz, CDCl_3) δ 8.07 (d, 4H, $^3J = 8.0$ Hz), 7.74-7.69 (m, 12H), 7.54 (d, 4H, $^3J = 7.7$ Hz), 7.45 (t, 4H, $^3J = 7.7$ Hz), 6.99 (s, 4H); ^{13}C NMR (100.1 MHz, CDCl_3) δ 66.5, 113.3, 119.0, 121.7, 122.9, 127.9, 129.9, 131.1, 131.7, 139.5, 141.7, 142.2, 150.0; MS (FAB, 3-nitrobenzyl alcohol) m/e 721 (M+1). Anal. Calcd for $\text{C}_{53}\text{H}_{28}\text{N}_4 \bullet 4.5 \text{ H}_2\text{O}$: C, 79.38; H, 4.65; N, 6.99. Found: C, 79.31; H, 4.78; N, 6.78.

X-ray Crystallographic Studies. X-ray diffraction data were collected with Cu K α radiation using a Bruker SMART 2000 CCD diffractometer. The structures were solved by direct methods using SHELXS-97 and refined with SHELXL-97.²⁶ All non-hydrogen atoms were refined anisotropically, except for those in disordered parts of ethyl acetate included in crystals of compound **6**. Hydrogen atoms were placed in ideal positions and refined as riding atoms.

Structure of 2,2',7,7'-Tetranitro-9,9'-spirobi[9H-fluorene] (4). Crystals of compound **4** proved to belong to the triclinic space group P-1 with $a = 8.7222(2)$ Å, $b = 10.4838(2)$ Å, $c = 16.7599(4)$ Å, $\alpha = 85.288(2)^\circ$, $\beta = 88.006(2)^\circ$, $\gamma = 70.332(2)^\circ$, $V = 1438.23(6)$ Å³, $D_{\text{calcd}} = 1.451$ g/cm³, and $Z = 2$ at 223 K. Full-matrix least-squares refinements on F^2 of 416

parameters led to final residuals $R_1 = 0.0616$ and $wR_2 = 0.1794$ for 5304 observed reflections with $I > 2\sigma(I)$.

Structure of 2,2',7,7'-Tetracyano-9,9'-spirobi[9H-fluorene] (5). Compound **5** crystallized in the monoclinic space group C2/c with $a = 14.0060(3)$ Å, $b = 15.8520(3)$ Å, $c = 14.3180(4)$ Å, $\beta = 99.780(2)^\circ$, $V = 3132.73(13)$ Å³, $D_{\text{calcd}} = 1.389$ g/cm³, and $Z = 4$ at 293 K. Full-matrix least-squares refinements on F^2 of 196 parameters led to final residuals $R_1 = 0.0690$ and $wR_2 = 0.1648$ for 3099 reflections with $I > 2\sigma(I)$.

Structure of 2,2',7,7'-Tetrakis(4-nitrophenyl)-9,9'-spirobi[9H-fluorene] (6). Crystals of compound **6** proved to belong to the triclinic space group P-1 with $a = 16.1160(8)$ Å, $b = 16.2973(8)$ Å, $c = 18.7307(9)$ Å, $\alpha = 64.223(3)^\circ$, $\beta = 69.471(3)^\circ$, $\gamma = 89.408(3)^\circ$, $V = 4089.3(3)$ Å³, $D_{\text{calcd}} = 1.372$ g/cm³, and $Z = 2$ at 223 K. Full-matrix least-squares refinements of 1153 parameters on F^2 led to final residuals $R_1 = 0.0686$ and $wR_2 = 0.1591$ for 14819 reflections with $I > 2\sigma(I)$.

Structure of 2,2',7,7'-Tetrakis(4-cyanophenyl)-9,9'-spirobi[9H-fluorene] (7). Compound **7** crystallized in the triclinic space group P-1 with $a = 13.3274(6)$ Å, $b = 14.2569(7)$ Å, $c = 14.8016(7)$ Å, $\alpha = 93.161(3)^\circ$, $\beta = 98.071(3)^\circ$, $\gamma = 109.723(3)^\circ$, $V = 2605.3(2)$ Å³, $D_{\text{calcd}} = 1.256$ g/cm³, and $Z = 2$ at 223 K. Full-matrix least-squares refinements on F^2 of 695 parameters led to final residuals $R_1 = 0.0567$ and $wR_2 = 0.1776$ for 9617 reflections with $I > 2\sigma(I)$.

Structure of 2,2',7,7'-Tetrakis(3-nitrophenyl)-9,9'-spirobi[9H-fluorene] (8). Crystals of compound **8** proved to belong to the tetragonal space group I4₁/a with $a = b = 12.3873(3)$ Å, $c = 24.1863(7)$ Å, $V = 3711.27(17)$ Å³, $D_{\text{calcd}} = 1.433$ g/cm³, and $Z = 4$ at 223 K. Full-matrix least-squares refinements on F^2 of 167 parameters led to final residuals $R_1 = 0.0429$ and $wR_2 = 0.1096$ for 1760 reflections with $I > 2\sigma(I)$.

Structure of 2,2',7,7'-Tetrakis(3-cyanophenyl)-9,9'-spirobi[9H-fluorene] (9).

Compound **9** crystallized in the tetragonal space group I4₁/a with $a = b = 13.2114(9)$ Å, $c = 21.539(3)$ Å, $V = 3759.4(6)$ Å³, $D_{\text{calcd}} = 1.274$ g/cm³, and $Z = 4$ at 223 K. Full-matrix least-squares refinements on F^2 of 129 parameters led to final residuals $R_1 = 0.0629$ and $wR_2 = 0.1509$ for 1780 reflections with $I > 2\sigma(I)$.

Acknowledgment. We are grateful to the Natural Sciences and Engineering Research Council of Canada, the Ministère de l'Éducation du Québec, the Canada Foundation for Innovation, the Canada Research Chairs Program, and Merck Frosst for financial support.

Supporting Information Available: ORTEP drawings and tables in CIF format for crystallographic data, atomic coordinates, anisotropic thermal parameters, and bond lengths and angles (including weak interactions) for compounds **4-9**. This material is available free of charge via the Internet at <http://pubs.acs.org>.

Notes and References

1. Fellow of the Ministère de l'Éducation du Québec, 2002-2004. Fellow of the Natural Sciences and Engineering Research Council of Canada, 2000-2002.
2. Fellow of the Natural Sciences and Engineering Research Council of Canada, 2003.
3. Fellow of the Ministère de l'Éducation du Québec, 2000-2002. Fellow of the Natural Sciences and Engineering Research Council of Canada, 1998-2000.
4. For recent reviews, see: Price, S. L. *Adv. Drug Deliv. Rev.* **2004**, *56*, 301. Price, S. L. *CrystEngComm* **2004**, *6*, 344.
5. Dunitz, J. D. *Chem. Commun.* **2003**, 545. Desiraju, G. R. *Nature Materials* **2002**, *1*, 77. Gavezzotti, A. *Acc. Chem. Res.* **1994**, *27*, 309. Maddox, J. *Nature* **1988**, *335*, 201.
6. Simard, M.; Su, D.; Wuest, J. D. *J. Am. Chem. Soc.* **1991**, *113*, 4696.
7. For recent references, see: Laliberté, D.; Maris, T.; Wuest, J. D. *J. Org. Chem.* **2004**, *69*, 1776. Laliberté, D.; Maris, T.; Wuest, J. D. *Can. J. Chem.* **2004**, *82*, 386. Le Fur, E.; Demers, E.; Maris, T.; Wuest, J. D. *Chem. Commun.* **2003**, 2966. Saied, O.; Maris, T.; Wuest, J. D. *J. Am. Chem. Soc.* **2003**, *125*, 14956. Fournier, J.-H.; Maris, T.; Wuest, J. D.; Guo, W.; Galoppini, E. *J. Am. Chem. Soc.* **2003**, *125*, 1002. Laliberté, D.; Maris, T.; Sirois, A.; Wuest, J. D. *Org. Lett.* **2003**, *5*, 4787. Sauriat-Dorizon, H.; Maris, T.; Wuest, J. D.; Enright, G. D. *J. Org. Chem.* **2003**, *68*, 240. Brunet, P.; Demers, E.; Maris, T.; Enright, G. D.; Wuest, J. D. *Angew. Chem., Int. Ed.* **2003**, *42*, 5303. Fournier, J.-H.; Maris, T.; Simard, M.; Wuest, J. D. *Cryst. Growth Des.* **2003**, *3*, 535.
8. Fournier, J.-H.; Maris, T.; Wuest, J. D. *J. Org. Chem.* **2004**, *69*, 1762.
9. For other recent studies in which molecules designed to associate by hydrogen bonding have been used in crystal engineering, see: Uemura, K.; Kitagawa, S.; Fukui, K.; Saito, K. *J. Am. Chem. Soc.* **2004**, *126*, 3817. Sada, K.; Inoue, K.; Tanaka, T.; Tanaka, A.; Epergyes, A.; Nagahama, S.; Matsumoto, A.; Miyata, M. *J. Am. Chem. Soc.* **2004**, *126*, 1764. Maspoch, D.; Domingo, N.; Ruiz-Molina, D.; Wurst, K.; Tejada, J.; Rovira, C.; Veciana, J. *J. Am. Chem. Soc.* **2004**, *126*, 730. Baudron, S. A.; Avarvari, N.; Canadell, E.; Auban-Senzier, P.; Batail, P. *Chem. Eur. J.* **2004**, *10*, 4498. Angeloni, A.;

Crawford, P. C.; Orpen, A. G.; Podesta, T. J.; Shore, B. J. *Chem. Eur. J.* **2004**, *10*, 3783. Murata, T.; Morita, Y.; Fukui, K.; Sato, K.; Shiomi, D.; Takui, T.; Maesato, M.; Yamochi, H.; Saito, G.; Nakasuji, K. *Angew. Chem., Int. Ed.* **2004**, *43*, 6343. Soldatov, D. V.; Moudrakovski, I. L.; Ripmeester, J. A. *Angew. Chem., Int. Ed.* **2004**, *43*, 6308. Du, Y.; Creighton, C. J.; Toungle, B. A.; Reitz, A. B. *Org. Lett.* **2004**, *6*, 309. Bhogala, B. R.; Vangala, V. R.; Smith, P. S.; Howard, J. A. K.; Desiraju, G. R. *Cryst. Growth Des.* **2004**, *4*, 647. Balasubramaniam, V.; Wong, L. G. J.; Vittal, J. J.; Valiyaveettil, S. *Cryst. Growth Des.* **2004**, *4*, 553. Dale, S. H.; Elsegood, M. R. J.; Coombs, A. E. L. *CrystEngComm* **2004**, *6*, 328. Hosseini, M. W. *CrystEngComm* **2004**, *6*, 318. Vinodu, M.; Goldberg, I. *CrystEngComm* **2004**, *6*, 215. Aakeröy, C. B.; Desper, J.; Helfrich, B. A. *CrystEngComm* **2004**, *6*, 19. Alshahateet, S. F.; Nakano, K.; Bishop, R.; Craig, D. C.; Harris, K. D. M.; Scudder, M. L. *CrystEngComm* **2004**, *6*, 5. Brown, R. J.; Camarasa, G.; Griffiths, J.-P.; Day, P.; Wallis, J. D. *Tetrahedron Lett.* **2004**, *45*, 5103. Pedireddi, V. R.; SeethaLekshmi, N. *Tetrahedron Lett.* **2004**, *45*, 1903. Martin, S. M.; Yonezawa, J.; Horner, M. J.; Macosko, C. W.; Ward, M. D. *Chem. Mater.* **2004**, *16*, 3045. Shimizu, L. S.; Hughes, A. D.; Smith, M. D.; Davis, M. J.; Zhang, B. P.; zur Loya, H.-C.; Shimizu, K. D. *J. Am. Chem. Soc.* **2003**, *125*, 14972. Ouyang, X.; Fowler, F. W.; Lauher, J. W. *J. Am. Chem. Soc.* **2003**, *125*, 12400. Kobayashi, K.; Sato, A.; Sakamoto, S.; Yamaguchi, K. *J. Am. Chem. Soc.* **2003**, *125*, 3035. Rakotondradany, F.; Whitehead, M. A.; Lebuis, A.-M.; Sleiman, H. F. *Chem. Eur. J.* **2003**, *9*, 4771. Jagadish, B.; Carducci, M. D.; Bosshard, C.; Günter, P.; Margolis, J. I.; Williams, L. J.; Mash, E. A. *Cryst. Growth Des.* **2003**, *3*, 811. Bhogala, B. R.; Nangia, A. *Cryst. Growth Des.* **2003**, *3*, 547. Olenik, B.; Smolka, T.; Boese, R.; Sustmann, R. *Cryst. Growth Des.* **2003**, *3*, 183. Kitamura, M.; Nakano, K. *Cryst. Growth Des.* **2003**, *3*, 25. Ma, B.-Q.; Coppens, P. *Chem. Commun.* **2003**, 2290. Yagai, S.; Karatsu, T.; Kitamura, A. *Chem. Commun.* **2003**, 1844. Walsh, R. D. B.; Bradner, M. W.; Fleischman, S.; Morales, L. A.; Moulton, B.; Rodríguez-Hornedo, R.; Zaworotko, M. J. *Chem. Commun.* **2003**, 186. Blay, G.; Fernández, I.; Pedro, J. R.; Ruiz-García, R.; Muñoz, M. C.; Cano, J.; Carrasco, R. *Eur. J. Org. Chem.* **2003**, 1627. Braga, D.; Polito, M.; Bracaccini, M.; D'Addario, D.; Tagliavini, E.; Sturba, L. *Organometallics* **2003**, *22*,

2142. Roesky, H. W.; Andruh, M. *Coord. Chem. Rev.* **2003**, *236*, 91. Ermer, O.; Kusch, A.; Röbke, C. *Helv. Chim. Acta* **2003**, *86*, 922. Arora, K. K.; Pedireddi, V. R. *J. Org. Chem.* **2003**, *68*, 9177. Wen, J.-F.; Hong, W.; Yuan, K.; Mak, T. C. W.; Wong, H. N. C. *J. Org. Chem.* **2003**, *68*, 8918. Moon, K.; Chen, W.-Z.; Ren, T.; Kaifer, A. E. *CrystEngComm* **2003**, *5*, 451. Trivedi, D. R.; Ballabh, A.; Dastidar, P. *CrystEngComm* **2003**, *5*, 358. Burke, N. J.; Burrows, A. D.; Mahon, M. F.; Pritchard, L. S. *CrystEngComm* **2003**, *5*, 355. Pérez, C.; Rodríguez, M. L.; Foces-Foces, C.; Pérez-Hernández, N.; Pérez, R.; Martín, J. D. *Org. Lett.* **2003**, *5*, 641. Shan, N.; Bond, A. D.; Jones, W. *New J. Chem.* **2003**, *27*, 365. Kobayashi, N.; Naito, T.; Inabe, T. *Bull. Chem. Soc. Jpn.* **2003**, *76*, 1351. Görbitz, C. H. *Acta Crystallogr.* **2002**, *B58*, 849. Tanaka, T.; Tasaki, T.; Aoyama, Y. *J. Am. Chem. Soc.* **2002**, *124*, 12453. Moorthy, J. N.; Natarajan, R.; Mal, P.; Venugopalan, P. *J. Am. Chem. Soc.* **2002**, *124*, 6530. Archer, E. A.; Krische, M. J. *J. Am. Chem. Soc.* **2002**, *124*, 5074. Kim, S.; Bishop, R.; Craig, D. C.; Dance, I. G.; Scudder, M. L. *J. Org. Chem.* **2002**, *67*, 3221. Lyssenko, K. A.; Lenev, D. A.; Kostyanovsky, R. G. *Tetrahedron* **2002**, *58*, 8525. Beatty, A. M.; Schneider, C. M.; Simpson, A. E.; Zaher, J. L. *CrystEngComm* **2002**, *4*, 282. Field, J. E.; Combariza, M. Y.; Vachet, R. W.; Venkataraman, D. *Chem. Commun.*, **2002**, 2260. Gauthier, D.; Baillargeon, P.; Drouin, M.; Dory, Y. L. *Angew. Chem., Int. Ed.* **2001**, *40*, 4635. Hong, B. H.; Lee, J. Y.; Lee, C.-W.; Kim, J. C.; Bae, S. C.; Kim, K. S. *J. Am. Chem. Soc.* **2001**, *123*, 10748. Papaefstathiou, G. S.; MacGillivray, L. R. *Org. Lett.* **2001**, *3*, 3835. Zaman, M. B.; Tomura, M.; Yamashita, Y. *J. Org. Chem.* **2001**, *66*, 5987. Dapporto, P.; Paoli, P.; Roelens, S. *J. Org. Chem.* **2001**, *66*, 4930. Vaid, T. P.; Sydora, O. L.; Douthwaite, R. E.; Wolczanski, P. T.; Lobkovsky, E. B. *Chem. Commun.* **2001**, 1300. Sharma, C. V. K.; Clearfield, A. *J. Am. Chem. Soc.* **2000**, *122*, 4394. Corbin, P. S.; Zimmerman, S. C. *J. Am. Chem. Soc.* **2000**, *122*, 3779. Cantrill, S. J.; Pease, A. R.; Stoddart, J. F. *J. Chem. Soc., Dalton Trans.* **2000**, 3715. Videnova-Adrabińska, V.; Janeczko, E. *J. Mater. Chem.* **2000**, *10*, 555. Akazome, M.; Suzuki, S.; Shimizu, Y.; Henmi, K.; Ogura, K. *J. Org. Chem.* **2000**, *65*, 6917. Baumeister, B.; Matile, S. *Chem. Commun.* **2000**, 913. Chowdhry, M. M.; Mingos, D. M. P.; White, A. J. P.; Williams, D. J. *J. Chem. Soc., Perkin Trans. 1* **2000**, 3495. Gong, B.; Zheng, C.;

- Skrzypczak-Jankun, E.; Zhu, J. *Org. Lett.* **2000**, *2*, 3273. Krische, M. J.; Lehn, J.-M.; Kyritsakas, N.; Fischer, J.; Wegelius, E. K.; Rissanen, K. *Tetrahedron* **2000**, *56*, 6701. Fuchs, K.; Bauer, T.; Thomann, R.; Wang, C.; Friedrich, C.; Mülhaupt, R. *Macromolecules* **1999**, *32*, 8404. Holý, P.; Závada, J.; Císařová, I.; Podlaha, J. *Angew. Chem., Int. Ed.* **1999**, *38*, 381. Karle, I. L.; Ranganathan, D.; Kurur, S. *J. Am. Chem. Soc.* **1999**, *121*, 7156. Chin, D. N.; Palmore, G. T. R.; Whitesides, G. M. *J. Am. Chem. Soc.* **1999**, *121*, 2115. Hanessian, S.; Saladino, R.; Margarita, R.; Simard, M. *Chem. Eur. J.* **1999**, *5*, 2169.
10. For a review of hydrogen bonding in the solid state, see: Steiner, T. *Angew. Chem., Int. Ed.* **2002**, *41*, 48.
 11. For recent reviews, see: James, S. L. *Chem. Soc. Rev.* **2003**, *32*, 276. Yaghi, O. M.; O'Keeffe, M.; Ockwig, N. W.; Chae, H. K.; Eddaoudi, M.; Kim, J. *Nature* **2003**, *423*, 705.
 12. For a review of molecular networks, see: Moulton, B.; Zaworotko, M. J. *Chem. Rev.* **2001**, *101*, 1629.
 13. For reviews of weak interactions, see: Desiraju, G. R. *Acc. Chem. Res.* **2002**, *35*, 565. Desiraju, G. R.; Steiner, T. *The Weak Hydrogen Bond in Structural Chemistry and Biology*; Oxford University Press: Oxford, 1999.
 14. For a review of aromatic interactions, see: Hunter, C. A.; Lawson, K. R.; Perkins, J.; Urch, C. J. *J. Chem. Soc., Perkin Trans. 2* **2001**, 651.
 15. Thaimattam, R.; Xue, F.; Sarma, J. A. R. P.; Mak, T. C. W.; Desiraju, G. R. *J. Am. Chem. Soc.* **2001**, *123*, 4432.
 16. Basavoju, S.; Aitipamula, S.; Desiraju, G. R. *CrystEngComm.* **2004**, *6*, 120.
 17. For recent related studies of weak interactions in the solid state, see: Choudhury, A. R.; Islam, K.; Kirchner, M. T.; Mehta, G.; Guru Row, T. N. *J. Am. Chem. Soc.* **2004**, *126*, 12274. Kumar, V. S. S.; Pigge, F. C.; Rath, N. P. *Cryst. Growth Des.* **2004**, *4*, 1217. Alshahateet, S. F.; Bishop, R.; Craig, D. C.; Scudder, M. L. *Cryst. Growth Des.* **2004**, *4*, 837. Arora, K. K.; Pedireddi, V. R. *Tetrahedron* **2004**, *60*, 919. Xu, W.; Lu, Y.-X.; Liu, C.-M.; Guo, P.; Lan, B.-J.; Zhou, H. *Acta Crystallogr.* **2004**, *E60*, o1049.

18. a) The composition was determined by X-ray crystallography. b) The composition was estimated by X-ray crystallography and by ^1H NMR spectroscopy of dissolved samples.
19. The dimensions of a channel in a particular direction correspond to those of an imaginary cylinder that could be passed through the hypothetical open network in the given direction in contact with the van der Waals surface. Such values are inherently conservative because 1) they measure the cross section at the most narrow constriction, and 2) they systematically underestimate the sizes of channels that are not uniform and linear.
20. The percentage of volume accessible to guests was estimated by the PLATON program.²¹ PLATON calculates the accessible volume by allowing a spherical probe of variable radius to roll over the internal van der Waals surface of the crystal structure. PLATON uses a default value of 1.20 Å for the radius of the probe, which is an appropriate model for small guests such as water. The van der Waals radii used to define surfaces for these calculations are as follows: C: 1.70 Å, H: 1.20 Å, N: 1.55 Å, and O: 1.52 Å. If V is the volume of the unit cell and V_g is the guest-accessible volume as calculated by PLATON, then the porosity P in % is given by $100V_g/V$.
21. Spek, A. L. *PLATON, A Multipurpose Crystallographic Tool*; Utrecht University: Utrecht, The Netherlands, 2001. van der Sluis, P.; Spek, A. L. *Acta Crystallogr.* **1990**, *A46*, 194.
22. C-H···N interactions are considered significant if they have H···N distances less than or equal to 2.65 Å.
23. Wu, R.; Schumm, J. S.; Pearson, D. L.; Tour, J. M. *J. Org. Chem.* **1996**, *61*, 6906.
24. Other C-H···O interactions can be considered to be present if the criteria are changed and longer H···O distances are accepted. If allowable H···O distances can reach 2.70 Å, then molecule **A** would have C-H···O interactions with 6 neighbors and molecule **B** with 8 neighbors (see Supporting Information).
25. For discussions of interpenetration in networks, see: Batten, S. R. *CrystEngComm* **2001**, *18*, 1. Batten, S. R.; Robson, R. *Angew. Chem., Int. Ed.* **1998**, *37*, 1460.

-
26. Sheldrick, G. M. *SHELXS-97, Program for the Solution of Crystal Structures and SHELXL-97, Program for the Refinement of Crystal Structures*; Universität Göttingen: Germany, 1997.

Figure 1. Selected C-H···O and C-H···N interactions in nitroarenes and benzonitriles.

Figure 2. View of the structure of crystals of 2,2',7,7'-tetranitro-9,9'-spirobi[9H-fluorene] (**4**) grown from dioxane/toluene, showing a central molecule (gray) and the four neighbors linked by C-H···O interactions involving nitro groups. Included molecules of dioxane are omitted for clarity. The central molecule 1) forms a cyclic pair of C-H···O interactions of type I (Figure 1) with one neighbor (blue); 2) serves as both donor and acceptor in single C-H···O interactions of type II (Figure 1) with two other neighbors (red); and 3) acts as both donor and acceptor in C-H···O interactions of type II (Figure 1) with a fourth neighbor (green). C-H···O interactions are represented by broken lines.

Figure 3. View along the *c* axis of the network formed by 2,2',7,7'-tetranitro-9,9'-spirobi[9H-fluorene] (**4**), showing a $4 \times 4 \times 3$ array of unit cells. Guests are omitted, and atoms are represented by spheres of van der Waals radii to show the cross sections of the channels. Atoms of carbon appear in gray, hydrogen in white, nitrogen in blue, and oxygen in red.

Figure 4. View along the *c* axis of the network formed by crystallizing 2,2',7,7'-tetracyano-9,9'-spirobi[9H-fluorene] (**5**) from CHCl₃/hexane, showing a $3 \times 3 \times 3$ array of unit cells. Guests are omitted, and atoms are represented by spheres of van der Waals radii to show the cross sections of the channels. Atoms of carbon appear in gray, hydrogen in white, and nitrogen in blue.

Figure 5. (a) Representation of π -stacking of a central molecule of 2,2',7,7'-tetracyano-9,9'-spirobi[9H-fluorene] (**5**) (shown in red) with two neighbors. (b) Representation of the resulting network, with π -stacking shown as straight red lines intersecting at the centers of neighboring molecules.

Figure 6. Views of the structure of crystals of 2,2',7,7'-tetrakis(4-nitrophenyl)-9,9'-spirobi[9H-fluorene] (**6**) grown from ethyl acetate/hexane, showing the two symmetry-independent molecules **A** (red) and **B** (blue) in the unit cell. Included molecules of ethyl acetate are omitted for clarity. (a) Aryl-aryl interactions between molecule **A** (red) and four neighbors (green) satisfying the condition that the centroids of the interacting phenyl rings are separated by less than 4.5 Å. (b) Molecule **B** (blue) and the five neighbors (green) that satisfy the same condition. Note that one of the neighbors is hidden behind molecule **B** and is not visible. (c) C-H···O interactions (largely type III) between molecule **A** (red) and four neighbors (green) with H···O distances less than or equal to 2.65 Å. The C-H···O interactions are represented by broken lines. (d) Similar view of C-H···O interactions (types II and III) involving molecule **B** (blue) and four neighbors (green).

Figure 7. View along the *b* axis of the network formed by crystallizing 2,2',7,7'-tetrakis(4-cyanophenyl)-9,9'-spirobi[9H-fluorene] (**7**) from dioxane/hexane, showing a $4 \times 2 \times 3$ array of unit cells. Guests are omitted, and atoms are represented by spheres of van der Waals radii to show the cross sections of the channels. Atoms of carbon appear in gray, hydrogen in white, and nitrogen in blue.

Figure 8. Representation of the principal aryl-aryl interactions between a central molecule of 2,2',7,7'-tetrakis(4-cyanophenyl)-9,9'-spirobi[9H-fluorene] (**7**) (shown in red) and three neighbors (green) satisfying the condition that the centroids of the interacting phenyl rings are separated by less than 4.5 Å.

Figure 9. Views of the closely related structures of crystals of 2,2',7,7'-tetrakis(3-nitrophenyl)-9,9'-spirobi[9H-fluorene] (**8**) and 2,2',7,7'-tetrakis(3-cyanophenyl)-9,9'-spirobi[9H-fluorene] (**9**), grown from CHCl₃/acetone and toluene/hexane, respectively. **(a)** Aryl-aryl interactions involving a central molecule of compound **8** (red) with four neighbors (green) satisfying the condition that the centroids of the interacting phenyl rings are separated by less than 4.5 Å. **(b)** C-H···O interactions (types III-IV) between a central molecule of compound **8** (red) and the four neighbors that also have aryl-aryl interactions (green), as well as those involving a second set of four neighbors (blue). C-H···O interactions are represented by broken lines. Together, the red and green molecules define a non-interpenetrated diamondoid network, and the red and blue molecules describe a diamond network with five-fold interpenetration. **(c)** Similar view of aryl-aryl interactions involving a central molecule of compound **9** (red) and its four neighbors (green). **(d)** Non-interpenetrated diamondoid network defined by connecting the centers of molecules of compound **9** linked by aryl-aryl interactions.

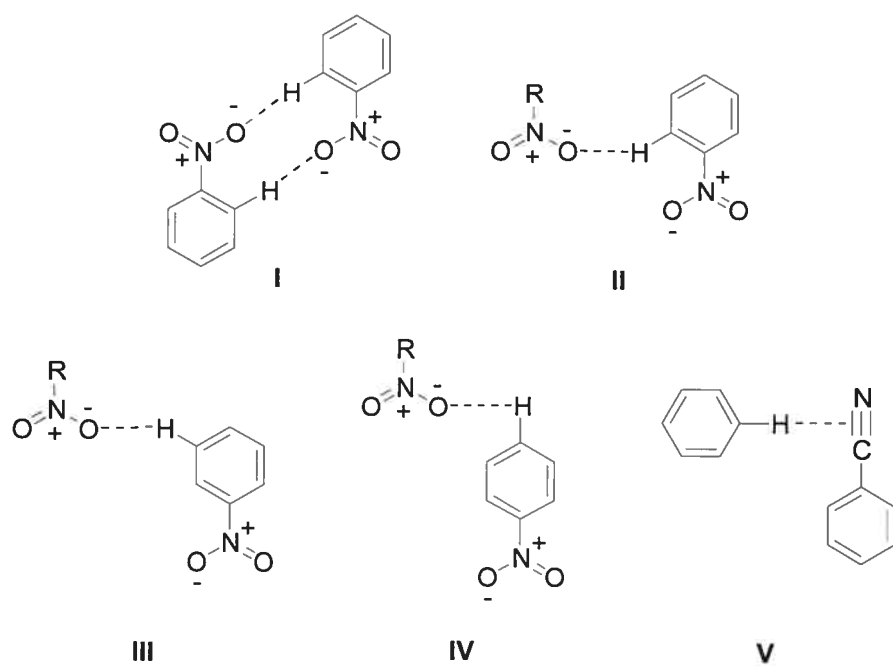


Figure 1. Selected C-H...O and C-H...N interactions in nitroarenes and benzonitriles.

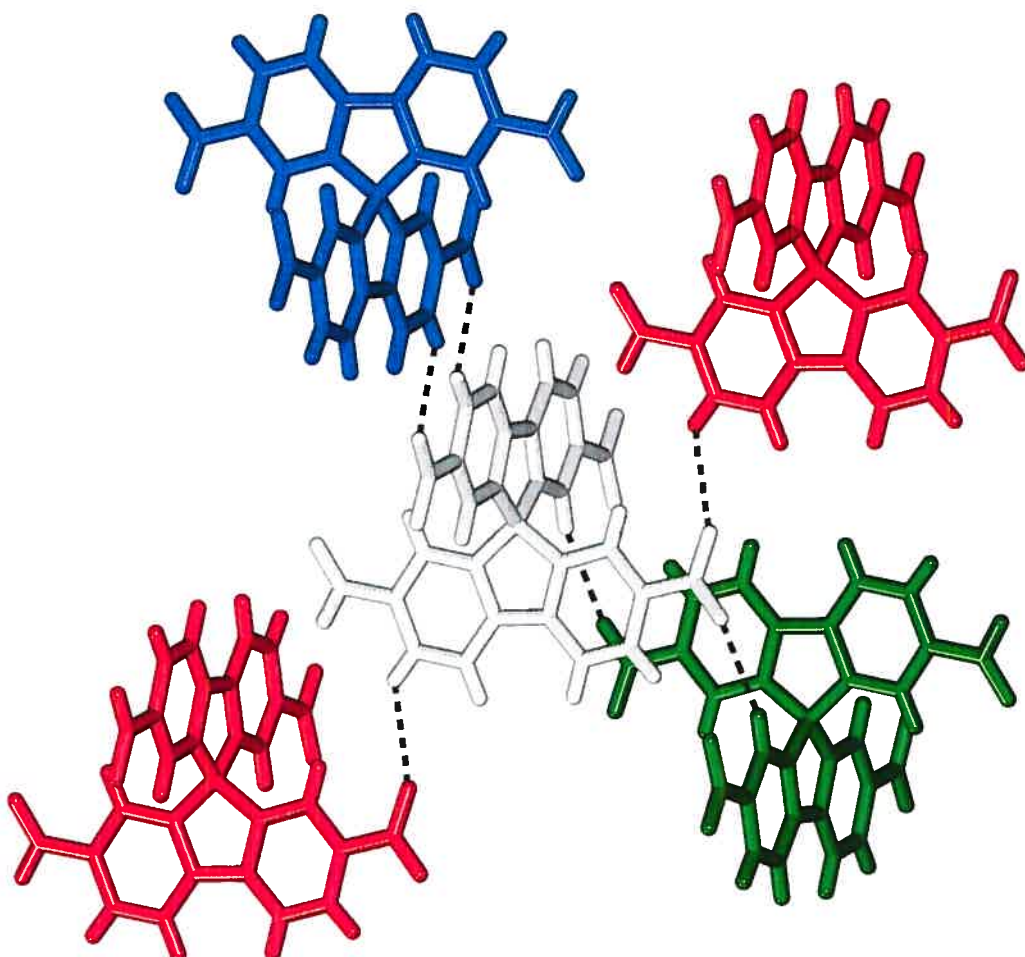


Figure 2. View of the structure of crystals of 2,2',7,7'-tetranitro-9,9'-spirobi[9H-fluorene] (4) grown from dioxane/toluene, showing a central molecule (gray) and the four neighbors linked by C-H...O interactions involving nitro groups. Included molecules of dioxane are omitted for clarity. The central molecule 1) forms a cyclic pair of C-H...O interactions of type I (Figure 1) with one neighbor (blue); 2) serves as both donor and acceptor in single C-H...O interactions of type II (Figure 1) with two other neighbors (red); and 3) acts as both donor and acceptor in C-H...O interactions of type II (Figure 1) with a fourth neighbor (green). C-H...O interactions are represented by broken lines.

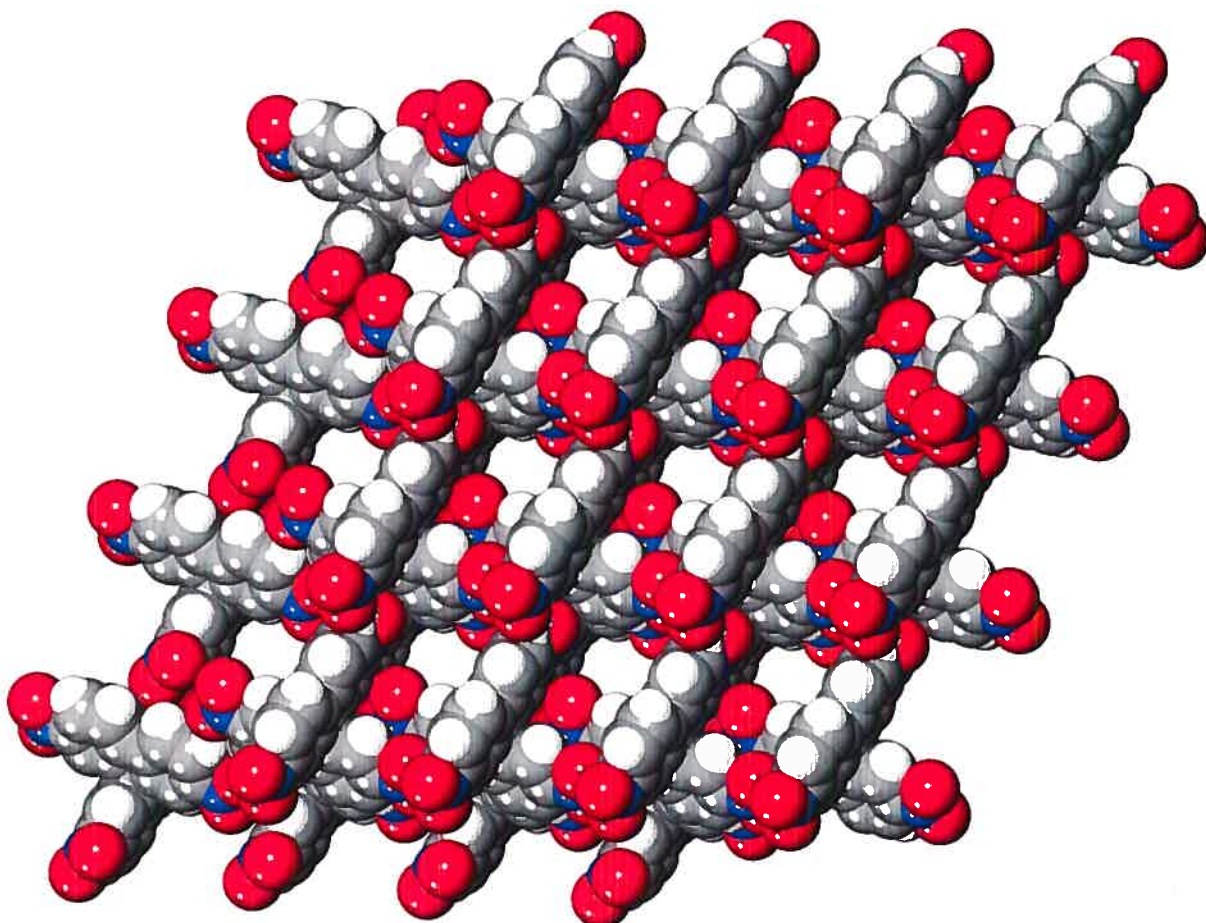


Figure 3. View along the *c* axis of the network formed by 2,2',7,7'-tetrtnitro-9,9'-spirobi[9H-fluorene] (**4**), showing a $4 \times 4 \times 3$ array of unit cells. Guests are omitted, and atoms are represented by spheres of van der Waals radii to show the cross sections of the channels. Atoms of carbon appear in gray, hydrogen in white, nitrogen in blue, and oxygen in red.

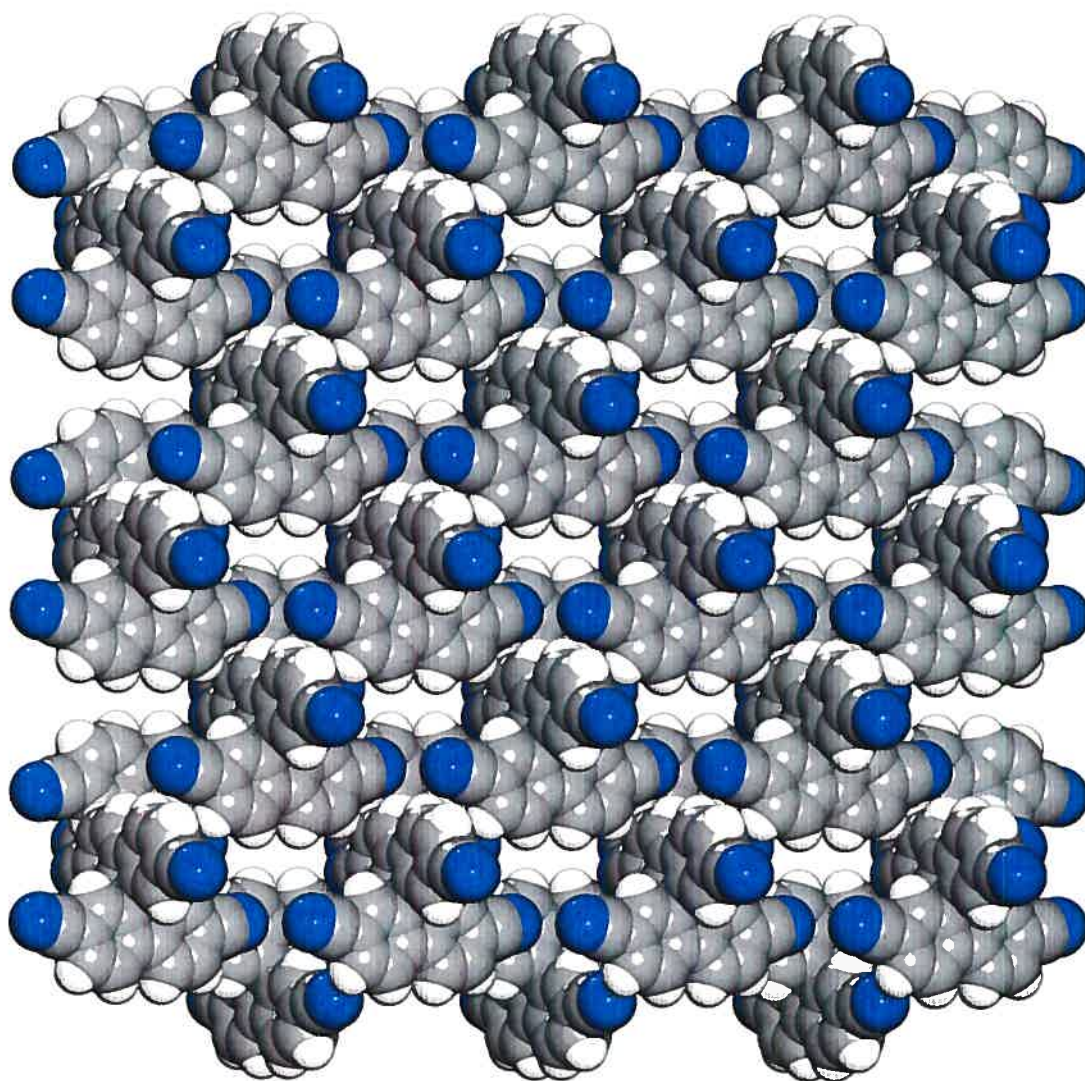


Figure 4. View along the c axis of the network formed by crystallizing 2,2',7,7'-tetracyano-9,9'-spirobi[9H-fluorene] (**5**) from $\text{CHCl}_3/\text{hexane}$, showing a $3 \times 3 \times 3$ array of unit cells. Guests are omitted, and atoms are represented by spheres of van der Waals radii to show the cross sections of the channels. Atoms of carbon appear in gray, hydrogen in white, and nitrogen in blue.

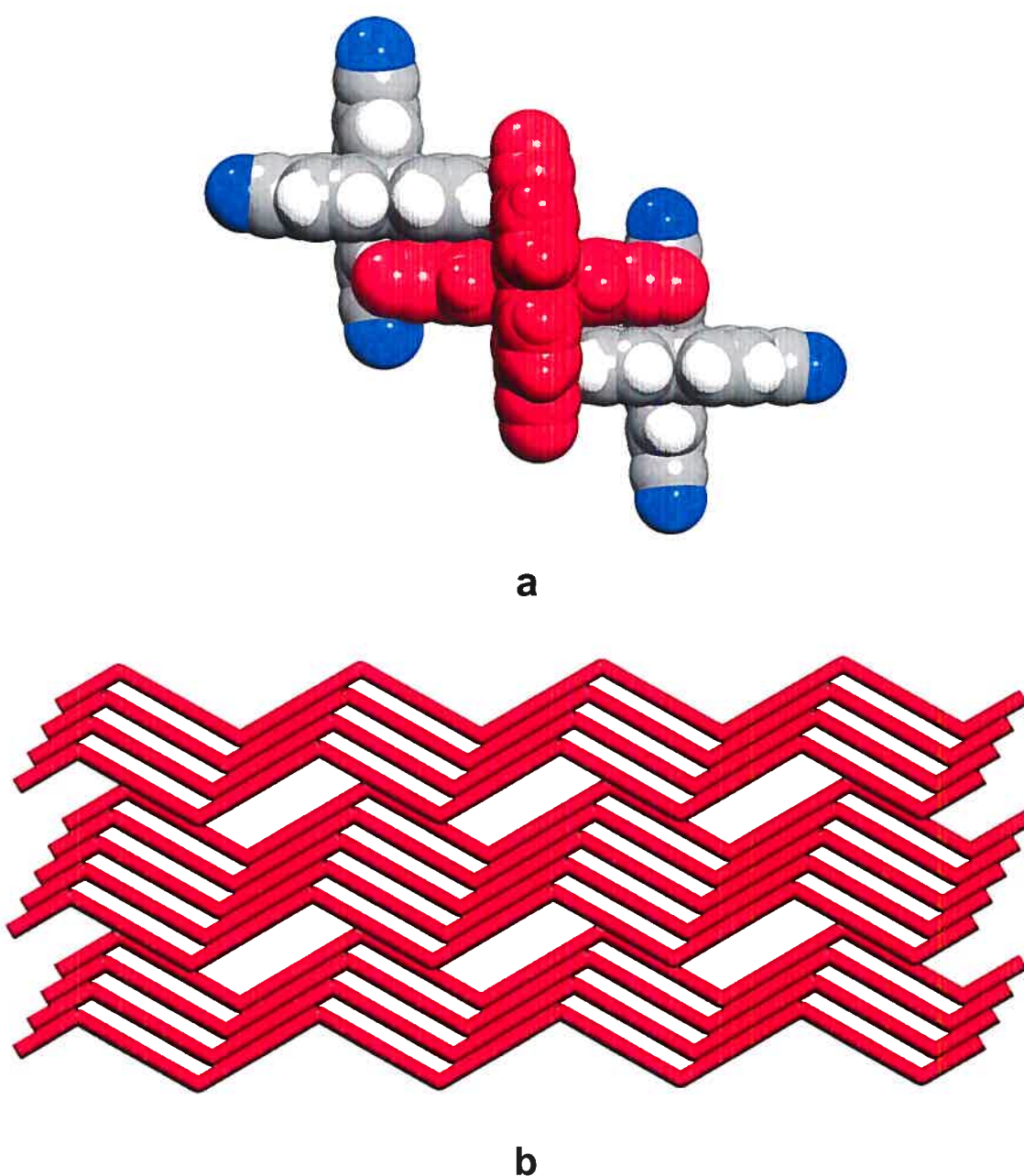


Figure 5. (a) Representation of π -stacking of a central molecule of 2,2',7,7'-tetracyano-9,9'-spirobi[9H-fluorene] (5) (shown in red) with two neighbors. (b) Representation of the resulting network, with π -stacking shown as straight red lines intersecting at the centers of neighboring molecules.

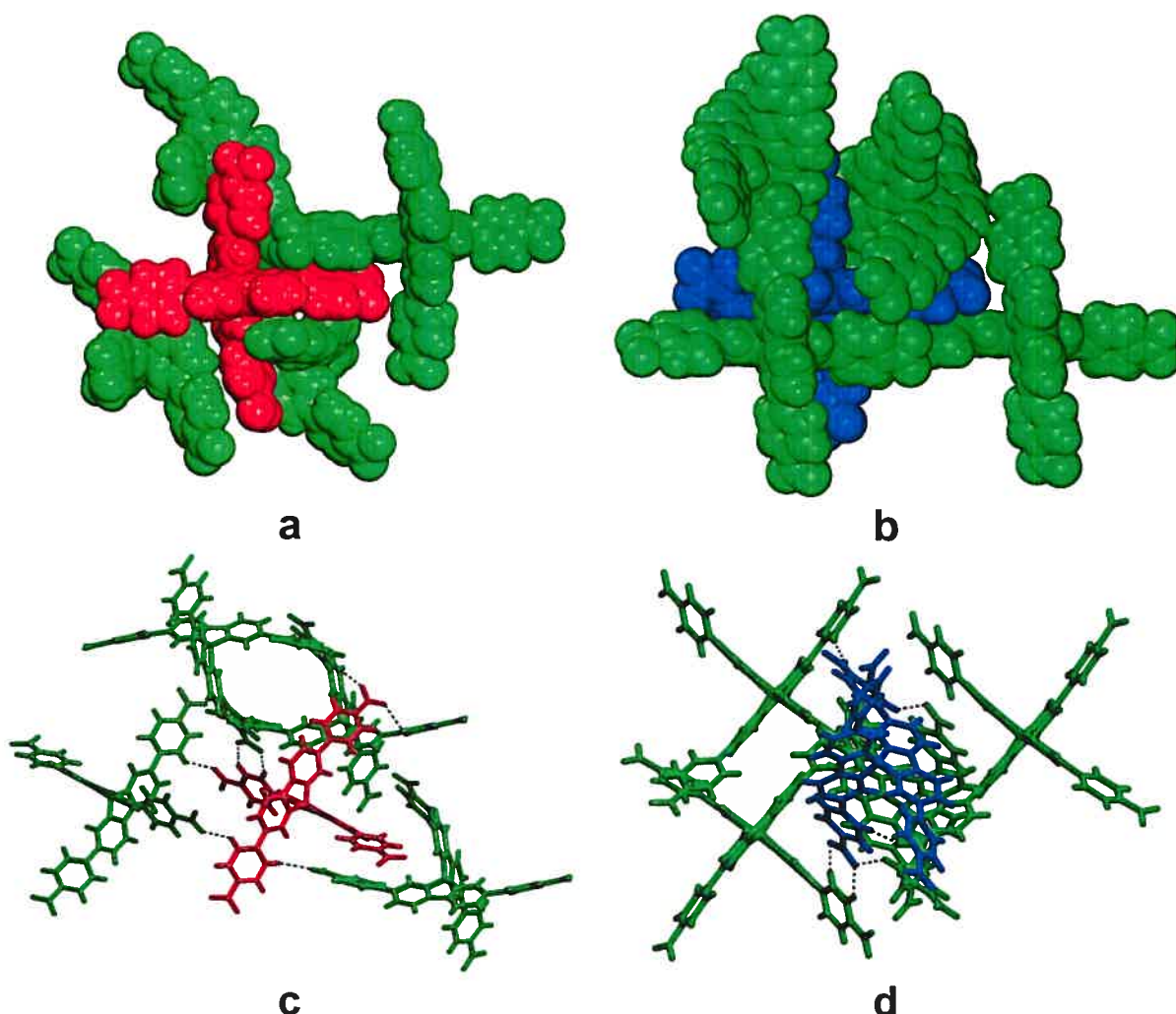


Figure 6. Views of the structure of crystals of 2,2',7,7'-tetrakis(4-nitrophenyl)-9,9'-spirobi[9H-fluorene] (**6**) grown from ethyl acetate/hexane, showing the two symmetry-independent molecules **A** (red) and **B** (blue) in the unit cell. Included molecules of ethyl acetate are omitted for clarity. **(a)** Aryl-aryl interactions between molecule **A** (red) and four neighbors (green) satisfying the condition that the centroids of the interacting phenyl rings are separated by less than 4.5 Å. **(b)** Molecule **B** (blue) and the five neighbors (green) that satisfy the same condition. Note that one of the neighbors is hidden behind molecule **B** and is not visible. **(c)** C-H···O interactions (largely type III) between molecule **A** (red) and four neighbors (green) with H···O distances less than or equal to 2.65 Å. The C-H···O interactions are represented by broken lines. **(d)** Similar view of C-H···O interactions (types II and III) involving molecule **B** (blue) and four neighbors (green).

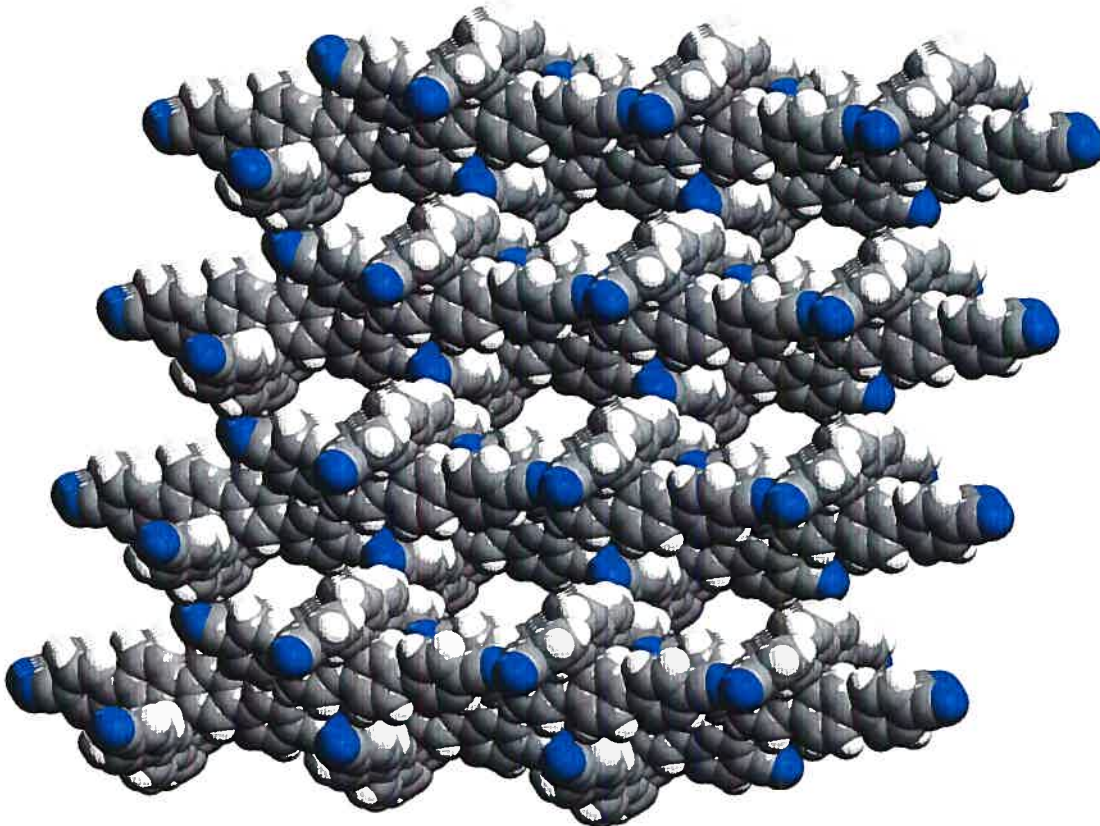


Figure 7. View along the *b* axis of the network formed by crystallizing 2,2',7,7'-tetrakis(4-cyanophenyl)-9,9'-spirobi[9H-fluorene] (**7**) from dioxane/hexane, showing a $4 \times 2 \times 3$ array of unit cells. Guests are omitted, and atoms are represented by spheres of van der Waals radii to show the cross sections of the channels. Atoms of carbon appear in gray, hydrogen in white, and nitrogen in blue.

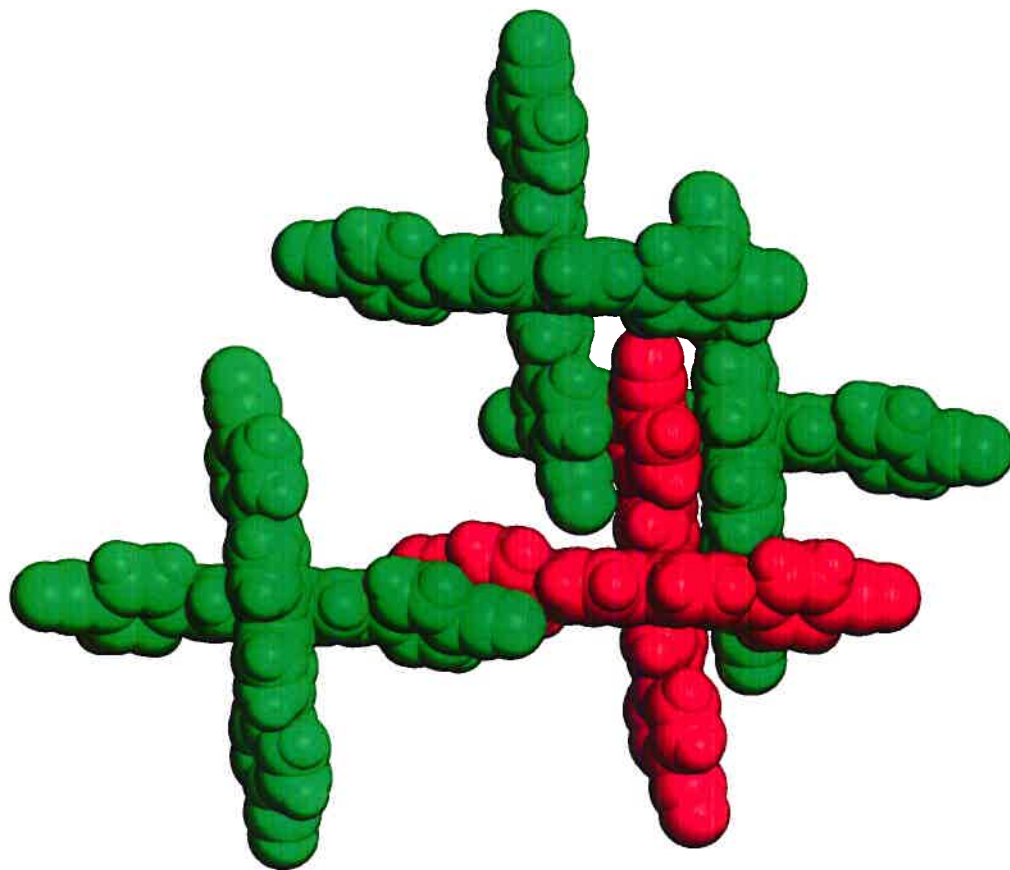


Figure 8. Representation of the principal aryl-aryl interactions between a central molecule of 2,2',7,7'-tetrakis(4-cyanophenyl)-9,9'-spirobi[9H-fluorene] (7) (shown in red) and three neighbors (green) satisfying the condition that the centroids of the interacting phenyl rings are separated by less than 4.5 Å.

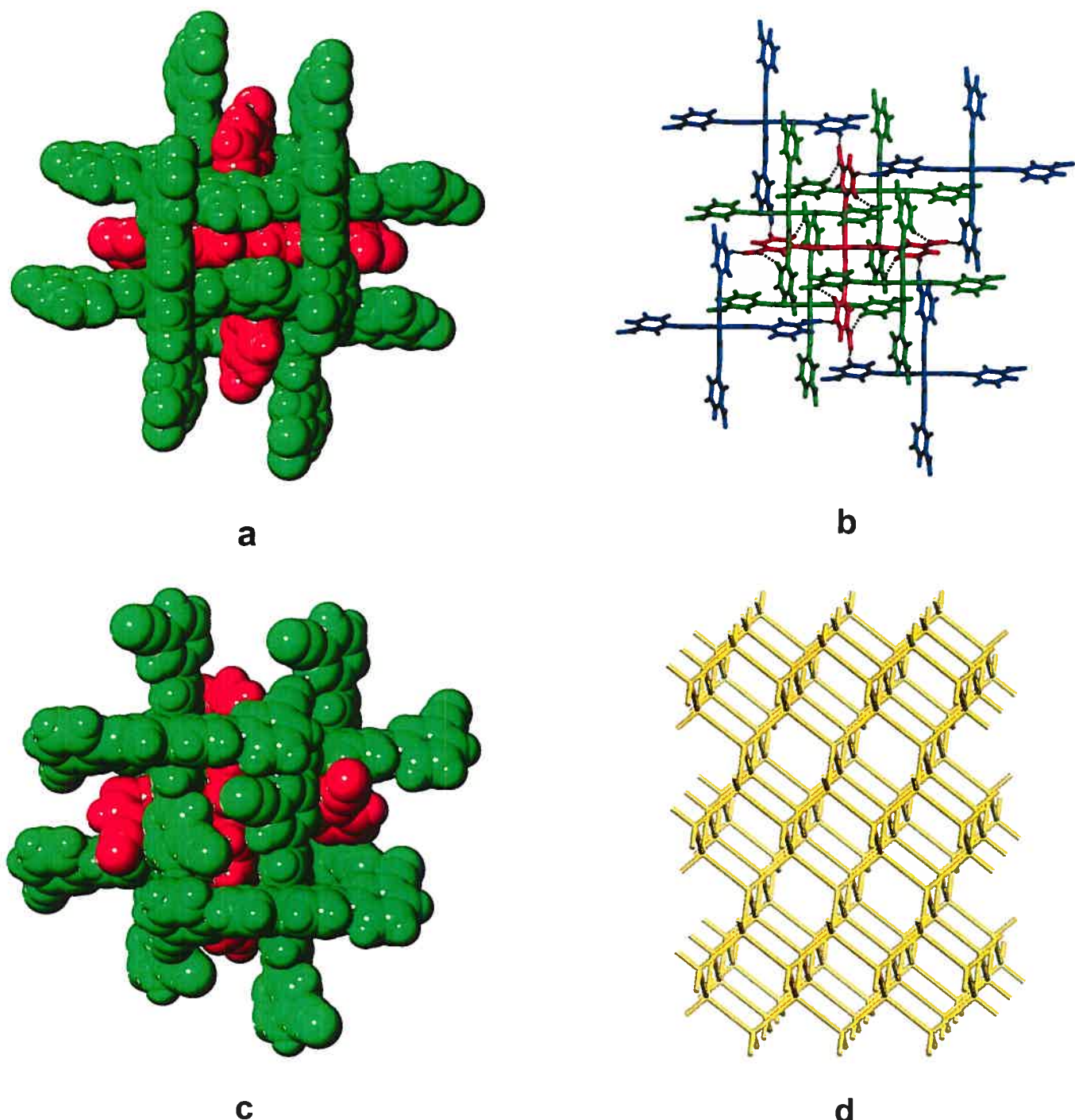
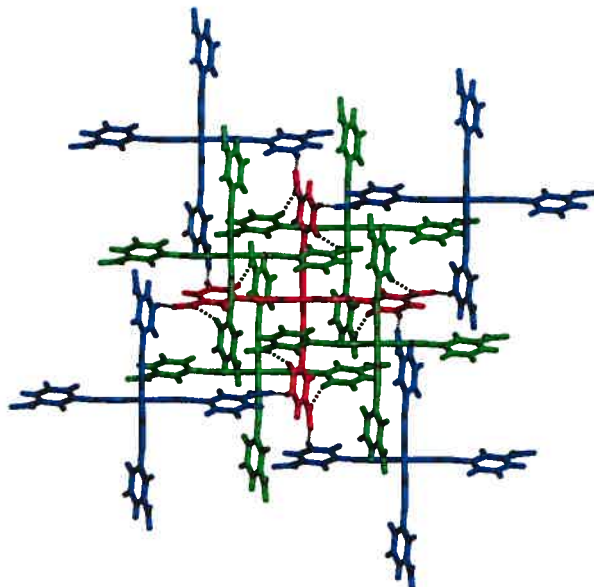
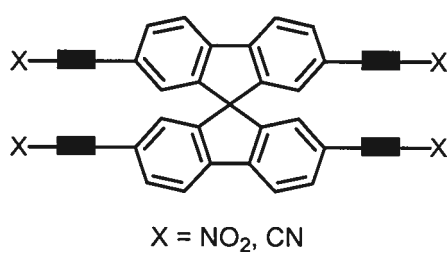


Figure 9. Views of the closely related structures of crystals of 2,2',7,7'-tetrakis(3-nitrophenyl)-9,9'-spirobi[9H-fluorene] (**8**) and 2,2',7,7'-tetrakis(3-cyanophenyl)-9,9'-spirobi[9H-fluorene] (**9**), grown from CHCl₃/acetone and toluene/hexane, respectively. (**a**) Aryl-aryl interactions involving a central molecule of compound **8** (red) with four

neighbors (green) satisfying the condition that the centroids of the interacting phenyl rings are separated by less than 4.5 Å. **(b)** C-H···O interactions (types III-IV) between a central molecule of compound **8** (red) and the set of four neighbors that also have aryl-aryl interactions (green), as well as those involving a second set of four neighbors (blue). C-H···O interactions are represented by broken lines. Together, the red and green molecules define a non-interpenetrated diamondoid network, and the red and blue molecules describe a diamond network with five-fold interpenetration. **(c)** Similar view of aryl-aryl interactions involving a central molecule of extended tetracyanospirobifluorene **9** (red) and its four neighbors (green). **(d)** Non-interpenetrated diamondoid network defined by connecting the centers of molecules of compound **9** linked by aryl-aryl interactions.

Table of Contents Graphic



4.6 Conclusion

Malgré plusieurs années d'étude, nous sommes forcés d'admettre que même pour des composés où la reconnaissance repose sur des ponts hydrogène, il est difficile de prévoir le résultat que l'on obtiendra de sa cristallisation. Il est donc prévisible et normal qu'une cristallisation n'impliquant que des interactions faibles soit d'autant plus difficile à prévoir. Par contre, nos études ont permis d'observer certaines tendances se dégageant des réseaux obtenus. Il semble ainsi que dans un réseau ayant la possibilité de faire intervenir à la fois des liaisons de type O···H-C provenant de fonctions nitro et des interactions π , il s'installe une grande compétition entre les deux types d'interactions. Le réseau obtenu résulte souvent en une combinaison de ces derniers. Par contre, lors d'une compétition entre des liens de type N···H-C, provenant de fonctions cyano, et des interactions π , il semble que ce soit principalement les interactions π qui contrôlent l'architecture du réseau.

On peut donc conclure en disant que même si le processus de cristallisation reste encore trop subtil pour permettre la prévision de l'agencement cristallin, il n'en reste pas moins que les interactions faibles demeurent un facteur à ne pas négliger lors de l'autoassemblage.

Chapitre 5

***Utilisation de ponts
hydrogène provenant de
l'aniline en génie cristallin***

5.1 La tectonique moléculaire et le pont hydrogène

La tectonique moléculaire est une stratégie efficace pour construire des réseaux ordonnés de manière prévisible. Pour ce faire, les molécules doivent interagir fortement et de façon bien définie avec leurs voisines. Les sous-unités tectoniques peuvent être conceptualisées par le simple procédé de greffer, sur un cœur central de géométrie définie, des sites de reconnaissance permettant l'auto-association des molécules entre elles. Plus le site de reconnaissance est fort, spécifique et directionnel, plus il joue un rôle déterminant dans la façon dont les molécules seront liées entre elles. Ainsi plusieurs unités de reconnaissance utilisant le pont hydrogène ont été étudiées par notre groupe, mais aussi par la majorité des groupes de recherche s'interessant à l'auto-assemblage intermoléculaire.¹

¹ Uemura, K.; Kitagawa, S.; Fukui, K.; Saito, K. *J. Am. Chem. Soc.* **2004**, *126*, 3817. Sada, K.; Inoue, K.; Tanaka, T.; Tanaka, A.; Eperges, A.; Nagahama, S.; Matsumoto, A.; Miyata, M. *J. Am. Chem. Soc.* **2004**, *126*, 1764. Maspoch, D.; Domingo, N.; Ruiz-Molina, D.; Wurst, K.; Tejada, J.; Rovira, C.; Veciana, J. *J. Am. Chem. Soc.* **2004**, *126*, 730. Baudron, S. A.; Avarvari, N.; Canadell, E.; Auban-Senzier, P.; Batail, P. *Chem. Eur. J.* **2004**, *10*, 4498. Angeloni, A.; Crawford, P. C.; Orpen, A. G.; Podesta, T. J.; Shore, B. *J. Chem. Eur. J.* **2004**, *10*, 3783. Murata, T.; Morita, Y.; Fukui, K.; Sato, K.; Shiomi, D.; Takui, T.; Maesato, M.; Yamochi, H.; Saito, G.; Nakasuji, K. *Angew. Chem., Int. Ed.* **2004**, *43*, 6343. Soldatov, D. V.; Moudrakovski, I. L.; Ripmeester, J. A. *Angew. Chem., Int. Ed.* **2004**, *43*, 6308. Du, Y.; Creighton, C. J.; Tounge, B. A.; Reitz, A. B. *Org. Lett.* **2004**, *6*, 309. Bhogala, B. R.; Vangala, V. R.; Smith, P. S.; Howard, J. A. K.; Desiraju, G. R. *Cryst. Growth Des.* **2004**, *4*, 647. Dale, S. H.; Elsegood, M. R. J.; Coombs, A. E. L. *CrystEngComm* **2004**, *6*, 328. Hosseini, M. W. *CrystEngComm* **2004**, *6*, 318. Vinodu, M.; Goldberg, I. *CrystEngComm* **2004**, *6*, 215. Aakeröy, C. B.; Desper, J.; Helfrich, B. A. *CrystEngComm* **2004**, *6*, 19.

Parmi les nombreux groupes fonctionnels pouvant permettre un auto-assemblage par pont hydrogène, on retrouve les acides carboxyliques. Ces derniers ont été l'un des premiers groupes de reconnaissance utilisés comme unité d'association en chimie supramoléculaire appliquée au problème de contrôler l'organisation de cristaux.² La Figure 5.1 montre les motifs d'association les plus souvent observés pour ce groupe de reconnaissance. On voit qu'il peut s'associer en chaîne, mais qu'il peut aussi former des dimères très directionnels.

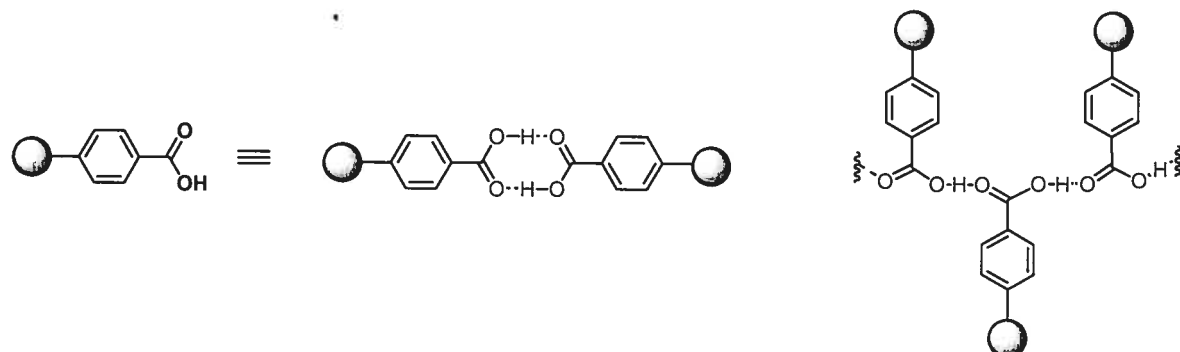


Figure 5.1 Motifs de reconnaissance couramment observés pour les interactions entre les acides carboxyliques.

La directionnalité est un atout important dans la reconnaissance moléculaire, car elle crée une prévisibilité lors de l'association intermoléculaire. De plus, moins il y a de motifs de reconnaissance, plus il est aisément de prédire la manière dont seront disposées les molécules dans un réseau. C'est pour ces raisons que la pyridone a été la première unité de reconnaissance à avoir été utilisée par notre groupe.³ Cette dernière s'associe sous forme de dimère directionnel par l'intermédiaire de deux ponts hydrogène rendant possible la prédiction de son association intermoléculaire (Figure 5.2). Ce motif de reconnaissance est encore aujourd'hui très présent dans nos études en génie cristallin.⁴

² Ermer, O. *J. Am. Chem. Soc.* **1988**, *110*, 3747.

³ Simard, M.; Su, D.; Wuest, J. D. *J. Am. Chem. Soc.* **1991**, *113*, 4696.

⁴ Saied, O.; Maris, T.; Wuest, J. D. *J. Am. Chem. Soc.* **2003**, *125*(49), 14956.

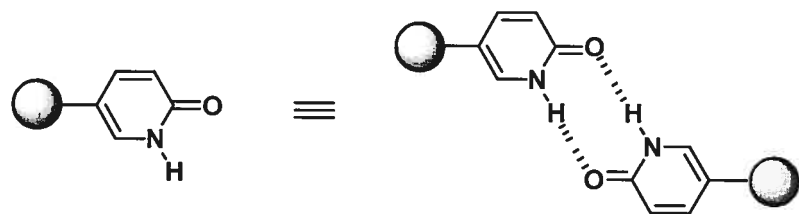


Figure 5.2 Reconnaissance dimérique directionnelle de la pyridone.

La diaminotriazine, quoi qu'étant un groupe dont l'association est moins directionnelle et dont le nombre de motifs de reconnaissance est plus élevé, est l'une des unités de reconnaissance les plus utilisées ces dernières années en tectonique moléculaire.⁵ En effet, le désavantage en terme de prédictibilité est largement compensé par son efficacité pour la reconnaissance intermoléculaire. Il faut voir ici que ses nombreuses possibilités d'interactions par pont hydrogène lui procurent une flexibilité favorisant l'association intermoléculaire. La Figure 5.3 illustre les trois principaux motifs de reconnaissance de la diaminotriazine.

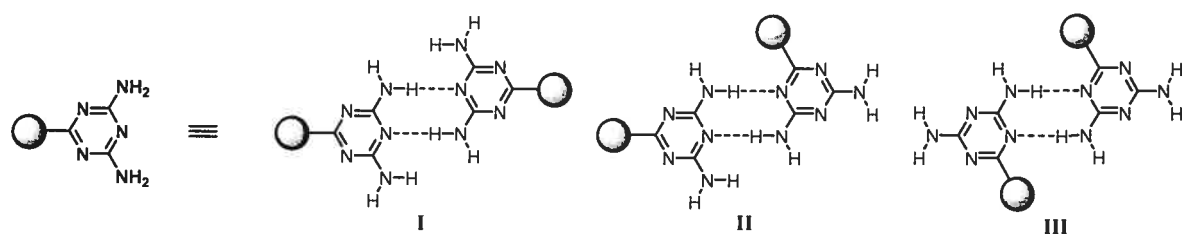


Figure 5.3 Les trois principaux motifs de reconnaissance de la diaminotriazine.

⁵ Malek, N. *Thèse de doctorat*, Université de Montréal, 2001. Brunet, P.; Simard, M.; Wuest, J. D. résultats non publiés. Lautman, M.; Maris, T.; Wuest, J. D., mémoire de maîtrise. Fournier, J.-H.; Maris, T.; Wuest, J. D. *J. Org. Chem.* 2004, 69, 1762. Brunet, P.; Simard, M.; Wuest, J. D. *J. Am. Chem. Soc.* 1997, 119, 2737. Sauriat-Dorizon, H.; Maris, T.; Wuest, J. D.; Enright, G. D. *J. Org. Chem.*, 2003, 68, 240.

Les quelques exemples qui viennent d'être discutés permettent de voir que chaque unité de reconnaissance peut avoir ses forces et ses faiblesses. On peut ainsi comprendre que dépendamment des objectifs visés lors de la conception d'un tecton, le choix de l'unité de reconnaissance se fera en considérant les atouts de chacun. Pour cette raison, l'un des objectifs constants de notre groupe est l'emploi et la caractérisation de diverses unités de reconnaissance. Dans cet ordre d'idée, on a étudié entre autre les acides boroniques ainsi que les groupements hydroxy des phénols comme unité de reconnaissance en chimie supramoléculaire (Figure 5.4).^{6,7}

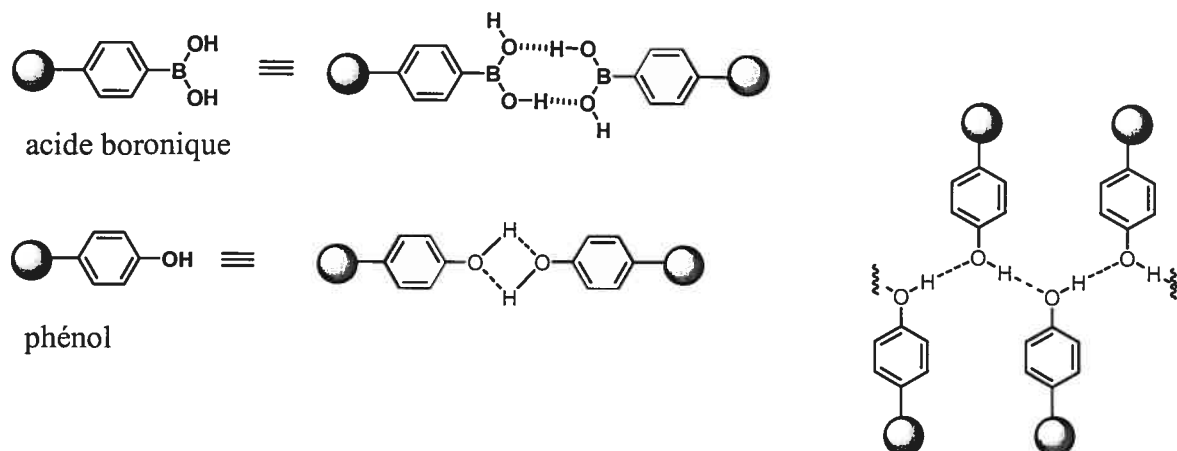


Figure 5.4 Exemple de motifs d'association connus pour les acides boroniques et les phénols.

Le groupe Wuest a donc utilisé de nombreux motifs de reconnaissance basés sur le pont hydrogène, mais il reste encore beaucoup de candidats potentiels. Parmi ces candidats, il y a les arylamines. En effet, de bons résultats ont été obtenus avec les phénols

⁶ Laliberté, D.; Maris, T.; Wuest, J. D., résultats non publiés. Demers, E.; Maris, T.; Wuest, J. D., résultats non publiés. Fournier, J.-H.; Maris, T.; Wuest, J. D.; Guo, W.; Galoppini, E. *J. Am. Chem. Soc.* **2003**, *125*(4), 1002.

⁷ Fournier, J.H.; Maris, T.; Wuest, J. D. *Crystal Growth & Design* **2003**, *3*(4), 539. Patenaude, G.; Maris, T.; Wuest, J. D., résultats non publiés.

et les arylamines sont très comparables à ces derniers. Elles sont à la fois donneur et accepteur de ponts hydrogène, à la différence près qu'elles ont la possibilité de donner deux ponts hydrogène. Le Chapitre 5 sera consacré aux études réalisées sur les arylamines comme unités de reconnaissance en tectonique moléculaire.

5.2 Article 3

Molecular Tectonics. Hydrogen-Bonded Networks

Built from Tetra- and Hexaanilines

Dominic Laliberté, Thierry Maris, Eric Demers,
Fatima Helzy, Mathieu Arseneault and James D. Wuest*

Crystal Growth & Design 2005, 5, 1451

Molecular Tectonics. Hydrogen-Bonded Networks

Built from Tetra- and Hexaanilines

Dominic Laliberté,¹ Thierry Maris, Eric Demers,²

Fatima Helzy, Mathieu Arseneault, and James D. Wuest*

Département de Chimie, Université de Montréal

Montréal, Québec H3C 3J7 Canada

*Author to whom correspondence may be addressed:



Abstract

A series of compounds with multiple PhNH₂ groups were synthesized and crystallized, and their structures were solved by X-ray diffraction to assess the ability of -NH₂ groups in anilines to direct molecular crystallization. 2,2',7,7'-Tetraamino-9,9'-spirobi[9H-fluorene] (**1c**) forms an inclusion complex held together in part by donation of hydrogen bonds from -NH₂ groups to guest molecules. Surprisingly, the -NH₂ groups do not engage in hydrogen bonding with each other. Tetrakis(4-aminophenyl)methane (**2c**) crystallizes to form a guest-free close-packed diamondoid network in which each -NH₂ group donates and accepts one N-H···N hydrogen bond. Tetrakis[(4-aminophenoxy)methyl]methane (**3c**), a more flexible analogue, also crystallizes as a close-packed structure maintained by an extensive network of N-H···N hydrogen bonds. Despite the structural similarity of tetraanilines **2c** and **3c**, their hydrogen-bonding patterns and network topologies are different. A flexible hexaaniline, 1,1'-oxybis[3-(4-aminophenoxy)-2,2-bis[(4-aminophenoxy)methyl]]propane (**4c**), produces a close-packed network joined by both N-H···N and N-H···O hydrogen bonds. Tetrakis(4-aminophenyl)ethylene (**5**) crystallizes as a hydrate to yield a structure consisting of layered hydrogen-bonded sheets. The diverse hydrogen-bonding motifs observed show that crystal engineering using direct interactions of the -NH₂ group of anilines is a challenging endeavor, and other intermolecular interactions can compete effectively with N-H···N hydrogen bonds to determine how crystallization occurs.

Introduction

In a recent review,³ Dunitz presented the following summary of current methods for predicting the structure of molecular crystals:

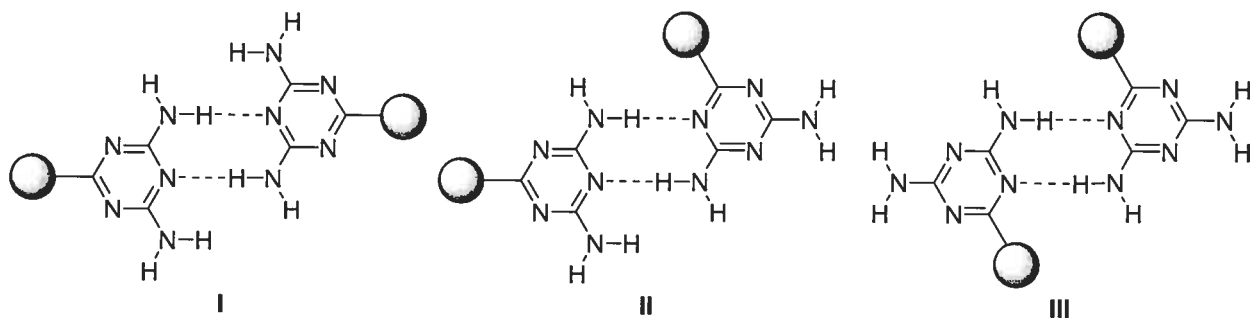
...Computational methods for predicting crystal structures of organic compounds cannot yet be regarded as reliable. From a more qualitative and descriptive viewpoint has come the notion that certain groupings in organic molecules exercise attractive intermolecular interactions and so guide the molecules into distinctive patterns in their crystal structures...This has indeed become one of the tenets of crystal engineering. The prime example of a structure directing interaction is, of course, the hydrogen bond...

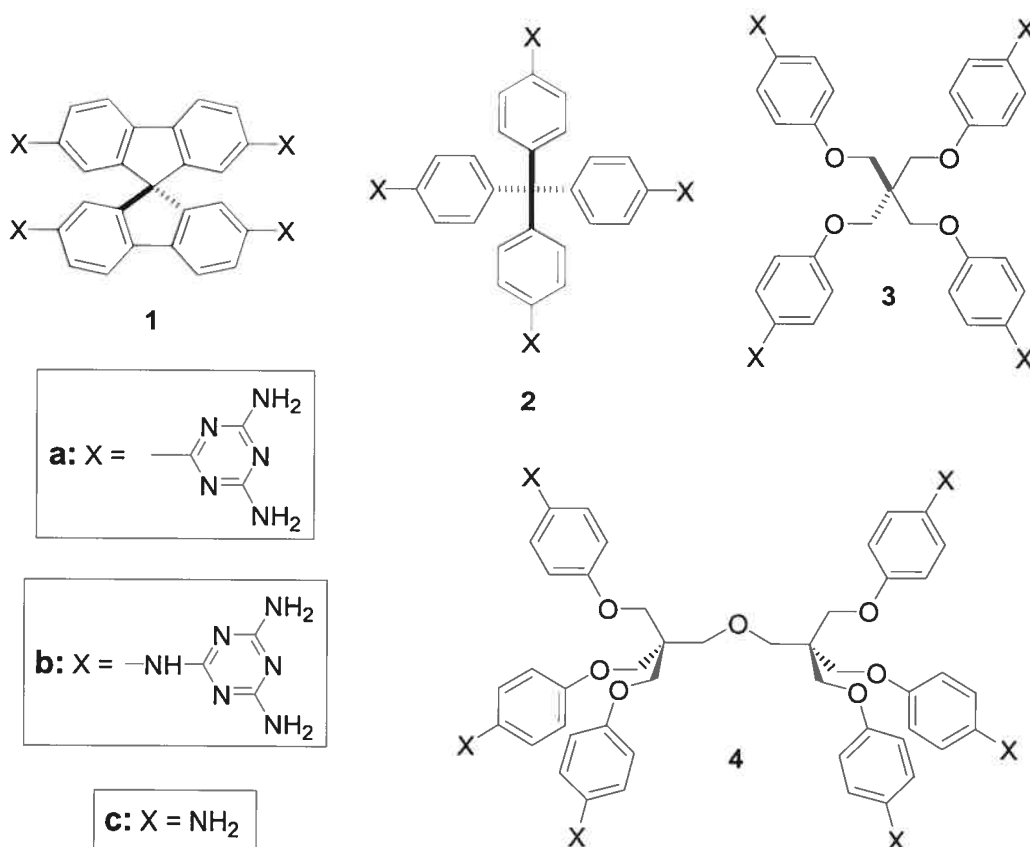
Successful use of this approach requires a set of especially favorable patterns of interaction that can be used to control molecular association. Such motifs, named supramolecular synthons by Desiraju,⁴ provide a crucial tool for constructing molecular aggregates by design. A particularly effective strategy in crystal engineering uses special molecules in which structurally well-defined cores are attached to multiple peripheral groups that can interact according to reliable supramolecular synthons. Such molecules, which have been called tectons from the Greek word for builder,⁵ are programmed to associate and to form networks with predictable architectures.⁶⁻¹³ Ideally, each tecton in the network will be positioned relative to its principal neighbors in a way predetermined by the geometry of the core and the characteristics of the supramolecular synthons that hold the network together.

Tectonic association can produce predictably ordered molecular crystals with unique features not encountered in crystals formed from normal molecules. For example, each tecton is held in place by multiple directional interactions, ensuring that the resulting network has high structural integrity and that polymorphs without these specific patterns of interaction are disfavored. In addition, the directional interactions involved in tectonic

association cannot normally be optimized at the same time that close molecular packing is achieved, leading to the formation of porous networks with significant space for the inclusion of guests.¹⁴

Certain supramolecular synthons have proven to be especially effective for engineering molecular crystals with predictable structural features. For example, we have made extensive use of multiply hydrogen-bonded synthons involving heterocyclic groups such as aminotriazines, which are easy to attach to various cores and typically associate according to motifs I-III.^{6,8}



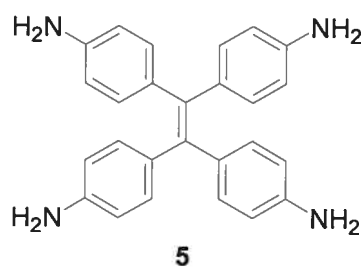


Previous research has established that aminotriazines **1a-4a** and **1b-2b**,⁶⁻⁹ despite their highly diverse molecular structures and widely different degrees of flexibility, all crystallize to form extensively hydrogen-bonded networks held together by 8-20 hydrogen bonds per tecton, primarily according to synthons **I-III**. Furthermore, the porosities of all these networks are impressively high (40-75%),¹⁵ and single crystals are robust enough to allow guests to be exchanged without loss of crystallinity. Overall, only about 15% of molecular structures in the Cambridge Structural Database are inclusion complexes,¹⁷ few of these complexes form crystals in which more than 10% of the volume is accessible to guests, and an even smaller fraction of these complexes allow guests to be exchanged in single crystals. The consistent realization of these properties in crystals of aminotriazines **1a-4a** and **1b-2b** underscores the effectiveness of molecular tectonics as a strategy for

engineering crystals, when used in conjunction with suitable supramolecular synthons involving multiple hydrogen bonds or comparable strong directional interactions.

To provide a point of reference for assessing the behavior of aminotriazines **1a-4a** and **1b-2b**, we decided to study anilines **1c-4c**,^{6,8,9,18,19} which have a related but much simpler hydrogen-bonding group attached to the same core structures. In principal, anilines **1c-4c** can associate to produce hydrogen-bonded networks held together by multiple N-H···N interactions, formed by -NH₂ groups that interact directly and serve simultaneously as both donors and acceptors of hydrogen bonds. Indeed, such interactions are ubiquitous in the structures of simple anilines.²⁰ Surprisingly, these interactions have not been used extensively in crystal engineering. In contrast, hydrogen bonding between the basic -NH₂ groups of anilines as acceptors and acidic groups as donors has been widely exploited,²¹ and related studies have analyzed the ability of the -OH group of phenols to direct crystallization by acting as donors and acceptors of O-H···O hydrogen bonds.^{10,13}

To assess the ability of the -NH₂ group of anilines to direct molecular crystallization, and to provide a firm basis for understanding the unusual properties of more complex derivatives **1a-4a** and **1b-2b**, we elected to crystallize anilines **1c-4c** and to solve their structures by X-ray crystallography. To this group, we added related compound **5**,²² in which four -NH₂ groups are attached to a tetraphenylethylene core.



Results and Discussion

Structure of 2,2',7,7'-Tetraamino-9,9'-spirobi[9H-fluorene] (1c). Spirobifluorene **1c** was synthesized by the reported method⁶ and was found to crystallize from DMF/H₂O in the monoclinic space group P2₁/c as an inclusion compound of well-defined composition **1c** • 0.5 DMF • 1 H₂O.²³ An extensively hydrogen-bonded network is formed, as expected, but the -NH₂ groups do not interact directly; instead, the network is maintained by hydrogen bonds involving the guests, as shown in Figure 1. In this view, three molecules of tetraaniline **1c** (red) each donate a single hydrogen bond to a hydrogen-bonded pair of H₂O molecules (blue), and a fourth molecule of compound **1c** (green) donates a single hydrogen bond to the oxygen atom of a molecule of DMF (yellow), which accepts an additional hydrogen bond from the H₂O dimer. In the resulting structure, tetraaniline **1c** serves exclusively as a donor of hydrogen bonds to molecules that are less basic. As observed in other anilines,²⁰ the -NH₂ groups in compound **1c** are somewhat pyramidalized. In the hypothetical structure created by removing DMF and H₂O from their positions as components of the network derived from tetraaniline **1c**, 18% of the volume is accessible to guests,¹⁵ which is similar to the values observed in structures of other simple derivatives of spirobifluorene.^{6,24}

Structure of Tetrakis(4-aminophenyl)methane (2c). Known tetraphenylmethane **2c** was synthesized by the reported method¹⁸ and crystallized from DMF/CHCl₃. The resulting crystals proved to belong to the tetragonal space group I4₁/a and to consist of a close-packed hydrogen-bonded network. The -NH₂ groups interact directly as both donors and acceptors of hydrogen bonds to define the symmetric motif shown in Figure 2 [N-H···N: 2.19(2) Å; N···N: 3.104(1) Å; \angle N-H···N: 167(1) $^{\circ}$]. Each molecule of tetraaniline **2c** forms a pair of hydrogen bonds with each of four neighbors, thereby creating a non-interpenetrated diamondoid network maintained by a total of eight hydrogen bonds per tecton.^{25,26} The resulting structure can be considered to be held together in part by helical chains of hydrogen-bonded -NH₂ group that run parallel to the *c* axis. In addition, the structure exhibits two-fold phenyl embraces in the same direction [C(3)-H(3)···C(4):

2.875(11) Å; C···C: 3.645(1) Å; \angle C-H···C: 136(1) $^\circ$.²⁷ The central carbon atoms of neighboring tectons are separated by 8.59 Å, and the -NH₂ groups are somewhat pyramidalized. Each -NH₂ group serves as a donor and acceptor of single hydrogen bonds, leaving a potential N-H donor unused and making the -NH₂ group resemble an -OH group in its hydrogen-bonding capacity. It is instructive to note that the resulting network is in fact isostructural with the one produced by hydrogen bonding of phenolic -OH groups in tetrakis(3-hydroxyphenyl)silane.¹⁰

Structure of Tetrakis[(4-aminophenoxy)methyl]methane (3c). Known pentaerythrityl tetraphenyl ether **3c** was synthesized by the reported method^{8,19} and crystallized from THF by slow evaporation. The resulting crystals proved to belong to the tetragonal space group I-4, and a close-packed hydrogen-bonded network was again formed, as in the case of more rigid analogue **2c**. In both cases, the -NH₂ groups interact directly as both donors and acceptors of hydrogen bonds [N-H···N: 2.54(2) Å; N···N: 3.182(3) Å; \angle N-H···N: 122.8(2) $^\circ$], but in the case of tetraaniline **3c** a new cyclic tetrameric motif is created (Figure 3). Each molecule of tecton **3c** now shares a single hydrogen bond with each of eight neighbors located at an intertectonic distance of 15.25 Å, producing a network again held together by a total of eight hydrogen bonds per tecton. Connecting virtual atoms placed at the center of each cyclic tetramer defines a three-fold interpenetrated diamondoid network.^{25,26} As in the case of analogue **2c**, further structural cohesion is maintained by phenyl embraces aligned with the *c* axis [C(5)-H(5)···centroid: 2.735(2) Å; C(5)···centroid: 3.743(2) Å; \angle C(5)-H(5)···centroid: 165(1) $^\circ$.²⁷ As noted in the structures of analogous tetraanilines **1c** and **2c**, the -NH₂ groups of tecton **3c** are slightly pyramidalized. Unlike rigid tetraphenylmethane **2c**, which directs its four -NH₂ groups tetrahedrally, flexible tetraphenyl ether **3c** favors a conformation far from the tetrahedral ideal, and the six C-C-C angles defined by the central carbon atom and the para phenyl carbon atoms of the core have the values 89.5(1) $^\circ$ (two angles) and 120.3(2) $^\circ$ (four angles). Similar values have been observed in the structures of other pentaerythrityl tetraphenyl ethers.^{8,28} Despite such deformations, tecton **3c** does not crystallize in a way that maximizes hydrogen bonding by allowing unused N-H groups to donate hydrogen bonds to latent oxygen acceptors.

Structure of 1,1'-Oxybis[3-(4-aminophenoxy)-2,2-bis[(4-aminophenoxy)methyl]]propane (4c). Dipentaerythrityl hexaphenyl ether **4c** was synthesized by the reported method⁹ and was found to crystallize from benzene/CH₃OH/hexane in the orthorhombic space group P2₁2₁2₁. The structure is a close-packed network in which each tecton forms a total of four N-H···N hydrogen bonds and four N-H···O hydrogen bonds with six neighbors as shown in Figure 4. Two neighbors (yellow) each share two N-H···N hydrogen bonds [N-H···N: 2.59(4) Å; N···N: 3.418(11) Å; \angle N-H···N: 153(6) $^{\circ}$] and two N-H···O hydrogen bonds [N-H···O: 2.31(2) Å; N···O: 3.161(5) Å; \angle N-H···O: 154(3) $^{\circ}$]; two other neighbors (green) each accept one hydrogen bond (one N-H···N and one N-H···O); and the remaining two neighbors (blue) each donate one hydrogen bond (one N-H···N and one N-H···O). Each tecton donates four hydrogen bonds and accepts four hydrogen bonds, and multiple donor and acceptor sites remain unused. It is noteworthy that pentaerythrityl tetraphenyl ether **3c** crystallizes without forming any N-H···O hydrogen bonds, whereas such interactions are important in the structure of dipentaerythrityl hexaphenyl ether **4c**, possibly because its increased flexibility and the larger number of donor and acceptor sites per molecule provide more options. Nevertheless, the number of hydrogen bonds per tecton remains constant in the two structures. As noted in the structures of tetraanilines **1c-3c**, the -NH₂ groups of tecton **4c** are slightly pyramidalized.

Examination of the structure of hexaaniline **4c** also reveals many inter- and intramolecular aromatic interactions, as observed in previous studies of dipentaerythrityl hexaphenyl ethers.^{9,29} In particular, each tecton **4c** adopts a characteristic \neq shaped conformation in which two pairs of the six phenoxyethyl arms lie parallel and interact intramolecularly by π -stacking.

Structure of Tetrakis(4-aminophenyl)ethylene (5). Tetraphenylethylene **5** was synthesized by the reported method²² and was found to crystallize from DMF/H₂O in the monoclinic space group P2₁/c as an inclusion compound of well-defined composition 3 **5** •

1 H₂O.²³ The structure is complex, incorporates three symmetry-independent molecules **5**, and consists of two types of extensively hydrogen-bonded layers (Figure 5). In one type of layer (red = R), each tecton shares a total of four N-H···N hydrogen bonds with four neighbors (Figure 5a). In the other type of layer (blue = B), each tecton forms a total of three N-H···N hydrogen bonds with three neighbors, and one of the neighbors also accepts a hydrogen bond from H₂O (Figure 5b). The layers then stack along the *a* axis according to the repeating pattern RBBRBB (Figure 5c). In the hypothetical structure created by removing networked H₂O, only 2% of the volume is accessible to guests.¹⁵

Conclusions

Anilines **1c-4c** and **5** incorporate multiple hydrogen-bonding -NH₂ groups connected to diverse molecular cores. As expected, their crystallization generates extensively hydrogen-bonded networks. However, no clear patterns of association emerge, whereas more complex relatives **1a-4a** and **1b-2b** reliably form networks held together by hydrogen bonding of aminotriazine units according to characteristic motifs I-III. In contrast, the corresponding anilines exhibit very diverse behavior, including cases in which 1) N-H···N hydrogen bonds are completely absent (spirobifluorene **1c**); 2) only N-H···N hydrogen bonds are present (tetraphenylmethane **2c** and pentaerythrityl tetraphenyl ether **3c**); and 3) both N-H···N hydrogen bonds and N-H···O hydrogen bonds are present (dipentaerythrityl hexaphenyl ether **4c**). These observations show that crystal engineering using direct interactions of the -NH₂ group of anilines is a challenging endeavor, and many other intermolecular interactions can compete effectively with N-H···N hydrogen bonds to determine how crystallization occurs.

Further understanding is provided by comparing the porosities of networks built from aminotriazines **1a-4a** and **1b-2b** with the porosities of networks constructed from simple anilines **1c-4c** and **5**. Porosities of the aminotriazines are very high (40-75%), whereas all the anilines form close-packed structures except two (**1c** and **5**), and in these two cases the porosities do not exceed 18%. Moreover, networks built from the aminotriazines are held together by 8-20 hydrogen bonds per tecton, whereas networks constructed from the corresponding anilines are maintained by a much smaller number of hydrogen bonds per molecule (3-8). These major differences in structure and properties, which are introduced simply by changing the identity of sticky sites grafted to the same molecular cores, underscore the versatility of molecular tectonics as a strategy for making ordered materials.

Experimental Section

2,2',7,7'-Tetraamino-9,9'-spirobi[9H-fluorene] (**1c**),⁶ tetrakis(4-aminophenyl)methane (**2c**),¹⁸ tetrakis[(4-aminophenoxy)methyl]methane (**3c**),^{8,19} 1,1'-oxybis[3-(4-aminophenoxy)-2,2-bis[(4-aminophenoxy)methyl]]propane (**4c**),⁹ and tetrakis(4-aminophenyl)ethylene (**5**)²² were all synthesized by known methods.

X-ray Crystallographic Studies. Structures were solved by direct methods using SHELXS-97 and refined with SHELXL-97.³⁰ All non-hydrogen atoms were refined anisotropically. Hydrogen atoms attached to aromatic rings were placed in ideal positions and refined as riding atoms, except in the cases of tetraanilines **2c** and **3c**, where they were fully refined. Hydrogen atoms associated with -NH₂ groups were located from difference Fourier maps and refined with restraints on distances.

Structure of 2,2',7,7'-Tetraamino-9,9'-spirobi[9H-fluorene] (1c**).** Small crystals were grown by slowly diffusing H₂O into a solution of compound **1c** in DMF. X-ray diffraction data were collected at 293 K with Cu K α radiation using a Bruker SMART 6000 CCD diffractometer equipped with a rotating anode generator. Crystals of compound **1c** proved to belong to the orthorhombic space group P2₁2₁2₁ with $a = 10.654(2)$ Å, $b = 14.404(3)$ Å, $c = 29.086(5)$ Å, $V = 4463.8(13)$ Å³, $D_{\text{calcd}} = 1.283$ g/cm³, and $Z = 8$. Full-matrix least-squares refinements on F^2 of 683 parameters led to final residuals $R_1 = 0.0700$ and $wR_2 = 0.2008$ for 5585 observed reflections with $I > 2\sigma(I)$.

Structure of Tetrakis(4-aminophenyl)methane (2c**).** Crystallization was induced by slowly diffusing CHCl₃ into a solution of compound **2c** in DMF. X-ray diffraction data were collected at 223 K with Cu K α radiation using a Bruker SMART 2000 CCD diffractometer. Crystals of compound **2c** were found to belong to the tetragonal space group I4₁/a with $a = b = 16.8018(8)$ Å, $c = 7.1674(4)$ Å, $V = 2023.4(2)$ Å³, $D_{\text{calcd}} = 1.249$

g/cm³, and $Z = 4$. Full-matrix least-squares refinements on F^2 of 90 parameters led to final residuals $R_1 = 0.0412$ and $wR_2 = 0.1191$ for 961 reflections with $I > 2\sigma(I)$.

Structure of Tetrakis[(4-aminophenoxy)methyl]methane (3c). Crystals were grown by slowly evaporating a solution of compound **3c** in THF. X-ray diffraction data were collected at 220 K with Cu K α radiation using a Bruker SMART 2000 CCD diffractometer. Crystals of compound **3c** proved to belong to the tetragonal space group I-4 with $a = b = 12.7089(1)$ Å, $c = 8.2149(1)$ Å, $V = 1326.84(2)$ Å³, $D_{\text{calcd}} = 1.253$ g/cm³, and $Z = 2$. Full-matrix least-squares refinements on F^2 of 117 parameters led to final residuals $R_1 = 0.0312$ and $wR_2 = 0.0849$ for 1183 reflections with $I > 2\sigma(I)$.

Structure of 1,1'-Oxybis[3-(4-aminophenoxy)-2,2-bis[(4-aminophenoxy)methyl]]propane (4c). Small needles were grown by slowly diffusing hexane into a solution of compound **4c** in a mixture of benzene and CH₃OH. X-ray diffraction data were collected at 293 K with Cu K α radiation using a Bruker SMART 6000 CCD diffractometer equipped with a rotating anode generator. Crystals of compound **4c** were found to belong to the orthorhombic space group P2₁2₁2₁ with $a = 6.0353(2)$ Å, $b = 24.6349(6)$ Å, $c = 28.1607(7)$ Å, $V = 4186.9(2)$ Å³, $D_{\text{calcd}} = 1.271$ g/cm³, and $Z = 4$. Full-matrix least-squares refinements on F^2 of 580 parameters led to final residuals $R_1 = 0.0495$ and $wR_2 = 0.1229$ for 5538 reflections with $I > 2\sigma(I)$.

Structure of Tetrakis(4-aminophenyl)ethylene (5). Needles were grown by diffusing H₂O into a solution of compound **5** in DMF. X-ray diffraction data were collected at 293 K with Cu K α radiation using a Bruker SMART 6000 CCD diffractometer equipped with a rotating anode generator. Compound **2** proved to crystallize in the monoclinic space group P2₁/c with $a = 32.927(3)$ Å, $b = 9.330(7)$ Å, $c = 21.448(2)$ Å, $\beta = 99.103(12)^\circ$, $V = 6506(5)$ Å³, $D_{\text{calcd}} = 1.221$ g/cm³, and $Z = 4$. Full-matrix least-squares refinements on F^2 of 820 parameters led to final residuals $R_1 = 0.0837$ and $wR_2 = 0.1889$ for 6341 reflections with $I > 2\sigma(I)$.

Acknowledgment. We are grateful to the Natural Sciences and Engineering Research Council of Canada, the Ministère de l'Éducation du Québec, the Canada Foundation for Innovation, the Canada Research Chairs Program, and Merck Frosst for financial support. In addition, we thank Prof. Jurgen Sygusch for providing access to a Bruker SMART 6000 CCD diffractometer equipped with a rotating anode.

Supporting Information Available: ORTEP drawings and tables of crystallographic data, atomic coordinates, anisotropic thermal parameters, bond lengths, bond angles, and packing diagrams for compounds **1c-4c** and **5**. This material is available free of charge via the Internet at <http://pubs.acs.org>.

Notes and References

1. Boehringer-Ingelheim Fellow, 2001-2002.
2. Fellow of the Ministère de l'Éducation du Québec, 2002-2004. Fellow of the Natural Sciences and Engineering Research Council of Canada, 2000-2002.
3. Dunitz, J. D. *Chem. Commun.* **2003**, 545.
4. Nangia, A.; Desiraju, G. R. *Top. Curr. Chem.* **1998**, *198*, 57. Desiraju, G. R. *Angew. Chem., Int. Ed.* **1995**, *34*, 2311.
5. Simard, M.; Su, D.; Wuest, J. D. *J. Am. Chem. Soc.* **1991**, *113*, 4696.
6. Fournier, J.-H.; Maris, T.; Wuest, J. D. *J. Org. Chem.* **2004**, *69*, 1762.
7. Brunet, P.; Demers, E.; Maris, T.; Enright, G. D.; Wuest, J. D. *Angew. Chem., Int. Ed.* **2003**, *42*, 5303. Le Fur, E.; Demers, E.; Maris, T.; Wuest, J. D. *Chem. Commun.* **2003**, 2966.
8. Laliberté, D.; Maris, T.; Wuest, J. D. *J. Org. Chem.* **2004**, *69*, 1776.
9. Laliberté, D.; Maris, T.; Sirois, A.; Wuest, J. D. *Org. Lett.* **2003**, *5*, 4787.
10. Fournier, J.-H.; Maris, T.; Simard, M.; Wuest, J. D. *Cryst. Growth Des.* **2003**, *3*, 535.
11. For recent related work, see: Laliberté, D.; Maris, T.; Wuest, J. D. *Can. J. Chem.* **2004**, *82*, 386. Saied, O.; Maris, T.; Wuest, J. D. *J. Am. Chem. Soc.* **2003**, *125*, 14956. Fournier, J.-H.; Maris, T.; Wuest, J. D.; Guo, W.; Galoppini, E. *J. Am. Chem. Soc.* **2003**, *125*, 1002. Sauriat-Dorizon, H.; Maris, T.; Wuest, J. D.; Enright, G. D. *J. Org. Chem.* **2003**, *68*, 240.
12. For other recent uses of hydrogen-bonded supramolecular synthons in crystal engineering, see: Uemura, K.; Kitagawa, S.; Fukui, K.; Saito, K. *J. Am. Chem. Soc.* **2004**, *126*, 3817. Sada, K.; Inoue, K.; Tanaka, T.; Tanaka, A.; Eperges, A.; Nagahama, S.; Matsumoto, A.; Miyata, M. *J. Am. Chem. Soc.* **2004**, *126*, 1764. Maspoch, D.; Domingo, N.; Ruiz-Molina, D.; Wurst, K.; Tejada, J.; Rovira, C.; Veciana, J. *J. Am. Chem. Soc.* **2004**, *126*, 730. Baudron, S. A.; Avarvari, N.; Canadell, E.; Auban-Senzier, P.; Batail, P. *Chem. Eur. J.* **2004**, *10*, 4498. Angeloni, A.; Crawford, P. C.; Orpen, A. G.; Podesta, T. J.; Shore, B. J. *Chem. Eur. J.* **2004**, *10*, 3783. Murata, T.; Morita, Y.; Fukui, K.; Sato, K.; Shiomi, D.; Takui, T.; Maesato, M.;

Yamochi, H.; Saito, G.; Nakasuji, K. *Angew. Chem., Int. Ed.* **2004**, *43*, 6343. Soldatov, D. V.; Moudrakovski, I. L.; Ripmeester, J. A. *Angew. Chem., Int. Ed.* **2004**, *43*, 6308. Du, Y.; Creighton, C. J.; Tounge, B. A.; Reitz, A. B. *Org. Lett.* **2004**, *6*, 309. Bhogala, B. R.; Vangala, V. R.; Smith, P. S.; Howard, J. A. K.; Desiraju, G. R. *Cryst. Growth Des.* **2004**, *4*, 647. Dale, S. H.; Elsegood, M. R. J.; Coombs, A. E. L. *CrystEngComm* **2004**, *6*, 328. Hosseini, M. W. *CrystEngComm* **2004**, *6*, 318. Vinodu, M.; Goldberg, I. *CrystEngComm* **2004**, *6*, 215. Aakeröy, C. B.; Desper, J.; Helfrich, B. A. *CrystEngComm* **2004**, *6*, 19. Alshahateet, S. F.; Nakano, K.; Bishop, R.; Craig, D. C.; Harris, K. D. M.; Scudder, M. L. *CrystEngComm* **2004**, *6*, 5. Brown, R. J.; Camarasa, G.; Griffiths, J.-P.; Day, P.; Wallis, J. D. *Tetrahedron Lett.* **2004**, *45*, 5103. Pedireddi, V. R.; SeethaLekshmi, N. *Tetrahedron Lett.* **2004**, *45*, 1903. Martin, S. M.; Yonezawa, J.; Horner, M. J.; Macosko, C. W.; Ward, M. D. *Chem. Mater.* **2004**, *16*, 3045. Shimizu, L. S.; Hughes, A. D.; Smith, M. D.; Davis, M. J.; Zhang, B. P.; zur Loya, H.-C.; Shimizu, K. D. *J. Am. Chem. Soc.* **2003**, *125*, 14972. Ouyang, X.; Fowler, F. W.; Lauher, J. W. *J. Am. Chem. Soc.* **2003**, *125*, 12400. Kobayashi, K.; Sato, A.; Sakamoto, S.; Yamaguchi, K. *J. Am. Chem. Soc.* **2003**, *125*, 3035. Rakotondradany, F.; Whitehead, M. A.; Lebuis, A.-M.; Sleiman, H. F. *Chem. Eur. J.* **2003**, *9*, 4771. Jagadish, B.; Carducci, M. D.; Bosshard, C.; Günter, P.; Margolis, J. I.; Williams, L. J.; Mash, E. A. *Cryst. Growth Des.* **2003**, *3*, 811. Bhogala, B. R.; Nangia, A. *Cryst. Growth Des.* **2003**, *3*, 547. Olenik, B.; Smolka, T.; Boese, R.; Sustmann, R. *Cryst. Growth Des.* **2003**, *3*, 183. Kitamura, M.; Nakano, K. *Cryst. Growth Des.* **2003**, *3*, 25. Ma, B.-Q.; Coppens, P. *Chem. Commun.* **2003**, 2290. Yagai, S.; Karatsu, T.; Kitamura, A. *Chem. Commun.* **2003**, 1844. Walsh, R. D. B.; Bradner, M. W.; Fleischman, S.; Morales, L. A.; Moulton, B.; Rodríguez-Hornedo, R.; Zaworotko, M. J. *Chem. Commun.* **2003**, 186. Blay, G.; Fernández, I.; Pedro, J. R.; Ruiz-García, R.; Muñoz, M. C.; Cano, J.; Carrasco, R. *Eur. J. Org. Chem.* **2003**, 1627. Braga, D.; Polito, M.; Braccaccini, M.; D'Addario, D.; Tagliavini, E.; Sturba, L. *Organometallics* **2003**, *22*, 2142. Roesky, H. W.; Andruh, M. *Coord. Chem. Rev.* **2003**, *236*, 91. Ermer, O.; Kusch, A.; Röbke, C. *Helv. Chim. Acta* **2003**, *86*, 922. Arora, K. K.; Pedireddi, V. R. *J. Org. Chem.* **2003**, *68*, 9177. Wen, J.-F.; Hong, W.; Yuan, K.; Mak, T. C. W.; Wong, H.

N. C. J. Org. Chem. 2003, 68, 8918. Moon, K.; Chen, W.-Z.; Ren, T.; Kaifer, A. E. CrystEngComm 2003, 5, 451. Trivedi, D. R.; Ballabh, A.; Dastidar, P. CrystEngComm 2003, 5, 358. Burke, N. J.; Burrows, A. D.; Mahon, M. F.; Pritchard, L. S. CrystEngComm 2003, 5, 355. Pérez, C.; Rodríguez, M. L.; Foces-Foces, C.; Pérez-Hernández, N.; Pérez, R.; Martín, J. D. Org. Lett. 2003, 5, 641. Shan, N.; Bond, A. D.; Jones, W. New J. Chem. 2003, 27, 365. Kobayashi, N.; Naito, T.; Inabe, T. Bull. Chem. Soc. Jpn. 2003, 76, 1351. Görbitz, C. H. Acta Crystallogr. 2002, B58, 849. Tanaka, T.; Tasaki, T.; Aoyama, Y. J. Am. Chem. Soc. 2002, 124, 12453. Moorthy, J. N.; Natarajan, R.; Mal, P.; Venugopalan, P. J. Am. Chem. Soc. 2002, 124, 6530. Archer, E. A.; Krische, M. J. J. Am. Chem. Soc. 2002, 124, 5074. Kim, S.; Bishop, R.; Craig, D. C.; Dance, I. G.; Scudder, M. L. J. Org. Chem. 2002, 67, 3221. Lyssenko, K. A.; Lenev, D. A.; Kostyanovsky, R. G. Tetrahedron 2002, 58, 8525. Beatty, A. M.; Schneider, C. M.; Simpson, A. E.; Zaher, J. L. CrystEngComm 2002, 4, 282. Field, J. E.; Combariza, M. Y.; Vachet, R. W.; Venkataraman, D. Chem. Commun., 2002, 2260. Gauthier, D.; Baillargeon, P.; Drouin, M.; Dory, Y. L. Angew. Chem., Int. Ed. 2001, 40, 4635. Hong, B. H.; Lee, J. Y.; Lee, C.-W.; Kim, J. C.; Bae, S. C.; Kim, K. S. J. Am. Chem. Soc. 2001, 123, 10748. Papaefstathiou, G. S.; MacGillivray, L. R. Org. Lett. 2001, 3, 3835. Zaman, M. B.; Tomura, M.; Yamashita, Y. J. Org. Chem. 2001, 66, 5987. Dapporto, P.; Paoli, P.; Roelens, S. J. Org. Chem. 2001, 66, 4930. Vaid, T. P.; Sydora, O. L.; Douthwaite, R. E.; Wolczanski, P. T.; Lobkovsky, E. B. Chem. Commun. 2001, 1300. Sharma, C. V. K.; Clearfield, A. J. Am. Chem. Soc. 2000, 122, 4394. Corbin, P. S.; Zimmerman, S. C. J. Am. Chem. Soc. 2000, 122, 3779. Cantrill, S. J.; Pease, A. R.; Stoddart, J. F. J. Chem. Soc., Dalton Trans. 2000, 3715. Videnova-Adrabińska, V.; Janeczko, E. J. Mater. Chem. 2000, 10, 555. Akazome, M.; Suzuki, S.; Shimizu, Y.; Henmi, K.; Ogura, K. J. Org. Chem. 2000, 65, 6917. Baumeister, B.; Matile, S. Chem. Commun. 2000, 913. Chowdhry, M. M.; Mingos, D. M. P.; White, A. J. P.; Williams, D. J. J. Chem. Soc., Perkin Trans. 1 2000, 3495. Gong, B.; Zheng, C.; Skrzypczak-Jankun, E.; Zhu, J. Org. Lett. 2000, 2, 3273. Krische, M. J.; Lehn, J.-M.; Kyritsakas, N.; Fischer, J.; Wegelius, E. K.; Rissanen, K. Tetrahedron 2000, 56, 6701. Fuchs, K.; Bauer, T.; Thomann, R.; Wang, C.; Friedrich, C.; Mülhaupt, R.

- Macromolecules* **1999**, *32*, 8404. Holý, P.; Závada, J.; Císařová, I.; Podlaha, J. *Angew. Chem., Int. Ed.* **1999**, *38*, 381. Karle, I. L.; Ranganathan, D.; Kurur, S. *J. Am. Chem. Soc.* **1999**, *121*, 7156. Chin, D. N.; Palmore, G. T. R.; Whitesides, G. M. *J. Am. Chem. Soc.* **1999**, *121*, 2115. Hanessian, S.; Saladino, R.; Margarita, R.; Simard, M. *Chem. Eur. J.* **1999**, *5*, 2169.
13. Balasubramaniam, V.; Wong, L. G. J.; Vittal, J. J.; Valiyaveettil, S. *Cryst. Growth Des.* **2004**, *4*, 553.
14. For reviews of porous molecular networks, see: Nangia, A. *Curr. Opin. Solid State Mater. Sci.* **2001**, *5*, 115. Langley, P. J.; Hulliger, J. *Chem. Soc. Rev.* **1999**, *28*, 279.
15. The percentage of volume accessible to guests was estimated by the PLATON program.¹⁶ PLATON calculates the accessible volume by allowing a spherical probe of variable radius to roll over the van der Waals surface of the network. PLATON uses a default value of 1.20 Å for the radius of the probe, which is an appropriate model for small guests such as water. The van der Waals radii used to define surfaces for these calculations are as follows: C: 1.70 Å, H: 1.20 Å, N: 1.55 Å, and O: 1.52 Å. If V is the volume of the unit cell and V_g is the guest-accessible volume as calculated by PLATON, then the porosity P in % is given by $100V_g/V$.
16. Spek, A. L. *PLATON, A Multipurpose Crystallographic Tool*; Utrecht University: Utrecht, The Netherlands, 2001. van der Sluis, P.; Spek, A. L. *Acta Crystallogr.* **1990**, *A46*, 194.
17. Nangia, A.; Desiraju, G. R. *Chem. Commun.* **1999**, 605.
18. Thaimattam, R.; Xue, F.; Sarma, J. A. R. P.; Mak, T. C. W.; Desiraju, G. R. *J. Am. Chem. Soc.* **2001**, *123*, 4432. Neugebauer, F. A.; Fischer, H.; Bernhardt, R. *Chem. Ber.* **1976**, *109*, 2389.
19. Ashley, J. N.; Collins, R. F.; Davis, M.; Sirett, N. E. *J. Chem. Soc.* **1958**, 3298.
20. a) For representative structural studies of simple anilines, see: Dey, A.; Jetti, R. K. R.; Boese, R.; Desiraju, G. R. *CrystEngComm* **2003**, *5*, 248. Dixon, D. A.; Calabrese, J. C.; Miller, J. S. *Angew. Chem., Int. Ed.* **1989**, *28*, 90. Colapietro, M.; Domenicano, A.; Portalone, G.; Schultz, G.; Hargittai, I. *J. Phys. Chem.* **1987**, *91*, 1728. Fukuyo, M.; Hirotsu, K.; Higuchi, T. *Acta Crystallogr.* **1982**, *B38*, 640. b) See the Supporting

- Information for 1) a list of the structures of all anilines containing intermolecular N-H···N hydrogen bonds and 2) an analysis of their bond lengths and angles.
21. For recent references, see: Vangala, V. R.; Mondal, R.; Broder, C. K.; Howard, J. A. K.; Desiraju, G. R. *Cryst. Growth Des.* **2004**, *4*, ASAP. Bhogala, B. R.; Vangala, V. R.; Smith, P. S.; Howard, J. A. K.; Desiraju, G. R. *Cryst. Growth Des.* **2004**, *4*, 647. Dey, A.; Desiraju, G. R.; Mondal, R.; Howard, J. A. K. *Chem. Commun.* **2004**, 2528. Bourne, S. A.; Corin, K. C.; Nassimbeni, L. R.; Weber, E. *CrystEngComm* **2004**, *6*, 54. Glidewell, C.; Low, J. N.; Skakle, J. M. S.; Wardell, S. M. S. V.; Wardell, J. L. *Acta Crystallogr.* **2004**, *B60*, 472. Vangala, V. R.; Bhogala, B. R.; Dey, A.; Desiraju, G. R.; Broder, C. K.; Smith, P. S.; Mondal, R.; Howard, J. A. K.; Wilson, C. C. *J. Am. Chem. Soc.* **2003**, *125*, 14495. Ermer, O.; Eling, A. *J. Chem. Soc., Perkin Trans. 2* **1994**, 925. Loehlin, J. H.; Etter, M. C.; Gendreau, C.; Cervasio, E. *Chem. Mater.* **1994**, *6*, 1218.
 22. Gorvin, J. H. *J. Chem. Soc.* **1959**, 678.
 23. The composition was determined by X-ray crystallography.
 24. Demers, E.; Maris, T.; Cabana, J.; Fournier, J.-H.; Wuest, J. D., submitted for publication.
 25. For discussions of interpenetration in networks, see: Batten, S. R. *CrystEngComm* **2001**, *18*, 1. Batten, S. R.; Robson, R. *Angew. Chem., Int. Ed.* **1998**, *37*, 1460.
 26. For a review of diamondoid hydrogen-bonded networks, see: Zaworotko, M. J. *Chem. Soc. Rev.* **1994**, *23*, 283.
 27. Scudder, M.; Dance, I. *Chem. Eur. J.* **2002**, *8*, 5456. Hunter, C. A.; Lawson, K. R.; Perkins, J.; Urch, C. J. *J. Chem. Soc., Perkin Trans. 2* **2001**, 651.
 28. Laliberté, D.; Maris, T.; Wuest, J. D. *Acta Crystallogr.* **2003**, *E59*, o799.
 29. Nättinen, K. I.; Rissanen, K. *Cryst. Growth Des.* **2003**, *3*, 339.
 30. Sheldrick, G. M. *SHELXS-97, Program for the Solution of Crystal Structures* and *SHELXL-97, Program for the Refinement of Crystal Structures*; Universität Göttingen: Germany, 1997.

Figure 1. Representation of the structure of crystals of 2,2',7,7'-tetraamino-9,9'-spirobi[9H-fluorene] (**1c**) grown from DMF/H₂O. Three molecules of tetraaniline **1c** (red) each donate a single hydrogen bond to a hydrogen-bonded pair of H₂O molecules (blue), and a fourth molecule of compound **1c** (green) donates a single hydrogen bond to the oxygen atom of a molecule of DMF (yellow), which accepts an additional hydrogen bond from the H₂O dimer. Hydrogen bonds appear as broken lines, and hydrogen atoms of the spirobifluorene cores are omitted for clarity.

Figure 2. View along the *c* axis of the structure of crystals of tetrakis(4-aminophenyl)methane (**2c**) grown from DMF/CHCl₃ showing a central molecule (red) and its four hydrogen-bonded neighbors (blue). Hydrogen bonds appear as broken lines, and hydrogen atoms of the tetraphenylmethyl cores are omitted for clarity.

Figure 3. View along the *c* axis of the structure of crystals of tetrakis[(4-aminophenoxy)methyl]methane (**3c**) grown from THF showing the characteristic cyclic hydrogen-bonded motif formed by four molecules of tetraaniline **3c**. Hydrogen bonds appear as broken lines, and hydrogen atoms of the pentaerythrityl tetraphenyl ether cores are omitted for clarity.

Figure 4. View of the structure of crystals of 1,1'-oxybis[3-(4-aminophenoxy)-2,2-bis[(4-aminophenoxy)methyl]]propane (**4c**) grown from benzene/CH₃OH/hexane showing a central tecton (red) surrounded by its six hydrogen-bonded neighbors. Two neighbors (yellow) each share two N-H···N hydrogen bonds with the central tecton, two other neighbors (green) each accept one hydrogen bond (one N-H···N and one N-H···O), and the remaining two neighbors (blue) each donate one hydrogen bond (one N-H···N and one N-H···O). Hydrogen bonds appear as broken lines, and hydrogen atoms of the dipentaerythrityl hexaphenyl ether cores are omitted for clarity.

Figure 5. View of the layered structure of crystals of tetrakis(4-aminophenyl)ethylene (**5**) grown from DMF/H₂O. Hydrogen bonds appear as broken lines, and hydrogen atoms of the tetraphenylethenyl cores are omitted for clarity. a) In one type of layer (red = R), each tecton shares a total of four N-H···N hydrogen bonds with four neighbors. b) In the other type of layer (blue = B), each tecton forms a total of three N-H···N hydrogen bonds with three neighbors, and one of the neighbors also accepts a hydrogen bond from H₂O. c) The layers then stack along the *a* axis according to the repeating pattern RBBRBB.

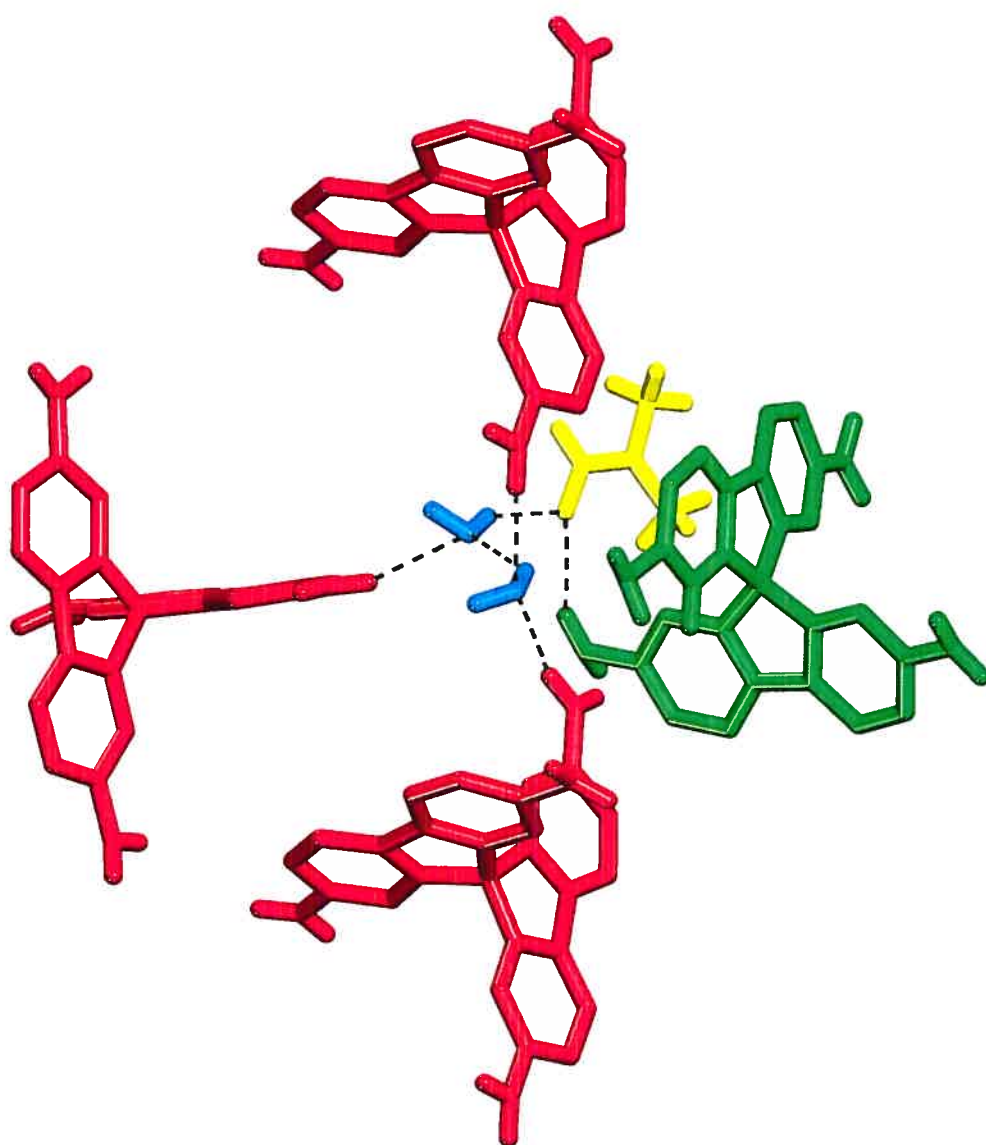


Figure 1. Representation of the structure of crystals of 2,2',7,7'-tetraamino-9,9'-spirobi[9H-fluorene] (**1c**) grown from DMF/H₂O. Three molecules of tetraaniline **1c** (red) each donate a single hydrogen bond to a hydrogen-bonded pair of H₂O molecules (blue), and a fourth molecule of compound **1c** (green) donates a single hydrogen bond to the oxygen atom of a molecule of DMF (yellow), which accepts an additional hydrogen bond from the H₂O dimer. Hydrogen bonds appear as broken lines, and hydrogen atoms of the spirobifluorene cores are omitted for clarity.

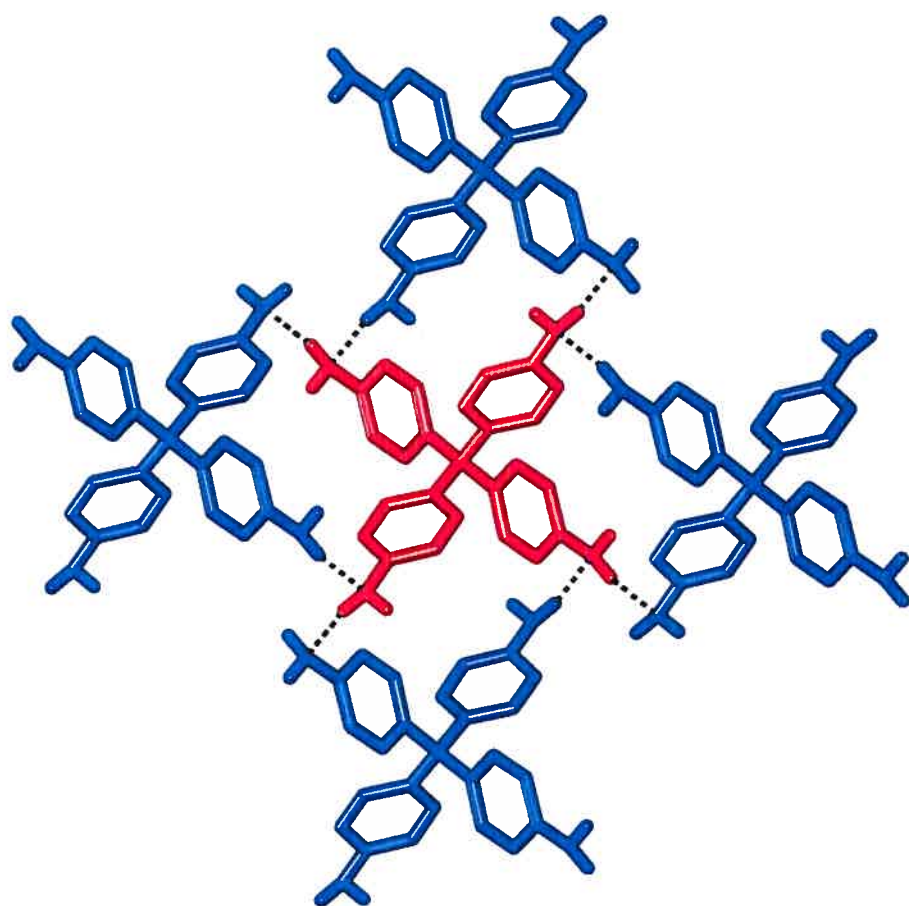


Figure 2. View along the c axis of the structure of crystals of tetrakis(4-aminophenyl)methane (**2c**) grown from DMF/CHCl₃ showing a central molecule (red) and its four hydrogen-bonded neighbors (blue). Hydrogen bonds appear as broken lines, and hydrogen atoms of the tetraphenylmethyl cores are omitted for clarity.

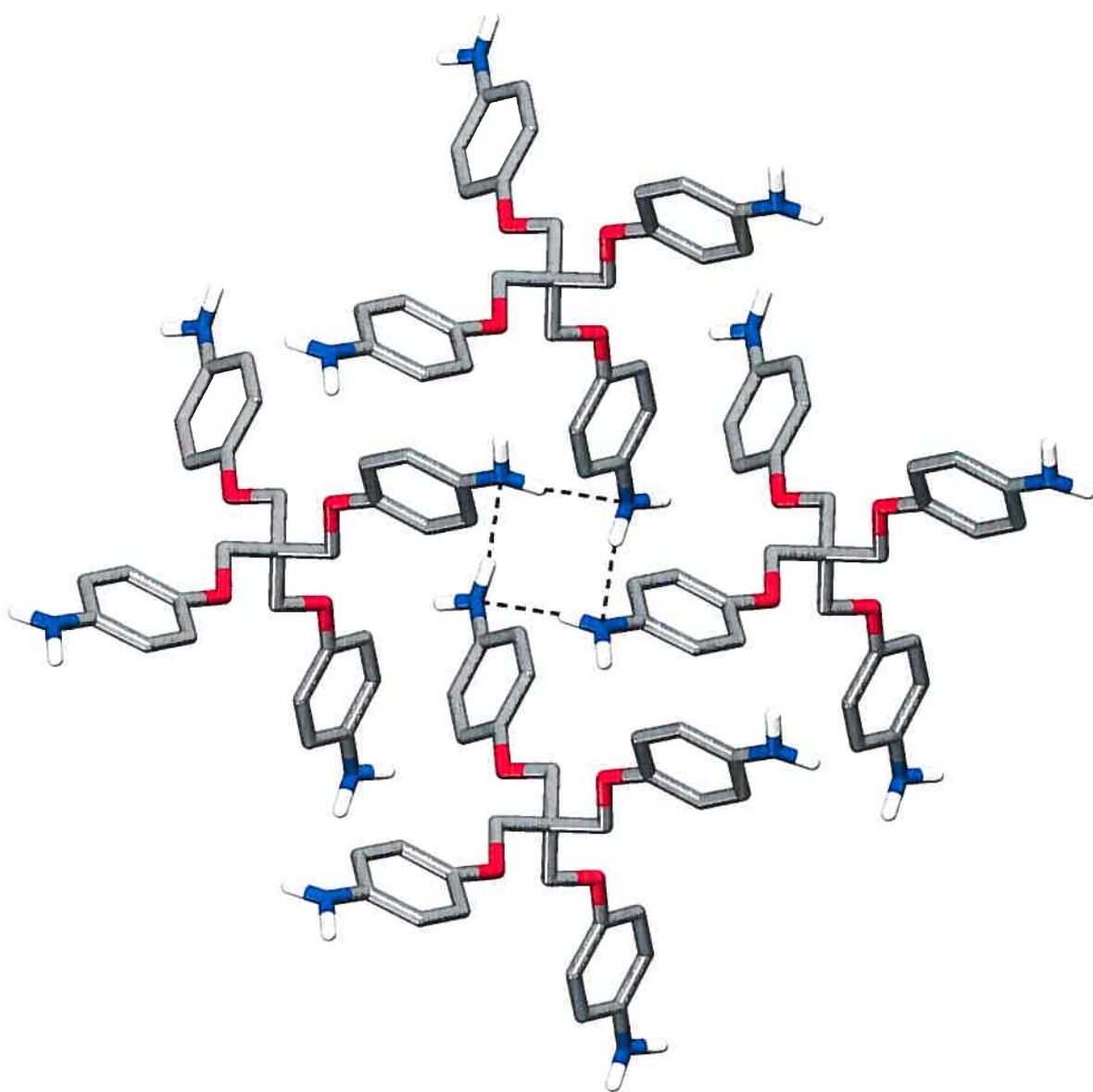


Figure 3. View along the *c* axis of the structure of crystals of tetrakis[(4-aminophenoxy)methyl]methane (**3c**) grown from THF showing the characteristic cyclic hydrogen-bonded motif formed by four molecules of tetraaniline **3c**. Hydrogen bonds appear as broken lines, and hydrogen atoms of the pentaerythrityl tetraphenyl ether cores are omitted for clarity.

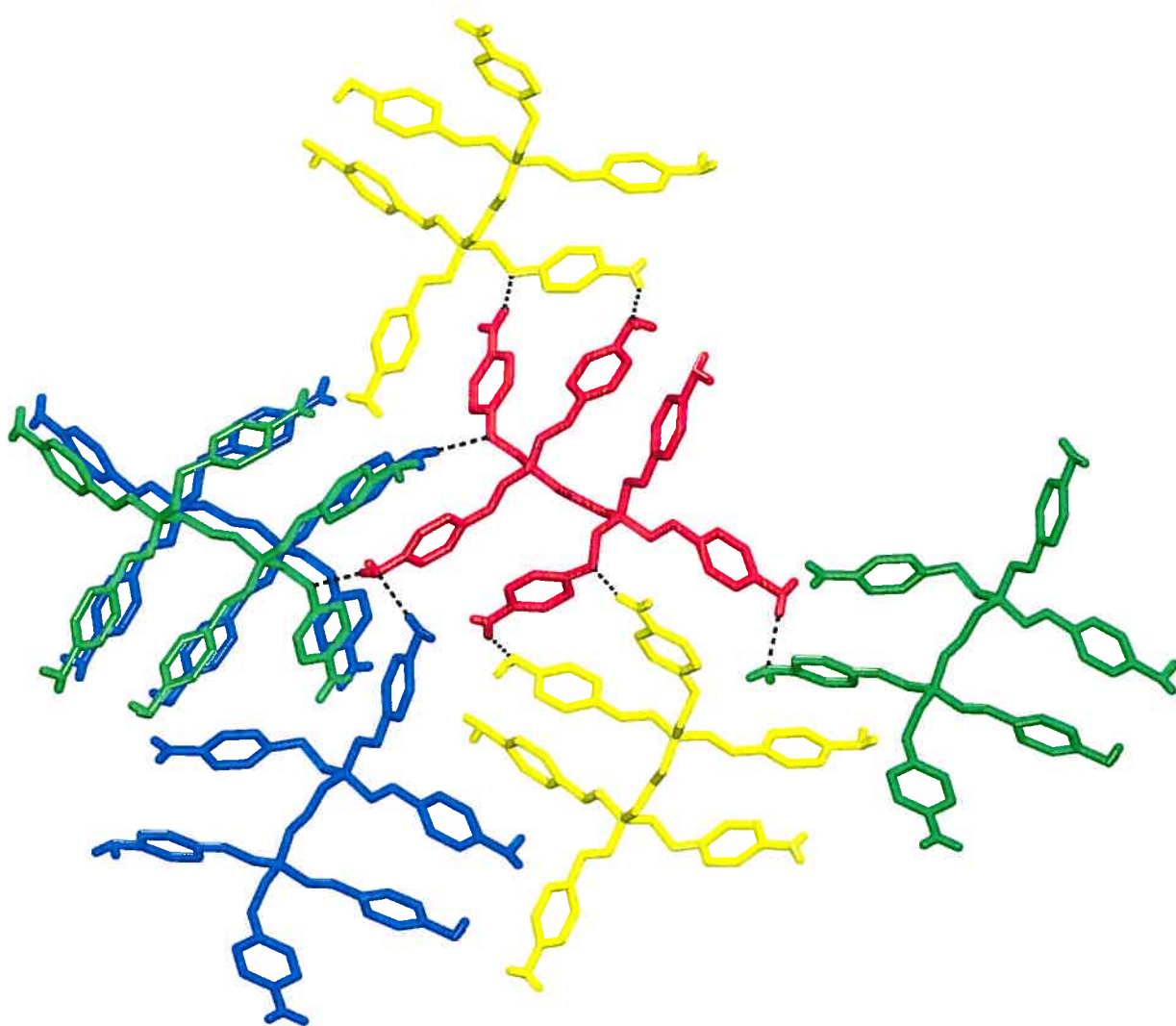


Figure 4. View of the structure of crystals of 1,1'-oxybis[3-(4-aminophenoxy)-2,2-bis[(4-aminophenoxy)methyl]]propane (**4c**) grown from benzene/CH₃OH/hexane showing a central tecton (red) surrounded by its six hydrogen-bonded neighbors. Two neighbors (yellow) each share two N-H...N hydrogen bonds with the central tecton, two other neighbors (green) each accept one hydrogen bond (one N-H...N and one N-H...O), and the remaining two neighbors (blue) each donate one hydrogen bond (one N-H...N and one N-H...O). Hydrogen bonds appear as broken lines, and hydrogen atoms of the dipentaerythrityl hexaphenyl ether cores are omitted for clarity.

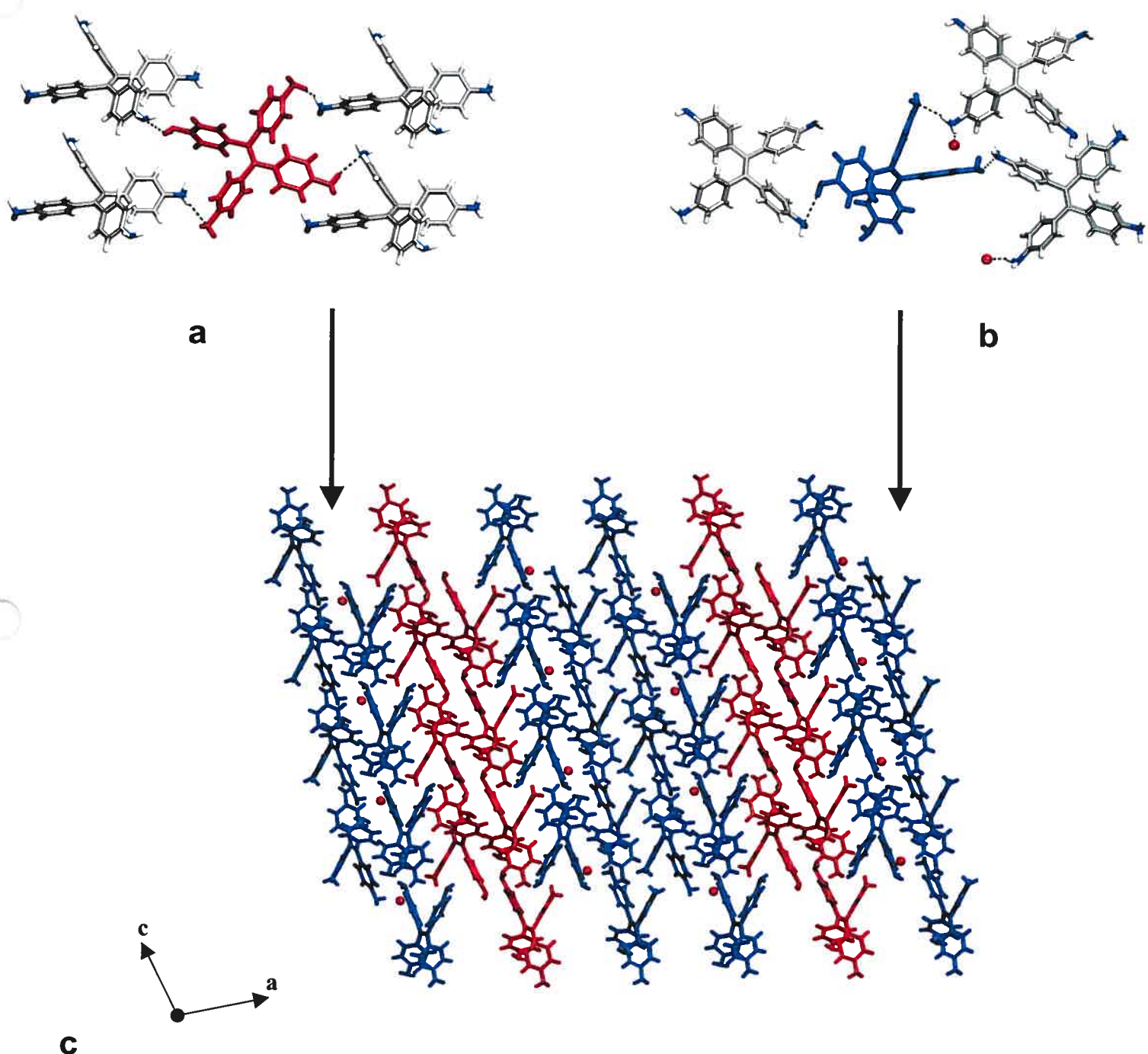
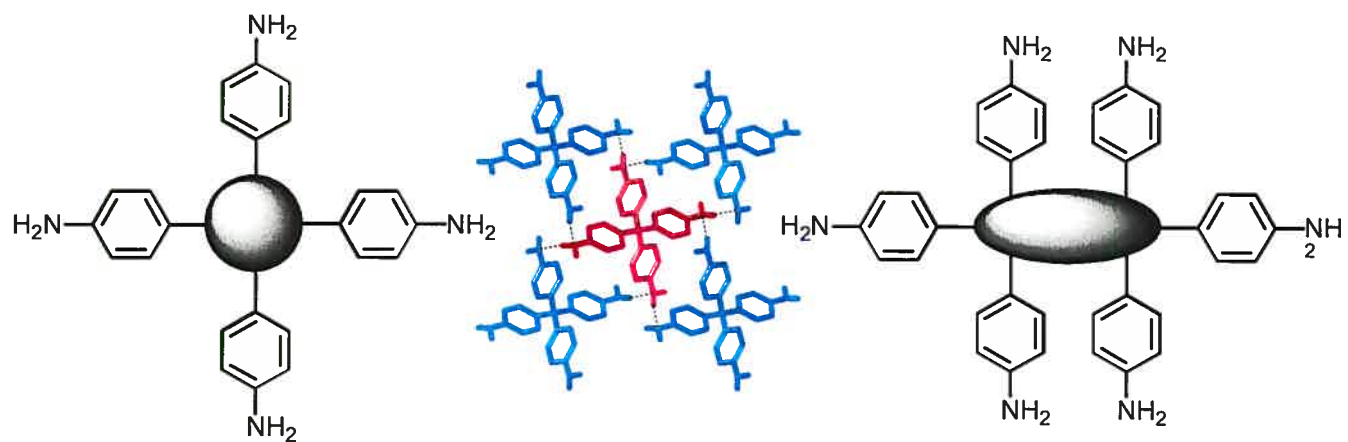


Figure 5. View of the layered structure of crystals of tetrakis(4-aminophenyl)ethylene (**5**) grown from DMF/H₂O. Hydrogen bonds appear as broken lines, and hydrogen atoms of the tetraphenylethylene cores and H₂O are omitted for clarity. a) In one type of layer (red = R), each tecton shares a total of four N-H...N hydrogen bonds with four neighbors. b) In the other type of layer (blue = B), each tecton forms a total of three N-H...N hydrogen bonds

with three neighbors, and one of the neighbors also accepts a hydrogen bond from H₂O. c) The layers then stack along the α axis according to the repeating pattern RBBRBB.

Table of Contents Graphic



5.3 Conclusion : la tectonique moléculaire et le pont hydrogène

L'analyse des résultats que nous avons présentés montre que les arylamines peuvent être utilisées en chimie supramoléculaire comme unité de reconnaissance. En effet, la cristallisation des composés **1c-4c** et **5** conduit à la formation de réseaux moléculaires retenus par de nombreux ponts hydrogène. Malheureusement, aucun motif d'association particulier n'est ressorti de cette étude.

Le comportement du composé **1c** a toutefois confirmé ce que l'on observe généralement avec les composés spirobifluorènes qui cristallisent afin de former des composés d'inclusion. D'un point de vue plus général, il faut mentionner qu'avec les unités centrales employées, il semble que la formation d'architectures découlant de l'association des arylamines privilégie un empilement plutôt compact où la porosité n'excède pas 18%. En effet, les seuls composés d'inclusion sont **1c** et **5**, mais les molécules incluses participent également à la structure du réseau. On ne peut donc pas considérer ces réseaux comme réellement poreux. Les arylamines demeurent tout de même une unité de reconnaissance utilisable en chimie supramoléculaire. Il sera intéressant de voir si les résultats futurs confirmeront les tendances observées jusqu'à présent.

Chapitre 6

***Réactions à l'intérieur de
cristaux poreux***

6.1 Introduction

Depuis quelques années, un des sujets d'actualité en chimie est la réalisation de réactions à l'état de solide cristallin. Comme il fallait s'y attendre, la nature nous a encore précédé de plusieurs millions d'années. Une belle illustration est la transformation de certains cristaux de minéraux en d'autres composés toujours cristallins. À titre d'exemple, on peut penser à l'azurite qui a comme pseudomorphe la malachite. En effet, l'azurite, carbonate basique de cuivre (II), réagit lentement avec l'eau pour donner la malachite, tel qu'illustré à la Figure 6.1.

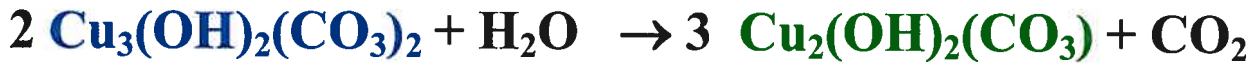


Figure 6.1 Illustration de l'azurite se transformant graduellement en son pseudomorphe, la malachite.

Inspiré une fois de plus par la nature, le chimiste s'est demandé s'il pouvait réaliser ce type de réaction dans des cristaux moléculaires. Bien entendu, il y a eu quelques cas isolés de réactions à l'état cristallin dans le passé, mais ce n'est que dans les années 60 que l'on a assisté à un vrai travail de génie cristallin où des réactions ont pris place à l'intérieur de cristaux. C'est en 1964 que Schmidt et ses collègues ont émis l'hypothèse que les réactions à l'état cristallin prenaient place avec un minimum de mouvements moléculaires.¹ En effet, ils ont montré que la photodimérisation [2+2] de l'acide cinnamique (Figure 6.2) dépend de la manière de cristalliser de ce dernier. L'acide cinnamique cristallise de trois façons différentes. La première, le cristal

¹ Cohen, M. D.; Schmidt, G. M. J. *J. Chem. Soc.* 1964, 1969.

de type α , place les groupements oléfines à une distance de 3,7 Å, avec une alternance entre le groupe phényle et le groupe carboxylique. Le type β , pour sa part, n'est pas alterné et la distance entre les oléfines est de 4,0 Å. Finalement, dans le cristal de type γ , les oléfines sont à une distance supérieure à 4,7 Å. Ainsi, lors de la photodimérisation, le cristal de type α forme l'acide truxinique de type α , le cristal β forme l'acide truxinique de type β et le cristal de type γ pour sa part est photostable puisque les oléfines sont trop éloignées pour réagir. En d'autres termes, Schmidt et ses collaborateurs ont montré que la stéréochimie du dimère formé par l'irradiation de l'acide cinnamique à l'état solide est directement corrélée à l'agencement du monomère à l'état cristallin. C'est le principe "topochimique".

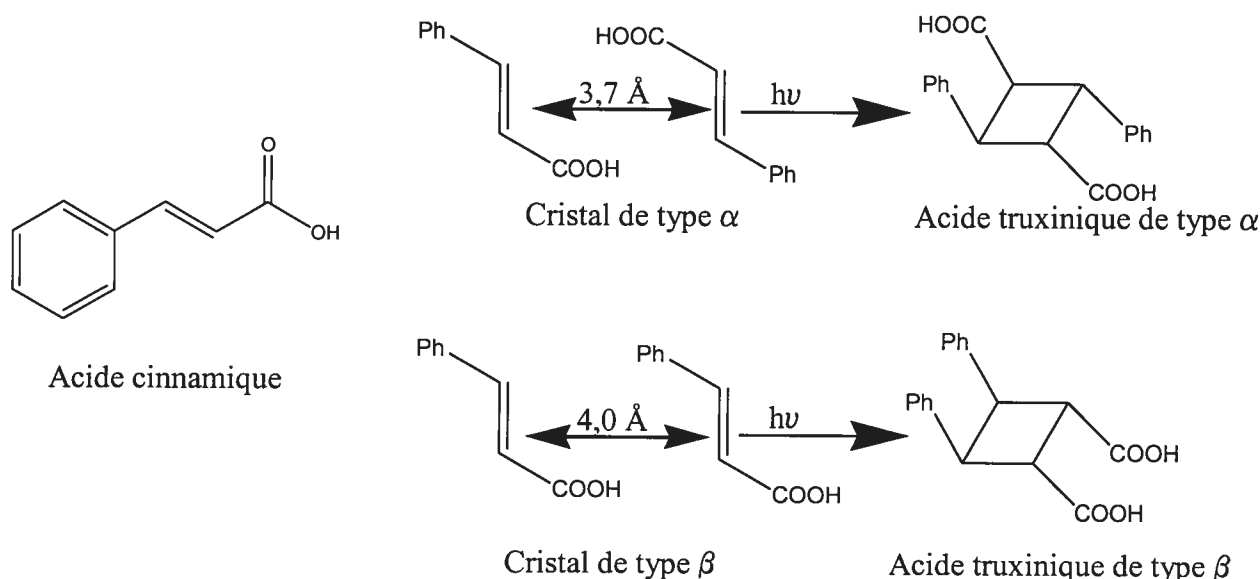


Figure 6.2 Représentation de l'acide cinnamique et de son agencement cristallin menant aux acides truxiniques.

Il a tout de même fallu attendre en 1993 pour que Enkelmann et Wegner réussissent à réaliser cette réaction de manière topotactique, c'est-à-dire dans une réaction où des monocristaux réagissent tout en conservant leur intégrité cristalline pour obtenir des cristaux avec une composition chimique différente.² Ainsi, Enkelmann et Wegner ont réalisé la

² Thomas, J. M. *Phil. Trans. Roy. Soc.* **1974**, 277, 251.

dimérisation d'un monocristal de l'acide cinnamique pour obtenir un monocristal de l'acide truxinique.³

Il existe quelques exemples de réactions topotactiques, mais la plupart d'entre elles reposent sur des photoadditions [2+2], où le positionnement des doubles liaisons est guidé par des groupes de reconnaissance. On retrouve ainsi plusieurs dimérisations et polymérisations basées sur ce concept (Figure 6.3).^{4,5} Il existe aussi d'autres types de réactions tels que des additions Diels-Alder⁶ ou encore des photoréarrangements (Figure 6.4).⁷

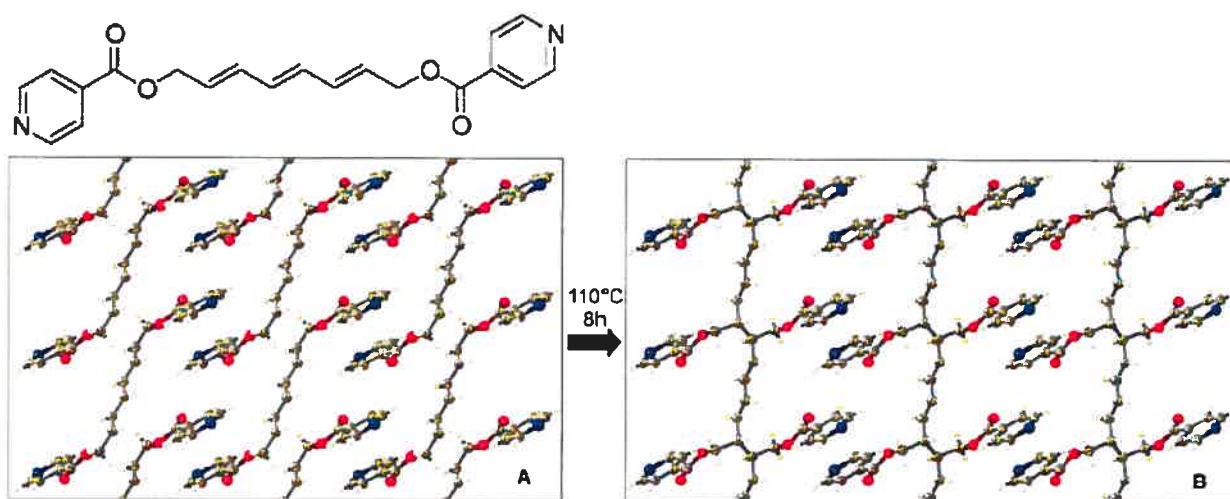


Figure 6.3 Polymérisation topochimique.^{4,5}

³ Enkelmann, V.; Wegner, G. *J. Am. Chem. Soc.* **1993**, *115*, 10390.

⁴ Takahashi, S.; Miura, H.; Kasai, H.; Okada, S.; Oikawa, H.; Nakanishi, H. *J. Am. Chem. Soc.* **2002**, *124*, 10944.

⁵ Hoang, T.; Lauher, J. W.; Fowler, F. W. *J. Am. Chem. Soc.* **2002**, *124*, 10656.

⁶ Kim, J. H.; Hubig, S. M.; Lindeman, S. V.; Kochi, J. K. *J. Am. Chem. Soc.* **2001**, *123*, 87.

⁷ Morimoto, M.; Kobatake, S.; Irie, M. *Chem. Eur. J.* **2003**, *9*, 621

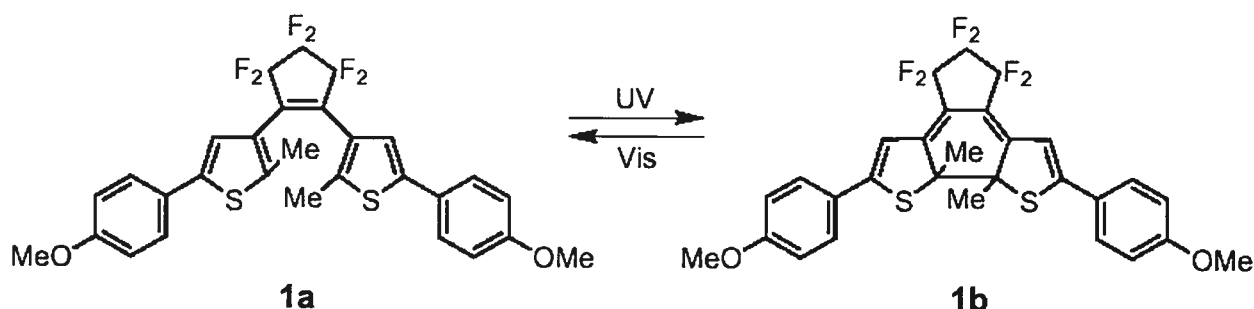


Figure 6.4 Photoréarrangement à l'état cristallin du 1,2-bis(2-méthyl-5-p-méthoxyphényl-3-thiènyle)perfluorocyclopentène.⁷

Le problème principal avec ce genre de réaction est le manque de versatilité. En effet, il faut soit être chanceux et cristalliser des composés qui ont la possibilité de réagir à l'état cristallin ou encore il faut un énorme travail de génie cristallin pour 1) installer des fonctions de reconnaissance dont les substituants sont bien placés pour satisfaire le principe topochimique et 2) trouver les conditions pour avoir une réaction topotactique.

6.2 La tectonique moléculaire et les réactions à l'état cristallin

La tectonique moléculaire propose une solution plus générale pour effectuer ce type de réaction. En effet, il a été démontré que la tectonique moléculaire permet de former des réseaux tridimensionnels poreux où les canaux formés sont occupés par des molécules provenant de la cristallisation.⁸ Il a aussi été démontré qu'il est possible de remplacer les molécules invitées par d'autres molécules par diffusion à l'intérieur des canaux, généralement sans perte de cristallinité.⁹

Il fallait à présent construire un tecton qui, en plus de former un réseau poreux suffisamment robuste pour permettre l'échange des molécules invitées, ait des groupes fonctionnels accessibles à l'intérieur des canaux formés. On a basé le squelette du tecton envisagé sur un cœur moléculaire déjà bien connu dans le groupe, soit le tecton 6.1 (Figure 6.5).¹⁰ Sa cristallisation conduit à la formation d'un réseau poreux, les canaux obtenus sont interconnectés, l'architecture est suffisamment robuste pour permettre les échanges avec plusieurs solvants sans perte de cristallinité et seulement un des deux atomes d'hydrogène des groupements amine de la triazine est utilisé pour former des ponts hydrogène. Il est donc permis de croire que la substitution d'un des hydrogènes par un groupe fonctionnel ne nuirait pas à la formation d'un réseau supramoléculaire poreux.

⁸ Wang, X.; Simard, M.; Wuest, J.D. *J. Am. Chem. Soc.* **1994**, *116*, 12119.

⁹ Brunet, P.; Simard, M.; Wuest, J.D. *J. Am. Chem. Soc.* **1997**, *119*, 2737.

¹⁰ Hetzel, S.; Maris, T.; Simard, M.; Wuest, J. D. résultats non publiés.

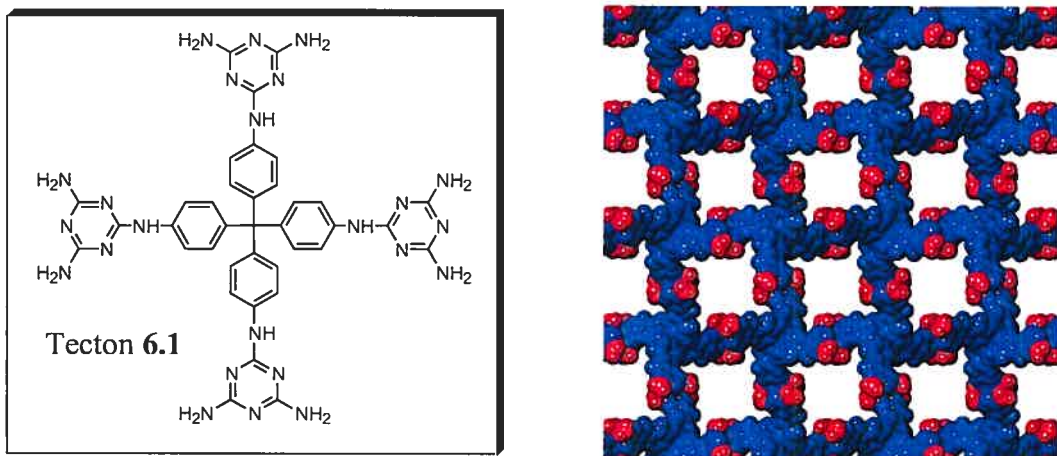


Figure 6.5 Représentation selon l'axe c, en rayons de van der Waals, du réseau formé par la cristallisation du tecton 6.1.

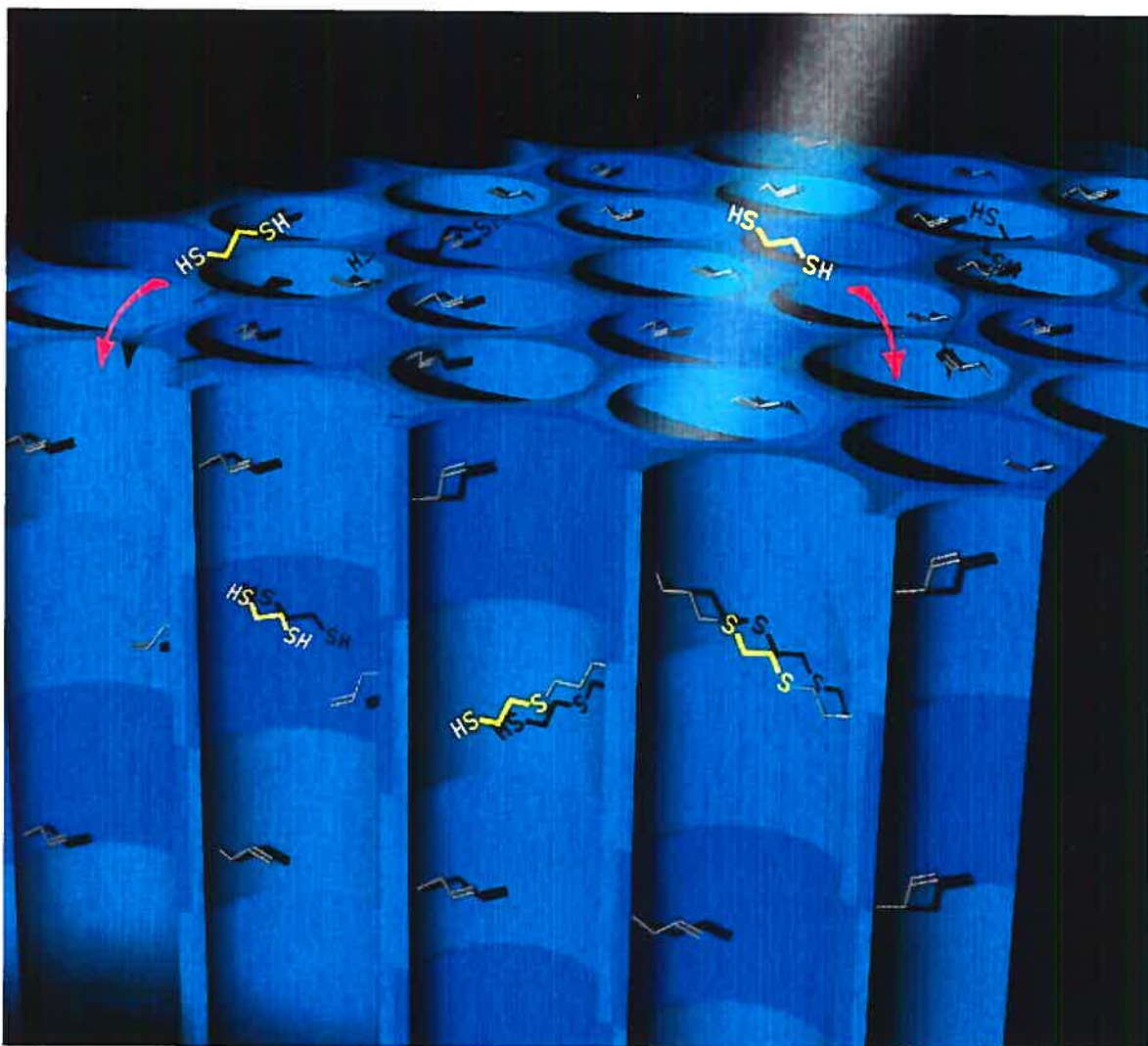
6.3 Article 4

Topotactic Reactions in Networks

*Designing Permeable Molecular Crystals that React with
External Agents To Give Crystalline Products*

Philippe Brunet, Eric Demers, Thierry Maris, Gary D. Enright and James D. Wuest

Angewandte Chemie, International Edition. 2003, 43, 5303-5305



Page de couverture de *Angewandte Chemie, International Edition*. 2003, 43, 5303-5305.

Topotactic Reactions in Networks

Designing Permeable Molecular Crystals that React with External Agents To Give Crystalline Products

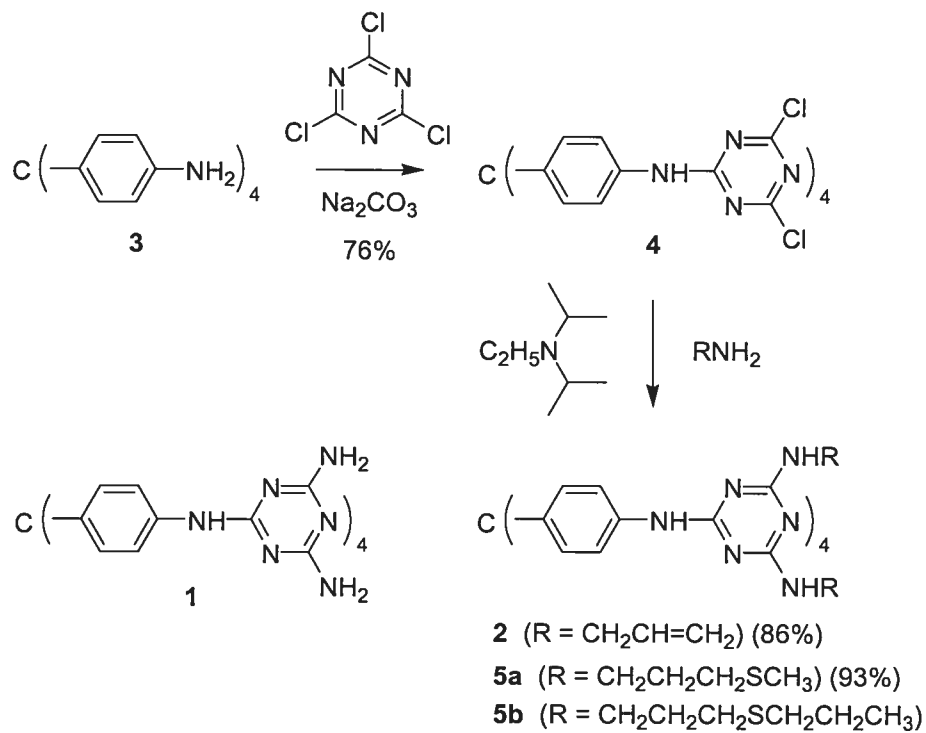
Topotactic reactions,[1] which convert single crystals of starting compounds directly into single crystals of products, are elegant and potentially useful processes that have fascinated solid-state chemists for many years. Unfortunately, such reactions are very rare. Mobility in solids is restricted, so known topotactic reactions in molecular crystals typically involve intramolecular processes or require that all necessary co-reactants be present within the solid, held in close proximity, and oriented properly.[2,3] These prerequisites can sometimes be satisfied by laborious crystal engineering, but new ways to devise topotactic reactions are needed. Here we describe a general strategy based on the use of permeable molecular crystals that are specifically designed to let external agents enter, react, and produce single crystals of new substances, with retention of the original crystalline architecture. Moreover, we show that such topotactic processes can be made to cross-link molecular crystals covalently, thereby capturing temporary supramolecular constructs as permanent crystalline macromolecular replicas.

Our strategy is related to the technique of isomorphous replacement in protein crystallography, a largely empirical process in which protein crystals are treated with agents that diffuse through water-filled channels in the crystal and bind at sites not normally determined in advance. We felt that single crystals of much smaller molecules might be made to react quantitatively with external agents at predetermined sites, thus providing a rational route to new substances in crystalline form. At present, such reactions are exceedingly rare, have been discovered by accident rather than by design, and involve only the smallest possible reactants.[3,4]

Suitable permeable molecular crystals can be made by an approach that has been called molecular tectonics.[5] This approach relies on the programmed association of special sticky molecules called tectons (derived from the Greek word for builder) that form directional

interactions with neighbors according to well-established motifs. Such molecules do not typically crystallize in normal close-packed arrays; instead, they tend to form open networks filled with potentially mobile guests.[6] Tectonic networks held together by multiple hydrogen bonds are normally robust enough to allow the original guests to be exchanged or even partially removed without the loss of crystallinity, which renders their interiors accessible to various reagents.[7]

Initial experiments showed that in the porous hydrogen bonded network formed by tecton **1** (Scheme 1), -NH₂ groups not used in intertectonic hydrogen bonding lie in guest-filled channels.[8] We reasoned that -NHR groups in substituted derivatives would be located similarly, thus making the substituents accessible to external agents. To test this hypothesis, we synthesized octaallyl derivative **2** by the route summarized in Scheme 1. X-ray diffraction established that tecton **2** crystallizes from dioxane in the tetragonal space group I 41 /a to give the network represented by Figures 1 and 2. Each tecton forms a total of 16 hydrogen bonds with four neighbors, which results in a robust non-interpenetrated network with diamondoid connectivity.[9,10]



Scheme 1. Tecton **1** and the synthesis of tectons **2** and **5a** in solution.

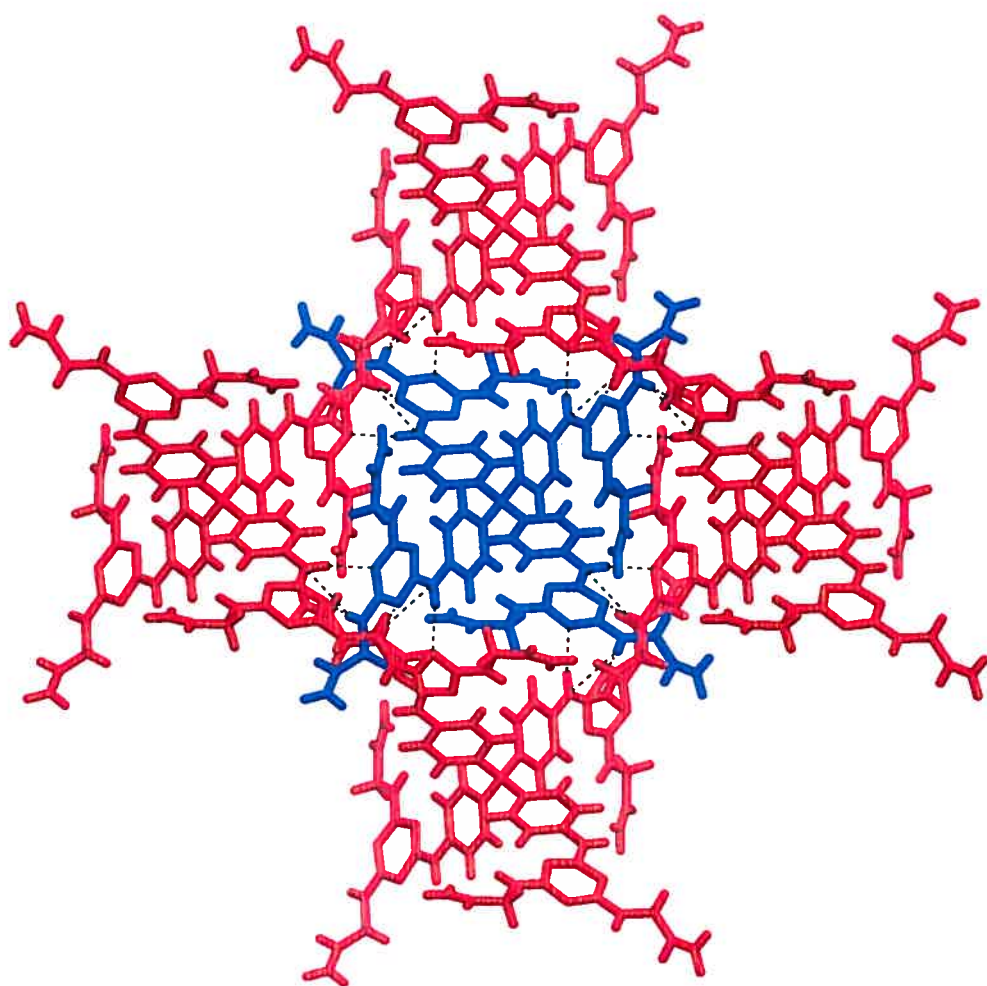


Figure 1. View along the c axis of the crystal structure of tecton **2** showing a single tecton (blue) and the four neighbors (red) with which it forms hydrogen bonds (----).

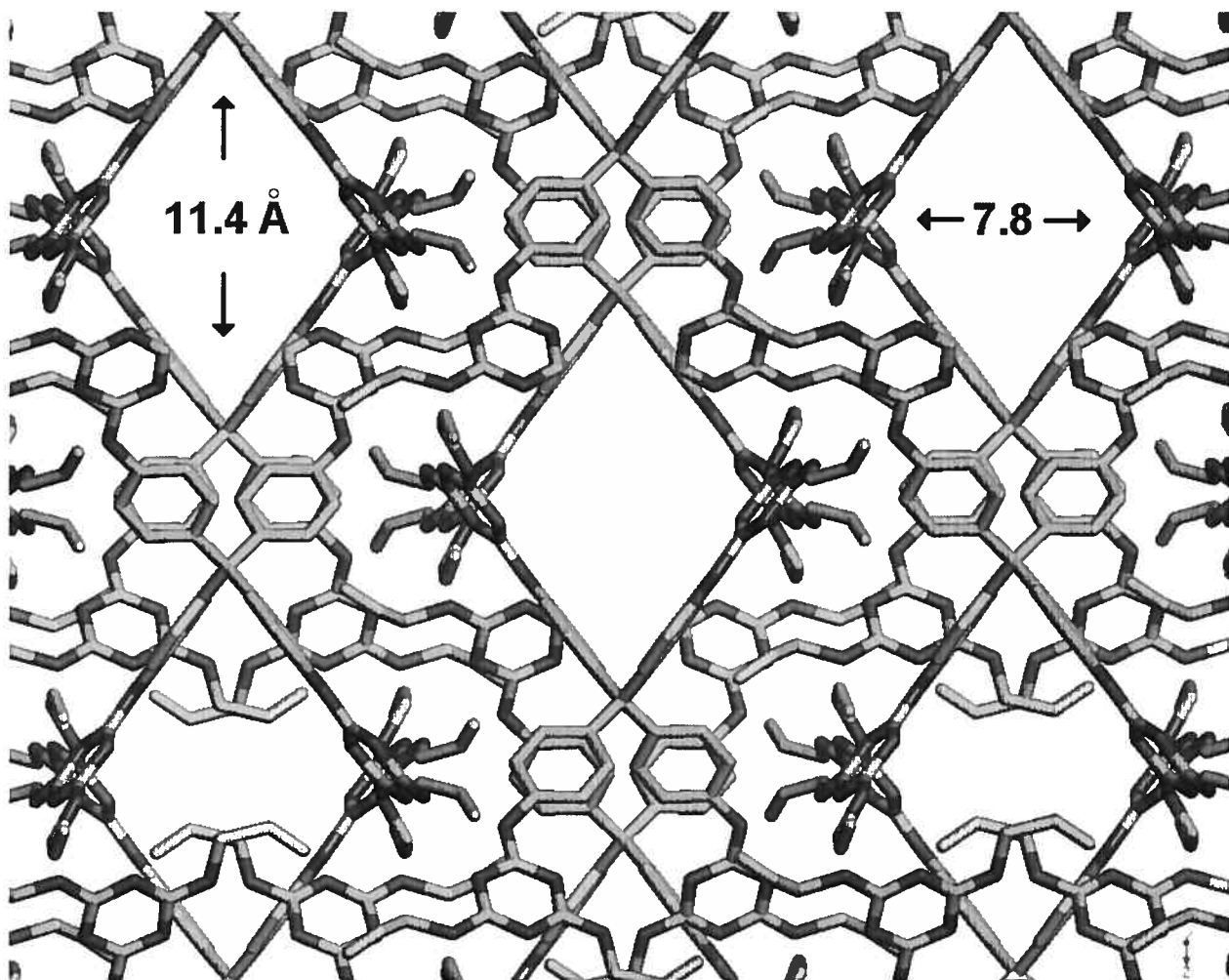


Figure 2. View along the *b* axis of the crystal structure of tecton **2** showing the cross sections of helical channels. Hydrogen atoms and some allyl groups (upper channels) have been removed for clarity.

Dioxane occupies nearly 40 % of the volume of the crystals, [11,12] which have the composition **2** • 6 dioxane, as determined by X-ray crystallography and ^1H NMR spectroscopy of dissolved samples. The guests fill interconnected helical channels that have a rhomboid cross section of approximately $7.8 \times 11.4 \text{ \AA}^2$ at the narrowest points (Figure 2). The channels themselves are represented by the surface shown in Figure 3.[13] In principle, guests diffusing inside the crystals can reach any point within the channels by multiple redundant pathways. As planned, the channels also include the allyl groups of tecton **2**.

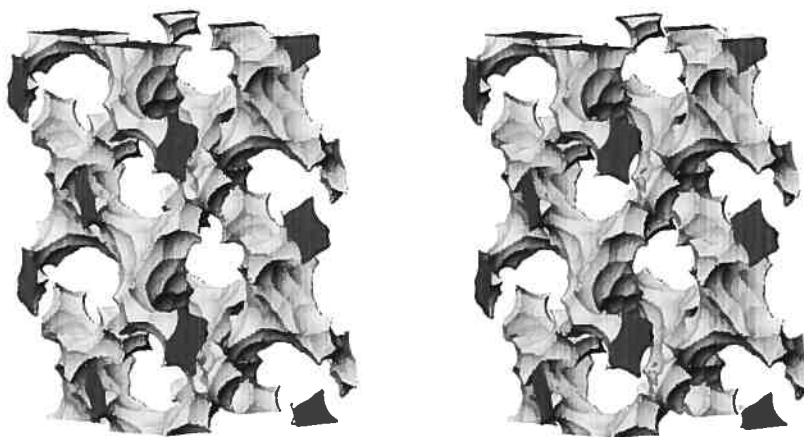


Figure 3. Stereoscopic representation of the channels in the structure of tecton 2.[13] The image shows a $1 \times 1 \times 2$ array of unit cells with the c axis vertical. The outsides of the channels appear in light gray, and dark gray is used to show where the channels are cut by the boundaries of the array. The surface is defined by the possible loci of the center of a sphere of diameter 3 as it rolls over the surface of the ordered tectonic network.

When single crystals of tecton **2** • 6 dioxane of dimensions $0.5 \times 0.5 \times 0.5$ mm were treated with excess toluene at 25°C for 24 h, they remained transparent and morphologically unchanged, continued to exhibit uniform extinction between crossed polarizers, and showed closely similar unit-cell parameters when studied by single-crystal X-ray diffraction. However, analysis of dissolved samples by ^1H NMR spectroscopy established that the initial guest, dioxane, had been replaced completely by toluene. As a result, these crystals are well designed to allow a suitable reagent to enter by diffusion and react predictably with the exposed allyl groups without changing the architecture of the network, thereby yielding isostructural crystals of a new substance.

This possibility was tested by placing single crystals of tecton **2** in degassed toluene in a quartz vessel, then exposing them to CH_3SH and irradiating them with a medium-pressure Hg

lamp at 25°C for 40 h. Under these conditions, photochemical solid-state addition of thiol to the allyl groups occurred to give thioether **5a**, [14,15] in which 70–85% of the allyl groups had reacted, as measured by ¹H NMR spectroscopy of dissolved samples. Moreover, the process proved to be topotactic. The resulting crystals were morphologically unchanged, remained transparent, and continued to exhibit uniform extinction between crossed polarizers. X-ray diffraction confirmed that thioether **5a** had been formed isostructurally as single crystals belonging to the tetragonal space group I 41 /a, with unit-cell parameters similar (\pm 9%) to those of precursor **2**.

A larger thiol ($\text{CH}_3\text{CH}_2\text{CH}_2\text{SH}$) also reacted topotactically in high yield with crystals of tecton **2** to give isostructural single crystals of thioether **5b** with similar (\pm 2%) unit cell parameters. In contrast, thiols that were too large to enter the channels in crystals of tecton **2** reacted negligibly under similar conditions, presumably because only the surfaces of the crystals are accessible. For example, photochemical additions of 3,5-dimethylbenzenethiol and 2,4,6-trimethylbenzylthiol proceeded only to the extent of \pm 3%. Such control experiments established that the observed solid-state photochemical additions to tecton **2** do not occur by a sequence of dissolution, reaction in solution, and subsequent recrystallization. The mass spectrum of thioether **5a** obtained topotactically showed the expected statistical distribution of molecules with reacted and unreacted allyl groups, which suggests that addition occurs relatively homogeneously throughout the crystal. A bimodal distribution, which would arise if addition occurred exclusively near the surface to leave an unreacted core, was not observed.

A sample of thioether **5a** prepared independently in solution by treating intermediate **4** (Scheme 1) with 3-methylthio-1-propanamine could be crystallized from $\text{CH}_3\text{OH}/\text{THF}$. In this case, the structure proved to be the same as the one obtained topotactically in the solid state. In other cases, however, we expect new polymorphs to be formed. Our strategy for devising topotactic reactions in porous crystals has two notable advantages: 1) It delivers single crystals of new compounds in polymorphic forms that are predetermined, based on the structure of the starting material, and 2) these polymorphs may be impossible to obtain by direct crystallization of the product, either because other polymorphs are favored or because crystallization does not occur at all.

A long-sought goal in supramolecular chemistry is covalent capture,[16] in which ordered structures formed reversibly by self-assembly are converted into analogues joined permanently by covalent bonds. Molecular tectonics allows predictable covalent capture to occur in the solid state by using permeable crystals with internally exposed reactive groups that can be cross-linked by external agents. This strategy extends conceptually related polymerizations, such as the cross-linking of porous protein crystals [17] and coordination complexes joined by metals,[18] to the realm of small molecular monomers and the production of single crystals of well-defined polymers.[19]

Single crystals of tecton **2** • 6 dioxane were exposed to a series of liquid dithiols $\text{HS}(\text{CH}_2)_n\text{SH}$ and irradiated under standard conditions. The resulting materials proved to be insoluble in DMSO, hot aqueous HCl, and CF_3COOH , even after crushing to expose internal surfaces. This result indicates that extensive cross-linking had taken place. When $\text{HSCH}_2\text{CH}_2\text{SH}$ was used as the cross-linker, detailed studies of the resulting polymer by solid-state ^{13}C NMR spectroscopy and Raman spectroscopy confirmed the addition of the thiol to the allyl groups.[20] Remarkably, cross-linking of crystals of tecton **2** by both $\text{HSCH}_2\text{CH}_2\text{SH}$ and $\text{HSCH}_2\text{CH}_2\text{CH}_2\text{SH}$ occurred topotactically to give isostructural single crystals of the macromolecular products. Detailed single-crystal X-ray crystallographic analysis of the products confirmed directly that cross-linking had occurred and showed that each molecule of tecton **2** becomes joined not to its immediate hydrogen-bonded neighbors but to those somewhat farther away (Figure 4).

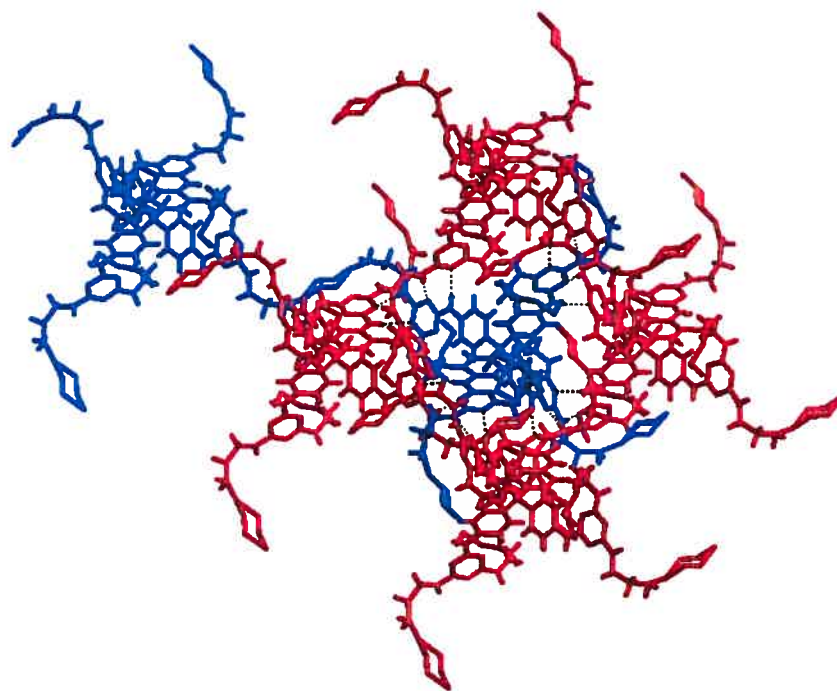


Figure 4. Structure of the macromolecule obtained by cross-linking crystals of tecton 2 with HSCH₂CH₂SH, as viewed approximately along the c axis. The image shows a central unit derived from tecton 2 (blue), four neighboring units (red) joined by hydrogen bonds (----), and one of the farther units (also in blue) to which the central unit has been linked covalently.

Despite close architectural similarity, the covalently cross-linked materials are vastly more stable than their hydrogen bonded supramolecular precursor. In particular, variable temperature X-ray powder diffraction established that the polymer derived from HSCH₂CH₂SH loses its crystallinity only when it decomposes irreversibly above 200°C whereas the precursor loses crystallinity at 25°C by spontaneous loss of included solvent. The topotactic cross-linking we observe in single crystals of tecton 2 has two unique characteristics: 1) Polymerization occurs in three dimensions to give a single crystalline macromolecular object, and 2) the composition of the product crystals is different from that of the starting crystals. In contrast, previously observed topotactic polymerizations have occurred in one direction to yield crystals with the same composition consisting of multiple copies of linear macromolecules.[2]

These observations demonstrate how molecular tectonics, by allowing the design of robust porous networks with reactive interiors, can give access to new molecular and

macromolecular materials with predictably ordered structures that would be difficult or impossible to obtain by conventional methods.

Keywords

materials science • supramolecular chemistry • crystal engineering • topotactic reactions • hydrogen bonding

Acknowledgments

We thank Drs. James F. Britten and Michel Simard for preliminary crystallographic studies, Marjolaine Arseneault for her help in obtaining Raman spectra, and Prof. Denis Gravel for his expertise in photochemistry. We are grateful to the Natural Sciences and Engineering Research Council of Canada, the Ministère de l'Éducation du Québec, the Canada Research Chairs Program, and the Canada Foundation for Innovation for financial support.

Experimental Section

X-ray structural analyses

Data were collected at 173 K using a Bruker SMART 1000 CCD diffractometer with Mo K α radiation ($\lambda = 0.71070 \text{ \AA}$). Intensities were integrated using SAINT^[16] and corrected for absorption and other effects using SADABS.^[17] Structures were solved and refined using the SHELX suite of programs.^[18]

Crystal data for tecton **2** • 6 dioxane: crystal size 0.15 x 0.20 x 0.30 mm, tetragonal, space group I4₁/a, $a = b = 23.0674(6) \text{ \AA}$, $c = 16.1892(6) \text{ \AA}$, $V = 8614.4(4) \text{ \AA}^3$, $Z = 4$. Least-squares refinement of 273 parameters based on 1759 reflections with $I > 2\sigma(I)$ (out of 2269 reflections) gave $R_1 = 0.0795$, $wR_2 = 0.230$, and GoF = 1.076.

Crystal data for thioether **5a** (as obtained from crystals of tecton **2**): crystal size 0.08 x 0.15 x 0.20 mm, tetragonal, space group I4₁/a, $a = b = 20.988(2) \text{ \AA}$, $c = 16.816(3) \text{ \AA}$, $V = 7407.6(16)$

\AA^3 , $Z = 4$. Least-squares refinement of 214 parameters based on 865 reflections with $I > 2\sigma(I)$ (out of 1976 reflections) gave $R_1 = 0.1210$, $wR_2 = 0.389$, and GoF = 1.306.

Crystal data for the product of cross-linking crystals of tecton **2** by $\text{HSCH}_2\text{CH}_2\text{CH}_2\text{SH}$: crystal size $0.15 \times 0.30 \times 0.30$ mm, tetragonal, space group $I4_1/a$, $a = b = 23.233(16)$ \AA , $c = 16.274(17)$ \AA , $V = 8785(13)$ \AA^3 , $Z = 4$. Least-squares refinement of 182 parameters (with 192 restraints) based on 462 reflections with $I > 2\sigma(I)$ (out of 688 reflections) gave $R_1 = 0.1888$, $wR_2 = 0.461$, and GoF = 1.766.

Estimation of porosity

The percentage of volume accessible to guests was estimated by the PLATON program (A. L. Spek, *PLATON, A Multipurpose Crystallographic Tool*; Utrecht University: Utrecht, The Netherlands, 2001. P. van der Sluis, A. L. Spek, *Acta Crystallogr.* **1990**, *A46*, 194). PLATON calculates the accessible volume by allowing a spherical probe of variable radius to roll over the internal van der Waals surface of the crystal structure. PLATON uses a default value of 1.20 \AA for the radius of the probe, which is an appropriate model for small guests such as water. The van der Waals radii used to define surfaces for these calculations are as follows: C: 1.70 \AA , H: 1.20 \AA , N: 1.55 \AA , O: 1.52 \AA , and S: 1.80 \AA . If V is the volume of the unit cell and V_g is the guest-accessible volume as calculated by PLATON, then the porosity P in % is given by $100V_g/V$.

Notes and References

- [1] J. M. Thomas, *Phil. Trans. Roy. Soc.* **1974**, *277*, 251.
- [2] M. Morimoto, S. Kobatake, M. Irie, *Chem. Eur. J.* **2003**, *9*, 621; S. Takahashi, H. Miura, H. Kasai, S. Okada, H. Oikawa, H. Nakanishi, *J. Am. Chem. Soc.* **2002**, *124*, 10944; T. Hoang, J. W. Lauher, F. W. Fowler, *J. Am. Chem. Soc.* **2002**, *124*, 10656; T. Tanaka, A. Matsumoto, *J. Am. Chem. Soc.* **2002**, *124*, 9676; J. H. Kim, S. M. Hubig, S. V. Lindeman, J. K. Kochi, *J. Am. Chem. Soc.* **2001**, *123*, 87; M. Irie, T. Lifka, S. Kobatake, N. Kato, *J. Am. Chem. Soc.* **2000**, *122*, 4871. K. Tanaka, E. Mochizuki, N. Yasui, Y. Kai, I. Miyahara, K. Hirotsu, F. Toda, *Tetrahedron*, **2000**, *56*, 6853; K. Honda, F. Nakanishi, N. Feeder, *J. Am. Chem. Soc.* **1999**, *121*, 8246; Y. Ohashi, *Acta Crystallogr. Sect. A*, **1998**, *54*, 842; H. Hosomi, Y. Ito, S. Ohba, *Acta Crystallogr. Sect. B*, **1998**, *54*, 907; C. J. Keppert, D. Hesek, P. D. Beer, M. J. Rosseinsky, *Angew. Chem.*, **1998**, *110*, 3335; *Angew. Chem. Int. Ed.*, **1998**, *37*, 3158; J. D. Ranford, J. J. Vittal, D. Wu, *Angew. Chem.*, **1998**, *110*, 1159; *Angew. Chem. Int. Ed.*, **1998**, *37*, 1114; M. Leibovitch, G. Olovsson, J. R. Scheffer, J. Trotter, *J. Am. Chem. Soc.*, **1997**, *119*, 1462; T. Suzuki, T. Fukushima, Y. Yamashita, T. Miyashi, *J. Am. Chem. Soc.*, **1994**, *116*, 2793; A. Mori, N. Kato, H. Takeshita, Y. Kurahashi, M. Ito, *J. Chem. Soc. Chem. Commun.*, **1994**, 869; V. Enkelmann, G. Wegner, K. Novak, K. B. Wagener, *J. Am. Chem. Soc.*, **1993**, *115*, 10390; W.-N. Wang, W. Jones, *Tetrahedron*, **1987**, *43*, 1273; B. Tieke, *J. Polym. Sci. Polym. Chem. Ed.*, **1984**, *22*, 2895; E. J. Miller, T. B. Brill, A. L. Rheingold, W. C. Fultz, *J. Am. Chem. Soc.*, **1983**, *105*, 7580; M. Hasegawa, *Chem. Rev.*, **1983**, *83*, 507; H. Nakanishi, W. Jones, J. M. Thomas, M. B. Hursthouse, M. Motellalli, *J. Phys. Chem.*, **1981**, *85*, 3636; R. Popovitz-Biro, H. C. Chang, C. P. Tang, N. R. Shochet, M. Lahav, L. Leiserowitz, *Pure Appl. Chem.*, **1980**, *52*, 2693; K. Cheng, B. M. Foxman, *J. Am. Chem. Soc.*, **1977**, *99*, 8102; G. M. J. Schmidt, *Pure Appl. Chem.*, **1971**, *27*, 647.
- [3] N. Tokitoh, Y. Arai, T. Sasamori, R. Okazaki, S. Nagase, H. Uekusa, Y. Ohashi, *J. Am. Chem. Soc.* **1998**, *120*, 433.
- [4] For related reactions of guests with hosts in molecular inclusion complexes, see: R. Popovitz-Biro, H. C. Chang, C. P. Tang, N. R. Shochet, M. Lahav, L. Leiserowitz, *Pure Appl. Chem.*, **1980**, *52*, 2693.

- [5] S. Mann, *Nature* **1993**, *365*, 499. M. Simard, D. Su, J. D. Wuest, *J. Am. Chem. Soc.* **1991**, *113*, 4696.
- [6] For recent references, see: J.-H. Fournier, T. Maris, J. D. Wuest, W. Guo, E. Galoppini, *J. Am. Chem. Soc.* **2003**, *125*, 1002.
- [7] P. Brunet, M. Simard, J. D. Wuest, *J. Am. Chem. Soc.* **1997**, *119*, 2737. X. Wang, M. Simard, J. D. Wuest, *J. Am. Chem. Soc.* **1994**, *116*, 12119.
- [8] S. Hetzel, T. Maris, M. Simard, J. D. Wuest, unpublished results.
- [9] S. R. Batten, R. Robson, *Angew. Chem., Int. Ed. Engl.* **1998**, *37*, 1460.
- [10] M. J. Zaworotko, *Chem. Soc. Rev.* **1994**, *23*, 283.
- [11] The percentage of volume accessible to guests was estimated by the PLATON program,^[10] as described in detail in the supporting information.
- [12] A. L. Spek, *PLATON, A Multipurpose Crystallographic Tool*, Utrecht University, Utrecht (The Netherlands), **2001**. P. van der Sluis, A. L. Spek, *Acta Crystallogr.* **1990**, *A46*, 194.
- [13] Representations of channels were generated by the Cavities option in the ATOMS program (ATOMS, Version 5.1;Shape Software:521 Hidden Valley Road, Kingsport, TN 37663; <http://www.shapesoftware.com>). We are grateful to Eric Dowty of Shape Software for integrating this capacity into ATOMS at our suggestion.
- [14] For a review of photochemical reactions in molecular crystals, see: V. Ramamurthy, K. Venkatesan, *Chem. Rev.*, **1987**, *87*, 433.
- [15] C. S. Marvel, R. R. Chambers, *J. Am. Chem. Soc.* **1948**, *70*, 993. W. E. Vaughan, F. F. Rust, *J. Org. Chem.* **1942**, *7*, 472.
- [16] E. A. Archer, M. J. Krische, *J. Am. Chem. Soc.*, **2002**, *124*, 5074.
- [17] A. L. Margolin, M. A. Navia, *Angew. Chem.*, **2001**, *113*, 2262; *Angew. Chem. Int. Ed.*, **2001**, *40*, 2204.
- [18] Z. Xu, S. Lee, Y.-H. Kiang, A. B. Mallik, N. Tsomaia, K. T. Mueller, *Adv. Mater.*, **2001**, *13*, 637.
- [19] For recent references to related polymerizations of guests in molecular inclusion complexes, see: K. Nakano, K. Sada, M. Miyata, *Polym. J.*, **2001**, *33*, 172; K. Tajima, T. Aida, *Chem. Commun.*, **2000**, 2399.
- [20] Some allyl groups remain unreacted, some molecules of HSCH₂CH₂SH react only once, leaving free –SH groups, and some unreacted HSCH₂CH₂SH may remain trapped in the

lattice. Spectroscopic and elemental analyses are consistent with the addition of approximately 6 equivalents of HSCH₂CH₂SH per tecton, rather than the 4 equivalents required for ideal cross-linking.

- [21] SAINT (Release 6.06), Integration Software for Single Crystal Data, Bruker AXS Inc., Madison, Wisconsin (USA), **1999**.
- [22] G. M. Sheldrick, SADABS, Bruker Area Detector Absorption Corrections, Bruker AXS Inc., Madison, Wisconsin (USA), **1996**.
- [23] G. M. Sheldrick, SHELXS-97, Program for the Solution of Crystal Structures and SHELXL-97, Program for the Refinement of Crystal Structures, University of Göttingen (Germany), **1997**.

6.4 Conclusions et perspectives

La réalisation de réactions dans des cristaux poreux par diffusion d'un réactif à l'intérieur des canaux crée maintenant de nouvelles opportunités pour la tectonique moléculaire. En effet, nous savons maintenant que ces réactions sont possibles et qu'il suffit de bien concevoir le tecton de départ pour permettre la réalisation de réactions à l'état solide avec de tels cristaux. De plus, on a maintenant la possibilité de rigidifier le réseau par polymérisation si l'on envisage des utilisations nécessitant une plus grande robustesse du cristal. Il reste maintenant à utiliser notre imagination pour concevoir de nouveaux tectons en vue d'applications pratiques.

Une extension intéressante à ce projet serait de tenter l'encapsulation des molécules invitées à l'intérieur du cristal. En effet, nous avons montré que des thiols d'une dimension trop élevée sont dans l'impossibilité de pénétrer à l'intérieur du cristal et de réagir avec les double liaisons des tectons. Ainsi, l'emploi de ces thiols ne menait qu'à des réactions de faibles rendements pouvant être attribués à des réactions de surface. Il serait donc intéressant de voir le résultat de ce même genre de réactions, avec un dithiol dont la dimension l'obligerait à ne réagir qu'en surface (Figure 6.6). Il est alors permis de se demander si cette réaction de surface permettrait de piéger les molécules invitées à l'intérieur du cristal.

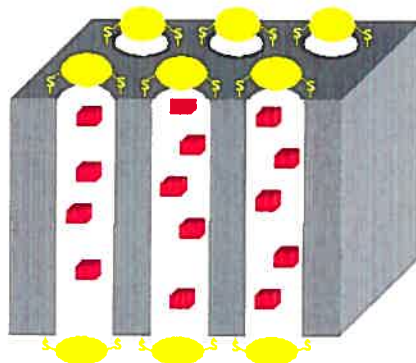


Figure 6.6 Représentation schématique de l'encapsulation de molécules invitées (cube rouge) à l'intérieur d'un cristal (cube gris) par une réaction de surface à l'aide d'un gros dithiol (jaune).

Chapitre 7

***Excavation de cristaux
moléculaires***

7.1 Introduction

Depuis plusieurs années, on compare les réseaux tectoniques aux zéolithes, composés inorganiques à base d'aluminosilicates ou d'aluminophosphates. En effet, les composés de la famille des zéolithes sont poreux et très utilisés tant en industrie qu'en recherche académique, et ce, notamment dans des processus de séparation, d'échange d'ions et de catalyse.¹ Par exemple, certains sont utilisés pour leurs capacités sorptives afin de piéger sélectivement en leur sein des molécules d'eau. Les zéolithes peuvent aussi servir de catalyseurs. Dans ce cas, les molécules diffusent à l'intérieur des cavités et subissent des transformations catalysées par la présence d'acides de Brønsted ou de Lewis faisant partie intégrante du réseau.

Les zéolithes ont l'avantage d'être très robustes et de résister à des conditions extrêmes, ce que les réseaux moléculaires ne tolèrent généralement pas. La préparation de ces réseaux poreux ne se veut pas une méthode pour fournir des substituants aux zéolithes, mais un outil complémentaire. Ainsi, certaines caractéristiques des réseaux tectoniques organiques peuvent sembler une faiblesse par rapport aux zéolithes, mais on verra qu'elles sont compensées par d'autres avantages.

Premièrement, le volume « libre » des zéolithes classiques dépasse rarement 50%² alors qu'il dépasse couramment cette valeur dans le cas des solides tectoniques. On a même répertorié des volumes libres de l'ordre de 70 à 75%.³

¹ Stein, A. *Adv. Mater.*, 2003, **15**, 763. A. Corma, *Chem. Rev.*, 1997, **97**, 2373.

² Cheetham, A. K.; Ferey, G.; Loiseau, T. *Angew. Chem. Int. Ed.* 1999, **38**, 3268.

³ Maley, K.; Gagnon, E.; Maris, T.; Wuest, J. D., résultats non publiés. Malek, N.; Simard, M.; Maris, T.; Wuest, J. D. *J. Am. Chem. Soc.* . 2005, **127** (16), 5910.

c) Fournier, J.-H.; Maris, T.; Wuest, J. D. *J. Org. Chem.* 2004, **69**, 1762.

Deuxièmement, il est possible d'incorporer, lors de la synthèse des tectons, des groupements fonctionnels pouvant servir de sites de catalyse. Par ce fait même, cette incorporation est plus facile et aussi plus versatile que de former une nouvelle zéolithe. En effet, la gamme de catalyseurs existants en chimie ne limite pas le choix aux sites catalytiques acides des zéolites. Il est aussi à noter qu'il est également possible d'incorporer des chromophores ou encore des éléments de chiralité selon l'usage souhaité.

Troisièmement, la modulation des dimensions des cavités est beaucoup plus aisée dans le cas de la tectonique moléculaire puisqu'il suffit en principe de modifier les dimensions des tectons pour observer une modification conséquente à l'échelle du réseau. De plus, les tectons peuvent incorporer certains éléments de flexibilité conférant aux réseaux une capacité d'adaptation aux déformations mécaniques.

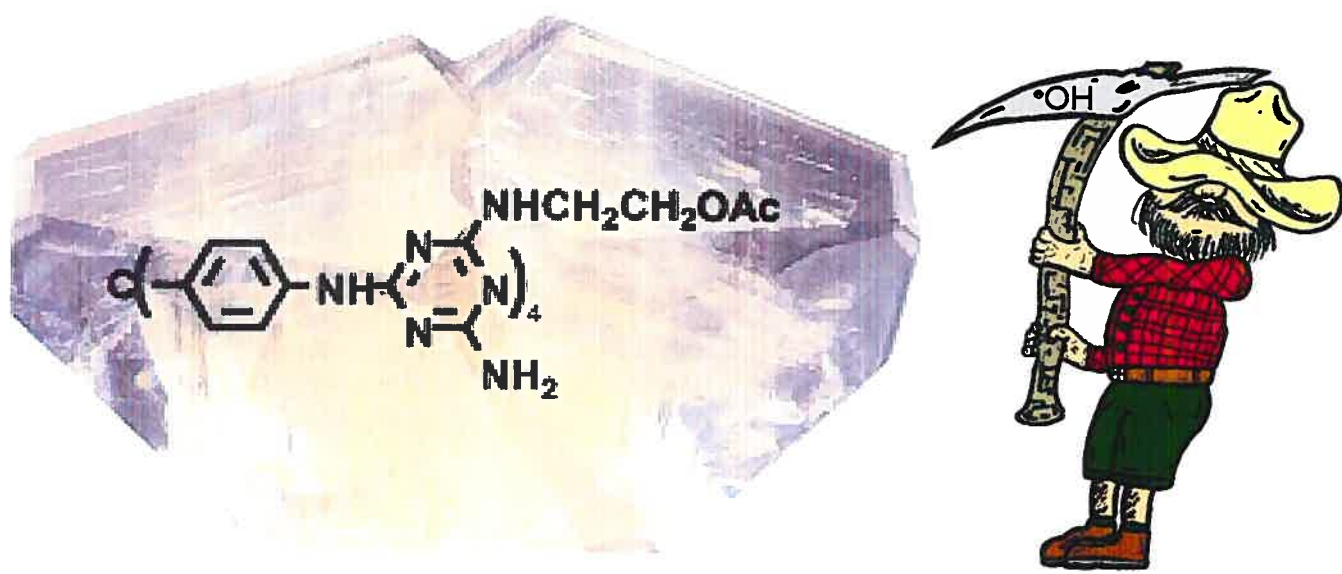
Les avantages mentionnés ci-dessus ont été jusqu'à ce jour des concepts théoriques. Il faut désormais montrer des exemples concrets afin de démontrer l'utilité de la tectonique moléculaire. Le présent chapitre sera consacré à deux des avantages mentionnés plus haut. Ainsi, on traitera du contrôle de la porosité du réseau ainsi que de l'incorporation de groupes fonctionnels à l'intérieur de ce dernier. Le contrôle de la porosité est d'une importance majeure pour différentes applications potentielles de la tectonique moléculaire. En effet, si l'on veut réaliser une certaine sélection lors d'applications telle que la chromatographie d'exclusion, il est nécessaire de pouvoir contrôler la grosseur des canaux formés. De plus, pour ce qui est de la réalisation de réactions à l'intérieur du réseau, il faut d'abord que les molécules puissent y pénétrer. Ensuite, il peut être nécessaire d'introduire des groupes fonctionnels pour catalyser les réactions à l'intérieur du réseau, donc il faut montrer la faisabilité de cette insertion. Finalement, si l'on veut effectuer la mimique d'un état de transition afin de catalyser une réaction, il faut également montrer qu'il est possible de retirer des fractions de molécules, par exemple un groupe fonctionnel faisant la mimique d'un état de transition, appartenant au réseau sans briser la cristallinité de ce dernier.

7.2 Article 5

Excavations in molecular crystals

Erwan Le Fur, Eric Demers, Thierry Maris and James D. Wuest

Chemical Communications, 2003, 2966-2967



Le concept de l'excavation illustré dans *Chemical Communications*, 2003, 2966-2967.

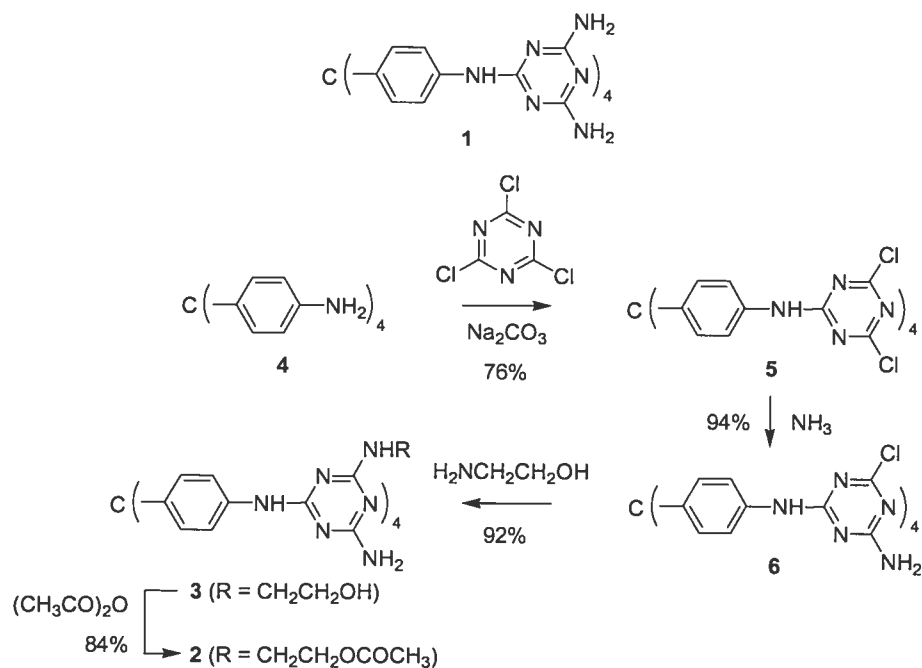
Excavations in molecular crystals

Single crystals built from porous molecular networks can react with agents that penetrate the crystals, cleave fragments from the network, and thereby increase the volume available for guests, all without loss of crystallinity.

Ordered microporous materials are indispensable in modern technology, particularly in catalysis and separation.^{1,2} The resulting need to control and enhance porosity has driven research in the field of zeolites and related inorganic materials for decades. More recently, impressive molecular analogues have been devised, using compounds joined by coordination to metals, hydrogen bonds, or other interactions to form open networks.¹⁻³ In both zeolites and their molecular analogues, the well-defined volume of the ordered host network normally sets a fixed upper limit on the volume available for accommodating guests. Here we describe a strategy for increasing the useable volume in porous molecular networks by excavating the interiors of single crystals.

Molecular crystals with accessible interiors can be made conveniently by an approach that has been called molecular tectonics.⁴ This approach is based on the programmed association of special sticky compounds, called tectons from the Greek word for builder, that form directional interactions with their neighbors according to reliable motifs. The crystallization of such molecules tends to produce open networks filled with potentially mobile guests. Porous networks joined by multiple hydrogen bonds are normally robust enough to allow guests in single crystals to be exchanged or even partially removed without loss of crystallinity, thereby making the interiors accessible to various agents.⁵ In principle, this allows the porosity to be increased rationally by introducing agents that 1) react with the constituent tectons at predetermined sites and 2) liberate small molecular fragments that can escape the network by diffusion, all without loss of crystallinity.

Initial work showed that tecton **1** (Scheme 1) crystallizes to form an open network held together by hydrogen bonding of triaminotriazine groups. In this network, $-\text{NH}_2$ groups not used in intertectonic hydrogen bonding lie in guest-filled channels. We expected $-\text{NHR}$ groups in substituted derivatives to be located similarly, making them accessible to external agents. To test this hypothesis, we made tetraacetate **2** by the route shown in Scheme 1. X-ray diffraction established that tecton **2** crystallizes from DMSO/acetone/ H_2O in the tetragonal space group $I4_1/a$ to give the network represented by Fig. 1-2.[‡] The 4 triaminotriazine groups of each tecton form a total of 16 hydrogen bonds with 4 neighboring tectons (Fig. 1), resulting in a robust non-interpenetrated network with diamondoid connectivity.⁶ In addition, the 4 $-\text{NH}(\text{CH}_2)_2\text{OCOCH}_3$ groups of each tecton are involved in a total of 8 hydrogen bonds with 4 additional neighbors (Fig. 2). This yields a structure in which each tecton forms a total of 24 hydrogen bonds with 8 neighbors.



Scheme 1. Tecton **1** and the synthesis of tecton **2**.

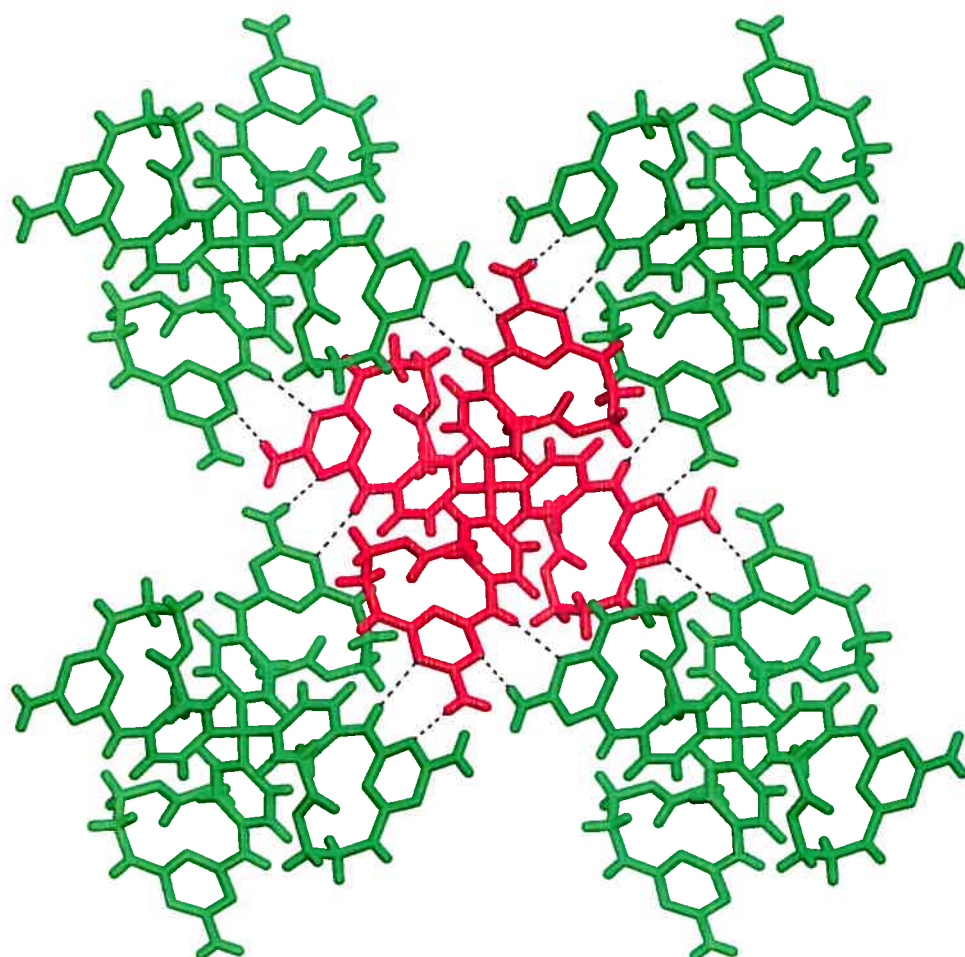


Figure 1. View along the *c* axis of the crystal structure of tecton 2 showing a central tecton (red) and the 4 neighbors (green) with which it interacts by hydrogen bonds (blue) involving triaminotriazine groups.

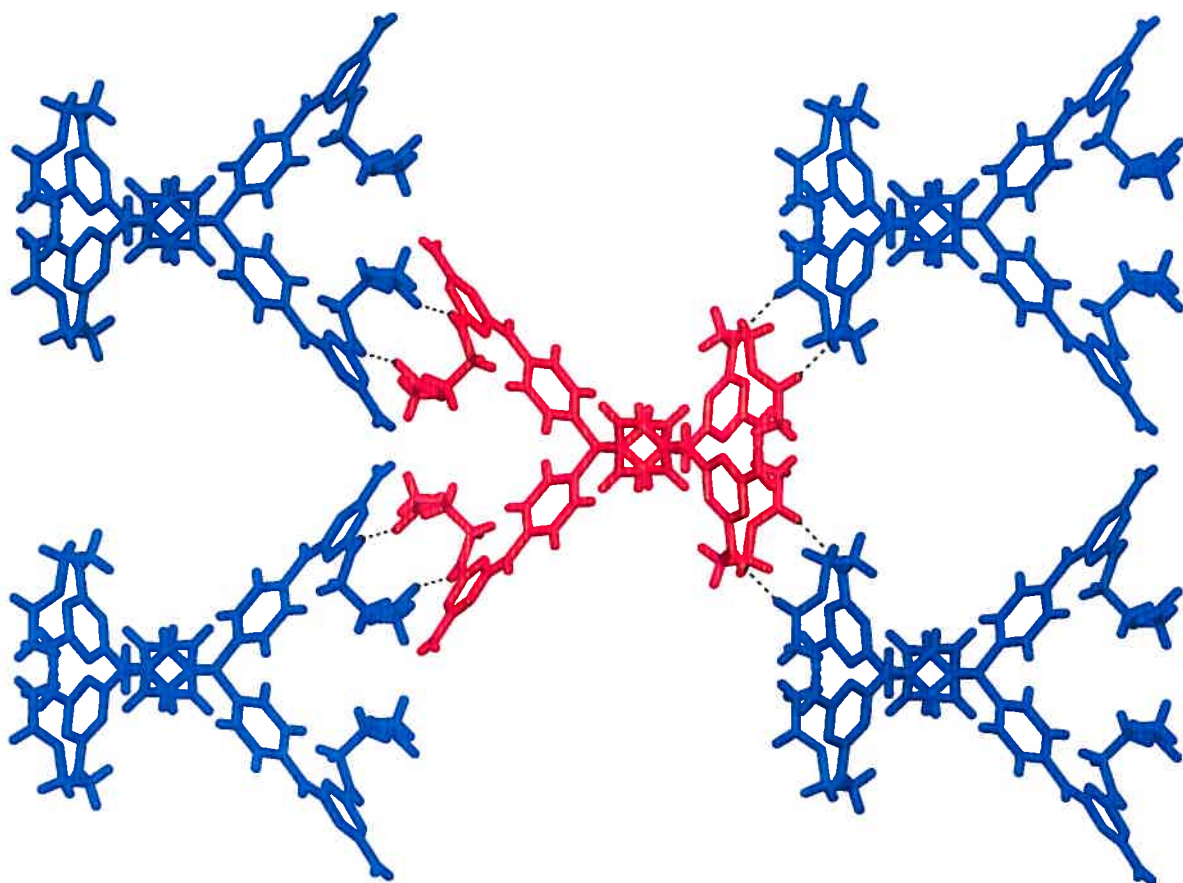


Figure 2. View along the α axis of the crystal structure of tecton 2 showing a central tecton (red) and the 4 neighbors (blue) with which it interacts by hydrogen bonds (blue) involving $-\text{NH}(\text{CH}_2)_2\text{OCOCH}_3$ groups.

Disordered guests occupy nearly 40% of the volume of the crystals,^{7,8} which have the approximate composition **2** • 3 DMSO • 1 acetone • n H₂O as estimated by ¹H NMR spectroscopy of dissolved samples.⁹ The guests occupy interconnected helical channels into which the acetate groups extend, as anticipated. In principle, guests diffusing inside crystals of tecton **2** can reach any point within the channels by multiple redundant pathways.

When single crystals of dimensions 0.8 mm x 0.5 mm x 0.3 mm were treated with acetone/H₂O at 25 °C for 24 h, they remained transparent and morphologically unchanged, continued to exhibit uniform extinction between crossed polarizers, and showed closely similar unit cell parameters when studied by single-crystal X-ray diffraction. However, analysis of dissolved samples by ¹H NMR spectroscopy established that the initial guest, DMSO, had been replaced completely. Similar exchanges in single crystals could be effected with CH₃OH, CH₃CN, THF, and dioxane. As a result, crystals of tecton **2** appear well designed to allow suitable reagents to enter by diffusion and cleave the exposed acetyl groups without necessarily changing the basic architecture of the network. In principle, such processes should yield isostructural single crystals of higher porosity, now built from tetrol **3** (Scheme 1).

This concept was tested by growing single crystals of tecton **2** from DMSO/acetone/H₂O, replacing included solvent with CH₃CN/H₂O, and then exposing the exchanged crystals to aqueous N(CH₃)₄⁺ OH⁻ at 25 °C for 2 weeks. Under these conditions, hydrolysis occurred within the crystal to give tetrol **3** in which 40-60% of the original acetate groups had been cleaved, as measured by ¹H NMR spectroscopy of dissolved samples. The resulting solid appeared morphologically identical to the original crystals, remained transparent, exhibited uniform extinction between crossed polarizers, and continued to diffract.

Single-crystal X-ray diffraction of the product confirmed the results of NMR spectroscopy and established that hydrolysis occurs isostructurally to give crystals

belonging to the tetragonal space group I4₁/a, with unit cell parameters similar ($\pm 2\%$) to those of tetraacetate **2**.‡ The resulting structure was solved and shown to be similar to that of precursor **2**, but refinement of the acetyl group with full occupancy led to thermal displacement parameters that converged at unreasonable values. Refinement with a variable occupancy factor yielded acceptable values for the thermal parameters and suggested that at least 30% of the acetyl groups had been cleaved, in agreement with measurements based directly on NMR spectroscopy of dissolved samples. Other nucleophiles with dimensions allowing access to the interior of crystals of tetraacetate **2**, such as NH₃ and N₂H₄, proved to be less effective than N(CH₃)₄⁺ OH⁻ for cleaving the acetyl groups with retention of crystallinity.

Longer contact of crystals of tetraacetate **2** with aqueous N(CH₃)₄⁺ OH⁻ increased the extent of hydrolysis, but the product was no longer crystalline.¹⁰ The acetyl groups are involved in one-third of the hydrogen bonds in the crystal structure of tecton **2**, so it is not surprising that extensive hydrolysis decreases the robustness of the network markedly. Quantitative formation of tetrol **3** from tetraacetate **2** in the solid state without changing the unit cell parameters or the geometry of the conserved molecular core would create a structure in which the volume available for including guests is increased from 40% to more than 50%.^{7,8} Most of this theoretical increase can be achieved in practice without loss of crystallinity, so our experiments establish that excavating permeable molecular crystals is an effective new strategy for increasing porosity.

It is instructive to compare this strategy with other procedures that increase the porosity of materials by post-synthetic modifications. For example, 1) templates can be removed from inside zeolites and their analogues by calcination; 2) imprinted polymers can be created by removing specific substituents;¹¹ and 3) dendrimers can be cored by similar procedures.¹² Our strategy for excavation is distinctly different because it produces crystalline products under mild conditions. Simple increases in porosity are an obvious application of this strategy, but more ambitious post-crystallization modifications could excavate covalently attached transition-state analogues or structural mimics from the

interior of permeable molecular crystals, leading to effective new ordered materials for selective catalysis and separation.

We thank the Natural Sciences and Engineering Research Council of Canada, the Ministère de l'Éducation du Québec, the Canada Research Chairs Program, the Canada Foundation for Innovation, and Valorisation-Recherche Québec for financial support.

Notes and references

‡ Crystallographic data were collected using a Bruker SMART 2000 CCD diffractometer with Cu K α radiation ($\lambda = 1.54178 \text{ \AA}$). Intensities were integrated using the SAINT program¹³ and corrected for absorption and other effects using the SADABS program.¹⁴ Structures were solved and refined using the SHELX suite of programs.¹⁵

Crystal data for tecton **2** • 3 DMSO • 1 acetone • n H₂O: T = 293 K, crystal size 0.41 x 0.14 x 0.14 mm, tetragonal, space group I4₁/a, $a = b = 25.6644(3) \text{ \AA}$, $c = 12.2028(3) \text{ \AA}$, $V = 8037.5(2) \text{ \AA}^3$, $Z = 4$, θ max = 72.95°, 32725 reflections measured, 3976 unique ($R_{\text{int}} = 0.055$). Final residual for 193 parameters and 2230 reflections with $I > 2\sigma(I)$: $R_1 = 0.0824$, $wR_2 = 0.1885$ and GoF = 1.097.

Crystal data for tetrol **3** produced by solid-state hydrolysis: T = 223 K, crystal size 0.30 x 0.20 x 0.15 mm, tetragonal, space group I4₁/a, $a = b = 25.6490(6) \text{ \AA}$, $c = 11.9240(4) \text{ \AA}$, $V = 7856.3(4) \text{ \AA}^3$, $Z = 4$, θ max = 59.19°, 18629 reflections measured, 2675 unique ($R_{\text{int}} = 0.046$). Final residual for 210 parameters, 75 restraints and 559 reflections with $I > 2\sigma(I)$: $R_1 = 0.1196$, $wR_2 = 0.3102$ and GoF = 1.094.

See <http://www.rsc.org/suppdata/cc> for crystallographic files in CIF or other electronic format.

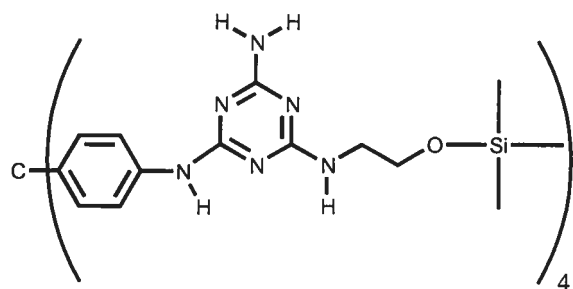
- 1 A Stein, *Adv. Mater.*, 2003, **15**, 763. A. Corma, *Chem. Rev.*, 1997, **97**, 2373.
- 2 P. J. Langley and J. Hulliger, *Chem. Soc. Rev.*, 1999, **28**, 279.
- 3 For recent references, see: J.-H. Fournier, T. Maris, J. D. Wuest, W. Guo and E. Galoppini, *J. Am. Chem. Soc.*, 2003, **125**, 1002.
- 4 S. Mann, *Nature*, 1993, **365**, 499. M. Simard, D. Su and J. D. Wuest, *J. Am. Chem. Soc.*, 1991, **113**, 4696.

- 5 P. Brunet, M. Simard and J. D. Wuest, *J. Am. Chem. Soc.*, 1997, **119**, 2737. X.
Wang, M. Simard and J. D. Wuest, *J. Am. Chem. Soc.*, 1994, **116**, 12119.
- 6 M. J. Zaworotko, *Chem. Soc. Rev.*, 1994, **23**, 283.
- 7 The percentage of volume accessible to guests was estimated by the PLATON program.⁸
- 8 A. L. Spek, *PLATON, A Multipurpose Crystallographic Tool*, Utrecht University, Utrecht (The Netherlands), 2001. P. van der Sluis and A. L. Spek, *Acta Crystallogr.*, 1990, **A46**, 194.
- 9 The amount of included H₂O could not be determined accurately.
- 10 The unchanged appearance of crystals after partial hydrolysis (40-60%), the loss of crystallinity upon extensive hydrolysis, and our inability to crystallize tetrol **3** independently all suggest that the observed process does not occur by a sequence of dissolution, hydrolysis, and recrystallization.
- 11 G. Wulff, *Chem. Rev.*, 2002, **102**, 1. K. Haupt and K. Mosbach, *Chem. Rev.*, 2000, **100**, 2495.
- 12 Y. Kim, M. F. Mayer and S. C. Zimmerman, *Angew. Chem., Int. Ed. Engl.*, 2003, **42**, 1121.
- 13 SAINT (Release 6.06), Integration Software for Single Crystal Data, Bruker AXS Inc., Madison, Wisconsin (USA), 1999.
- 14 G. M. Sheldrick, SADABS, Bruker Area Detector Absorption Corrections, Bruker AXS Inc., Madison, Wisconsin (USA), 1996.
- 15 G. M. Sheldrick, SHELXS-97, Program for the Solution of Crystal Structures and SHELXL-97, Program for the Refinement of Crystal Structures, University of Göttingen (Germany), 1997.

7.3 Conclusions et perspectives

L'article du Chapitre 7.2 fait une contribution importante au sujet de l'ingénierie de cristaux. Il ouvre d'abord la voie vers une nouvelle façon d'augmenter la porosité de la structure en faisant des modifications subséquentes à la cristallisation. Il démontre ensuite la possibilité d'incorporer des groupes fonctionnels sur le réseau et surtout la faisabilité de retirer des parties de molécule du réseau sans altérer sa cristallinité.

La poursuite logique de ce projet serait l'emploi de groupes protecteurs ne pouvant participer à la formation de ponts hydrogène afin de prévenir son implication dans la formation du réseau. De cette manière, la réalisation d'une déprotection totale sans altérer l'architecture cristalline serait envisageable. Comme l'illustre le tecton 7.1, l'emploi du groupement triméthylsilyle élimine la formation de ponts hydrogène avec le réseau. Ce tecton se verrait ainsi un excellent candidat de départ pour de prochaines études.



Tecton 7.1

Parallèlement, il serait très intéressant de se servir de cette faiblesse, soit la participation du groupe protecteur dans la formation du réseau et de l'utiliser à notre avantage. En effet, un projet plus ambitieux serait l'utilisation d'un groupement pouvant mimer un état de transition qui participerait à la formation du réseau. Ainsi, le retrait d'un groupe fonctionnel comme le groupement phosphate pourrait, en théorie, laisser

l'empreinte digitale de la mimique d'un état de transition comme l'hydrolyse d'un groupement ester (Figure 7.1). Cette empreinte pourrait alors servir à catalyser l'hydrolyse de certains esters.

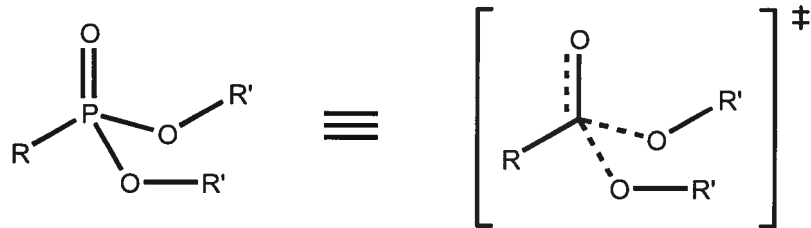


Figure 7.1 Le groupement phosphate est comparable à l'état de transition de l'hydrolyse d'une fonction ester.

Chapitre 8

***Conclusions et
perspectives***

8.1 Conclusions

Le premier objectif de cette thèse consistait en une meilleure compréhension des phénomènes d'auto assemblage en génie cristallin. Pour se faire, on a réalisé de nombreuses études basées sur une unité centrale simple et rigide, soit le 9,9'-spirobifluorène.

On a d'abord fait l'historique du 9,9'-spirobifluorène, de sa première synthèse à aujourd'hui, puis on a regardé ses modes de substitutions et son utilisation en tectonique moléculaire. On a vu ses forces, ses faiblesses et les études potentielles qui pourraient découler de cette unité centrale.

Le chapitre 3 portait sur l'étude des effets que peuvent avoir un espaceur phényle entre l'unité centrale et son groupement de reconnaissance. Les résultats obtenus ont démontré que cette stratégie était efficace afin d'augmenter la distance entre les unités centrales de chaque tecton. Ils ont aussi permis de conclure que dans le cas de la porosité, même si cette dernière est reliée à ce phénomène d'éloignement, on ne peut en tirer un lien de causalité unilatérale. En effet, il semble que la topologie du réseau aurait un rôle prépondérant dans la détermination de la porosité résultant d'un agencement cristallin. Pour répondre à plusieurs questions pouvant être soulevées par ces résultats, des études ont été proposées afin d'étudier les effets de topologie sur la porosité du réseau.

L'utilisation des interactions faibles en génie cristallin a fait l'objet du chapitre 4. On réalisa ainsi plusieurs architectures cristallines basées sur le 9,9'-spirobifluorène. Les études ont permis d'analyser à la fois le comportement des interactions faibles en génie cristallin, mais aussi l'effet que peut avoir un espaceur phényle entre l'unité centrale et son groupement de reconnaissance. Les résultats obtenus semblent montrer que les interactions de type O···H-C, provenant de fonctions nitro, sont déterminantes lors de la cristallisation de composés. En effet, même lors d'une compétition avec des interactions de type π , il

arrive que le réseau soit totalement gouverné par les interactions de type O···H-C. On remarque toutefois qu'il semble y avoir une prépondérance pour une combinaison de ces deux types d'interactions lors de la cristallisation. À l'opposé, lors d'une compétition avec des liens de type N···H-C provenant de fonctions cyano et des interactions de type π , l'architecture du réseau semble contrôlée en totalité par les interactions π . Il faut quand même admettre que le processus de cristallisation par le biais d'interactions faibles reste encore trop subtil pour permettre la prévision de l'architecture et aucune conclusion trop hâtive ne saurait en être tirée. Il n'en demeure pas moins que les interactions faibles ont un rôle non négligeable lors de la cristallisation.

Le chapitre 5 portait sur l'emploi des arylamines comme groupement de reconnaissance en chimie supramoléculaire. Ce groupement s'est avéré efficace comme donneur et accepteur de pont hydrogène dans la formation de réseau supramoléculaire. Nos études semblent montrer que les arylamines ont une tendance marquée à former des empilements compacts. En effet, mis à part le spirobifluorène reconnu pour former des composés d'inclusions, tous les composés étudiés ont révélé une architecture cristalline compacte. Les membres du groupe Wuest continuent d'étudier ce groupement de reconnaissance, et il sera intéressant de voir si cette tendance se maintiendra.

Une grande partie des applications potentielles de la tectonique moléculaire nécessitera des réactions à l'intérieur du réseau cristallin formé par les tectons. Il était donc essentiel de démontrer la faisabilité de ce concept. Le second objectif de cette thèse portait ainsi sur la réalisation de réactions à l'intérieur de cristaux poreux fabriqués par la stratégie de la tectonique moléculaire.

Au chapitre 6, on a développé une stratégie permettant la réalisation de réactions topotactiques à l'intérieur de réseaux cristallins poreux. Nos études ont d'abord montré que la tectonique moléculaire est une stratégie efficace dans la formation de réseaux cristallins poreux. On a ensuite démontré que les réseaux formés peuvent être suffisamment robustes pour permettre l'échange de molécules invitées du réseau par d'autres molécules. Ainsi,

par cette stratégie de diffusion, il nous a été possible de réaliser de nombreuses réactions topotactiques consistant en l'ajout de divers thiols sur des fonctions allyliques du réseau. Cette même stratégie, combinée à l'emploi de dithiols comme réactifs, a permis de démontrer qu'il est possible de renforcer les réseaux obtenus par l'ajout d'interactions covalentes.

La réalisation de réactions dans des cristaux poreux par diffusion de réactifs à l'intérieur de canaux ouvre maintenant une nouvelle voie pour la tectonique moléculaire. En effet, nous savons maintenant que ces réactions sont possibles et qu'il suffit de bien concevoir le tecton de départ pour permettre la réalisation de réactions à l'état solide avec de tels cristaux.

Le chapitre 7 traitait également de réactions à l'état cristallin. On voulait utiliser la même stratégie de diffusion et de réaction subséquente afin de contrôler la porosité d'un cristal. Pour ce faire nous avons cristallisé un tecton comportant un groupe fonctionnel offrant la possibilité d'être retiré à l'état cristallin. Le concept s'est avéré efficace en ce sens qu'il est possible d'augmenter la porosité d'un cristal en enlevant des groupes d'atomes à l'intérieur de ce dernier. Cependant, le clivage de groupements pouvant intervenir dans la structure du réseau peut mener à l'effondrement de ce dernier.

8.2 Perspectives et voies futures

La première partie de cette thèse portant sur l'ingénierie du cristal a soulevé plus de questions qu'elle n'a apporté de réponse, ce qui est souvent le cas en science. On peut ainsi penser, comme nous l'avons soulevé tout au cours de cette thèse, à plusieurs expériences de contrôle afin de mieux comprendre les différents facteurs intervenant lors de la cristallisation. En effet, le domaine de la cristallisation reste jusqu'à aujourd'hui un domaine de la chimie où il reste encore beaucoup à faire, car nous sommes encore loin du jour où nous pourrons prédire avec exactitude le réseau formé par une molécule simplement en connaissant sa structure.

À titre d'exemple, voici quelques avenues intéressantes qu'on pourrait étudier afin de faire des percés dans le domaine du génie cristallin :

- Une comparaison systématique entre différentes unités centrales similaires, comme par exemple le tétraphénylméthane et le spirobifluorène, mais substitué de la même manière.
- L'utilisation de différents espaces ne permettant pas les interactions aryl-aryl comme une triple liaison afin d'étudier les comportements cristallins.
- L'emploi de groupes de reconnaissance plus directionnels et possédant le moins de motifs de reconnaissance possible.

Pour ce qui est des interactions faibles, comme leur nom l'indique, elles ne sont pas très fortes, donc subtiles et difficiles à prévoir. Des milliers d'études pourraient être proposées. Il faudra encore longtemps avant que l'on puisse dégager des conclusions solides sur leurs emplois. Ces conclusions ne viendront que lorsque plusieurs groupes de recherche auront creusé la question à leur manière et selon leur vision. Ainsi, une

multitude de façons de voir, une quantité d'études réalisées et une expertise du domaine permettront un jour de mieux répondre aux questions soulevées par les interactions faibles.

L'utilisation d'arylamines comme groupe de reconnaissance en tectonique moléculaire n'en est qu'à ses débuts. Pour l'instant, elles semblent privilégier un empilement compact, mais nous n'avons que quelques composés à l'appuis. Toutefois, le groupe Wuest est très prolifique dans l'emploi d'unités centrales différentes en tectonique moléculaire et sous peu, il sera sans aucun doute possible de comparer nos résultats préliminaires avec une banque plus complète de composés afin de confirmer ou d'infirmer cette hypothèse et d'en poser d'autres.

La seconde partie de cette thèse, les chapitres 6 et 7, a démontré la viabilité de la stratégie de diffusion pour permettre la réalisation de réactions topotactiques à l'intérieur de cristaux poreux. Par cette méthode, on a également montré qu'il est possible d'induire la modification chimique du réseau après sa cristallisation. Plusieurs utilisations ambitieuses se dégagent de ces résultats. En effet, il est maintenant envisageable d'utiliser cette stratégie pour des fins comme la catalyse. On peut désormais penser à incorporer des groupes fonctionnels utiles en catalyse après la cristallisation d'un composé ou encore libérer un groupe fonctionnel après la cristallisation. Des projets plus ambitieux encore peuvent être envisagés. Par exemple, le retrait d'un groupe fonctionnel mimant un état de transition pourrait permettre au cristal de devenir un catalyseur similaire aux enzymes.

La stratégie de diffusion pour les réactions topotactiques a également montré la possibilité de rigidifier un réseau par l'ajout de liaisons covalentes. Ce concept vient donc palier une des principales faiblesses de nos réseaux et rendent envisageable des applications nécessitant une robustesse accrue des cristaux. Toutes les applications potentielles de ces nouveaux matériaux n'ont donc de limite que notre imagination et notre capacité à mettre nos idées en œuvre. Les prochaines années de la tectonique moléculaire risquent donc de nous réservé de belles surprises.

Annexe 1

Supporting Information

Molecular Tectonics. Porous Hydrogen-Bonded Networks

Built from Derivatives of 2,2',7,7'-Tetraphenyl-9,9'-spirobi[9H-fluorene]

Eric Demers, Thierry Maris, and James D. Wuest*

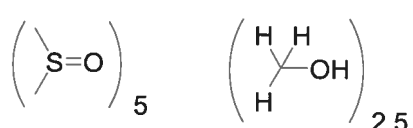
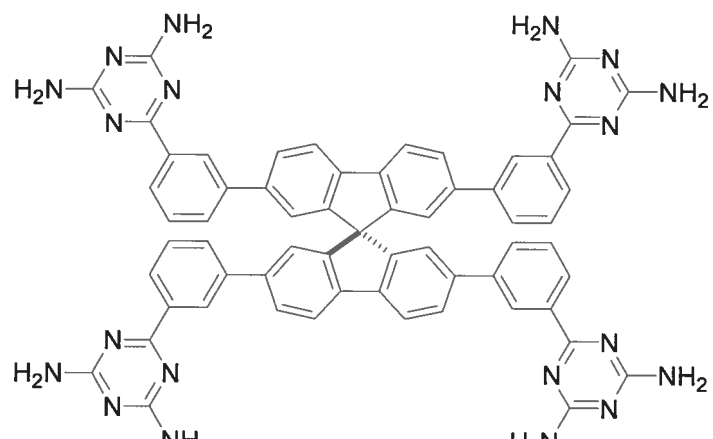
Contents

- I Crystal and molecular structure of compound 3.....(A1-3)-(A1-8)**
- II Crystal and molecular structure of compound 2.....(A1-9)-(A1-16)**

I

CRYSTAL AND MOLECULAR STRUCTURE OF

COMPOUND 3



X-Ray Crystal Structure Determination and Refinement

A crystal was mounted on a cryoloop and placed under a low-temperature device at 223 K on the platform of a Bruker diffractometer equipped with a SMART CCD 2K detector system, a Cu sealed Siemens ceramic diffraction tube with an oriented graphite monochromator ($\lambda = 1.54178 \text{ \AA}$), and a generator operating at 40 kV and 30 mA. The lattice parameters and standard deviations were obtained by a least-squares fit using 120 frames with 5 sec exposures per frame using the Bruker SMART software. Different frame sets with the detector at $2\theta = 38^\circ$ and 110° (6 + 8 runs) were collected by phi and omega scans with 15 sec exposures per frame. The crystal-to-detector distance was 4.908 cm, and the data collection was carried out in 512 x 512 pixel mode, utilizing 4 x 4 pixel binning. The collected data were processed and reduced using Bruker SAINTPLUS, and empirical absorption and other effects were corrected using SADABS.

The crystal was found to be very weakly diffracting, with a sharp drop in the number of spots at higher angles. No significant diffraction was observed beyond $2\theta > 110^\circ$, though some meaningful reflections with moderate intensities could be collected up to $2\theta < 140^\circ$. Some runs for the sets at $2\theta = 110^\circ$ were removed to improve the global data statistics.

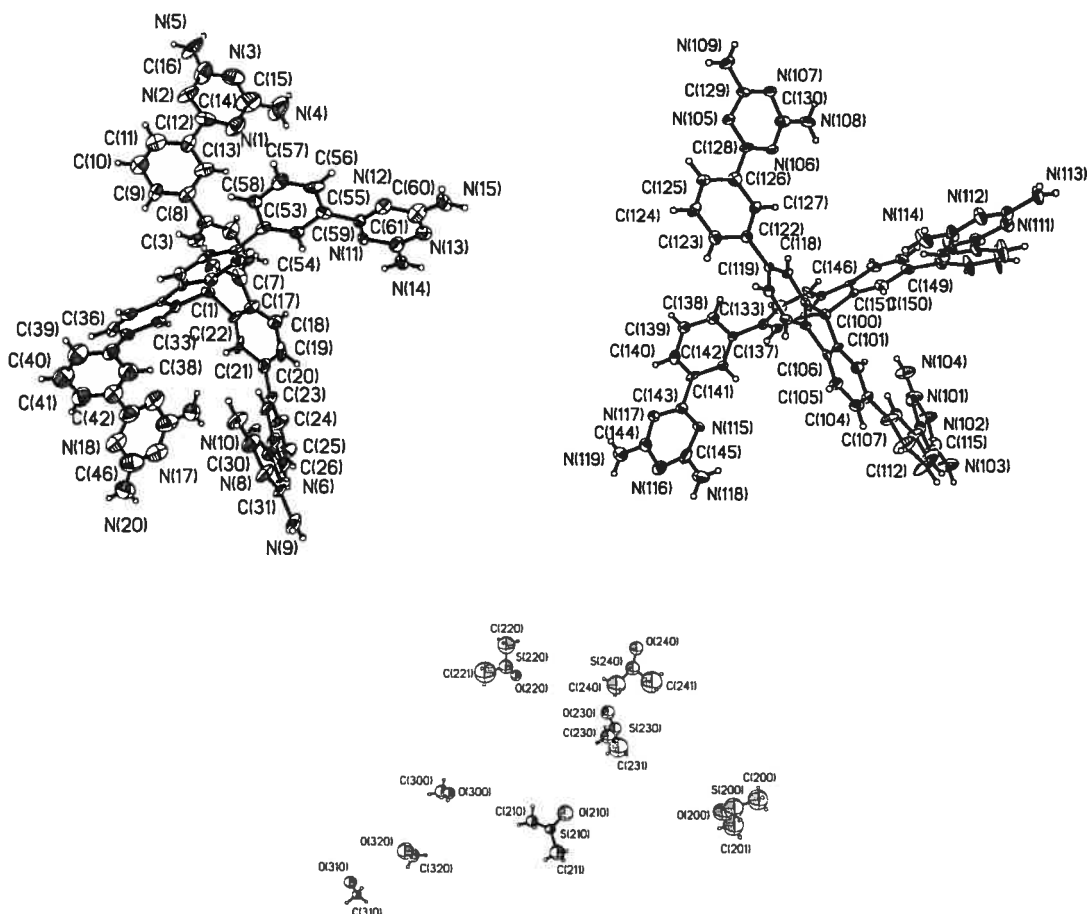
The structure was partially solved with SIR2000 and completed by Fourier difference map in the subsequent refinement step. Two symmetry-independent molecules of compound **3** could be completed and refined with some restraints at this stage of refinement to compensate for the effect of missing guests. Refinement by full-matrix least-squares based on F^2 was carried out using the SHELX suite of programs, in this case with the refinement program ShelxH, which is suited for large structural problems. Hydrogen atoms were included in ideal positions with fixed isotropic U values and were allowed to ride with their respective non-hydrogen atoms and refined. Some peaks belonging to disordered guests in the void volume could be identified, notably sulfur atoms from DMSO molecules. Subsequent Fourier recycling permitted the identification of approximately 5 DMSO and

2.5 methanol guest molecules (one being disordered over an inversion center). Refinement was attempted over these molecules (some of them being hydrogen-bonded with diaminotriazine units of the host network). However, the poor data-to-parameter ratio (8975 reflections with $I > 2 \sigma(I)$ over a total of 25334), combined with the low symmetry of the crystal lattice and the large number of disordered guests remaining to be found, caused refinement of the disordered guests to behave poorly despite extensive use of restraints.

As a result, the ordered part of the structure was subjected to the SQUEEZE option in PLATON. The procedure was performed keeping the located DMSO and methanol molecules. The remaining potential solvent area volume found by PLATON was 1743.9 \AA^3 (22%), and the analysis converged after 5 cycles to a residual $R_f = 13\%$, with a calculated electron count by cell of 40. The solvent-modified data were used to refine the structure anisotropically, except for the guests, and (still using restraints to stabilize the refinement) gave final residual factors $R_1 = 9.29\%$ and $wR_2 = 23.32\%$ for 8975 reflections with $I > 2 \sigma(I)$.

**Table S1. Crystal data and structure refinement for C135 H130 N40 O8 S5.
Refinement after PLATON / SQUEEZE**

Empirical formula	C134.50 H128 N40 O7.50 S5	
Formula weight	2585.07	
Temperature	223 (2) K	
Wavelength	1.54178 Å	
Crystal system	Triclinic	
Space group	P-1	Z = 2
Unit cell dimensions	a = 12.2162(10) Å b = 21.2975(17) Å c = 30.884(2) Å	α = 93.026(3)° β = 94.690(4)° γ = 96.419(3)°
Volume	7942.6(10) Å ³	
Density (calculated)	1.081 g/cm ³	
Absorption coefficient	1.164 mm ⁻¹	
Crystal size	0.20 x 0.20 x 0.12 mm	
Theta range for data collection	1.44 to 69.99°	
Index ranges	-14 ≤ h ≤ 14, -25 ≤ k ≤ 25, -34 ≤ l ≤ 34	
Reflections collected	97194	
Independent reflections	25334 [R _{int} = 0.058]	
Absorption correction	Semi-empirical from equivalents	
Max. and min. transmission	0.8720 and 0.8000	
Refinement method	Full-matrix least-squares on F ²	
Data / restraints / parameters	25334 / 147 / 1533	
Goodness-of-fit on F ²	1.025	
Final R indices [I>2sigma(I)]	R ₁ = 0.0929, wR ₂ = 0.2332	
R indices (all data)	R ₁ = 0.1295, wR ₂ = 0.2400	
Largest diff. peak and hole	0.352 and -0.557 e/Å ³	



ORTEP view of the C_{134.50} H₁₂₈ N₄₀ O_{7.50} S₅ compound with the numbering scheme adopted. Ellipsoids drawn at 30% probability level. Hydrogen atoms represented by sphere of arbitrary size.

Table S2. Bond lengths [Å] and angles [°] related to the hydrogen bonding for C134.50 H128 N40 O7.50 S5.

D-H	...A	d (D-H)	d (H...A)	d (D...A)	<DHA
N(4)-H(4A)	N(102) #1	0.87	2.43	3.247(9)	157.5
N(5)-H(5B)	O(310)	0.87	2.05	2.836(14)	150.0
N(9)-H(9A)	N(111) #2	0.87	2.47	3.328(6)	169.7
N(9)-H(9B)	N(18) #3	0.87	2.01	2.851(13)	161.4
N(10)-H(10A)	O(230)	0.87	2.27	3.123(9)	165.0
N(10)-H(10B)	N(110)	0.87	2.27	3.088(6)	155.8
N(14)-H(14A)	N(106)	0.87	2.10	2.965(5)	174.4
N(14)-H(14B)	O(210) #4	0.87	2.50	3.364(8)	173.8
N(15)-H(15B)	N(13) #4	0.87	2.26	3.110(6)	166.1
N(15)-H(15A)	O(210)	0.87	2.01	2.793(8)	148.5
N(20)-H(20B)	O(230) #3	0.87	2.30	2.967(9)	133.2
N(20)-H(20A)	N(8) #3	0.87	2.77	3.200(8)	111.8
N(103)-H(10D)	O(200)	0.87	1.99	2.843(9)	165.4
N(103)-H(10C)	N(107) #5	0.87	2.34	3.121(6)	149.1
N(104)-H(10F)	N(116) #6	0.87	2.11	2.933(7)	157.9
N(104)-H(10E)	O(320) #7	0.87	2.67	3.412(10)	144.4
N(108)-H(10G)	N(11)	0.87	2.21	3.010(5)	152.2
N(108)-H(10H)	O(300)	0.87	2.06	2.909(7)	165.0
N(109)-H(10I)	N(100) #1	0.87	2.12	2.977(6)	169.9
N(109)-H(10J)	N(2) #2	0.87	2.18	2.975(6)	152.5
N(113)-H(11A)	N(112) #8	0.87	2.23	3.096(6)	177.0
N(113)-H(11B)	O(220) #8	0.87	2.25	2.867(6)	128.0
N(114)-H(11C)	N(7)	0.87	2.26	3.105(6)	165.2
N(114)-H(11D)	O(220)	0.87	2.03	2.864(7)	161.8
N(118)-H(11E)	O(240)	0.87	2.01	2.836(8)	159.1
N(119)-H(11G)	O(210) #2	0.87	1.83	2.614(6)	149.3
O(300)-H(300)	O(200) #1	0.83	1.93	2.729(9)	160.8

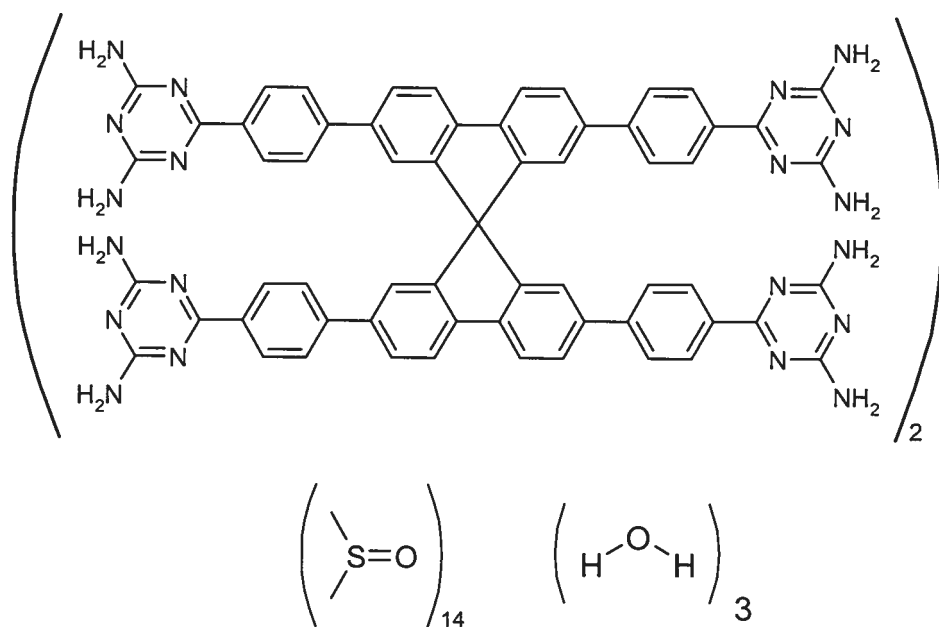
Symmetry transformations used to generate equivalent atoms:

#1 x,y+1,z	#2 x+1,y,z	#3 -x+2,-y+1,-z
#4 -x+2,-y+1,-z+1	#5 x,y-1,z	#6 x-1,y,z
#7 -x+1,-y+1,-z+1	#8 -x+1,-y+1,-z	

II

CRYSTAL AND MOLECULAR STRUCTURE OF

COMPOUND 2



X-Ray Crystal Structure Determination and Refinement

A small crystal mounted in a cryoloop was flash-cooled at 100 K on the platform of a Bruker diffractometer equipped with a SMART CCD 4K detector system, Montel 200 optics, and a FR591 copper rotating-anode generator ($\lambda = 1.54178 \text{ \AA}$) operating at 40 kV and 25 mA.

The lattice parameters with associated standard deviations were calculated by a least-squares fit on the theta angle from reflections collected in 120 frames with 3 sec exposures per frame using the Bruker SMART software, which found a triclinic unit cell. Data collection by phi and omega scans with 8 sec exposures per frame was carried out for a total of 15 runs with the detector at $2\theta = 38^\circ$ and 110° . The crystal-to-detector distance was 5.095 cm, and the data collection was carried out in 512×512 pixel mode. The collected data were processed and reduced using Bruker SAINTPLUS, and empirical absorption and other effects were corrected using SADABS.

Analysis by XPREP suggested the space group P1 based on the intensity statistics and the merging value. The structure solution was challenging due to the large amount of DMSO guest molecules in the unit cell, and SHELXS was not successful during several attempts performed in both P1 and P-1 space groups. Trials were then performed using SIR2000 in both P-1 and P1 and succeeded only in P1, whereas the $n(z)$ cumulative probability calculated distribution was found closer to the acentric distribution. The solution found by SIR2000 included two molecules in the asymmetric unit (one being incomplete at this stage), three well-defined DMSO molecules, and many peaks arising from non-resolved guest molecules. The initial model was completed by Fourier difference map following least-squares refinement using SHELXH (the part of SHELXL adapted for large-scale problems).

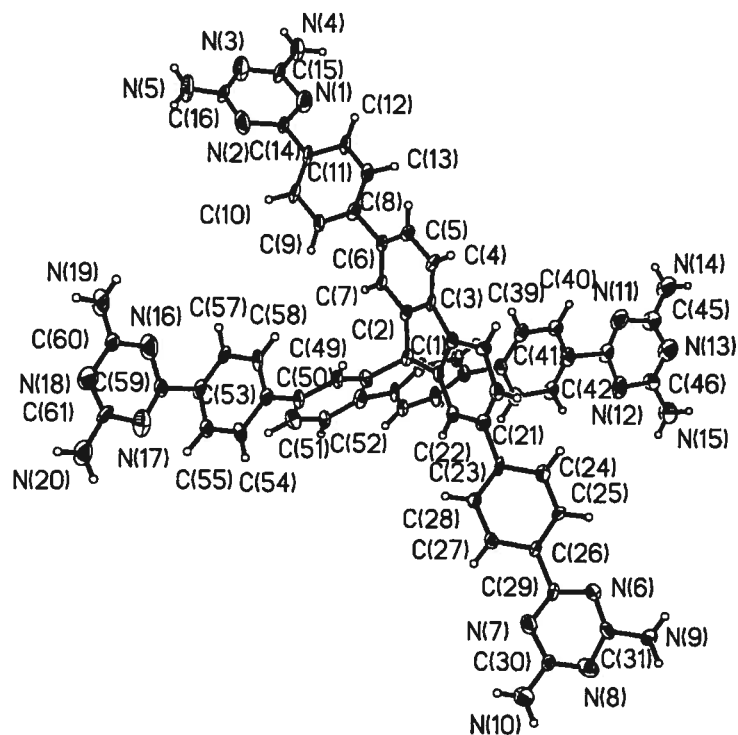
Subsequent Fourier recycling allowed the identification of up to 14 DMSO and 3 water molecules. Refinement was carried out by using blocks at the beginning, then by applying restraints while modeling two-site disorder for the DMSO molecules. However, the overall low quality of the data and high correlations arising from the presence of two symmetry-independent molecules made refinement difficult. After some refinement cycles, part of the guest was poorly modeled, and the resulting model included some short intermolecular contacts with the host network involving molecules of DMSO and water.

Consequently, the ordered part of the structure was subjected to the SQUEEZE option in PLATON. The procedure was performed keeping only the 11 DMSO molecules and 2 water molecules that were well located. The remaining potential solvent area volume found by PLATON was 940 \AA^3 (21%), and the analysis converged after 11 cycles to a residual $R_f = 12\%$, with a calculated electron count by cell of 97. The guest-modified data were used to refine the structure anisotropically, except for the located guest molecules, and (still using restraints to stabilize the refinement) analysis gave final residual factors $R_I = 9.57\%$ and $wR_2 = 22.36\%$ for 9973 reflections with $I > 2 \sigma(I)$ and 729 restraints. The structure is reported with the guest content determined before the application of the SQUEEZE treatment.

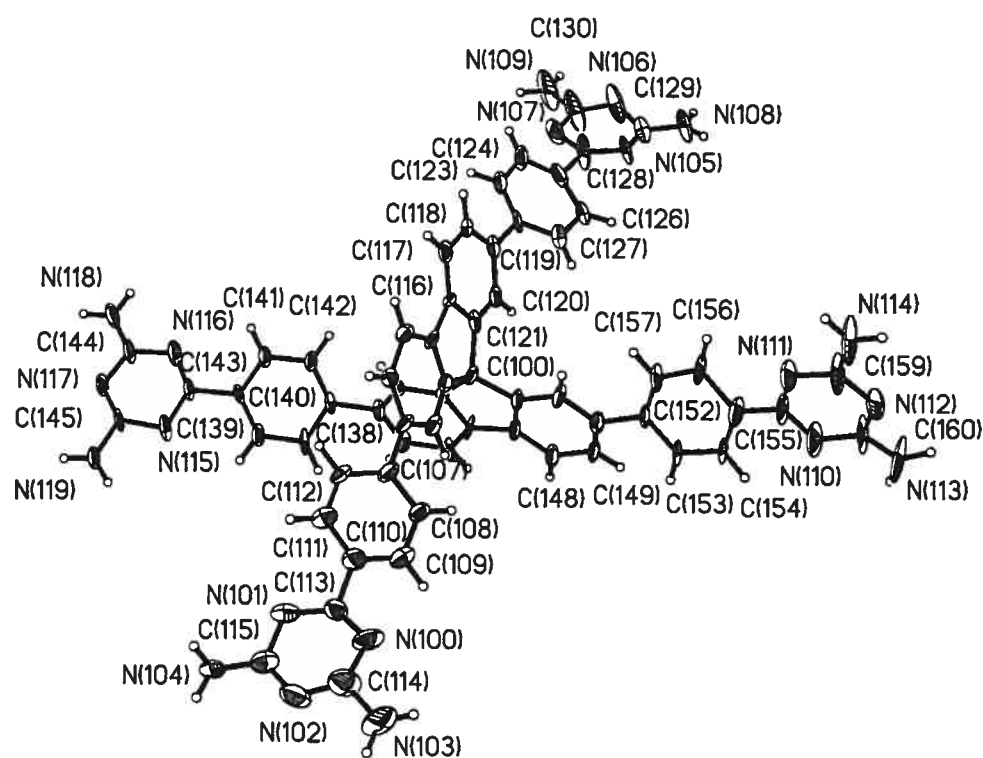
The absolute structure could not be determined with confidence because of the important disorder involving DMSO molecules and the treatment of the data by the SQUEEZE procedure. Checks for higher symmetry were performed with the routine ADDSYM to find missed symmetry or potential missed inversion centers, on the whole structure first and then on the structure without the guest molecules.

Table S3. Crystal data and structure refinement for C150 H180 N40 O17 S14.

Empirical formula	C150 H180 N40 O17 S14	
Formula weight	3264.18	
Temperature	100(2) K	
Wavelength	1.54178 Å	
Crystal system	Triclinic	
Space group	P1	$Z = 1$
Unit cell dimensions	$a = 13.458(2)$ Å	$\alpha = 81.076(8)^\circ$
	$b = 17.788(2)$ Å	$\beta = 74.960(8)^\circ$
	$c = 20.721(3)$ Å	$\gamma = 70.755(8)^\circ$
Volume	4509.6(11) Å ³	
Density (calculated)	1.201 g/cm ³	
Absorption coefficient	2.113 mm ⁻¹	
Crystal size	0.12 x 0.10 x 0.08 mm	
Theta range for data collection	2.21 to 68.61°	
Index ranges	$-15 \leq h \leq 16$, $-20 \leq k \leq 21$, $-24 \leq l \leq 24$	
Reflections collected	30221	
Independent reflections	15187 [R _{int} = 0.078]	
Absorption correction	Semi-empirical from equivalents	
Max. and min. transmission	0.8500 and 0.7900	
Refinement method	Full-matrix least-squares on F ²	
Data / restraints / parameters	15187 / 729 / 1731	
Goodness-of-fit on F ²	1.107	
Final R indices [I>2sigma(I)]	$R_1 = 0.0957$, $wR_2 = 0.2236$	
R indices (all data)	$R_1 = 0.1040$, $wR_2 = 0.2289$	
Largest diff. peak and hole	0.416 and -0.432 e/Å ³	



ORTEP view of the C₁₅₀ H₁₈₀ N₄₀ O₁₇ S₁₄ compound with the numbering scheme adopted. Ellipsoids drawn at 30% probability level. Hydrogen atoms represented by sphere of arbitrary size. Molecule A.



ORTEP view of the C₁₅₀H₁₈₀N₄₀O₁₇S₁₄ compound with the numbering scheme adopted. Ellipsoids drawn at 30% probability level. Hydrogen atoms represented by sphere of arbitrary size. Molecule B.

Table S4. Bond lengths [Å] and angles [°] related to the hydrogen bonding for C150 H180 N40 O17 S14.

D-H	..A	d (D-H)	d (H..A)	d (D..A)	<DHA
N(4)-H(4A)	O(240) #1	0.88	1.88	2.712(10)	158.1
N(4)-H(4A)	N(114) #1	0.88	2.64	3.136(13)	116.8
N(4)-H(4B)	N(18) #1	0.88	2.06	2.932(9)	173.1
N(5)-H(5B)	N(6) #2	0.88	2.16	3.036(10)	177.1
N(9)-H(9A)	N(2) #3	0.88	2.22	3.078(9)	165.3
N(9)-H(9B)	O(230) #3	0.88	1.86	2.741(10)	174.2
N(9)-H(9B)	O(231) #3	0.88	2.14	2.945(13)	152.2
N(10)-H(10A)	O(221) #3	0.88	1.91	2.706(13)	149.9
N(10)-H(10A)	O(220) #3	0.88	2.03	2.827(9)	149.3
N(10)-H(10B)	N(13) #4	0.88	2.05	2.911(10)	166.7
N(14)-H(14A)	N(7) #1	0.88	2.41	3.281(8)	172.6
N(15)-H(15A)	O(220) #5	0.88	2.09	2.892(11)	151.2
N(15)-H(15A)	O(221) #5	0.88	2.31	3.033(16)	139.3
N(15)-H(15B)	O(290) #3	0.88	2.22	3.049(16)	157.7
N(19)-H(19A)	O(270) #2	0.88	1.98	2.860(13)	175.0
N(19)-H(19A)	O(271) #2	0.88	2.03	2.845(13)	153.2
N(20)-H(20A)	N(1) #4	0.88	2.14	2.994(10)	163.0
N(113)-H(11A)	N(107) #4	0.88	2.32	3.171(13)	163.5
N(113)-H(11B)	N(12) #6	0.88	2.27	3.092(16)	156.0
N(114)-H(11D)	O(240)	0.88	1.95	2.825(15)	170.2
N(114)-H(11D)	N(4) #4	0.88	2.66	3.136(13)	115.3
N(118)-H(11E)	N(100) #1	0.88	2.53	3.401(11)	172.2
N(118)-H(11F)	O(210) #1	0.88	2.24	3.078(14)	158.7
N(118)-H(11F)	O(211) #1	0.88	2.46	3.26(2)	152.3
N(119)-H(11G)	O(280) #7	0.88	2.18	3.015(11)	157.9
N(119)-H(11G)	O(281) #7	0.88	1.96	2.825(13)	168.9
N(119)-H(11H)	O(250) #8	0.88	2.14	3.006(13)	167.2
N(103)-H(10C)	O(280) #9	0.88	2.02	2.830(13)	152.5
N(103)-H(10C)	O(281) #9	0.88	2.01	2.710(17)	135.9
N(103)-H(10D)	N(117) #4	0.88	2.12	2.948(13)	156.9
N(104)-H(10F)	N(105) #3	0.88	2.23	3.082(10)	163.3
N(108)-H(10G)	N(101) #2	0.88	2.24	3.099(12)	164.2
N(108)-H(10H)	O(200) #10	0.88	2.09	2.931(11)	160.3

Symmetry transformations used to generate equivalent atoms:

#1 x,y-1,z	#2 x,y,z-1	#3 x,y,z+1
#4 x,y+1,z	#5 x,y-1,z+1	#6 x+1,y+1,z-1
#7 x+1,y-1,z+1	#8 x+1,y,z	#9 x+1,y,z+1
#10 x+1,y,z-1		

References:

Bruker (2003). SAINT Release 7.06. Integration Software for Single Crystal Data. Bruker AXS Inc., Madison, USA.

Bruker (2001). SMART Release 5.625, Bruker Molecular Analysis Research Tool, Bruker AXS Inc., Madison, USA.

Burla, M. C.; Camalli, M.; Carrozzini, B. ; Cascarano, G. L.; Giacovazzo, C.; Polidori, G.; Spagna, R. *Acta. Crystallogr.* **2000**, *A56*, 451-457.

Le Page, Y. *J. Appl. Cryst.* **1987**, *20*, 264-269.

Le Page, Y. *J. Appl. Cryst.* **1988**, *21*, 983-984.

Sheldrick, G. M. (1996). SADABS, Bruker Area Detector Absorption Corrections. Bruker AXS Inc., Madison, USA.

Sheldrick, G. M. (1997a). SHELXS97. Program for Crystal Structure Solution. University of Göttingen, Germany.

Sheldrick, G. M. (1997b). SHELXL97. Program for Crystal Structure Refinement. University of Göttingen, Germany.

Spek, A. L. (2000). PLATON, Molecular Geometry Program, 2000 version. University of Utrecht, Utrecht, Holland.

van der Sluis, P.; Spek, A. L. *Acta Crystallogr.* **1990**, *A46*, 194.

Annexe 2

Supporting Information

Weakly Bonded Molecular Networks

Built from Tetranitro- and Tetracyanospirobifluorenes

Eric Demers, Thierry Maris, Janie Cabana,
Jean-Hugues Fournier, and James D. Wuest

Contents

- I **Crystal and molecular structure of 2,2',7,7'-tetranitro-9,9'-spirobi[9H-fluorene]**
 - 1.5 dioxane (compound 4).....(A2-3)-(A2-7)
- II **Crystal and molecular structure of 2,2',7,7'-tetracyano-9,9'-spirobi[9H-fluorene]**
 - 2 CHCl₃ (compound 5).....(A2-8)-(A2-10)
- III **Crystal and molecular structure of 2,2',7,7'-tetrakis(4-nitrophenyl)-9,9'-spirobi[9H-fluorene]** • 0.5 ethyl acetate (compound 6)(A2-11)-(A2-16)
- IV **Crystal and molecular structure of 2,2',7,7'-tetrakis(4-cyanophenyl)-9,9'-spirobi[9H-fluorene]** • 3 dioxane (compound 7)(A2-17)-(A2-20)
- V **Crystal and molecular structure of 2,2',7,7'-tetrakis(3-nitrophenyl)-9,9'-spirobi[9H-fluorene] (compound 8)**(A2-21)-(A2-24)
- VI **Crystal and molecular structure of 2,2',7,7'-tetrakis(3-cyanophenyl)-9,9'-spirobi[9H-fluorene] (compound 9)**(A2-25)-(A2-28)

CRYSTAL AND MOLECULAR STRUCTURE OF
2,2',7,7'-TETRANITRO-9,9'-SPIROBI[9H-FLUORENE] 1.5 DIOXANE
(COMPOUND 4)

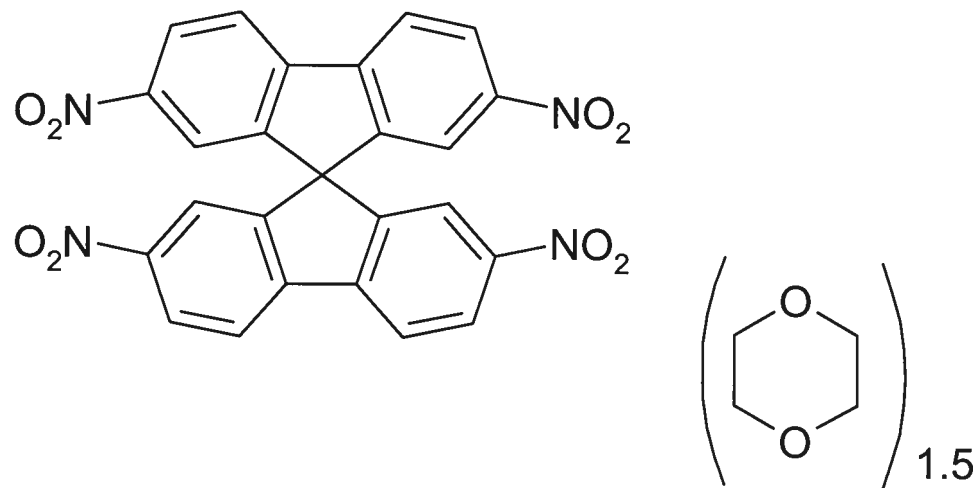


Table S1. Crystal data and structure refinement for 2,2',7,7'-tetrinitro-9,9'-spirobi[9H-fluorene] • 1.5 dioxane (**4**)

Empirical formula	C ₃₁ H ₂₄ N ₄ O ₁₁					
Formula weight	628.54					
Temperature	223(2) K					
Wavelength	1.54178 Å					
Crystal system	Triclinic					
Space group	P-1	Z = 2				
Unit cell dimensions	a = 8.7222(2) Å	α = 85.288(2)°	b = 10.4838(2) Å	β = 88.006(2)°	c = 16.7599(4) Å	γ = 70.332(2)°
Volume	1438.23(6) Å ³					
Density (calculated)	1.451 g/cm ³					
Absorption coefficient	0.951 mm ⁻¹					
Crystal size	0.38 x 0.27 x 0.19 mm					
Theta range for data collection	2.65 to 70.03°					
Index ranges	-10 ≤ h ≤ 10, -12 ≤ k ≤ 12, -20 ≤ l ≤ 20					
Reflections collected	17189					
Independent reflections	5304 [R _{int} = 0.032]					
Absorption correction	Semi-empirical from equivalents					
Max. and min. transmission	0.7300 and 0.6700					
Refinement method	Full-matrix least-squares on F ²					
Data / restraints / parameters	5304 / 0 / 416					
Goodness-of-fit on F ²	1.073					
Final R indices [I>2sigma(I)]	R ₁ = 0.0616, wR ₂ = 0.1794					
R indices (all data)	R ₁ = 0.0692, wR ₂ = 0.1879					
Largest diff. peak and hole	0.378 and -0.337 e/Å ³					

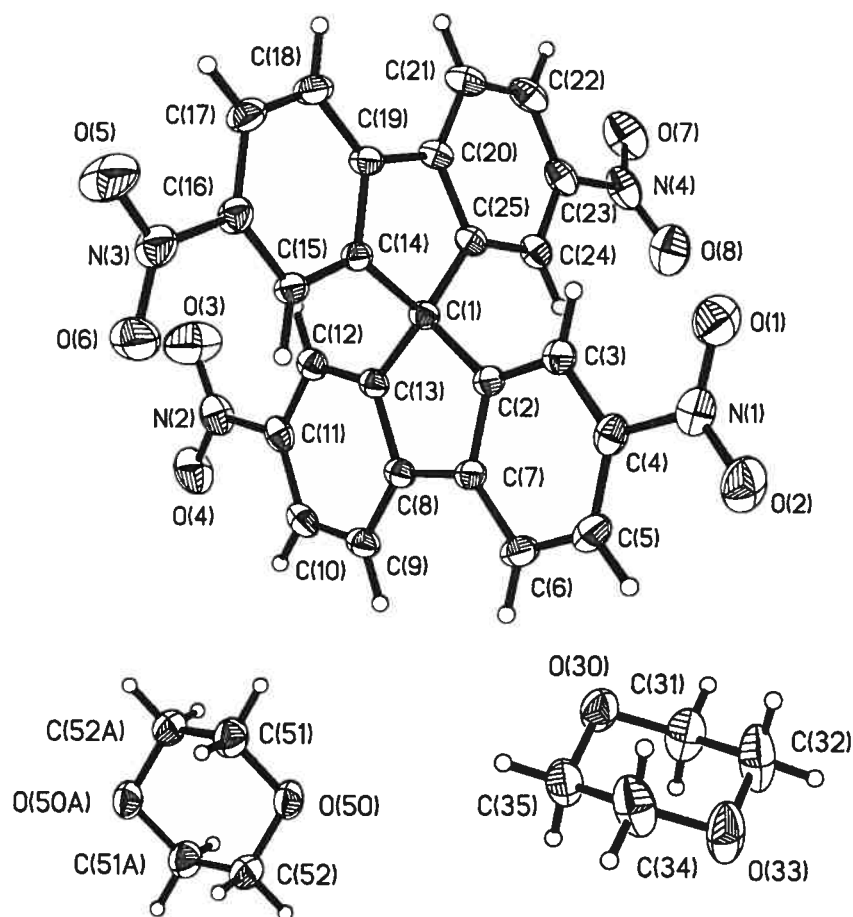


Figure S1. ORTEP view of molecular structure with the numbering scheme adopted for 2,2',7,7'-tetrinitro-9,9'-spirobi[9H-fluorene] • 1.5 dioxane (**4**). Ellipsoids drawn at 30% probability level. Hydrogens represented by sphere of arbitrary size.

Table S2. Bond lengths [Å] and angles [°] related to the hydrogen bonding for 2,2',7,7'-tetrinitro-9,9'-spirobi[9H-fluorene] • 1.5 dioxane (4).

D-H	..A	d (D-H)	d (H..A)	d (D..A)	<DHA
C(5)-H(5)	O(2) #1	0.94	2.50	3.295 (3)	142.7
C(12)-H(12)	O(5) #2	0.94	2.60	3.515 (3)	163.6
C(22)-H(22)	O(6) #3	0.94	2.66	3.351 (3)	130.9

Symmetry transformations used to generate equivalent atoms:

#1 -x+1, -y+1, -z+1 #2 -x, 1-y, -z #3 x, y-1, z

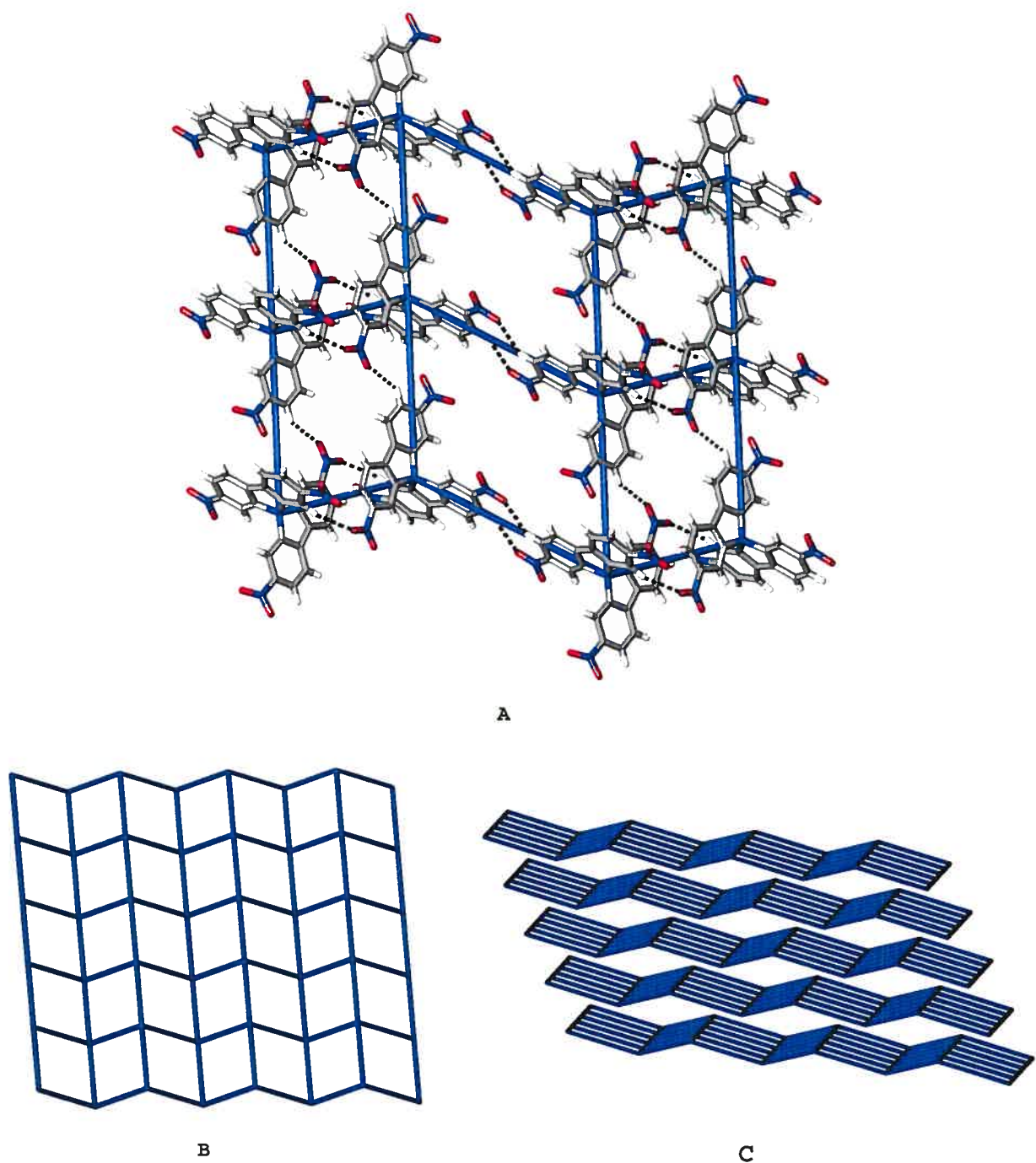


Figure S2. Network defined by the C-H...O interactions observed in the structure of 2,2',7,7'-tetrtnitro-9,9'-spirobi[9H-fluorene] • 1.5 dioxane (**4**). **A.** View of one network showing the molecules and the C-H...O interactions involving nitro groups. Each molecule is linked to four neighbors by a total of six C-H...O interactions, defining a 2D network. **B.** View of the same network without the molecules. **C.** View of the stacking of planar networks along the *a* axis.

CRYSTAL AND MOLECULAR STRUCTURE OF
2,2',7,7'-TETRACYANO-9,9'-SPIROBI[9H-FLUORENE] 2 CHCl₃
(COMPOUND 5)

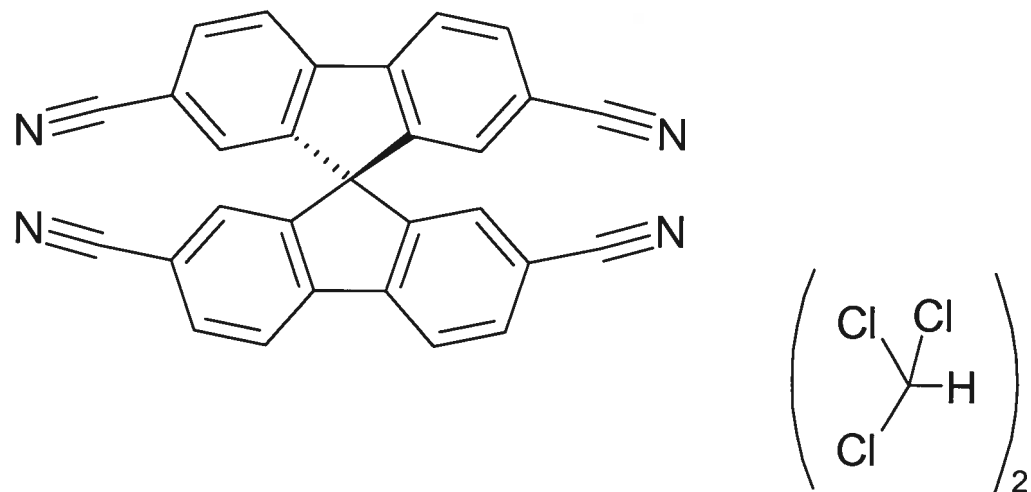


Table S3. Crystal data and structure refinement for 2,2',7,7'-tetracyano-9,9'-spirobi[9H-fluorene] • 2 CHCl₃ (**5**)

Empirical formula	C ₃₁ H ₁₄ Cl ₆ N ₄		
Formula weight	655.16		
Temperature	293 (2) K		
Wavelength	1.54180 Å		
Crystal system	Monoclinic		
Space group	C2/c	Z = 4	
Unit cell dimensions	a = 14.0060 (3) Å	α = 90°	
	b = 15.8520 (3) Å	β = 99.780 (2) °	
	c = 14.3180 (4) Å	γ = 90°	
Volume	3132.73 (13) Å ³		
Density (calculated)	1.389 g/cm ³		
Absorption coefficient	5.226 mm ⁻¹		
Crystal size	0.21 x 0.18 x 0.18 mm		
Theta range for data collection	4.25 to 72.89°		
Index ranges	-17 ≤ h ≤ 17, -19 ≤ k ≤ 19, -17 ≤ l ≤ 17		
Reflections collected	19040		
Independent reflections	3099 [R _{int} = 0.075]		
Absorption correction	Semi-empirical from equivalents		
Max. and min. transmission	0.4000 and 0.3000		
Refinement method	Full-matrix least-squares on F ²		
Data / restraints / parameters	3099 / 6 / 196		
Goodness-of-fit on F ²	1.019		
Final R indices [I>2sigma(I)]	R ₁ = 0.0690, wR ₂ = 0.1648		
R indices (all data)	R ₁ = 0.0719, wR ₂ = 0.1665		
Largest diff. peak and hole	0.315 and -0.675 e/Å ³		

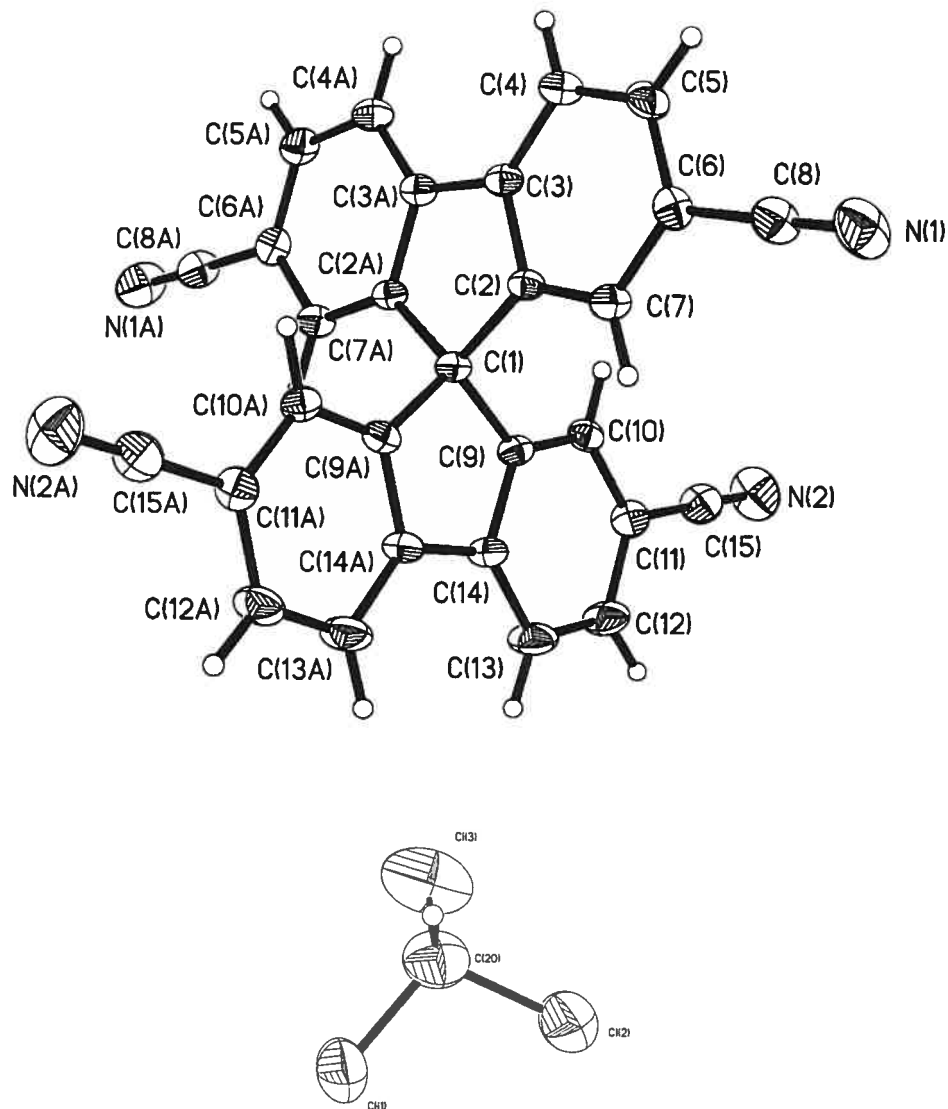


Figure S3. ORTEP view of the molecular structure of 2,2',7,7'-tetracyano-9,9'-spirobi[9H-fluorene] • 2 CHCl₃ (5) with the numbering scheme adopted. Ellipsoids drawn at 30% probability level. Hydrogens represented by sphere of arbitrary size. Only the main part of the disordered CHCl₃ molecule is shown.

CRYSTAL AND MOLECULAR STRUCTURE OF
2,2',7,7'-TETRAKIS(4-NITROPHENYL)-9,9'-SPIROBI[9H-FLUORENE]
0.5 ETHYL ACETATE (COMPOUND 6)

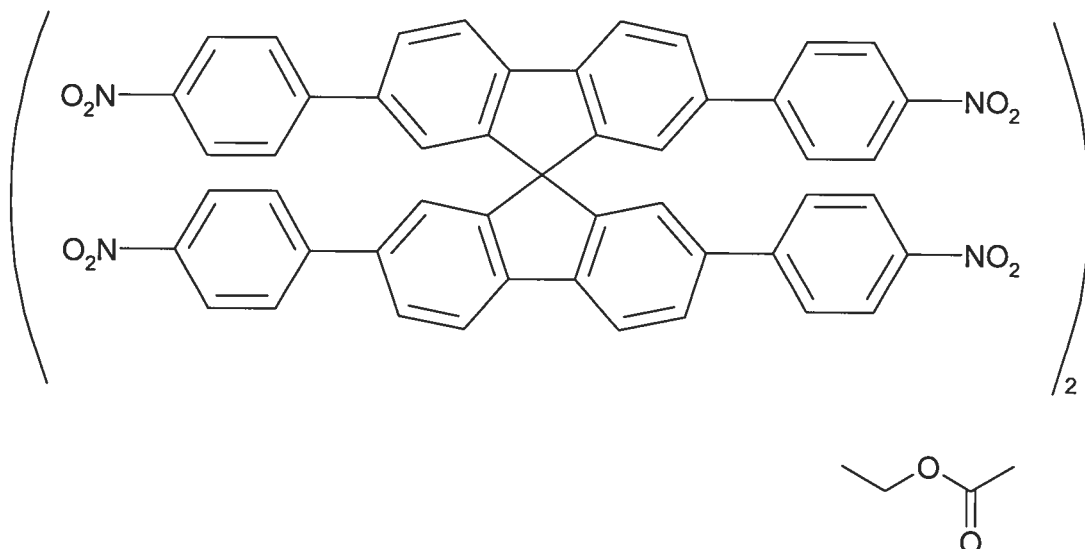


Table S4. Crystal data and structure refinement for 2,2',7,7'-tetrakis(4-nitrophenyl)-9,9'-spirobi[9H-fluorene] • 0.5 ethyl acetate (**6**).

Empirical formula	C ₁₀₂ H ₆₄ N ₈ O ₁₈	
Formula weight	1689.61	
Temperature	223 (2) K	
Wavelength	1.54178 Å	
Crystal system	Triclinic	
Space group	P-1	Z = 2
Unit cell dimensions	a = 16.1160 (8) Å	α = 64.223 (3) °
	b = 16.2973 (8) Å	β = 69.471 (3) °
	c = 18.7307 (9) Å	γ = 89.408 (3) °
Volume	4089.3 (3) Å ³	
Density (calculated)	1.372 g/cm ³	
Absorption coefficient	0.786 mm ⁻¹	
Crystal size	0.60 x 0.30 x 0.07 mm	
Theta range for data collection	2.84 to 70.22°	
Index ranges	-18 ≤ h ≤ 19, -17 ≤ k ≤ 19, -22 ≤ l ≤ 22	
Reflections collected	36709	
Independent reflections	14819 [R _{int} = 0.030]	
Absorption correction	Semi-empirical from equivalents	
Max. and min. transmission	0.8500 and 0.6600	
Refinement method	Full-matrix least-squares on F ²	
Data / restraints / parameters	14819 / 1 / 1153	
Goodness-of-fit on F ²	1.005	
Final R indices [I>2sigma(I)]	R ₁ = 0.0686, wR ₂ = 0.1591	
R indices (all data)	R ₁ = 0.0785, wR ₂ = 0.1605	
Largest diff. peak and hole	0.350 and -0.310 e/Å ³	

Table S5. Bond lengths [Å] and angles [°] related to the hydrogen bonding for 2,2',7,7'-tetrakis(4-nitrophenyl)-9,9'-spirobi[9H-fluorene] • 0.5 ethyl acetate (**6**).

D-H	..A	d (D-H)	d (H..A)	d (D..A)	<DHA
C(9) -H(9)	O(7)#1	0.94	2.59	3.337(5)	136.5
C(13) -H(13)	O(16)#2	0.94	2.60	3.499(6)	161.1
C(45) -H(45)	O(10)#3	0.94	2.50	3.394(6)	158.3
C(46) -H(46)	O(9)#3	0.94	2.49	3.246(6)	138.1
C(58) -H(58)	O(3)#4	0.94	2.43	3.348(6)	165.8
C(82) -H(82)	O(4)#4	0.94	2.59	3.208(6)	123.8
C(98) -H(98)	O(9)#5	0.94	2.52	3.292(6)	139.5

Symmetry transformations used to generate equivalent atoms:

```
#1 -x+1, -y+1, -z      #2 x-1, y-1, z
#3 -x+1, -y+1, -z+1    #4 x+1,y,z
#5 -x+2, -y+1, -z+1
```

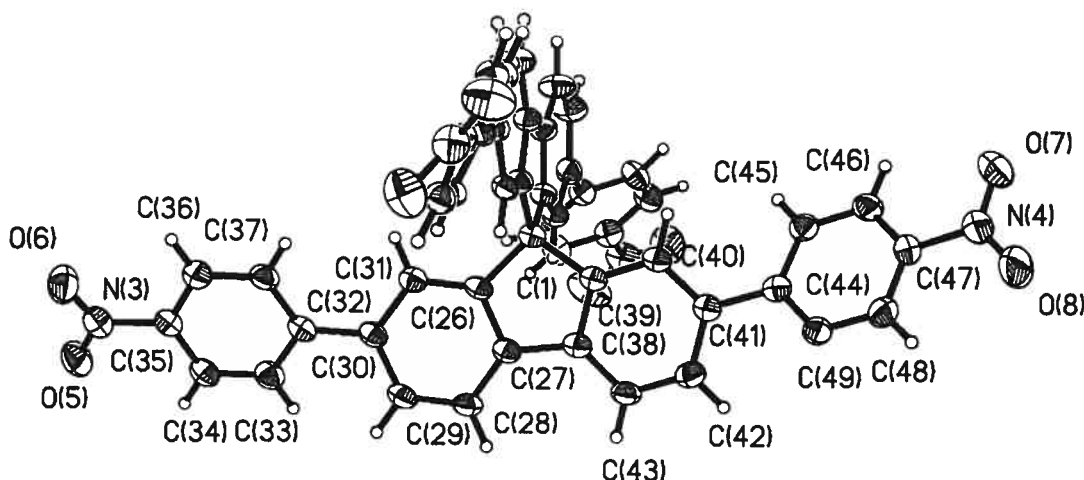
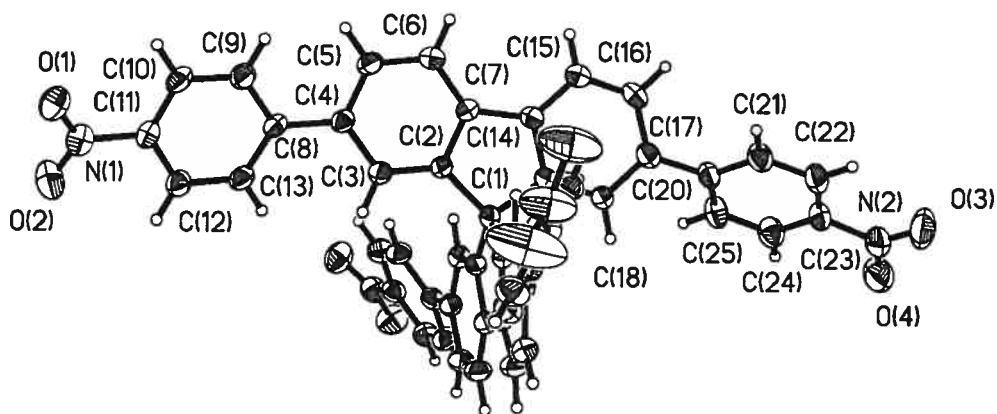


Figure S4. ORTEP view of the molecular structure of 2,2',7,7'-tetrakis(4-nitrophenyl)-9,9'-spirobi[9H-fluorene] • 0.5 ethyl acetate (**6**) with the numbering scheme adopted. Ellipsoids drawn at 30% probability level. Hydrogens represented by sphere of arbitrary size.

Molecule A

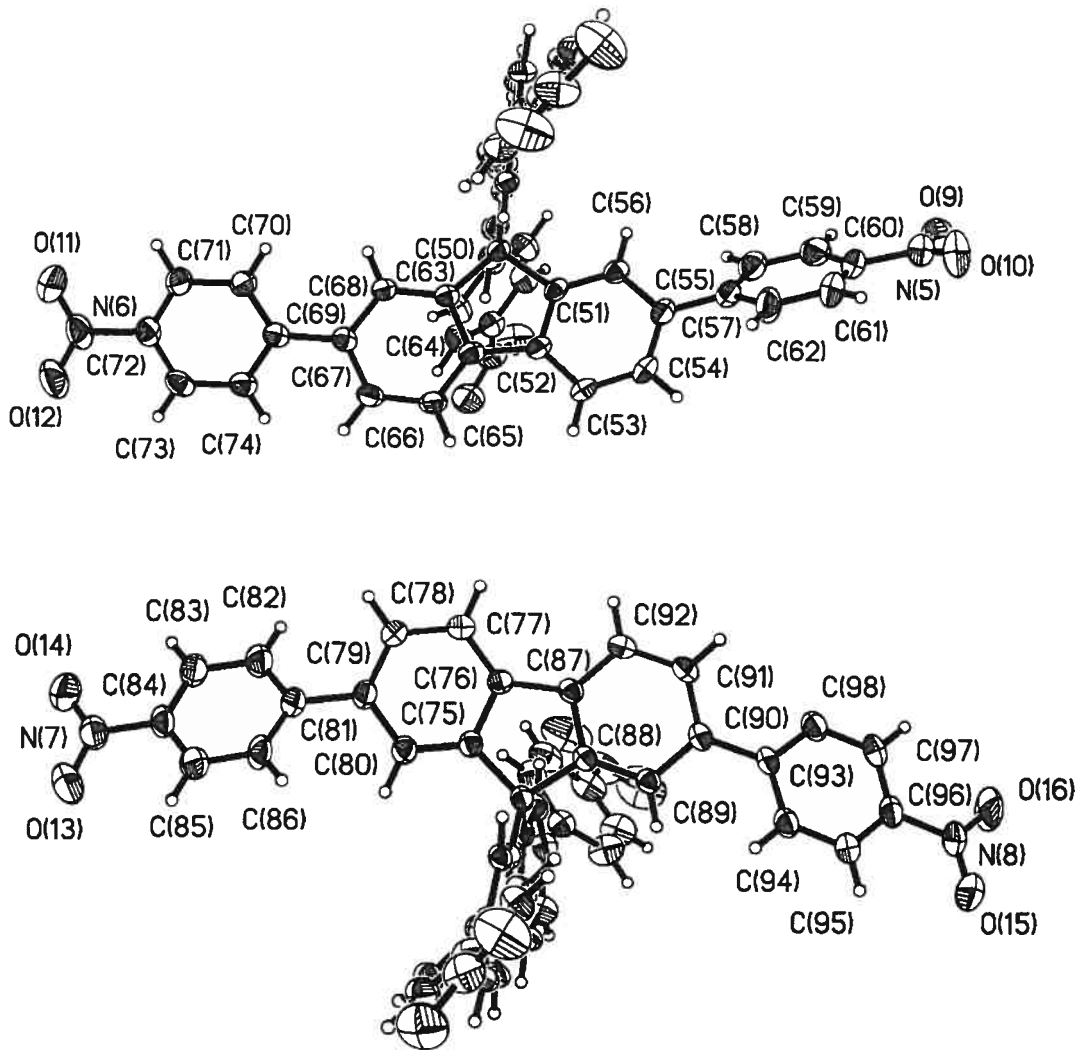


Figure S5. ORTEP view of the molecular structure of 2,2',7,7'-tetrakis(4-nitrophenyl)-9,9'-spirobi[9H-fluorene] • 0.5 ethyl acetate (6) with the numbering scheme adopted. Ellipsoids drawn at 30% probability level. Hydrogens represented by sphere of arbitrary size.

Molecule B

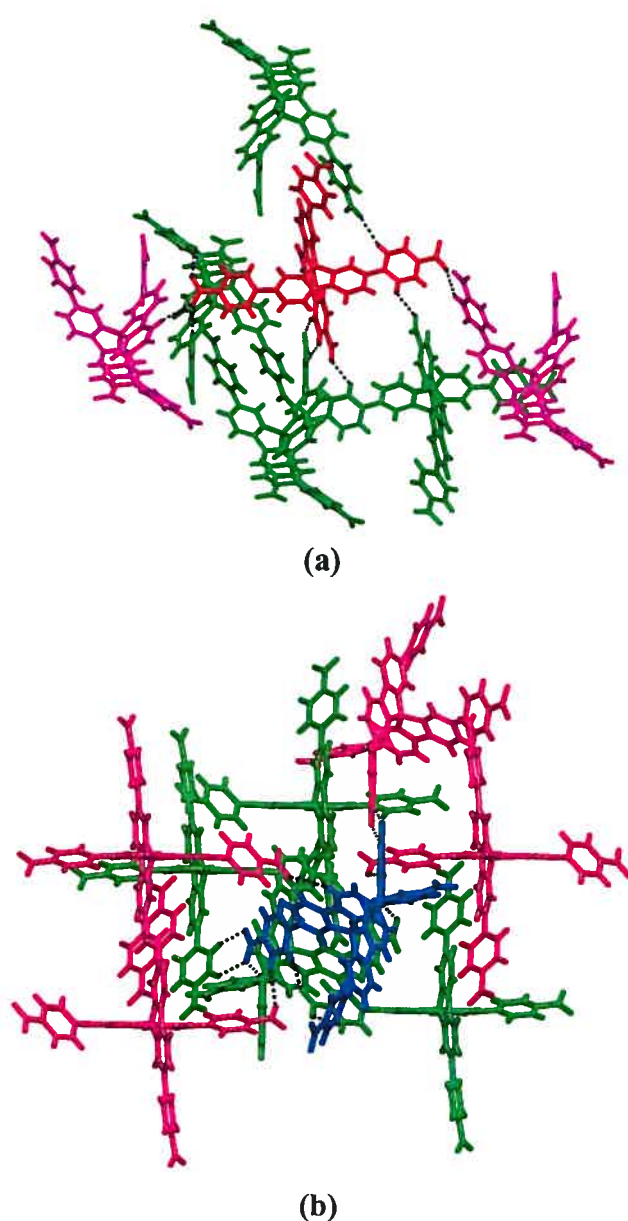


Figure S6. Views of the structure of crystals of 2,2',7,7'-tetrakis(4-nitrophenyl)-9,9'-spirobi[9H-fluorene] • 0.5 ethyl acetate (**6**) grown from ethyl acetate/hexane, showing the two symmetry-independent molecules **A** (red) and **B** (blue) in the unit cell. Included molecules of ethyl acetate are omitted for clarity. (a) C-H...O interactions between molecule **A** (red) and four neighbors (green) with H...O distances less than or equal to 2.65 Å, and two other neighbors (purple) with H...O distances less than or equal to 2.70 Å. The C-H...O interactions are represented by broken lines. (b) Similar view of C-H...O interactions involving molecule **B** (blue), four neighbors (green) with H...O distances less than or equal to 2.65 Å, and four other neighbors (purple) with H...O distances less than or equal to 2.70 Å.

CRYSTAL AND MOLECULAR STRUCTURE OF
2,2',7,7'-TETRAKIS(4-CYANOPHENYL)-9,9'-SPIROBI[9H-FLUORENE] 3
DIOXANE
(COMPOUND 7)

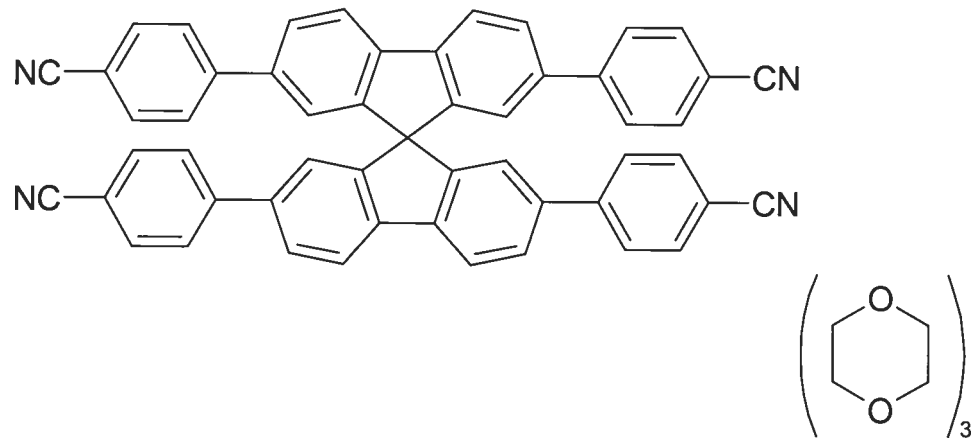


Table S6. Crystal data and structure refinement for 2,2',7,7'-tetrakis(4-cyanophenyl)-9,9'-spirobi[9H-fluorene] • 3 dioxane (7)

Empirical formula	C ₆₅ H ₅₂ N ₄ O ₆	
Formula weight	985.11	
Temperature	223 (2) K	
Wavelength	1.54178 Å	
Crystal system	Triclinic	
Space group	P-1	Z = 2
Unit cell dimensions	a = 13.3274 (6) Å b = 14.2569 (7) Å c = 14.8016 (7) Å	α = 93.161 (3) ° β = 98.071 (3) ° γ = 109.723 (3) °
Volume	2605.3 (2) Å ³	
Density (calculated)	1.256 g/cm ³	
Absorption coefficient	0.644 mm ⁻¹	
Crystal size	0.40 x 0.35 x 0.09 mm	
Theta range for data collection	3.03 to 70.04 °	
Index ranges	-16 ≤ h ≤ 15, -17 ≤ k ≤ 17, -18 ≤ l ≤ 18	
Reflections collected	31034	
Independent reflections	9617 [R _{int} = 0.028]	
Absorption correction	Semi-empirical from equivalents	
Max. and min. transmission	0.9200 and 0.7000	
Refinement method	Full-matrix least-squares on F ²	
Data / restraints / parameters	9617 / 12 / 695	
Goodness-of-fit on F ²	1.102	
Final R indices [I>2sigma(I)]	R ₁ = 0.0567, wR ₂ = 0.1776	
R indices (all data)	R ₁ = 0.0719, wR ₂ = 0.1884	
Largest diff. peak and hole	0.228 and -0.317 e/Å ³	

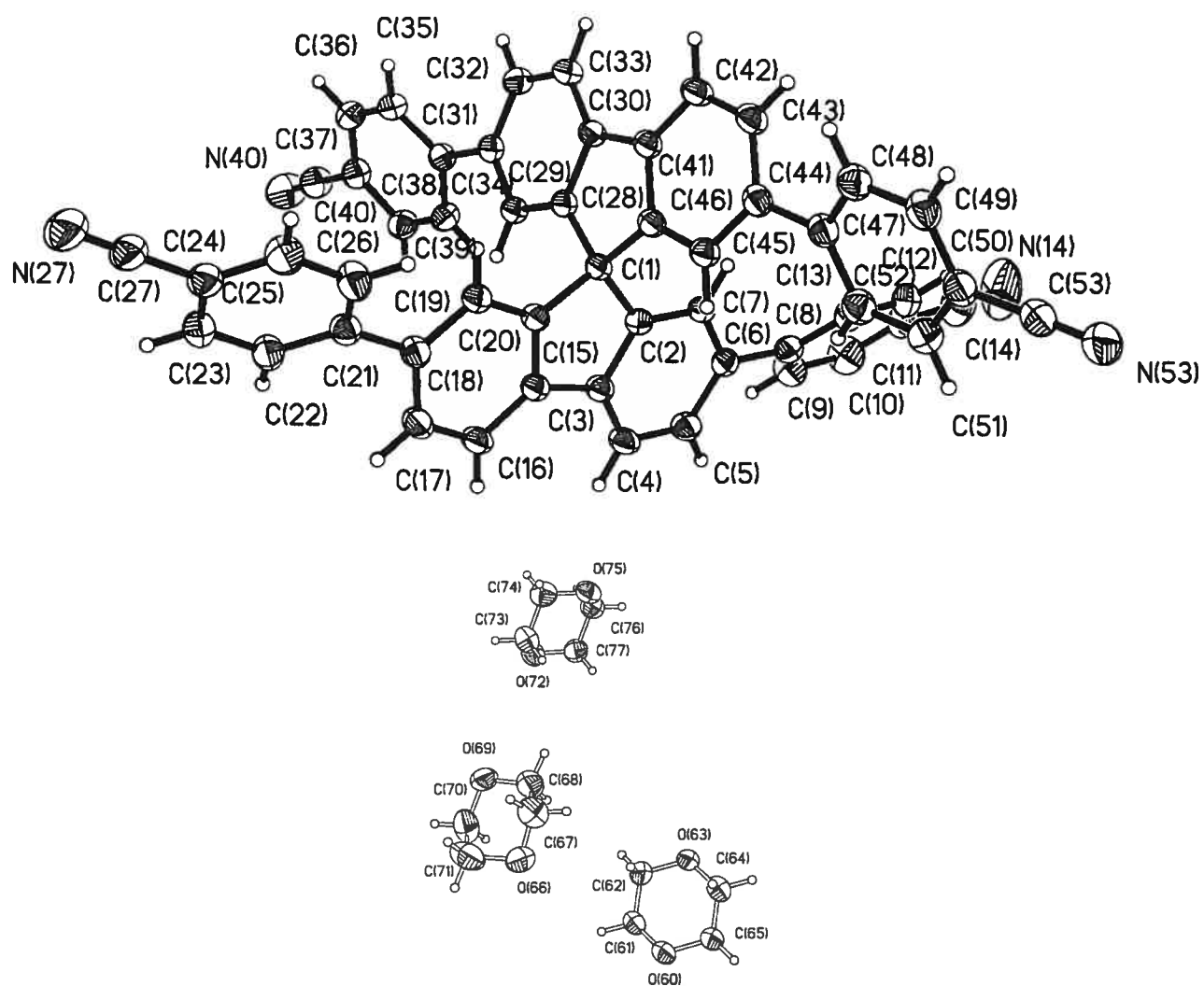


Figure S7. ORTEP view of the molecular structure of 2,2',7,7'-tetrakis(4-cyanophenyl)-9,9'-spirobi[9H-fluorene] • 3 dioxane (7) with the numbering scheme adopted. Ellipsoids drawn at 30% probability level. Hydrogens represented by sphere of arbitrary size.

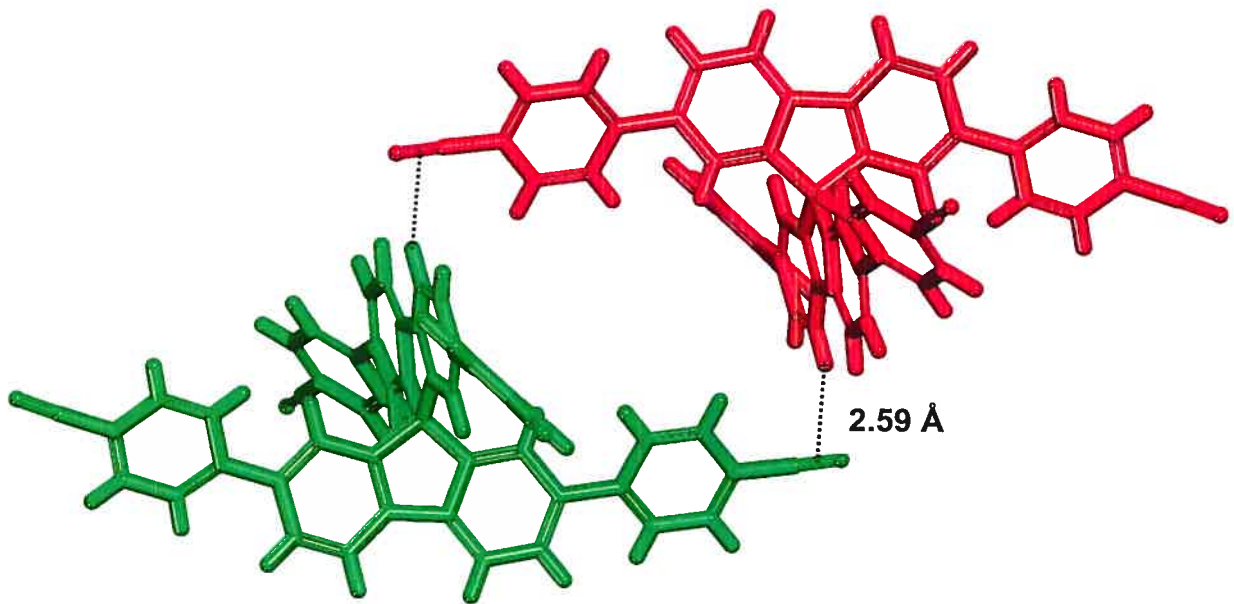


Figure S8. View of the structure of 2,2',7,7'-tetrakis(4-cyanophenyl)-9,9'-spirobi[9H-fluorene] • 3 dioxane (7) showing two molecules linked via C-H···N interactions of type V.

CRYSTAL AND MOLECULAR STRUCTURE OF
2,2',7,7'-TETRAKIS(3-NITROPHENYL)-9,9'-SPIROBI[9H-FLUORENE]
(COMPOUND 8)

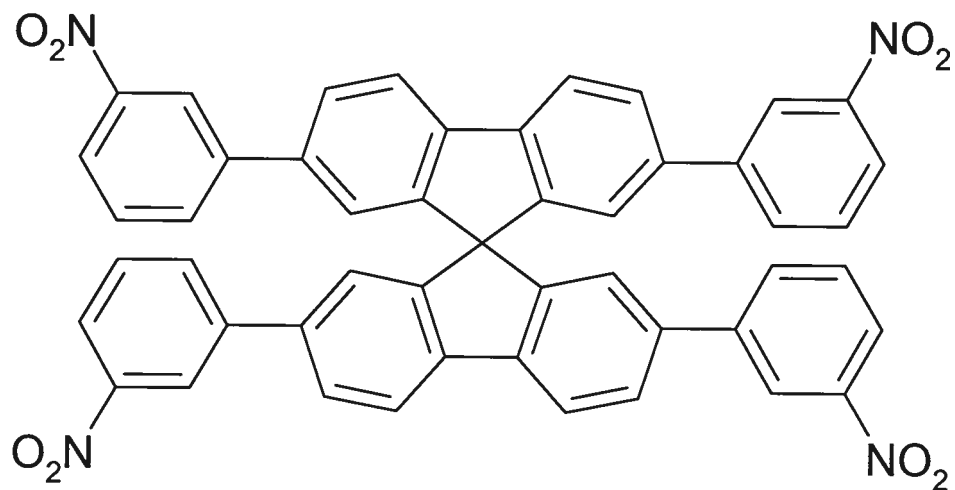


Table S7. Crystal data and structure refinement for 2,2',7,7'-tetrakis(3-nitrophenyl)-9,9'-spirobi[9H-fluorene] (**8**)

Empirical formula	C ₄₉ H ₂₈ N ₄ O ₈		
Formula weight	800.75		
Temperature	223 (2) K		
Wavelength	1.54178 Å		
Crystal system	Tetragonal		
Space group	I41/a	Z = 4	
Unit cell dimensions	a = 12.3873 (3) Å	α = 90°	
	b = 12.3873 (3) Å	β = 90°	
	c = 24.1863 (7) Å	γ = 90°	
Volume	3711.27 (17) Å ³		
Density (calculated)	1.433 g/cm ³		
Absorption coefficient	0.813 mm ⁻¹		
Crystal size	0.45 x 0.35 x 0.32 mm		
Theta range for data collection	4.01 to 70.01°		
Index ranges	-14 ≤ h ≤ 15, -14 ≤ k ≤ 15, -29 ≤ l ≤ 29		
Reflections collected	10167		
Independent reflections	1760 [R _{int} = 0.024]		
Absorption correction	Semi-empirical from equivalents		
Max. and min. transmission	0.87000 and 0.8200		
Refinement method	Full-matrix least-squares on F ²		
Data / restraints / parameters	1760 / 0 / 167		
Goodness-of-fit on F ²	1.034		
Final R indices [I>2sigma(I)]	R ₁ = 0.0429, wR ₂ = 0.1096		
R indices (all data)	R ₁ = 0.0440, wR ₂ = 0.1104		
Largest diff. peak and hole	0.266 and -0.319 e/Å ³		

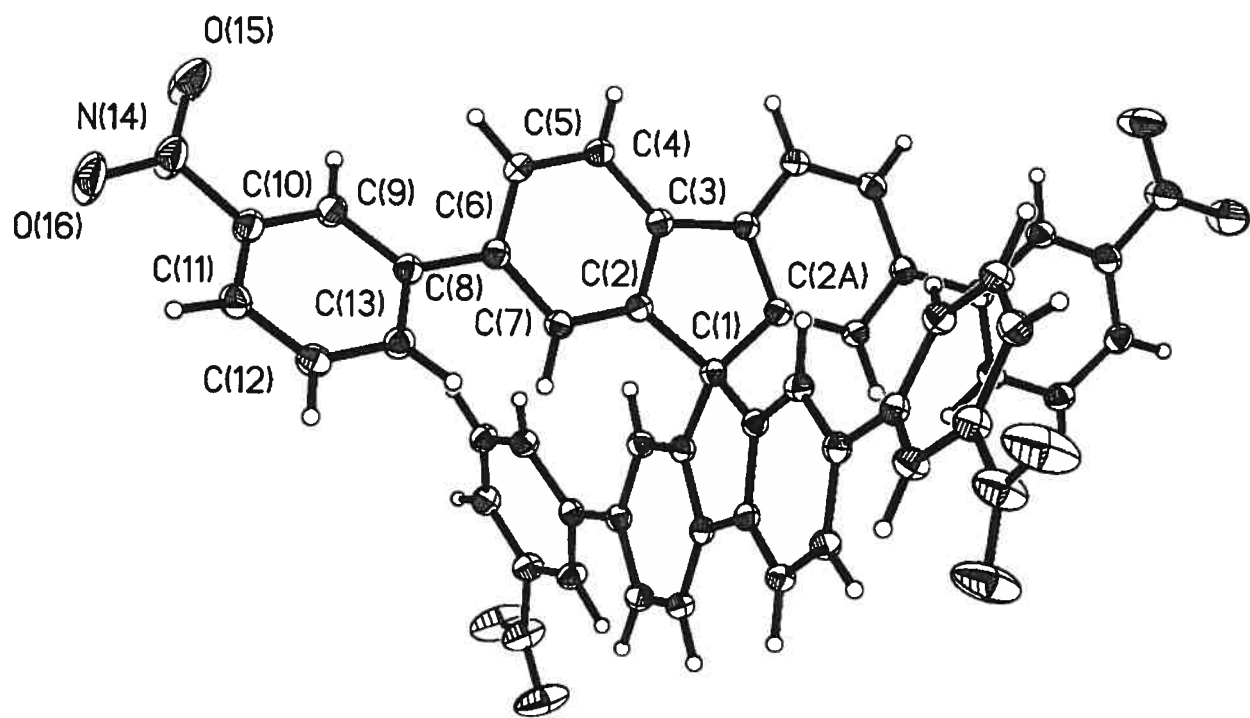


Figure S9. ORTEP view of molecular structure of 2,2',7,7'-tetrakis(3-nitrophenyl)-9,9'-spirobi[9H-fluorene] (**8**) with the numbering scheme adopted. Ellipsoids drawn at 30% probability level. Hydrogens represented by sphere of arbitrary size.

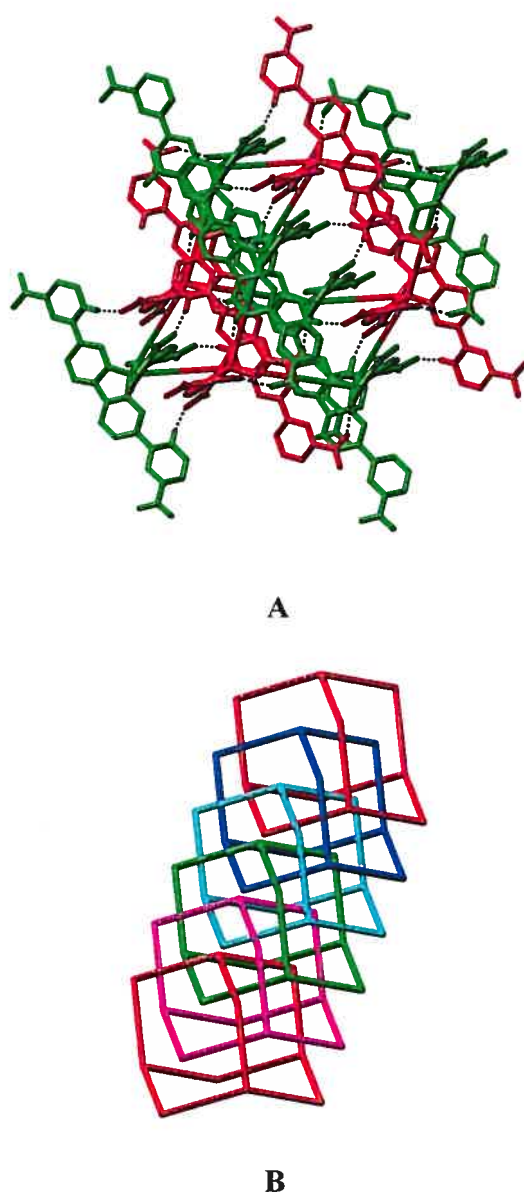


Figure S10. Diamondoid networks in the molecular structure of 2,2',7,7'-tetrakis(3-nitrophenyl)-9,9'-spirobi[9H-fluorene] (**8**). **A.** View of one non-interpenetrated diamondoid network defined by π -stacking interactions and C-H···O interactions of type **IV** (Figure 1), with H···O distances less than or equal to 2.65 Å. The centers of neighboring molecules displayed alternately in red and green are separated by 8.65 Å. **B.** View of the five-fold interpenetrated diamondoid networks defined by the additional C-H···O interactions that are slightly longer (2.652 Å). In each diamondoid network, the centers of neighboring molecules are separated by 15.11 Å, and the distance between two adjacent diamondoid networks is 12.387 Å.

CRYSTAL AND MOLECULAR STRUCTURE OF
2,2',7,7'-TETRAKIS (3-CYANOPHENYL) -9,9'-SPIROBI [9H-FLUORENE]
(COMPOUND 9)

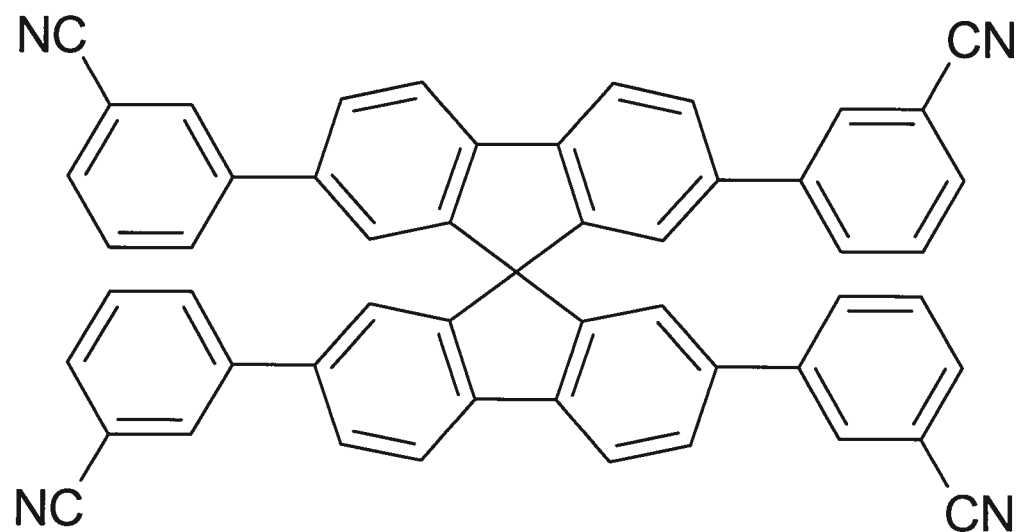


Table S8. Crystal data and structure refinement for 2,2',7,7'-tetrakis(3-cyanophenyl)-9,9'-spirobi[9H-fluorene] (9)

Empirical formula	C53 H28 N4
Formula weight	720.79
Temperature	223 (2) K
Wavelength	1.54178 Å
Crystal system	Tetragonal
Space group	I41/a
Unit cell dimensions	a = 13.2114 (9) Å α = 90° b = 13.2114 (9) Å β = 90° c = 21.539 (3) Å γ = 90°
Volume	3759.4 (6) Å ³
Density (calculated)	1.274 g/cm ³
Absorption coefficient	0.583 mm ⁻¹
Crystal size	0.25 x 0.20 x 0.15 mm
Theta range for data collection	3.93 to 70.04°
Index ranges	-10 ≤ h ≤ 11, -16 ≤ k ≤ 16, -26 ≤ l ≤ 26
Reflections collected	11979
Independent reflections	1780 [R _{int} = 0.076]
Absorption correction	Semi-empirical from equivalents
Max. and min. transmission	0.8900 and 0.8700
Refinement method	Full-matrix least-squares on F ²
Data / restraints / parameters	1780 / 0 / 129
Goodness-of-fit on F ²	1.063
Final R indices [I>2sigma(I)]	R ₁ = 0.0629, wR ₂ = 0.1509
R indices (all data)	R ₁ = 0.0664, wR ₂ = 0.1517
Largest diff. peak and hole	0.215 and -0.215 e/Å ³

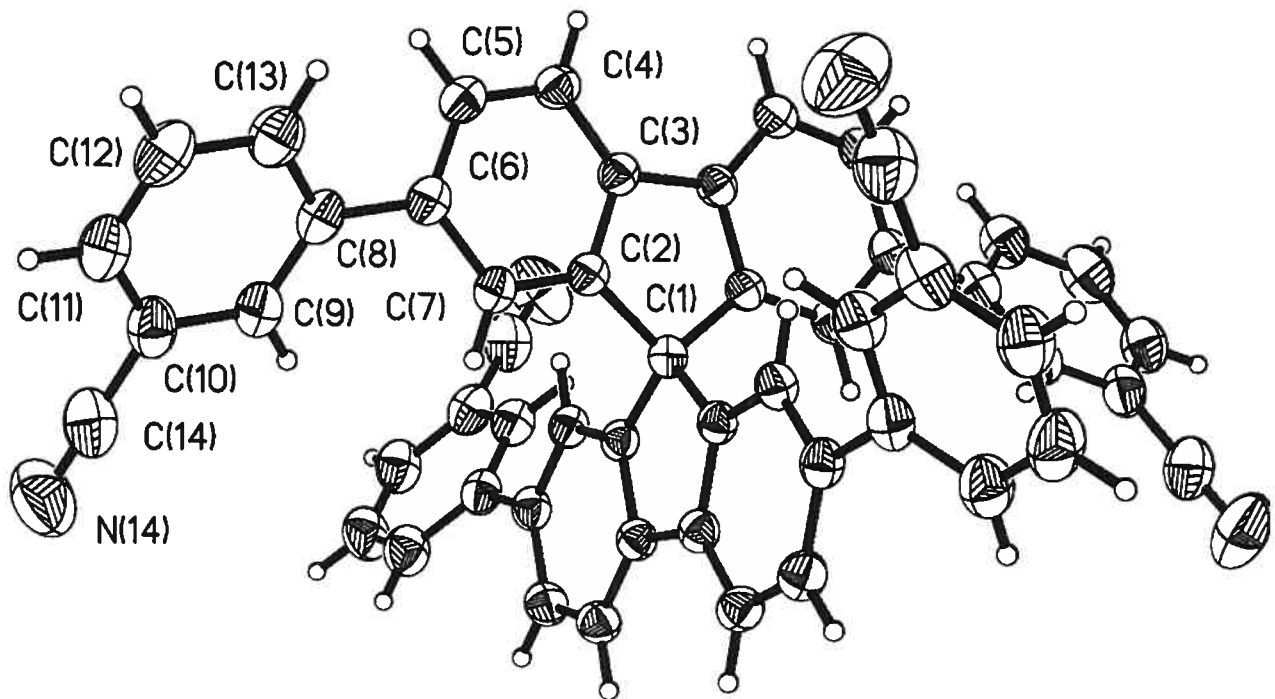


Figure S11. ORTEP view of the molecular structure of 2,2',7,7'-tetrakis(3-cyanophenyl)-9,9'-spirobi[9H-fluorene] (**9**) with the numbering scheme adopted. Ellipsoids drawn at 30% probability level. Hydrogens represented by sphere of arbitrary size.

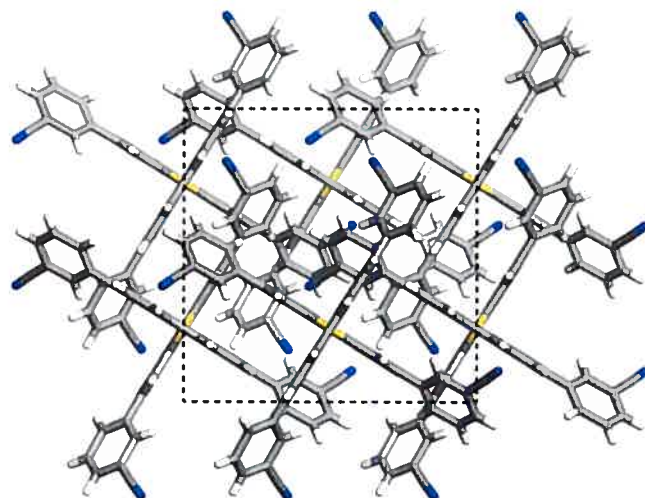


Figure S12. View along the *c* axis of the unit cell of 2,2',7,7'-tetrakis(3-cyanophenyl)-9,9'-spirobi[9*H*-fluorene] (**9**).

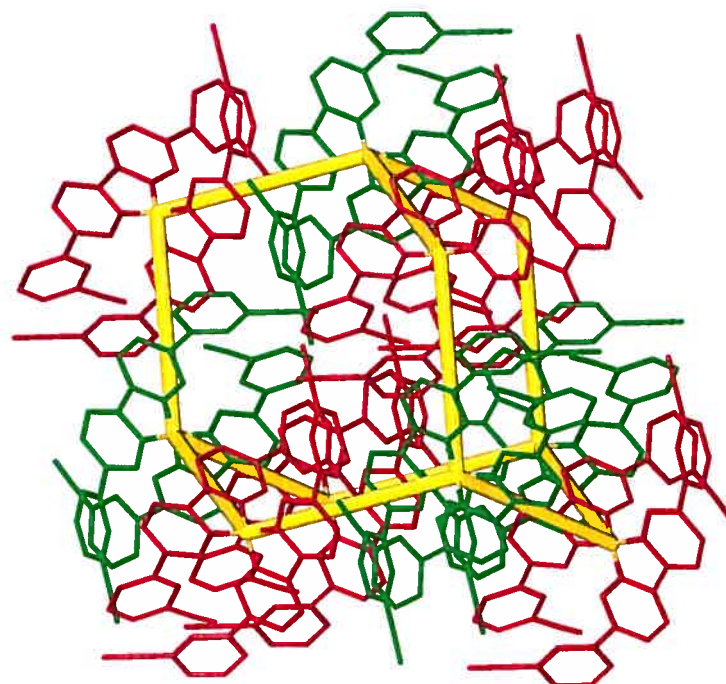


Figure S13. View of one diamondoid network generated by aryl-aryl interactions in the structure of 2,2',7,7'-tetrakis(3-cyanophenyl)-9,9'-spirobi[9*H*-fluorene] (**9**). The centers of neighboring molecules (displayed alternately in red and green) are separated by 8.522 Å.

Annexe 3

Supporting Information

Molecular Tectonics. Hydrogen-Bonded Networks

Built from Tetra- and Hexaanilines

Dominic Laliberté, Thierry Maris, Eric Demers,
Fatima Helzy, Mathieu Arseneault, and James D. Wuest

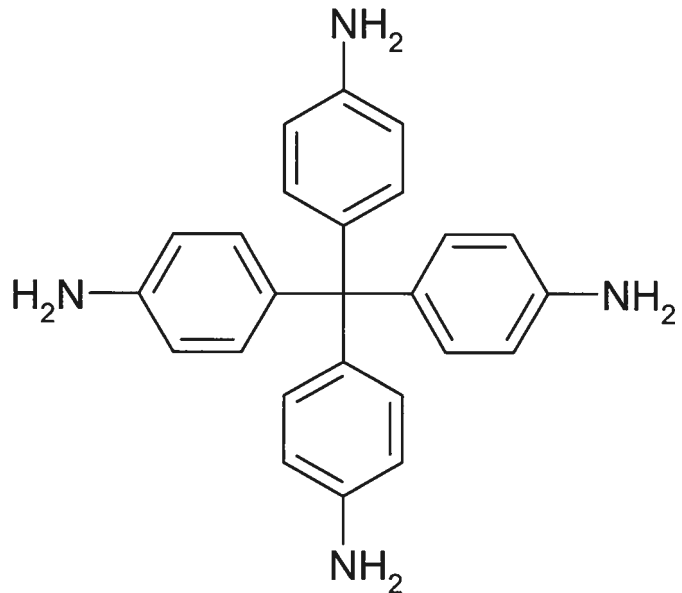
Contents

- I Crystal Structure of Tetrakis(4-aminophenyl)methane (2c).....(A3-3)-(A3-9)**
- II Crystal Structure of Tetrakis[(4-aminophenoxy)methyl]methane (3c)(A3-10)-(A3-17)**
- III Crystal Structure of 2,2',7,7'-Tetraamino-9,9'-spirobi[9H-fluorene] (1c)(A3-18)-(A3-23)**
- IV Crystal Structure of Tetrakis(4-aminophenyl)ethylene (5)(A3-24)-(A3-27)**
- V Crystal Structure of 1,1'-Oxybis[3-(4-aminophenoxy)-2,2-bis[(4-aminophenoxy)methyl]]propane (4c)(A3-28)-(A3-33)**

CRYSTAL AND MOLECULAR STRUCTURE OF
C25 H24 N4 COMPOUND (JIW547)

Equipe WUEST

Département de chimie, Université de Montréal,
C.P. 6128, Succ. Centre-Ville, Montréal, Québec, H3C 3J7 (Canada)



Structure solved and refined in the Laboratory of X-Ray Diffraction, Université de Montréal by Dr. Thierry Maris.

Table S1. Crystal data and structure refinement for C₂₅ H₂₄ N₄.

Empirical formula	C ₂₅ H ₂₄ N ₄	
Formula weight	380.48	
Temperature	223 (2) K	
Wavelength	1.54178 Å	
Crystal system	Tetragonal	
Space group	I4 ₁ /a	Z = 4
Unit cell dimensions	a = 16.8018(8) Å	α = 90°
	b = 16.8018(8) Å	β = 90°
	c = 7.1674(4) Å	γ = 90°
Volume	2023.36(18) Å ³	
Density (calculated)	1.249 g/cm ³	
Absorption coefficient	0.584 mm ⁻¹	
Crystal size	0.35 x 0.25 x 0.10 mm	
Theta range for data collection	5.27 to 69.81°	
Index ranges	-20 ≤ h ≤ 20, -20 ≤ k ≤ 20, -8 ≤ l ≤ 8	
Reflections collected	9513	
Independent reflections	961 [R _{int} = 0.028]	
Absorption correction	Semi-empirical from equivalents	
Max. and min. transmission	0.9400 and 0.8100	
Refinement method	Full-matrix least-squares on F ²	
Data / restraints / parameters	961 / 0 / 90	
Goodness-of-fit on F ²	1.082	
Final R indices [I>2sigma(I)]	R ₁ = 0.0412, wR ₂ = 0.1191	
R indices (all data)	R ₁ = 0.0475, wR ₂ = 0.1245	
Largest diff. peak and hole	0.143 and -0.191 e/Å ³	

Table S7. Bond lengths [\AA] and angles [$^\circ$] related to the hydrogen bonding for C25 H24 N4.

D-H	..A	d (D-H)	d (H..A)	d (D..A)	<DHA
N(8)-H(8B)	N(8) #4	0.929 (18)	2.192 (19)	3.1033 (14)	166.70 (14)

Symmetry transformations used to generate equivalent atoms:

#1 $y+1/4, -x-1/4, -z+7/4$ #2 $-y-1/4, x-1/4, -z+7/4$
#3 $-x, -y-1/2, z$ #4 $y+1/4, -x-3/4, z+1/4$

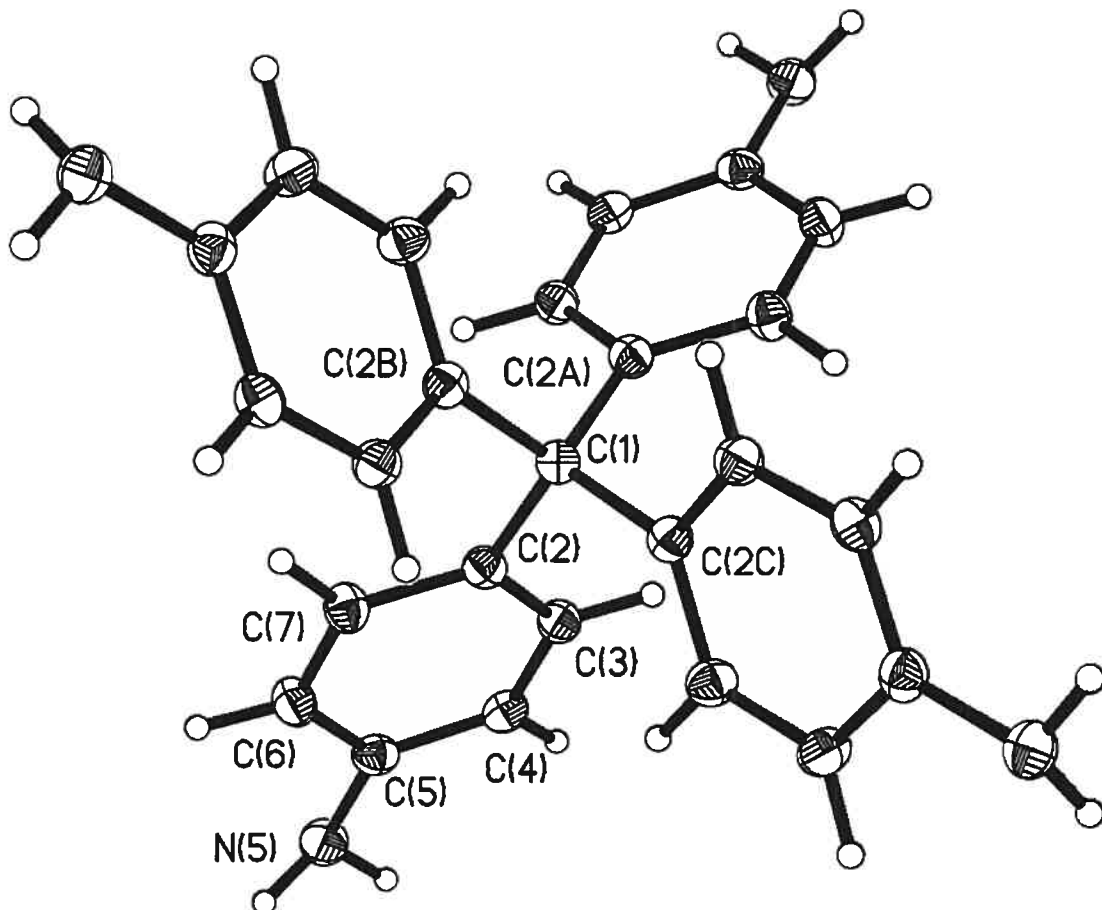


Figure S1

ORTEP view of the C₂₅ H₂₄ N₄ compound with the numbering scheme adopted. Ellipsoids drawn at 30% probability level. Hydrogen atoms represented by sphere of arbitrary size.

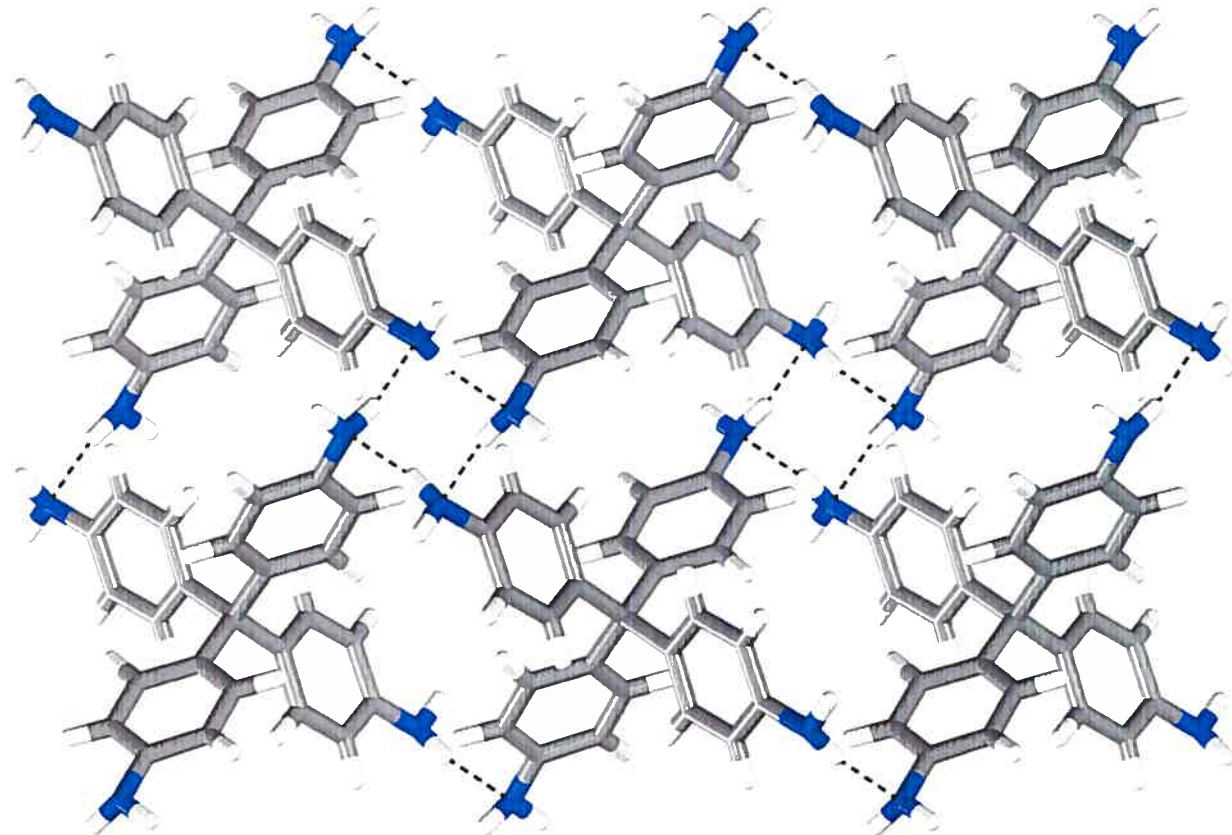


Figure S2

Packing diagram of the C₂₅ H₂₄ N₄ compound viewed along the c axis showing the hydrogen bonds.

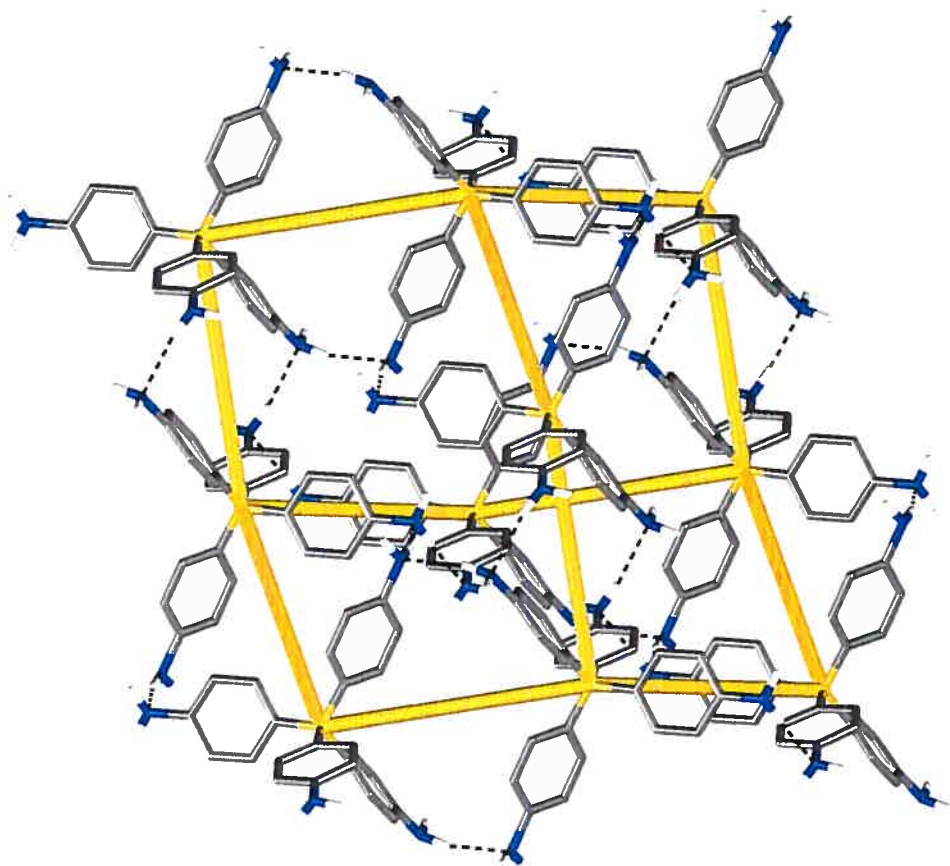


Figure S3

View of a diamondoid network in the structure of the C₂₅ H₂₄ N₄ compound defined by the intermolecular hydrogen bonds.

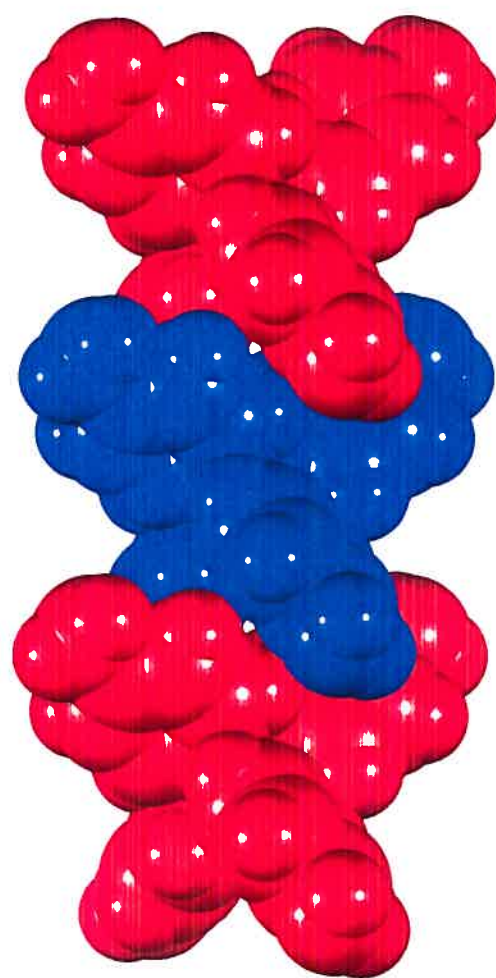


Figure S4

View of the structure of the C₂₅ H₂₄ N₄ compound showing the chain parallel to the c axis generated by two-fold phenyl embraces.



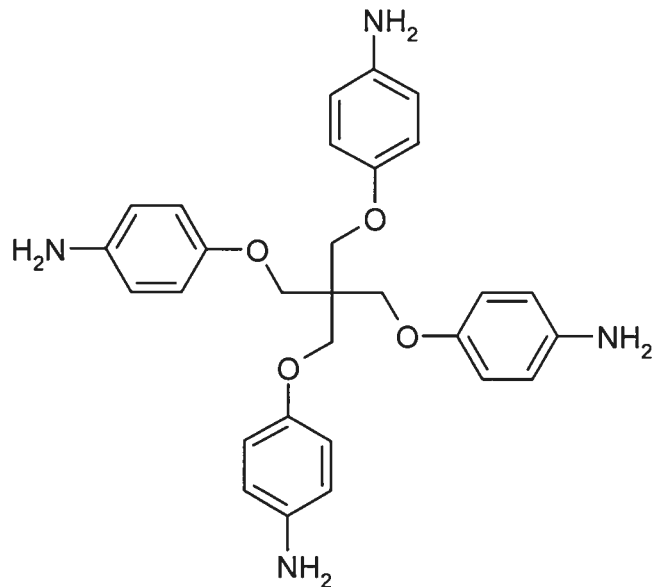
CRYSTAL AND MOLECULAR STRUCTURE OF

C29 H32 N4 O4 COMPOUND (JIW692)

Equipe WUEST

Département de chimie, Université de Montréal,

C.P. 6128, Succ. Centre-Ville, Montréal, Québec, H3C 3J7 (Canada)



Structure solved and refined in the Laboratory of X-Ray Diffraction, Université de Montréal by Dr. Thierry Maris.

Table S8. Crystal data and structure refinement for C₂₉ H₃₂ N₄ O₄.

Empirical formula	C ₂₉ H ₃₂ N ₄ O ₄		
Formula weight	500.59		
Temperature	220 (2) K		
Wavelength	1.54178 Å		
Crystal system	Tetragonal		
Space group	I-4	Z = 2	
Unit cell dimensions	a = 12.7089(1) Å	α = 90°	
	b = 12.7089(1) Å	β = 90°	
	c = 8.2149(1) Å	γ = 90°	
Volume	1326.84 (2) Å ³		
Density (calculated)	1.253 g/cm ³		
Absorption coefficient	0.684 mm ⁻¹		
Crystal size	0.35 x 0.34 x 0.30 mm		
Theta range for data collection	4.92 to 69.63°		
Index ranges	-14 ≤ h ≤ 14, -14 ≤ k ≤ 14, -7 ≤ l ≤ 9		
Reflections collected	3420		
Independent reflections	1232 [R _{int} = 0.025]		
Absorption correction	Semi-empirical from equivalents		
Max. and min. transmission	0.8140 and 0.7200		
Refinement method	Full-matrix least-squares on F ²		
Data / restraints / parameters	1232 / 0 / 117		
Goodness-of-fit on F ²	1.075		
Final R indices [I>2sigma(I)]	R ₁ = 0.0312, wR ₂ = 0.0849		
R indices (all data)	R ₁ = 0.0321, wR ₂ = 0.0857		
Absolute structure parameter	0.3 (2)		
Largest diff. peak and hole	0.096 and -0.099 e/Å ³		

Table S14. Bond lengths [\AA] and angles [°] related to the hydrogen bonding for C29 H32 N4 O4.

D-H	..A	d (D-H)	d (H..A)	d (D..A)	<DHA
N(7)-H(71)	N(7) #4	0.99 (2)	2.54 (2)	3.182 (3)	122.80 (17)

Symmetry transformations used to generate equivalent atoms:

#1 y-1/2,-x-1/2,-z-5/2 #2 -y-1/2,x+1/2,-z-5/2
#3 -x-1,-y,z #4 y,-x-1,-z-1

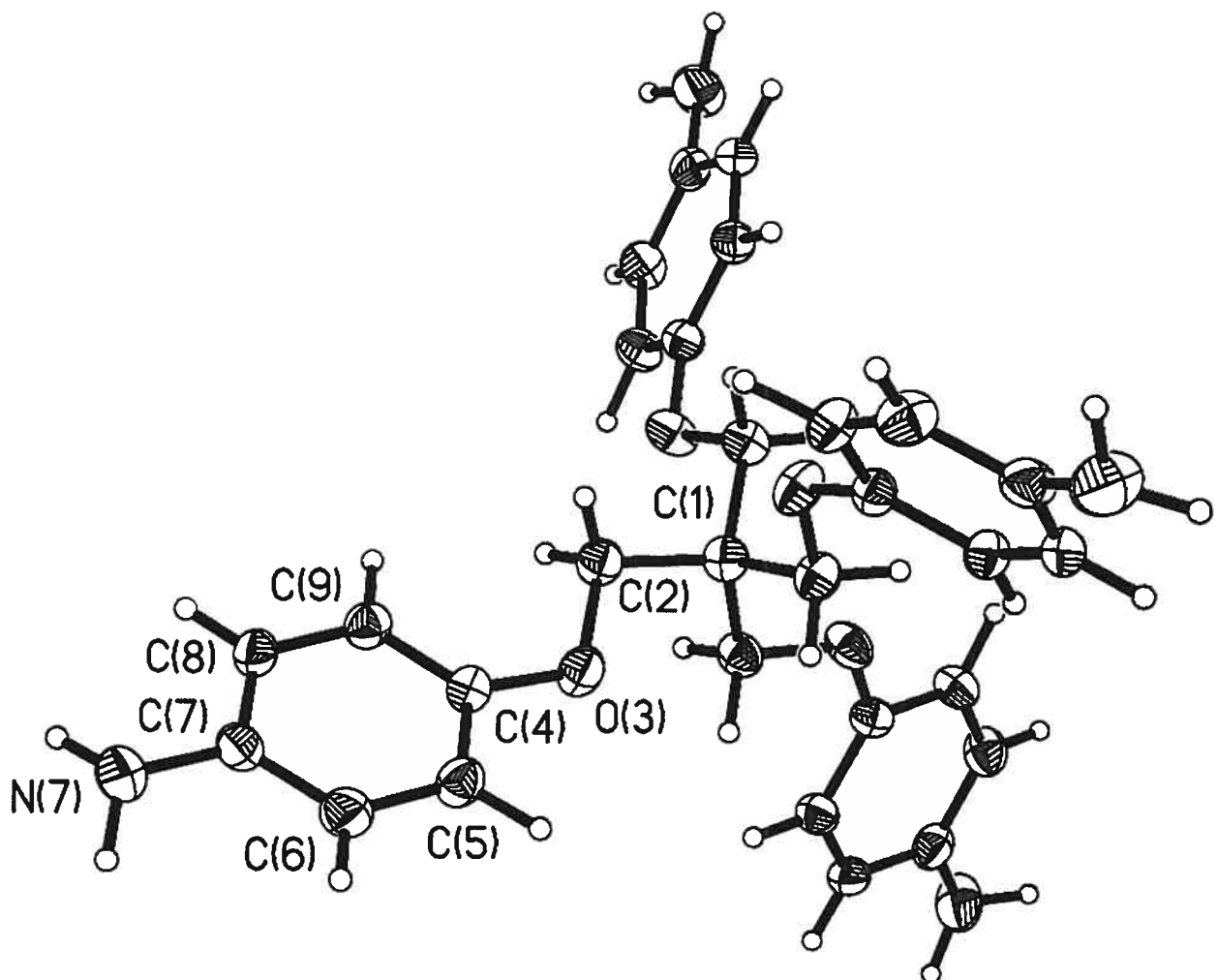


Figure S5

ORTEP view of the C₂₉ H₃₂ N₄ O₄ compound with the numbering scheme adopted. Ellipsoids drawn at 30% probability level. Hydrogens represented by sphere of arbitrary size.

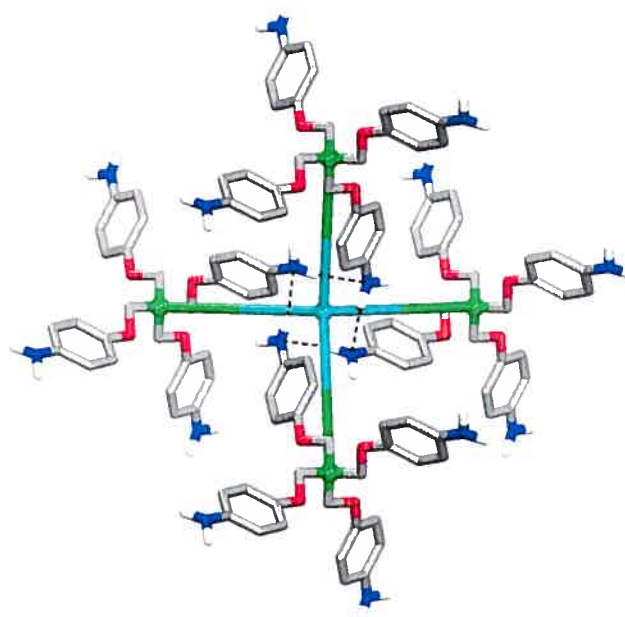


Figure S6

View along the *c* axis of the structure of the C₂₉ H₃₂ N₄ O₄ compound showing the hydrogen bonds and defining the nodes that generate the diamondoid network.

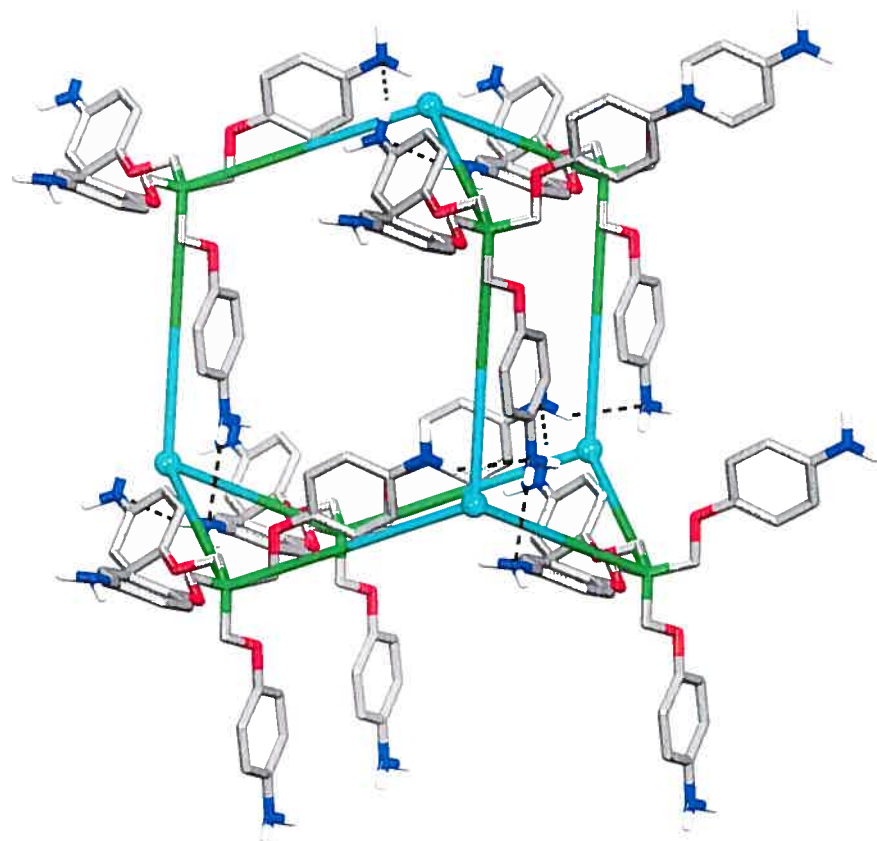


Figure S7

View of part of a diamondoid network in the structure of the C₂₉ H₃₂ N₄ O₄ compound. Blue spheres lie at the centers of cyclic hydrogen-bonded tetramers.

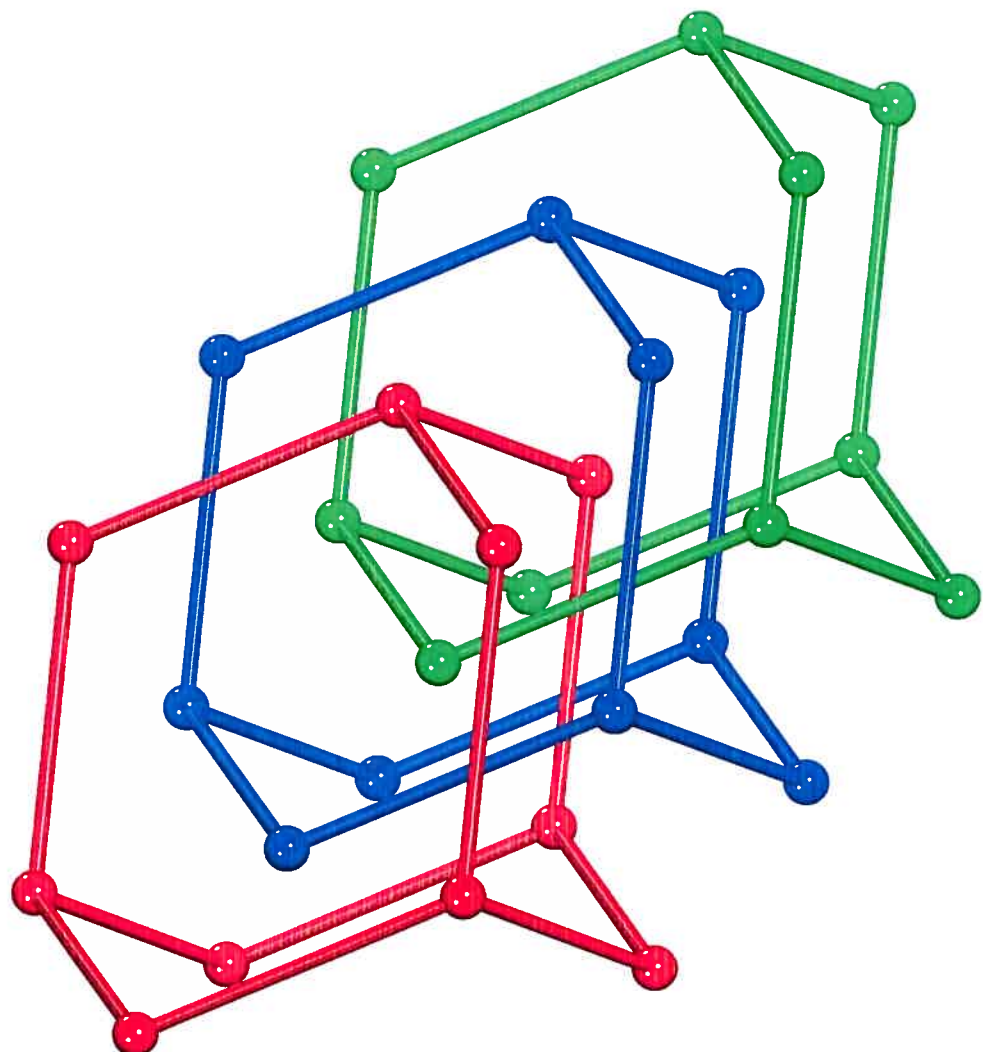


Figure S8

View of the three-fold interpenetrated diamondoid networks in the structure of the C₂₉ H₃₂ N₄ O₄ compound.

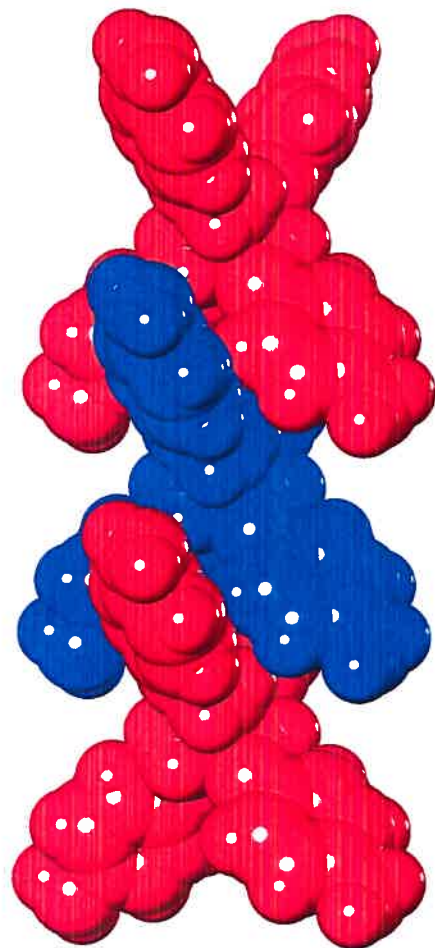


Figure S9

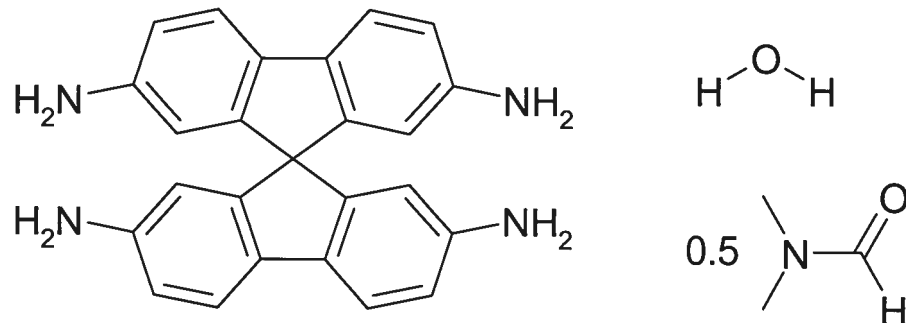
View of the structure of the C₂₉ H₃₂ N₄ O₄ compound showing the chain parallel to the c axis generated by two-fold phenyl embraces.



CRYSTAL AND MOLECULAR STRUCTURE OF
C26.50 H25.50 N4.50 O1.50 COMPOUND (JIW793)

Equipe WUEST

Département de chimie, Université de Montréal,
C.P. 6128, Succ. Centre-Ville, Montréal, Québec, H3C 3J7 (Canada)



Structure solved and refined in the Laboratory of X-Ray Diffraction, Université de Montréal by Dr. Thierry Maris.

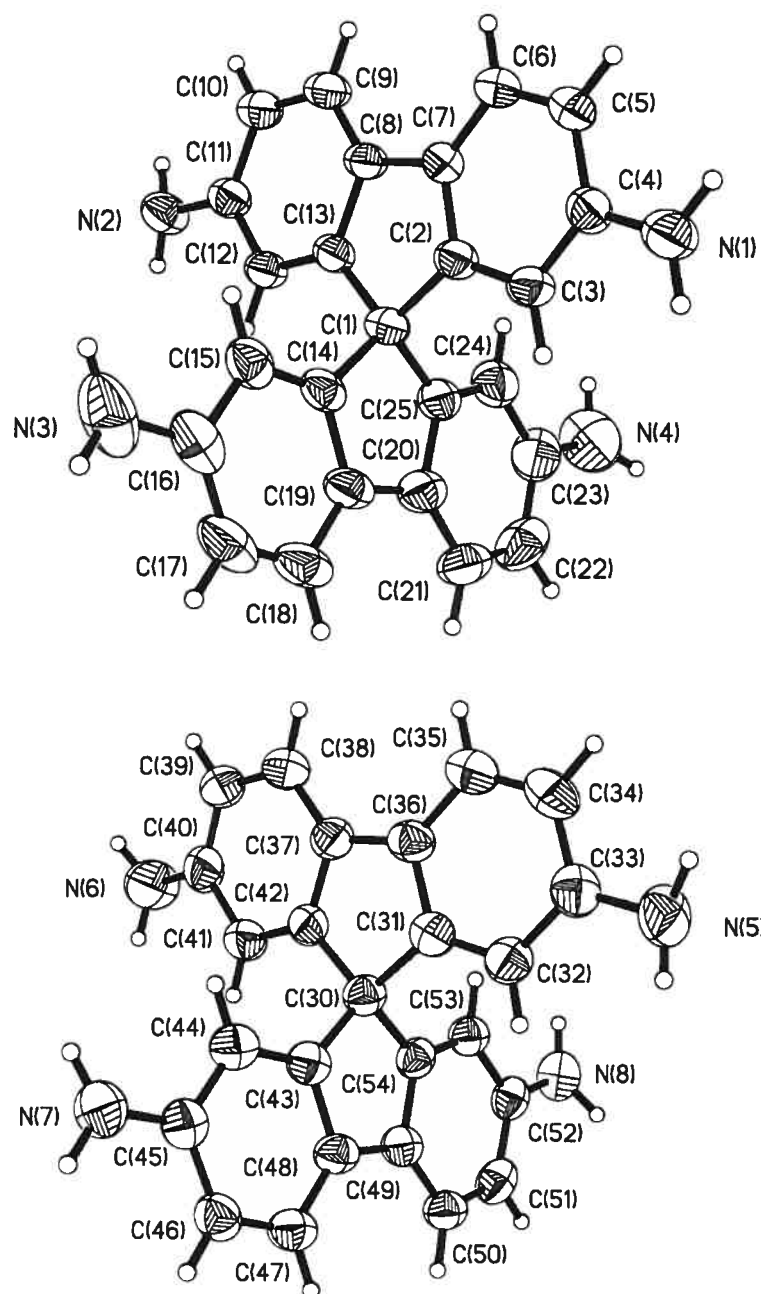
Table S15.	Crystal data and structure refinement for C26.5 H25.5 N4.5 O1.5.		
Empirical formula	C26.5	H25.5	N4.5 O1.5
Formula weight	431.01		
Temperature	293 (2) K		
Wavelength	1.54178 Å		
Crystal system	Orthorhombic		
Space group	P2 ₁ 2 ₁ 2 ₁	Z = 8	
Unit cell dimensions	a = 10.654 (2) Å	α = 90°	
	b = 14.404 (3) Å	β = 90°	
	c = 29.086 (5) Å	γ = 90°	
Volume	4463.8 (13) Å ³		
Density (calculated)	1.283 g/cm ³		
Absorption coefficient	0.651 mm ⁻¹		
Crystal size	0.18 x 0.15 x 0.06 mm		
Theta range for data collection	3.04 to 68.02°		
Index ranges	-13 ≤ h ≤ 13, -17 ≤ k ≤ 17, -33 ≤ l ≤ 33		
Reflections collected	43904		
Independent reflections	7454 [R _{int} = 0.052]		
Absorption correction	Semi-empirical from equivalents		
Max. and min. transmission	0.9600 and 0.8500		
Refinement method	Full-matrix least-squares on F ²		
Data / restraints / parameters	7454 / 20 / 683		
Goodness-of-fit on F ²	1.232		
Final R indices [I>2sigma(I)]	R ₁ = 0.0700, wR ₂ = 0.2008		
R indices (all data)	R ₁ = 0.0879, wR ₂ = 0.2314		
Absolute structure parameter	0.0 (8)		
Largest diff. peak and hole	0.266 and -0.298 e/Å ³		

Table S21. Bond lengths [Å] and angles [°] related to the hydrogen bonding for C26.5 H25.5 N4.5 O1.5.

D-H	..A	d(D-H)	d(H..A)	d(D..A)	<DHA
N(1)-H(1B)	O(70) #1	0.90(3)	2.398(16)	3.257(7)	160(4)
N(3)-H(3B)	O(71)	0.90(8)	2.24(4)	3.109(13)	161(10)
N(4)-H(4B)	O(71) #2	0.90(8)	2.26(4)	3.142(12)	168(15)
N(5)-H(5B)	O(70) #3	0.90(5)	2.400(13)	3.293(9)	171(5)
N(8)-H(8A)	O(60)	0.90(10)	2.24(7)	3.046(7)	148(12)
O(70)-H(70A)	O(60)	0.95(12)	2.08(9)	2.923(8)	147(13)
O(70)-H(70B)	N(1) #4	0.95(9)	2.82(15)	3.257(7)	109(11)
O(71)-H(71A)	O(70) #5	0.95(14)	2.59(10)	3.383(15)	141(13)

Symmetry transformations used to generate equivalent atoms:

#1 -x,y-1/2,-z+1/2	#2 x,y+1,z	#3 x+1,y,z
#4 -x,y+1/2,-z+1/2	#5 x,y-1,z	



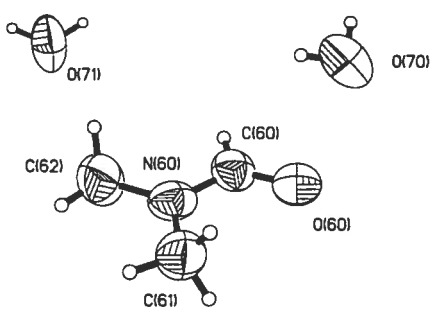


Figure S10

ORTEP view of the C_{26.5} H_{25.5} N_{4.5} O_{1.5} compound with the numbering scheme adopted. Ellipsoids drawn at 30% probability level. Hydrogens represented by sphere of arbitrary size.

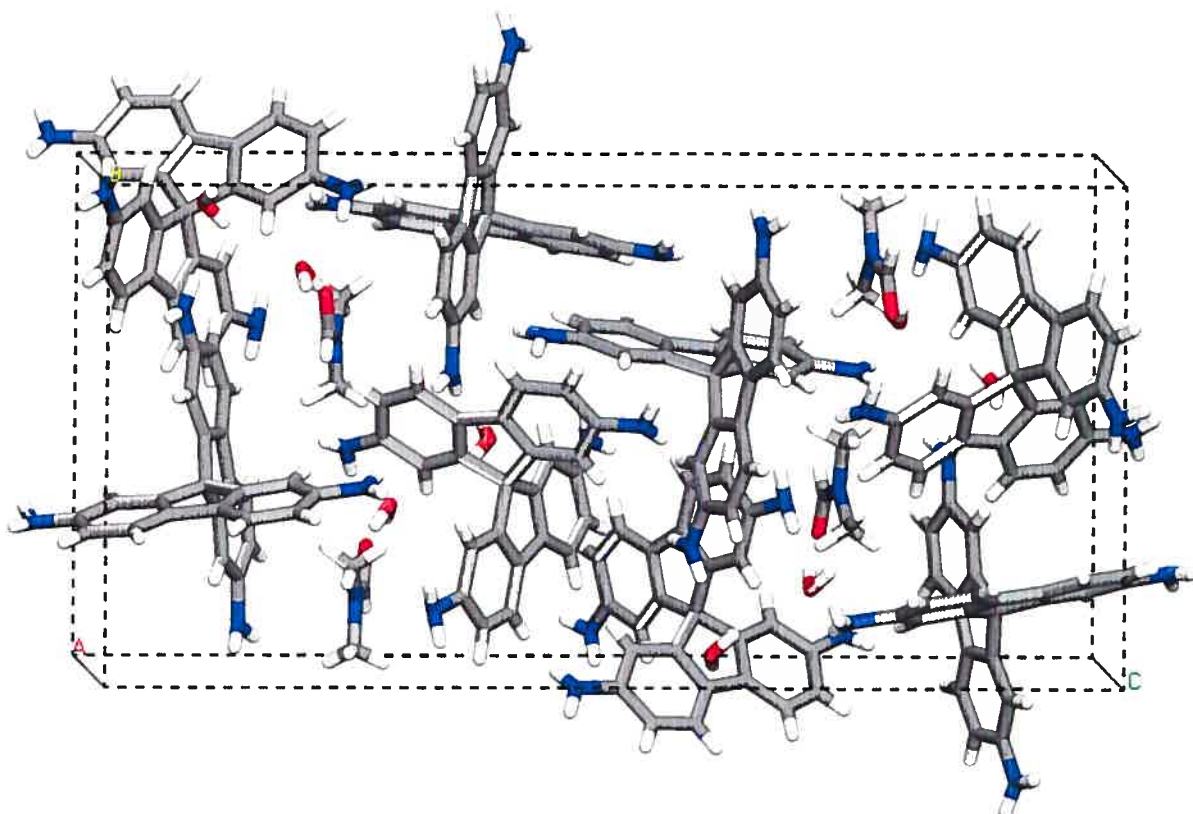


Figure S11

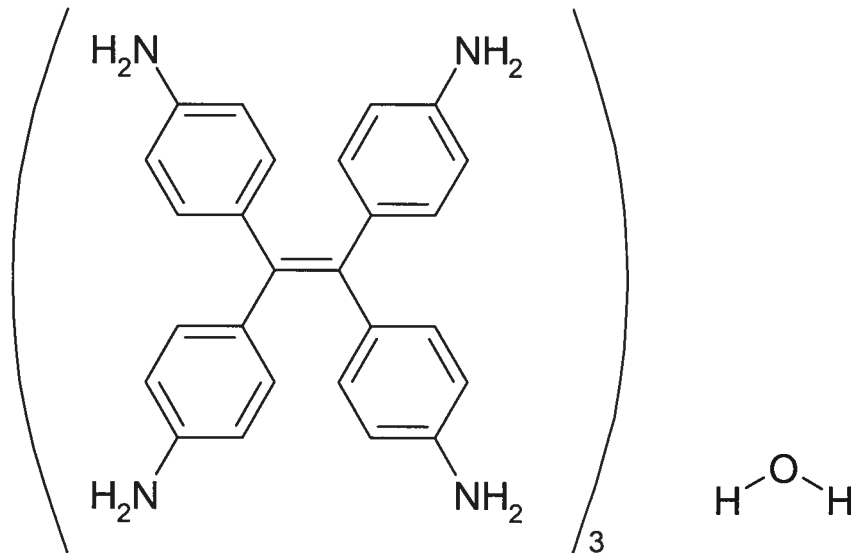
View of one unit cell of the C_{26.5} H_{25.5} N_{4.5} O_{1.5} compound.



CRYSTAL AND MOLECULAR STRUCTURE OF
C78 H74 N12 O COMPOUND (JIW744)

Equipe WUEST

Département de chimie, Université de Montréal,
C.P. 6128, Succ. Centre-Ville, Montréal, Québec, H3C 3J7 (Canada)



Structure solved and refined in the Laboratory of X-Ray Diffraction, Université de Montréal by Dr. Thierry Maris.

Table S22. Crystal data and structure refinement for C₇₈ H₇₄ N₁₂ O.

Empirical formula	C ₇₈ H ₇₄ N ₁₂ O	
Formula weight	1195.49	
Temperature	290(2) K	
Wavelength	1.54178 Å	
Crystal system	Monoclinic	
Space group	P21/c	Z = 4
Unit cell dimensions	a = 32.9270(17) Å	α = 90°
	b = 9.330(7) Å	β = 99.103(12)°
	c = 21.448(3) Å	γ = 90°
Volume	6506(5) Å ³	
Density (calculated)	1.221 Mg/m ³	
Absorption coefficient	0.580 mm ⁻¹	
Crystal size	0.15 x 0.09 x 0.05 mm	
Theta range for data collection	1.36 to 69.39°	
Index ranges	-39 ≤ h ≤ 39, -11 ≤ k ≤ 11, -25 ≤ l ≤ 25	
Reflections collected	70888	
Independent reflections	11980 [R _{int} = 0.081]	
Absorption correction	Semi-empirical from equivalents	
Max. and min. transmission	0.9700 and 0.9300	
Refinement method	Full-matrix least-squares on F ²	
Data / restraints / parameters	11980 / 0 / 820	
Goodness-of-fit on F ²	1.021	
Final R indices [I>2sigma(I)]	R ₁ = 0.0837, wR ₂ = 0.1889	
R indices (all data)	R ₁ = 0.0898, wR ₂ = 0.1907	
Largest diff. peak and hole	0.269 and -0.280 e/Å ³	
Table S28. Bond lengths [Å] and angles [°] related to the hydrogen bonding for C ₇₈ H ₇₄ N ₁₂ O.		

D-H	..A	d (D-H)	d (H..A)	d (D..A)	<DHA
N(3)-H(3A)	N(4) #1	0.89	2.58	3.444 (4)	163.3
N(4)-H(4A)	N(1) #2	0.89	2.56	3.450 (4)	175.1
N(4)-H(4B)	O(80) #3	0.89	1.93	2.772 (6)	158.3
N(6)-H(6A)	N(7) #4	0.89	2.67	3.309 (5)	129.7
N(7)-H(7A)	N(2) #1	0.89	2.52	3.266 (4)	142.3
N(8)-H(8A)	N(5) #5	0.89	2.35	3.212 (4)	162
N(9)-H(9A)	N(3) #6	0.89	2.65	3.433 (4)	146.9
N(11)-H(11A)	O(80)	0.89	1.78	2.645 (6)	163.1
N(11)-H(11B)	N(10) #5	0.89	2.41	3.275 (4)	165

Symmetry transformations used to generate equivalent atoms:

#1 x,y+1,z	#2 x,-y-1/2,z-1/2	#3 x,-y+1/2,z-1/2
#4 x,-y+5/2,z+1/2	#5 x,-y+3/2,z-1/2	#6 x,y,z+1

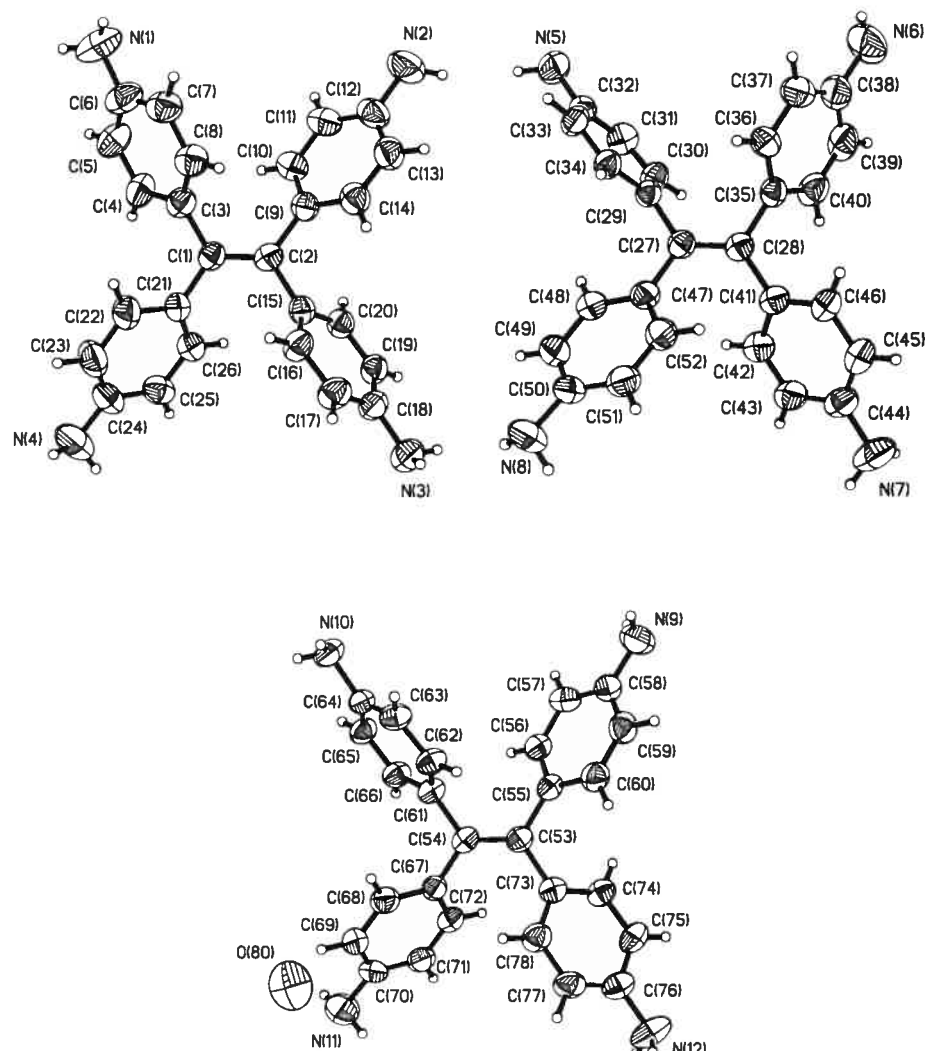


Figure S12

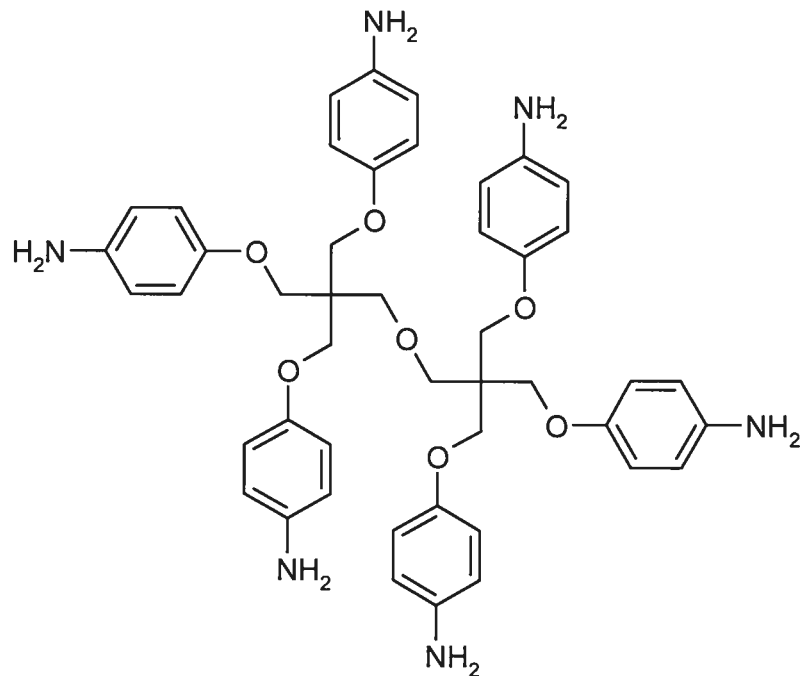
ORTEP view of the C₇₈ H₇₄ N₁₂ O compound with the numbering scheme adopted. Ellipsoids drawn at 30% probability level. Hydrogen atoms represented by spheres of arbitrary size.



CRYSTAL AND MOLECULAR STRUCTURE OF
C46 H52 N6 O7 COMPOUND (JIW753)

Equipe WUEST

Département de chimie, Université de Montréal,
C.P. 6128, Succ. Centre-Ville, Montréal, Québec, H3C 3J7 (Canada)



Structure solved and refined in the Laboratory of X-Ray Diffraction, Université de Montréal by Dr. Thierry Maris.

Table S29. Crystal data and structure refinement for C₄₆ H₅₂ N₆ O₇.

Empirical formula	C ₄₆ H ₅₂ N ₆ O ₇	
Formula weight	800.94	
Temperature	293 (2) K	
Wavelength	1.54178 Å	
Crystal system	Orthorhombic	
Space group	P2 ₁ 2 ₁ 2 ₁	Z = 4
Unit cell dimensions	a = 6.0353 (2) Å b = 24.6349 (6) Å c = 28.1607 (7) Å	α = 90° β = 90° γ = 90°
Volume	4186.9 (2) Å ³	
Density (calculated)	1.271 g/cm ³	
Absorption coefficient	0.701 mm ⁻¹	
Crystal size	0.25 x 0.02 x 0.02 mm	
Theta range for data collection	2.38 to 69.10°	
Index ranges	-6 ≤ h ≤ 7, -24 ≤ k ≤ 29, -34 ≤ l ≤ 34	
Reflections collected	42268	
Independent reflections	7649 [R _{int} = 0.099]	
Absorption correction	Semi-empirical from equivalents	
Max. and min. transmission	1.0000 and 0.7500	
Refinement method	Full-matrix least-squares on F ²	
Data / restraints / parameters	7649 / 12 / 580	
Goodness-of-fit on F ²	1.028	
Final R indices [I>2sigma(I)]	R ₁ = 0.0495, wR ₂ = 0.1229	
R indices (all data)	R ₁ = 0.0725, wR ₂ = 0.1408	
Absolute structure parameter	-0.2 (2)	
Largest diff. peak and hole	0.160 and -0.140 e/Å ³	

Table S35. Bond lengths [\AA] and angles [°] related to the hydrogen bonding for C46 H52 N6 O7.

D-H	..A	d(D-H)	d(H..A)	d(D..A)	<DHA
N(10)-H(11A)	N(60) #1	0.90(2)	2.59(4)	3.418(11)	153(6)
N(20)-H(21A)	N(40) #2	0.87(2)	2.36(2)	3.224(5)	173(4)
N(40)-H(41A)	O(50) #3	0.91(2)	2.36(3)	3.161(3)	147(4)
N(50)-H(51A)	O(10) #4	0.92(2)	2.31(2)	3.161(5)	154(3)

Symmetry transformations used to generate equivalent atoms:

#1 $-x+1, y+1/2, -z+1/2$	#2 $-x+1/2, -y+2, z-1/2$
#3 $x-1/2, -y+3/2, -z+1$	#4 $-x+1, y-1/2, -z+1/2$

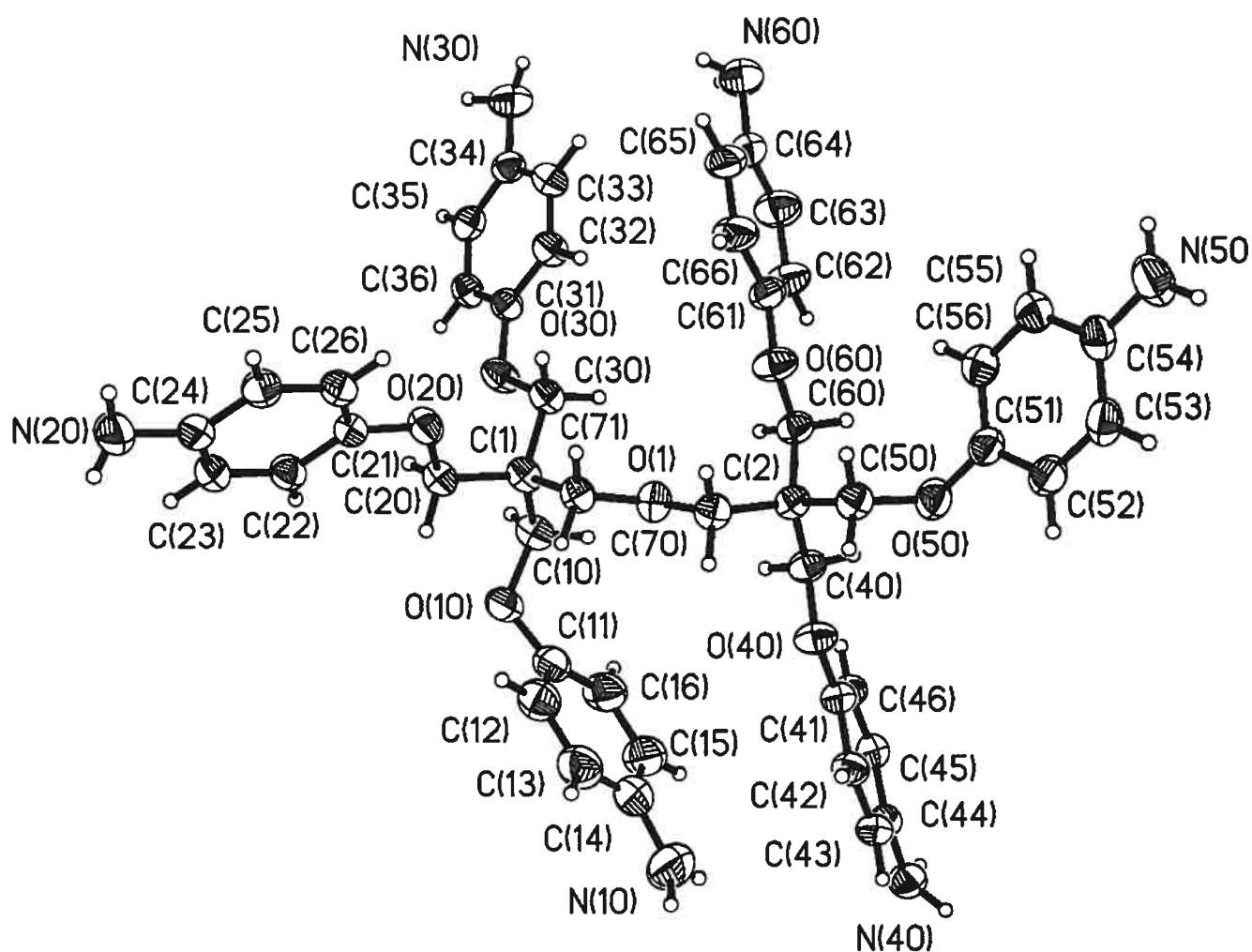


Figure S13

ORTEP view of the C₄₆ H₅₂ N₆ O₇ compound with the numbering scheme adopted. Ellipsoids drawn at 30% probability level. Hydrogens represented by sphere of arbitrary size.

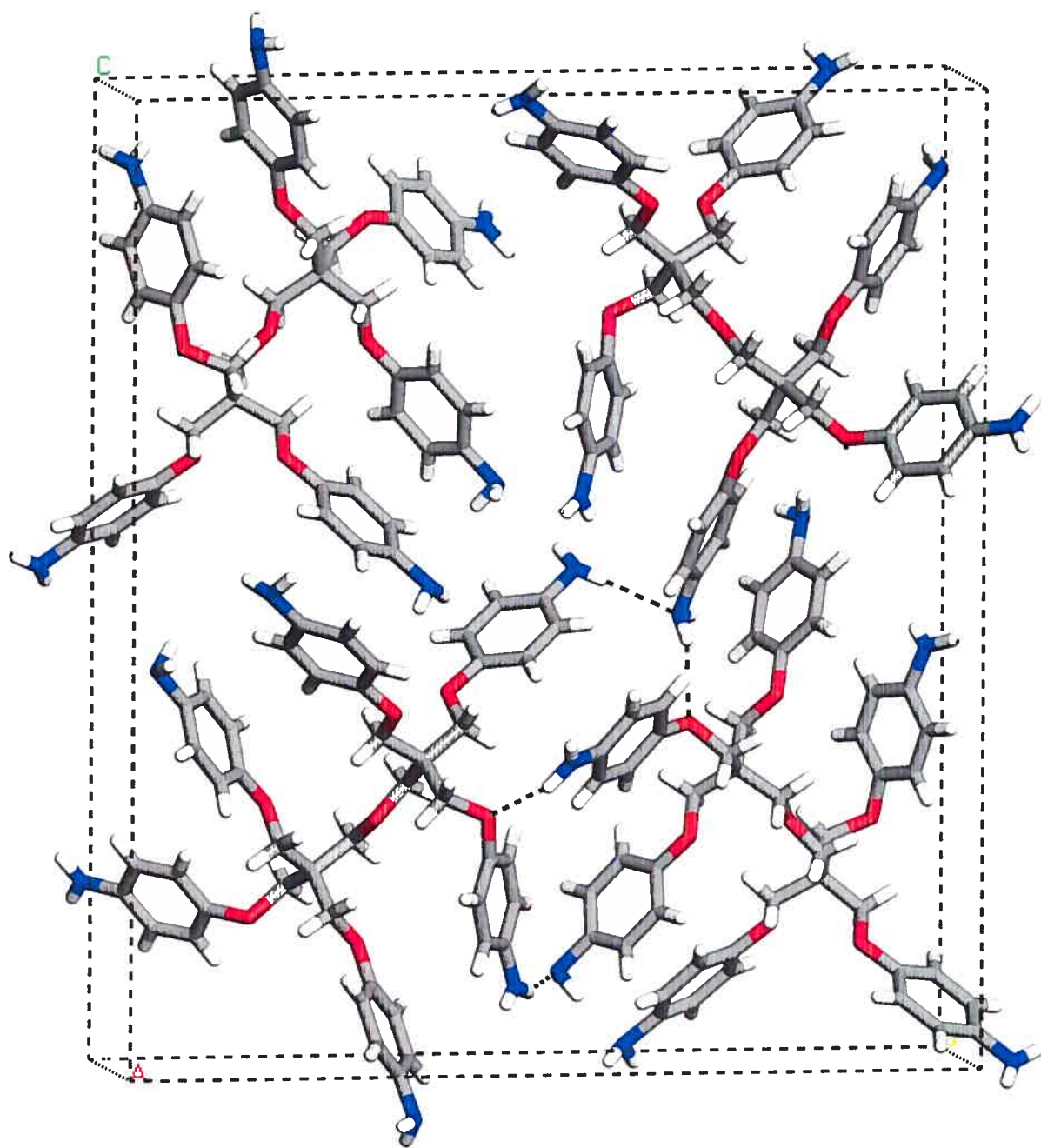


Figure S14

View of one unit cell of the C₄₆ H₅₂ N₆ O₇ compound.

REFERENCES

- Flack, H.D. (1983). *Acta Crystallogr.* A39, 876-881.
- Flack, H.D. and Schwarzenbach, D. (1988). *Acta Crystallogr.* A44, 499-506.
- SAINT (1999) Release 6.06; Integration Software for Single Crystal Data. Bruker AXS Inc., Madison, WI 53719-1173.
- Sheldrick, G.M. (1996). SADABS, Bruker Area Detector Absorption Corrections. Bruker AXS Inc., Madison, WI 53719-1173.
- Sheldrick, G.M. (1997). SHELXS97, Program for the Solution of Crystal Structures. Univ. of Gottingen, Germany.
- Sheldrick, G.M. (1997). SHELXL97, Program for the Refinement of Crystal Structures. Univ. of Gottingen, Germany.
- SHELXTL (1997) Release 5.10; The Complete Software Package for Single Crystal Structure Determination. Bruker AXS Inc., Madison, WI 53719-1173.
- SMART (1999) Release 5.059; Bruker Molecular Analysis Research Tool. Bruker AXS Inc., Madison, WI 53719-1173.
- Spek, A.L. (2000). PLATON, Molecular Geometry Program, 2000 version. University of Utrecht, Utrecht, Holland.
- XPREP (1997) Release 5.10; X-Ray Data Preparation and Reciprocal Space Exploration Program. Bruker AXS Inc., Madison, WI 53719-1173.

Annexe 4

Supporting Information

Topotactic Reactions in Networks

Designing Permeable Molecular Crystals that React with External Agents To Give Crystalline Products

Philippe Brunet, Eric Demers, Thierry Maris,

Gary D. Enright & James D. Wuest

Contents

- I Selected experimental procedures(A4-3)-(A4-5)
- II Crystal structure of tecton 2 • 6 dioxane(A4-6)-(A4-10)
- III Crystal structure of thioether 5a, as prepared from crystals of tecton 2 by photochemical addition of CH₃SH in the solid state(A4-11)-(A4-15)
- IV Crystal structure of the cross-linked product obtained from crystals of tecton 2 by photochemical addition of HSCH₂CH₂CH₂SH in the solid state..(A4-16)-(A4-20)

Selected experimental procedures

Tetrakis[4-[(2,4-dichloro-1,3,5-triazin-6-yl)amino]phenyl]methane (4). Tetrakis(4-amino-phenyl)methane (**3**) was prepared by a published procedure (F. A. Neugebauer, H. Fischer, R. Bernhardt, *Chem. Ber.* 1976, 109, 2389), modified by using THF instead of ethyl acetate in the reduction of tetrakis(4-nitrophenyl)methane. A solution of tetrakis(4-aminophenyl)methane (**3**; 0.761 g, 2.00 mmol) in acetone (16 mL) was added dropwise at 0 °C to a stirred solution of cyanuric chloride (1.51 g, 8.19 mmol) in acetone (24 mL). The resulting mixture was kept at 0 °C for 1 hour, treated with Na₂CO₃ (0.869 g, 8.20 mmol), and poured into water (160 mL). The precipitate was separated by filtration, washed, and dried to give tetrakis[4-[(2,4-dichloro-1,3,5-triazin-6-yl)amino]phenyl]methane (**4**; 1.48 g, 1.52 mmol, 76%) as a colorless solid: mp >310 °C; ¹H NMR (400 MHz, DMSO-*d*₆, 25 °C) δ 7.18 (d, 8H, ³J = 8.7 Hz), 7.55 (d, 8H, ³J = 8.7 Hz), 11.18 (s, 4H); ¹³C NMR (75.4 MHz, DMSO-*d*₆, 25 °C) δ 64.1, 121.7, 131.7, 135.8, 143.8, 164.6, 169.7, 170.7; MS (FAB, 3-nitrobenzyl alcohol) *m/e* 969. Anal. Calcd for C₃₇H₂₀Cl₈N₁₆: C, 45.71; H, 2.07; N, 23.05. Found: C, 46.03; H, 2.09; N, 22.61.

Tetrakis[4-[[2,4-bis(allylamino)-1,3,5-triazin-6-yl]amino]phenyl]methane (2). A solution containing tetrakis[4-[(2,4-dichloro-1,3,5-triazin-6-yl)amino]phenyl]methane (**4**; 0.226 g, 0.232 mmol), allylamine (0.35 mL, 4.7 mmol), and *N,N*-diisopropylethylamine (0.40 mL, 2.3 mmol) in dioxane (6 mL) was sealed in a glass tube, which was then heated at 110 °C for 6 h. Addition of the contents to cold water caused the precipitation of a solid, which was separated by filtration and washed with water and ether to give tetrakis[4-[[2,4-bis(allylamino)-1,3,5-triazin-6-yl]amino]phenyl]methane (**2**; 0.228 g, 0.200 mmol, 86%) as a light yellow solid. To effect crystallization, the compound (0.300 g, 0.264 mmol) was first dissolved in hot dioxane (3 mL). The hot solution was then divided into several portions, which were placed in closed 4 mL vials and allowed to cool slowly to room temperature in a pre-warmed insulated oil bath. Crystals were obtained within several days: mp 175 °C (dec); ¹H NMR (300 MHz, DMSO-*d*₆, 150 °C) δ 3.92 (s, 16H), 5.03 (d, 8H, ³J = 10.3 Hz), 5.16 (d, 8H, ³J = 17.2 Hz), 5.91 (m, 8H), 6.22 (s, 8H), 7.02 (d, 8H, ³J = 8.7 Hz),

7.63 (d, 8H, $^3J = 8.7$ Hz), 8.16 (4H); ^{13}C NMR (75.4 MHz, DMSO- d_6 , 150 °C) δ 43.0, 63.2, 115.1, 119.1, 130.8, 136.5, 138.5, 140.9, 164.6, 166.2; MS (FAB, 3-nitrobenzyl alcohol) m/e 1137. Anal. Calcd for $\text{C}_{61}\text{H}_{68}\text{N}_{24} + 1 \text{ H}_2\text{O}$: C, 63.41; H, 6.11; N, 29.10. Found: C, 63.34; H, 6.07; N, 28.92.

Tetrakis[4-[[2,4-bis[3-(methylthio)propanamino]-1,3,5-triazin-6-yl]amino]phenyl]methane (5a) (Synthesis in solution). A solution containing tetrakis[4-[[2,4-dichloro-1,3,5-triazin-6-yl]amino]phenyl]methane (**2**; 0.320 g, 0.329 mmol), 3-(methylthio)propanamine (0.312 g, 2.97 mmol), and *N,N*-diisopropylethylamine (0.52 mL, 3.0 mmol) in dioxane (5 mL) was sealed in a glass tube, which was then heated at 116 °C for 23 h. Addition of the contents to cold water caused the precipitation of a solid, which was separated by filtration and washed with water and ether to give tetrakis[4-[[2,4-bis[3-(methylthio)propanamino]-1,3,5-triazin-6-yl]amino]phenyl]methane (**5a**; 0.466 g, 0.306 mmol, 93%) as a colorless solid. Crystallization was effected by allowing methanol (1 mL) to diffuse into a solution of the crude product (0.010 mg, 0.0066 mmol) in THF (0.5 mL): ^1H NMR (300 MHz, DMSO- d_6 , 150 °C) δ 1.81 (m, 16H), 2.02 (s, 24H), 2.50 (t, 16H, $^3J = 7.1$ Hz), 3.35 (t, 16H, $^3J = 6.7$ Hz), 6.10 (bs, 8H), 7.01 (d, 8H, $^3J = 8.9$ Hz), 7.62 (d, 8H, $^3J = 8.9$ Hz), 8.05 (bs, 4H); ^{13}C NMR (75.4 MHz, DMSO- d_6 , 150 °C) δ 14.1, 28.7, 30.7, 38.9, 62.0, 117.9, 129.7, 137.5, 139.8, 163.6, 165.4; MS (FAB, 3-nitrobenzyl alcohol) m/e 1521.

Exchange of dioxane in single crystals of tecton **2 • 6 dioxane.** Crystals of tecton **2** • 6 dioxane with approximate dimensions 0.5 mm x 0.5 mm x 0.5 mm were grown in the normal way. The mother liquors were removed by pipette, and the crystals were immediately covered with toluene and kept at 25 °C for 24 h without stirring. The liquid phase was removed by pipette, then the crystals were washed with pentane and dried briefly in air. Analysis by ^1H NMR spectroscopy of dissolved samples showed complete replacement of dioxane by toluene.

Reaction of CH₃SH with single crystals of tecton **2.** Dioxane in single crystals of tecton **2** • 6 dioxane (10 mg, 0.0059 mmol) was replaced with toluene in the normal way. The

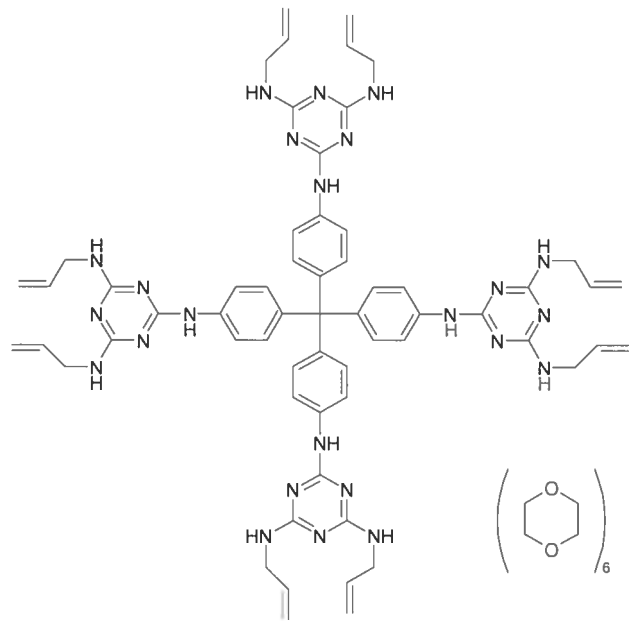
exchanged crystals, covered with toluene (5 mL), were placed in a jacketed quartz reactor, and He was bubbled through the stirred mixture at 25 °C. After 1 h, CH₃SH was added to the stream of He passing through the reactor, and after an additional 45 minutes, irradiation of the reactor was begun, using a medium-pressure 450-watt Hg lamp held at a distance of 10 cm. Irradiation was continued for 40 h with a constant current of CH₃SH/He. Analysis of the recovered crystals by mass spectrometry and by ¹H NMR spectroscopy of dissolved samples showed that an average of 70-85% of the allyl groups had reacted to give tetrakis[4-[[2,4-bis[3-(methylthio)propanamino]-1,3,5-triazin-6-yl]amino]phenyl]methane (**5a**), which was identified by comparison with authentic samples.

Cross-linking single crystals of tecton 2 with ethanedithiol. Single crystals of tecton **2** • 6 dioxane (10 mg, 0.0059 mmol) were placed in a jacketed quartz reactor and exposed briefly to neat ethanedithiol (5 mL), which was then replaced with a second portion (10 mL). He was bubbled through the stirred mixture at 25 °C for 1 h, and then the reactor was irradiated for 24 h using a medium-pressure 450-watt Hg lamp held at a distance of 10 cm. The recovered crystals were analyzed by optical microscopy, thermogravimetry, Raman spectroscopy, solid-state ¹³C NMR spectroscopy, and X-ray diffraction. Anal. Calcd for C₆₉H₁₀₀N₂₄S₈ + 6 HSCH₂CH₂SH: C, 51.50; H, 6.16; N, 19.75. Found: C, 50.83; H, 6.60; N, 19.17.

CRYSTAL AND MOLECULAR STRUCTURE OF
C85 H116 N24 O12 COMPOUND (JIW233)

Equipe WUEST

Département de chimie, Université de Montréal,
C.P. 6128, Succ. Centre-Ville, Montréal, Québec, H3C 3J7 (Canada)



Structure résolue à Ottawa par Dr. Gary Enright.

Table 1.Crystal data and structure refinement for C₈₅ H₁₁₆ N₂₄ O₁₂.

Empirical formula	C ₈₅ H ₁₁₆ N ₂₄ O ₁₂	
Formula weight	1666.018	
Temperature	173 (2) K	
Wavelength	0.71073 Å	
Crystal system	Tetragonal	
Space group	I 41/a	Z = 4
Unit cell dimensions	a = 23.0674(6) Å	α = 90°
	b = 23.0674(6) Å	β = 90°
	c = 16.1892(6) Å	γ = 90°
Volume	8614.4 (4) Å ³	
Density (calculated)	1.2846 Mg/m ³	
Absorption coefficient	0.089 mm ⁻¹	
Crystal size	0.15 x 0.20 x 0.30 mm	
Theta range for data collection	1.54 to 20.85°	
Index ranges	-23 ≤ h ≤ 23, -23 ≤ k ≤ 23, -16 ≤ l ≤ 16	
Reflections collected	25463	
Independent reflections	2269 [R _{int} = 0.0478]	
Absorption correction	Multi-scan	
Refinement method	Full-matrix least-squares on F ²	
Data / restraints / parameters	2269 / 0 / 273	
Goodness-of-fit on F ²	1.071	
Final R indices [I>2sigma(I)]	R ₁ = 0.0795, wR ₂ = 0.2308	
R indices (all data)	R ₁ = 0.0974, wR ₂ = 0.2496	
Largest diff. peak and hole	0.536 and -0.415 e/Å ³	

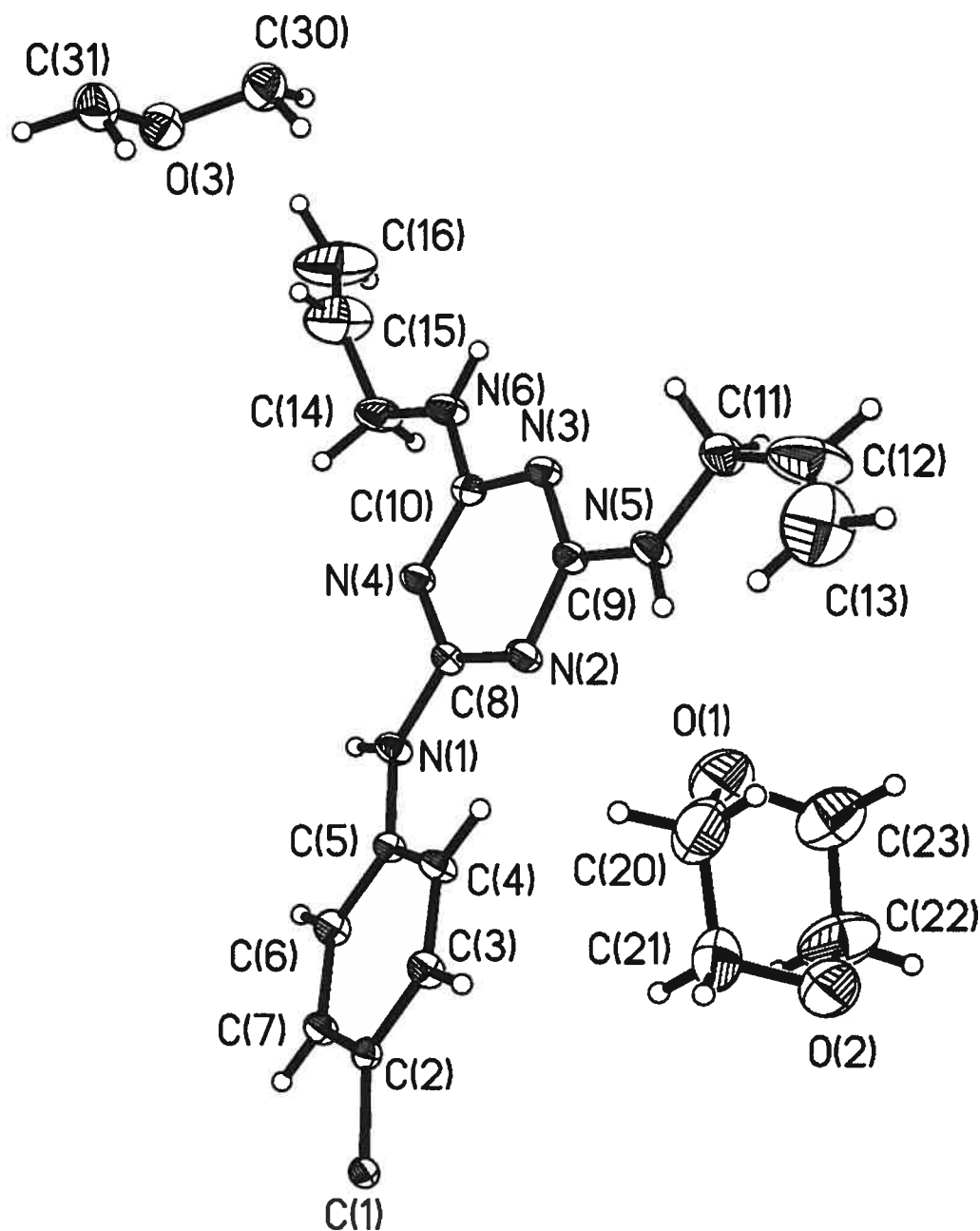
Table 6. Hydrogen bond lengths [\AA] and angles [°] for C85 H116 N24 O12

D	H	A	D - H	H...A	D...A	<DHA
N1	H1	N3#1	0.8800	2.1573	3.0278	170.02
N5	H5	O1#2	0.8800	2.2228	3.0488	156.23
N6	H6	N4#3	0.8800	2.1204	2.9929	171.11

#1 1/4+y, 1/4-x, 1/4+z

#2 1/2-x, 1/2-y, 1/2-z

#3 1/4-y, x-1/4, z-1/4



ORTEP view of the C₈₅ H₁₁₆ N₂₄ O₁₂ compound
(Asymmetric unit) with the numbering scheme adopted.
Ellipsoids drawn at 30% probability level. Hydrogens
represented by sphere of arbitrary size.

REFERENCES

- International Tables for Crystallography (1992). Vol. C. Tables 4.2.6.8 and 6.1.1.4, Dordrecht: Kluwer Academic Publishers.
- SAINT (1999) Release 6.06; Integration Software for Single Crystal Data. Bruker AXS Inc., Madison, WI 53719-1173.
- Sheldrick, G.M. (1996). SADABS, Bruker Area Detector Absorption Corrections. Bruker AXS Inc., Madison, WI 53719-1173.
- Sheldrick, G.M. (1997). SHELXS97, Program for the Solution of Crystal Structures. Univ. of Gottingen, Germany.
- Sheldrick, G.M. (1996). SHELXL96, Program for the Refinement of Crystal Structures. Univ. of Gottingen, Germany.
- SHELXTL (1997) Release 5.10; The Complete Software Package for Single Crystal Structure Determination. Bruker AXS Inc., Madison, WI 53719-1173.
- SMART (1999) Release 5.059; Bruker Molecular Analysis Research Tool. Bruker AXS Inc., Madison, WI 53719-1173.
- Spek, A.L. (1995. PLATON, Molecular Geometry Program, July 1995 version. University of Utrecht, Utrecht, Holland.
- XPREP (1997) Release 5.10; X-ray data Preparation and Reciprocal space Exploration Program. Bruker AXS Inc., Madison, WI 53719-1173.

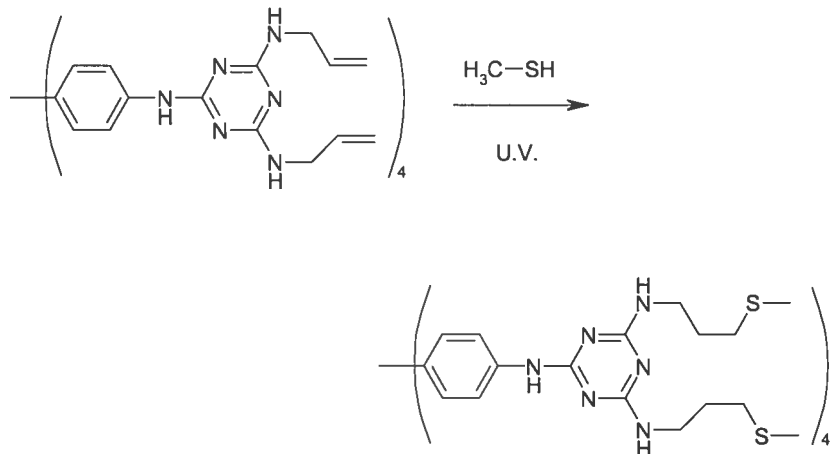


CRYSTAL AND MOLECULAR STRUCTURE OF
C64.2 H80.8 N24 S3.2 COMPOUND (JIW301)

lundi, septembre 12, 2005

Equipe WUEST

Département de chimie, Université de Montréal,
C.P. 6128, Succ. Centre-Ville, Montréal, Québec, H3C 3J7 (Canada)



Structure solved and refined by Dr. Thierry Maris in the laboratory of X-ray diffraction, Université de Montréal, Québec and by Dr Gary Enright, Steacie Institute for Molecular Sciences, National Research Council, Ottawa, Ontario.

Table 1. Crystal data and structure refinement for C_{64.2} H_{80.8} N₂₄ S_{3.2}

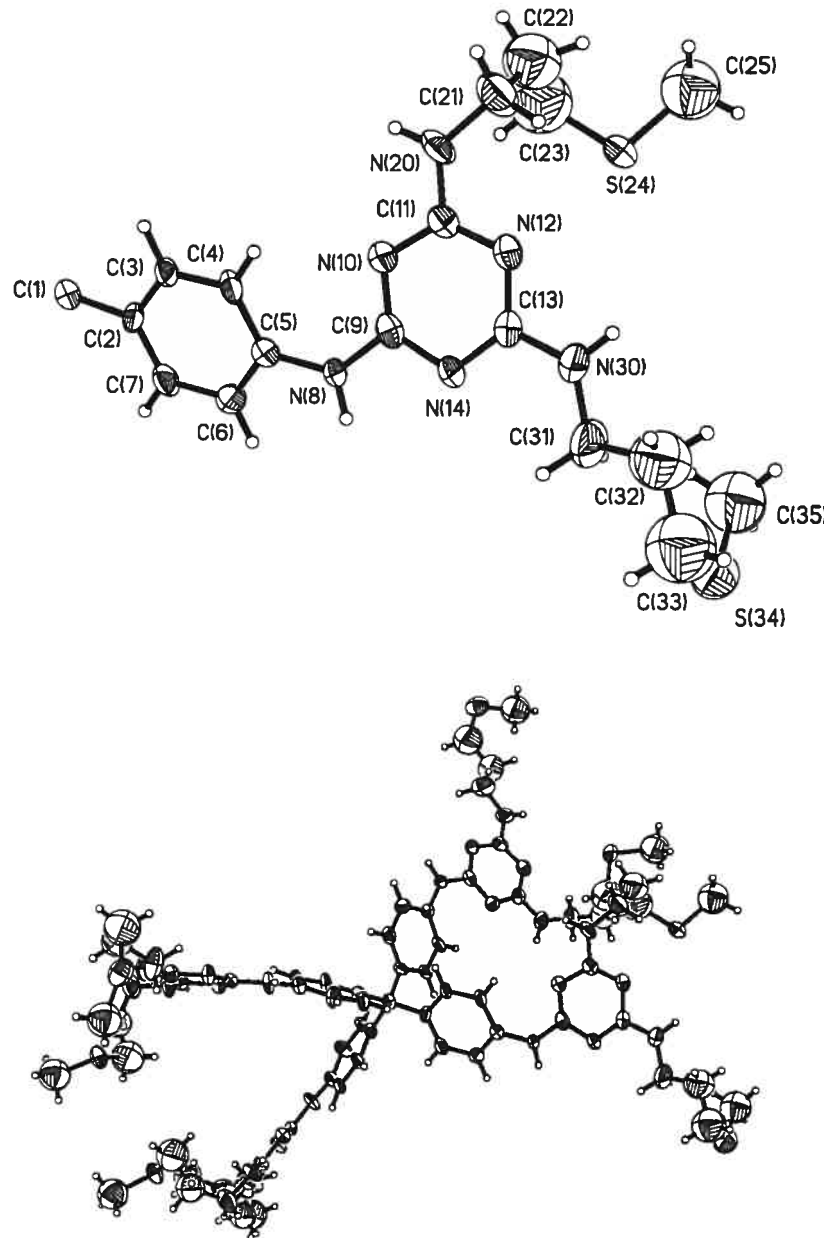
Empirical formula	C _{64.2} H _{80.8} N ₂₄ S _{3.2}	
Formula weight	1522.21	
Temperature	173 (2) K	
Wavelength	0.71073 Å	
Crystal system	Tetragonal	
Space group	I41/a	<i>Z</i> = 4
Unit cell dimensions	a = 20.988(2) Å b = 20.988(2) Å c = 16.816(3) Å	α = 90° β = 90° γ = 90°
Volume	7407.6(16) Å ³	
Density (calculated)	1.365 Mg/m ³	
Absorption coefficient	0.301 mm ⁻¹	
Crystal size	0.20 x 0.15 x 0.08 mm	
Theta range for data collection	1.55 to 20.99°	
Index ranges	-21 ≤ <i>h</i> ≤ 21, -21 ≤ <i>k</i> ≤ 21, -16 ≤ <i>l</i> ≤ 16	
Reflections collected	17939	
Independent reflections	1976 [R _{int} = 0.2328]	
Max. and min. transmission	0.9763 and 0.9422	
Refinement method	Full-matrix least-squares on F ²	
Data / restraints / parameters	1976 / 45 / 214	
Goodness-of-fit on F ²	1.306	
Final R indices [I>2σ(I)]	R ₁ = 0.1210, wR ₂ = 0.3894	
R indices (all data)	R ₁ = 0.2324, wR ₂ = 0.3894	
Largest diff. peak and hole	0.620 and -0.570 e/Å ³	

Table 7. Bond lengths [\AA] and angles [$^\circ$] related to the hydrogen bonding for C64.2 H80.8 N24 S3.2

D-H	..A	d(D-H)	d(H..A)	d(D..A)	<DHA
N(8)-H(8)	N(12) #4	0.88	2.08	2.956 (3)	174.2
N(20)-H(20)	S(24) #5	0.88	2.81	3.585 (4)	147.8
N(30)-H(30)	N(14) #6	0.88	2.18	3.045 (4)	166.5

Symmetry transformations used to generate equivalent atoms:

#1 $y-3/4, -x+3/4, -z-1/4$	#2 $-x, -y+3/2, z$
#3 $-y+3/4, x+3/4, -z-1/4$	#4 $y-1/4, -x+3/4, z-1/4$
#5 $y-3/4, -x+3/4, -z+3/4$	#6 $-y+3/4, x+1/4, z+1/4$



ORTEP view of the C_{64.2} H_{80.8} N₂₄ S_{3.2} compound with the numbering scheme adopted. Ellipsoids drawn at 30% probability level. Hydrogens represented by sphere of arbitrary size. For clarity, the remaining allyl functions are not represented.

REFERENCES

International Tables for Crystallography (1992). Vol. C. Tables 4.2.6.8 and
6.1.1.4, Dordrecht: Kluwer Academic Publishers.

SAINT (1999) Release 6.06; Integration Software for Single Crystal Data.
Bruker AXS Inc., Madison, WI 53719-1173.

Sheldrick, G.M. (1996). SADABS, Bruker Area Detector Absorption
Corrections.
Bruker AXS Inc., Madison, WI 53719-1173.

Sheldrick, G.M. (1997). SHELXS97, Program for the Solution of Crystal
Structures. Univ. of Gottingen, Germany.

Sheldrick, G.M. (1997). SHELXL97, Program for the Refinement of Crystal
Structures. Univ. of Gottingen, Germany.

SHELXTL (1997) Release 5.10; The Complete Software Package for Single
Crystal Structure Determination. Bruker AXS Inc., Madison, WI 53719-
1173.

SMART (1999) Release 5.059; Bruker Molecular Analysis Research Tool.
Bruker AXS Inc., Madison, WI 53719-1173.

Spek, A.L. (2000). PLATON, Molecular Geometry Program, 2000 version.
University of Utrecht, Utrecht, Holland.

XPREP (1997) Release 5.10; X-ray data Preparation and Reciprocal space
Exploration Program. Bruker AXS Inc., Madison, WI 53719-1173.

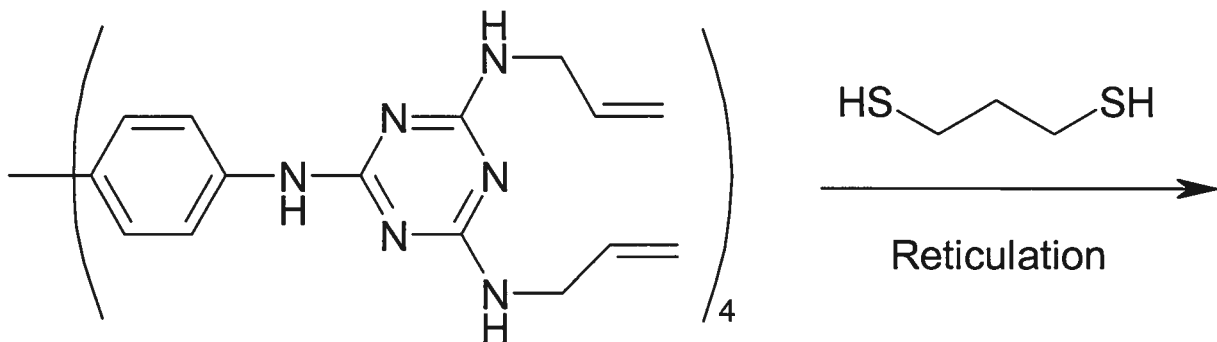


CRYSTAL AND MOLECULAR STRUCTURE OF
C46 H30 N12 S COMPOUND (JIW278)

lundi, septembre 12, 2005

Equipe WUEST

Département de chimie, Université de Montréal,
C.P. 6128, Succ. Centre-Ville, Montréal, Québec, H3C 3J7 (Canada)



ED-255-B

Structure solved and refined by Dr. Thierry Maris in the laboratory of X-ray diffraction, Université de Montréal, Québec and by Dr Gary Enright, Steacie Institute for Molecular Sciences, National Research Council, Ottawa, Ontario.

Table 1. Crystal data and structure refinement for C₄₆ H₃₀ N₁₂ S.

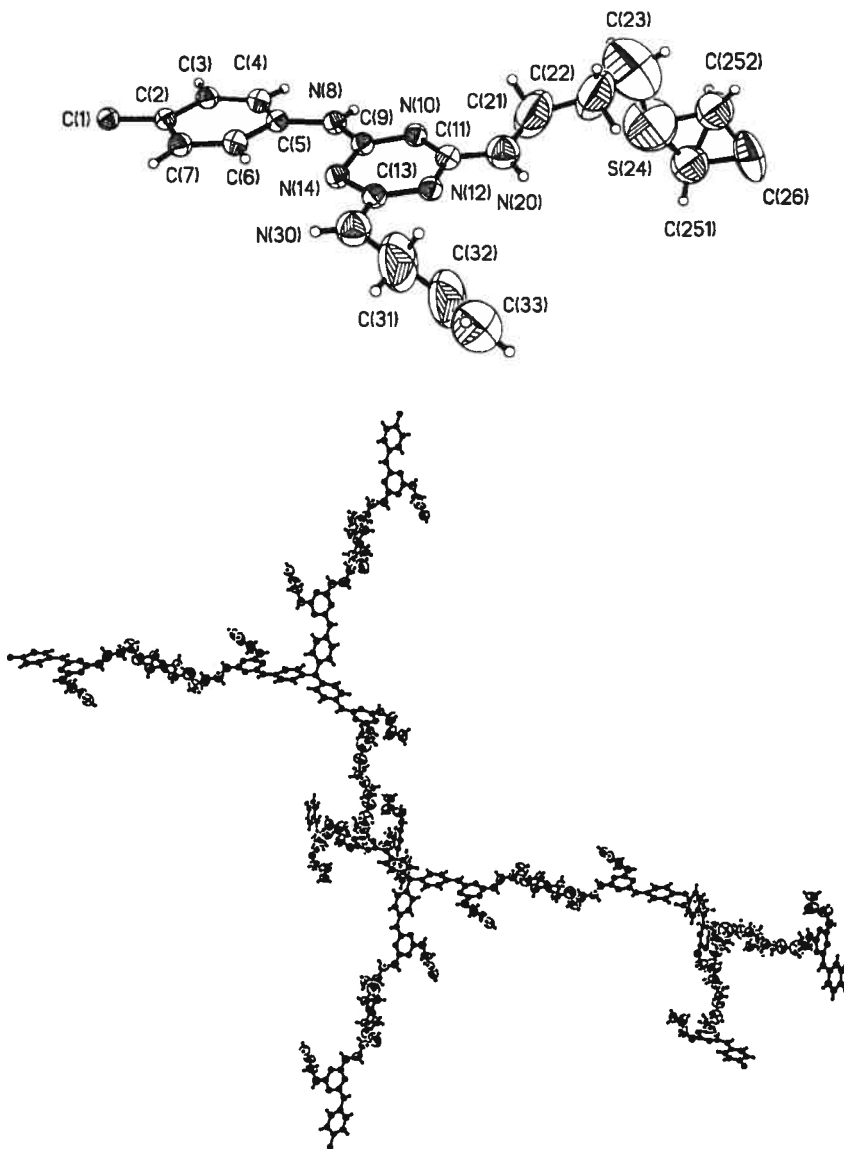
Empirical formula	C ₄₆ H ₃₀ N ₁₂ S	
Formula weight	782.88	
Temperature	173 (2) K	
Wavelength	0.71073 Å	
Crystal system	Tetragonal	
Space group	I41/a	Z = 8
Unit cell dimensions	a = 23.233(16) Å b = 23.233(16) Å c = 16.274(17) Å	α = 90° β = 90° γ = 90°
Volume	8785(13) Å ³	
Density (calculated)	1.184 Mg/m ³	
Absorption coefficient	0.120 mm ⁻¹	
Crystal size	0.30 x 0.30 x 0.15 mm	
Theta range for data collection	1.53 to 13.77°	
Index ranges	-15 ≤ h ≤ 15, -15 ≤ k ≤ 15, -10 ≤ l ≤ 10	
Reflections collected	6088	
Independent reflections	688 [R _{int} = 0.1523]	
Max. and min. transmission	0.9823 and 0.9650	
Refinement method	Full-matrix least-squares on F ²	
Data / restraints / parameters	688 / 192 / 182	
Goodness-of-fit on F ²	1.766	
Final R indices [I>2sigma(I)]	R ₁ = 0.1888, wR ₂ = 0.4611	
R indices (all data)	R ₁ = 0.2278, wR ₂ = 0.4611	
Largest diff. peak and hole	0.342 and -0.372 e/Å ³	

Table 6. Bond lengths [\AA] and angles [°] related to the hydrogen bonding for C46 H30 N12 S.

D-H	..A	d (D-H)	d (H..A)	d (D..A)	<DHA
N(8)-H(8)	N(12) #5	0.88	2.14	3.00 (3)	165.6
N(20)-H(20)	N(10) #6	0.88	2.24	3.05 (4)	152.8

Symmetry transformations used to generate equivalent atoms:

#1 $y-1/4, -x+5/4, -z+9/4$	#2 $-x+1, -y+3/2, z+0$
#3 $-y+5/4, x+1/4, -z+9/4$	#4 $-x, -y+2, -z+1$
#5 $y-3/4, -x+5/4, z+1/4$	#6 $-y+5/4, x+3/4, z-1/4$



ORTEP view of the C₄₆H₃₀N₁₂S compound with the numbering scheme adopted. Ellipsoids drawn at 30% probability level. Hydrogens represented by spheres of arbitrary size.

REFERENCES

- International Tables for Crystallography (1992). Vol. C. Tables 4.2.6.8 and 6.1.1.4, Dordrecht: Kluwer Academic Publishers.
- SAINT (1999) Release 6.06; Integration Software for Single Crystal Data. Bruker AXS Inc., Madison, WI 53719-1173.
- Sheldrick, G.M. (1996). SADABS, Bruker Area Detector Absorption Corrections. Bruker AXS Inc., Madison, WI 53719-1173.
- Sheldrick, G.M. (1997). SHELXS97, Program for the Solution of Crystal Structures. Univ. of Gottingen, Germany.
- Sheldrick, G.M. (1997). SHELXL97, Program for the Refinement of Crystal Structures. Univ. of Gottingen, Germany.
- SHELXTL (1997) Release 5.10; The Complete Software Package for Single Crystal Structure Determination. Bruker AXS Inc., Madison, WI 53719-1173.
- SMART (1999) Release 5.059; Bruker Molecular Analysis Research Tool. Bruker AXS Inc., Madison, WI 53719-1173.
- Spek, A.L. (2000). PLATON, Molecular Geometry Program, 2000 version. University of Utrecht, Utrecht, Holland.
- XPREP (1997) Release 5.10; X-ray data Preparation and Reciprocal space Exploration Program. Bruker AXS Inc., Madison, WI 53719-1173.

Annexe 5

Supporting Information

Excavations in molecular crystals

Erwan Le Fur, Eric Demers, Thierry Maris and James D. Wuest

Contents

- I Selected experimental procedures(A5-3)-(A5-5)**
- II Crystal structure of tecton 2 • 3 DMSO • 1 acetone • n H₂O(A5-6)-(A5-10)**
- III Crystal structure of tetrol 3, as prepared from crystals of tecton 2 by hydrolysis
in the solid state(A5-11)-(A5-16)**

Selected experimental procedures

Tetrakis[4-[(2,4-dichloro-1,3,5-triazin-6-yl)amino]phenyl]methane (5). Tetrakis(4-amino-phenyl)methane (**4**) was prepared by a published procedure (F. A. Neugebauer, H. Fischer and R. Bernhardt, *Chem. Ber.*, 1976, **109**, 2389), modified by using THF instead of ethyl acetate in the reduction of tetrakis(4-nitrophenyl)methane. A solution of tetrakis(4-aminophenyl)methane (**4**; 0.761 g, 2.00 mmol) in acetone (16 mL) was added dropwise at 0 °C to a stirred solution of cyanuric chloride (1.51 g, 8.19 mmol) in acetone (24 mL). The resulting mixture was kept at 0 °C for 1 hour, treated with Na₂CO₃ (0.869 g, 8.20 mmol), and poured into water (160 mL). The precipitate was separated by filtration, washed, and dried to give tetrakis[4-[(2,4-dichloro-1,3,5-triazin-6-yl)amino]phenyl]methane (**5**; 1.48 g, 1.52 mmol, 76%) as a colorless solid: mp >310 °C; ¹H NMR (400 MHz, DMSO-*d*₆, 25 °C) δ 7.18 (d, 8H, ³J = 8.7 Hz), 7.55 (d, 8H, ³J = 8.7 Hz), 11.18 (s, 4H); ¹³C NMR (75.4 MHz, DMSO-*d*₆, 25 °C) δ 64.1, 121.7, 131.7, 135.8, 143.8, 164.6, 169.7, 170.7; MS (FAB, 3-nitrobenzyl alcohol) *m/e* 969. Anal. Calcd for C₃₇H₂₀Cl₈N₁₆: C, 45.71; H, 2.07; N, 23.05. Found: C, 46.03; H, 2.09; N, 22.61.

Tetrakis[4-[[4-amino-2-chloro-1,3,5-triazin-6-yl]amino]phenyl]methane (6). A solution of tetrakis[4-[(2,4-dichloro-1,3,5-triazin-6-yl)amino]phenyl]methane (**5**; 0.250 g, 0.257 mmol) in dioxane (10 mL) was stirred at 0 °C and treated with concentrated aqueous ammonia (5 mL). The resulting white suspension was kept at 0 °C for 12 h, then excess ammonia was removed by partial evaporation of the mixture under reduced pressure. The

concentrate was poured into water (20 mL), and the precipitated solid was separated by filtration, washed twice with water (10 mL), and dried under vacuum to give tetrakis[4-[(4-amino-2-chloro-1,3,5-triazin-6-yl)amino]phenyl]methane (**6**; 0.217 g, 0.242 mmol, 94%) as a light yellow solid. To effect crystallization, the compound (0.050 g, 0.056 mmol) was first dissolved in DMSO (10 mL). The solution was then filtered and divided into 10 portions, which were placed in open 4 mL vials and transferred to a closed chamber containing CH₃CN. Crystals were obtained within several days: mp >250 °C ; ¹H NMR (300 MHz, DMSO-*d*₆, 90 °C) δ 7.05 (d, 8H, ³J = 8.7 Hz), 7.19 (bs, 8H), 7.64 (d, 8H, ³J = 8.7 Hz), 9.63 (bs, 4H); ¹³C NMR (75.4 MHz, DMSO-*d*₆, 25 °C) δ 62.8, 119.7, 130.8, 137.0, 141.4, 164.1, 167.2, 168.6. Anal. Calcd for C₃₇H₂₈Cl₄N₂₀ + 1 DMSO: C, 45.75; H, 4.11; N, 24.81. Found: C, 45.42; H, 3.60; N, 24.96.

Tetrakis[4-[(4-amino-2-(2-hydroxyethyl)amino-1,3,5-triazin-6-yl)amino]phenyl]methane (3). A mixture of tetrakis[4-[(4-amino-2-chloro-1,3,5-triazin-6-yl)amino]phenyl]methane (**6**; 0.300 g, 0.335 mmol), excess ethanolamine (12 mL), and THF (5 mL) was stirred and heated at 110 °C for 5 h. The mixture was then poured into a mixture of ice and water (50 mL), and the resulting precipitate was separated by filtration, washed four times with water (20 mL), and dried under vacuum to give tetrakis[4-[(4-amino-2-(2-hydroxyethyl)amino-1,3,5-triazin-6-yl)amino]phenyl]methane (**3**; 0.305 g, 0.307 mmol, 92%) as a light yellow solid: mp >250 °C; ¹H NMR (300 MHz, DMSO-*d*₆, 90 °C) δ 3.36 (dt, 8H, ³J = 5.9 Hz, ³J = 5.8 Hz), 3.53 (t, 8H, ³J = 5.9 Hz), 4.25 (s, 4H), 5.90 (bs, 8H), 6.18 (t, 4H, ³J = 5.8 Hz), 6.99 (d, 8H, ³J = 8.8 Hz), 7.66 (d, 8H, ³J = 8.8 Hz), 8.41

(bs, 4H); ^{13}C NMR (75.4 MHz, DMSO- d_6 , 25 °C) δ 43.0, 60.5, 62.4, 118.6, 130.7, 138.6, 140.0, 164.5, 166.4, 167.2; HRMS (electrospray) calcd for $\text{C}_{45}\text{H}_{53}\text{N}_{24}\text{O}_4$ m/e 993.46820, found 993.46814.

Tetrakis[4-[[4-amino-2-(2-acetoxyethyl)amino-1,3,5-triazin-6-yl]amino]phenyl]methane (2).

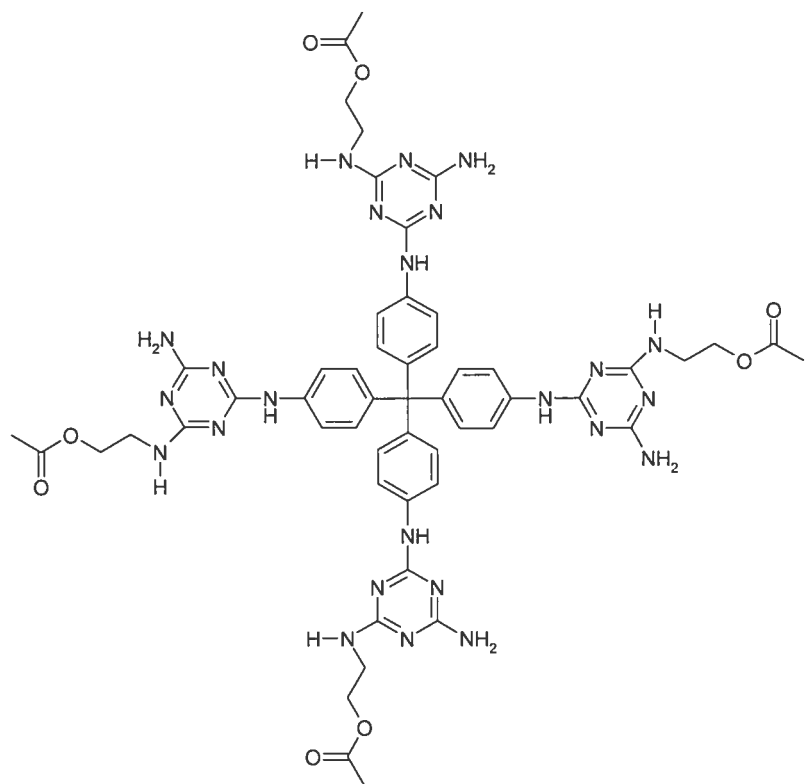
Excess acetic anhydride (5 mL) was added to tetrakis[4-[(4-amino-2-(2-hydroxyethyl)amino-1,3,5-triazin-6-yl)amino]phenyl]methane (**3**; 0.050 g, 0.050 mmol) and pyridine (0.68 mL, 8.4 mmol), and the resulting suspension was stirred at 25 °C for 24 h. The mixture was then concentrated by partial evaporation under reduced pressure, and the resulting precipitate was separated by filtration, washed twice with water (10 mL), and dried under vacuum to give tetrakis[4-[[4-amino-2-(2-acetoxyethyl)amino-1,3,5-triazin-6-yl]amino]phenyl]methane (**2**; 0.049 g, 0.042 mmol, 84%) as a light yellow solid. To effect crystallization, the compound (0.040 g, 0.034 mmol) was first dissolved in DMSO (0.8 mL). The solution was then filtered and divided into 8 portions, which were placed in open 4 mL vials and transferred to a closed chamber containing a 5:1 mixture of acetone and water. Crystals suitable for X-ray diffraction were obtained within 48 h: mp >250 °C; ^1H NMR (300 MHz, DMSO- d_6 , 90 °C) δ 1.96 (s, 12H), 3.48 (dt, 8H, $^3J = 5.9$ Hz, $^3J = 4.5$ Hz), 4.12 (t, 8H, $^3J = 5.9$ Hz), 5.99 (bs, 8H), 6.48 (t, 4H, $^3J = 4.5$ Hz), 6.98 (d, 8H, $^3J = 8.7$ Hz), 7.66 (d, 8H, $^3J = 8.7$ Hz), 8.52 (bs, 4H); ^{13}C NMR (75.4 MHz, DMSO- d_6 , 25 °C) δ 21.0, 40.5, 62.4, 63.0, 118.6, 130.7, 138.6, 140.1, 164.6, 166.3, 167.2, 170.7; MS (FAB, 3-nitrobenzyl alcohol) m/e 1162 (M + 1).



CRYSTAL AND MOLECULAR STRUCTURE OF
C53 H60 N24 O8 COMPOUND (JIW249)

Equipe WUEST

Département de chimie, Université de Montréal,
C.P. 6128, Succ. Centre-Ville, Montréal, Québec, H3C 3J7 (Canada)



Solvent: DMSO/acetone/H₂O

Table 1. Crystal data and structure refinement for C₅₃ H₆₀ N₂₄ O₈.

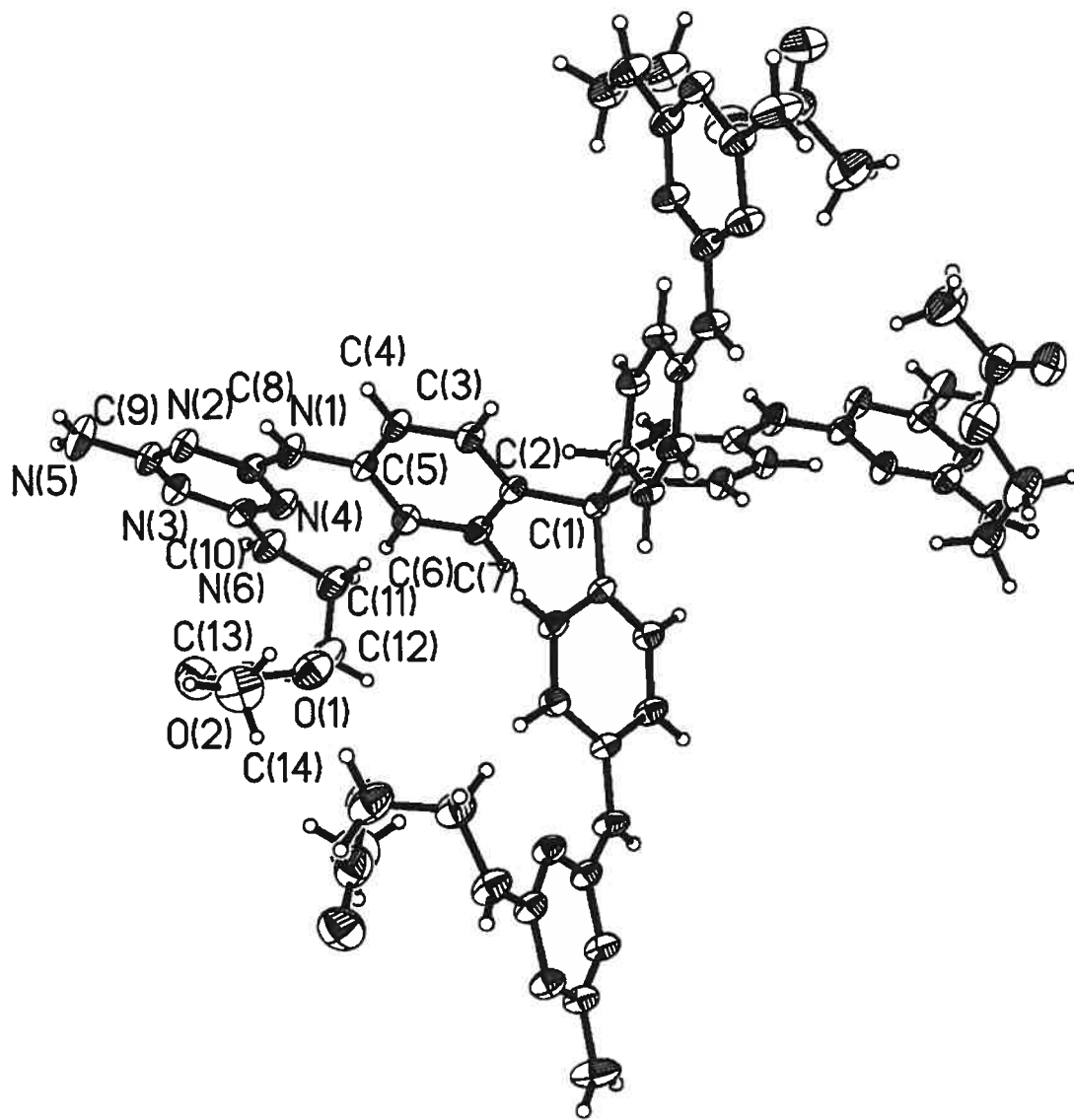
Empirical formula	C ₅₃ H ₆₀ N ₂₄ O ₈					
Formula weight	1161.25					
Temperature	293 (2) K					
Wavelength	1.54178 Å					
Crystal system, Space group	Tetragonal, I4 ₁ /a Z = 4					
Unit cell dimensions	a = 25.6644 (3) Å	α = 90°	b = 25.6644 (3) Å	β = 90°	c = 12.2028 (3) Å	γ = 90°
Volume	8037.5 (2) Å ³					
Density (without solvent)	0.960 g/cm ³					
Absorption coefficient	0.567 mm ⁻¹					
Crystal size	0.41 x 0.14 x 0.14 mm					
Theta range for data collection	3.44 to 72.95°					
Index ranges	-31 ≤ h ≤ 30, -31 ≤ k ≤ 31, -12 ≤ l ≤ 14					
Reflections collected	32725					
Independent reflections	3976 [R _{int} = 0.055]					
Absorption correction	Semi-empirical from equivalents					
Max. and min. transmission	1.0000 and 0.3300					
Refinement method	Full-matrix least-squares on F ²					
Data / restraints / parameters	3976 / 0 / 193					
Goodness-of-fit on F ²	1.097					
Final R indices [I>2sigma(I)]	R ₁ = 0.0824, wR ₂ = 0.1885					
R indices (all data)	R ₁ = 0.1568, wR ₂ = 0.2306					
Largest diff. peak and hole	0.202 and -0.235 e/Å ³					

Table 7. Bond lengths [\AA] and angles [$^\circ$] related to the hydrogen bonding for C53 H60 N24 O8.

D-H	..A	d (D-H)	d (H..A)	d (D..A)	<DHA
N(1)-H(1)	N(3) #4	0.86	2.46	3.288 (4)	161.9
N(5)-H(5A)	N(2) #5	0.86	2.12	2.975 (4)	174.6
N(6)-H(6)	O(2) #6	0.86	2.11	2.907 (4)	153.3

Symmetry transformations used to generate equivalent atoms:

#1 $-y+5/4, x-3/4, -z-3/4$	#2 $y+3/4, -x+5/4, -z-3/4$
#3 $-x+2, -y+1/2, z+0$	#4 $-y+5/4, x-1/4, z-1/4$
#5 $y+1/4, -x+5/4, z+1/4$	#6 $-x+3/2, -y+1/2, -z+1/2$



ORTEP view of the C₅₃H₆₀N₂₄O₈ compound with the numbering scheme adopted. Ellipsoids drawn at 30% probability level. Hydrogens represented by sphere of arbitrary size.

Experimental details

X-ray crystallographic data for JIW249 were collected from a single crystal mounted on a glass fiber. Data were collected using a Bruker Platform diffractometer, equipped with a Bruker SMART 2K charge-coupled device (CCD) area detector, using the program SMART and normal focus sealed-tube source graphite-monochromated Cu-K α radiation. The crystal-to-detector distance was 4.908 cm, and the data collection was carried out in 512 x 512 pixel mode, utilizing 4 x 4 pixel binning. The initial unit cell parameters were determined by a least-squares fit of the angular setting of strong reflections, collected by a 9.0 degree scan in 30 frames over four different parts of the reciprocal space (120 frames total). One complete sphere of data was collected, to better than 0.8 Å resolution. Upon completion of the data collection, the first 101 frames were recollected in order to improve the decay correction analysis.

The space group I4₁/a was determined based on systematic absences and intensity statistics. A successful direct-methods solution was calculated, which provided most non-hydrogen atoms from the E-map. Several full-matrix least-squares/difference Fourier cycles were performed, which located the remainder of the non-hydrogen atoms. In this way, the host network could easily be found and refined, but no resolved solvent molecules (DMSO/acetone/H₂O) could be found within the cavities. Most solvent molecules were disordered to such an extent that few significant difference peaks were found by Fourier difference. Refining the structure with isolated solvent peaks for modeling the disordered solvent gave a residual R1 close to 20% at this point, even though what appeared to be a correct solution was found. The data were treated with the Platon/Squeeze option to remove as much of the effects of solvent disorder as possible.

Platon found a potential solvent void of 3166 Å³ in the unit cell volume of 8037.5 Å³, or 39%. The Squeeze option found 760 electrons of diffuse scattering, a value giving 18 DMSO solvent molecules per unit cell or 4.5 per molecule of tecton. This figure is close to the value of 3.5 DMSO per tecton found by NMR, but acetone and H₂O may also be included in the cavities in the unit cell (see text).

Note that use of the Squeeze option from Platon has some effect on the values of the standard uncertainties of the geometric data.

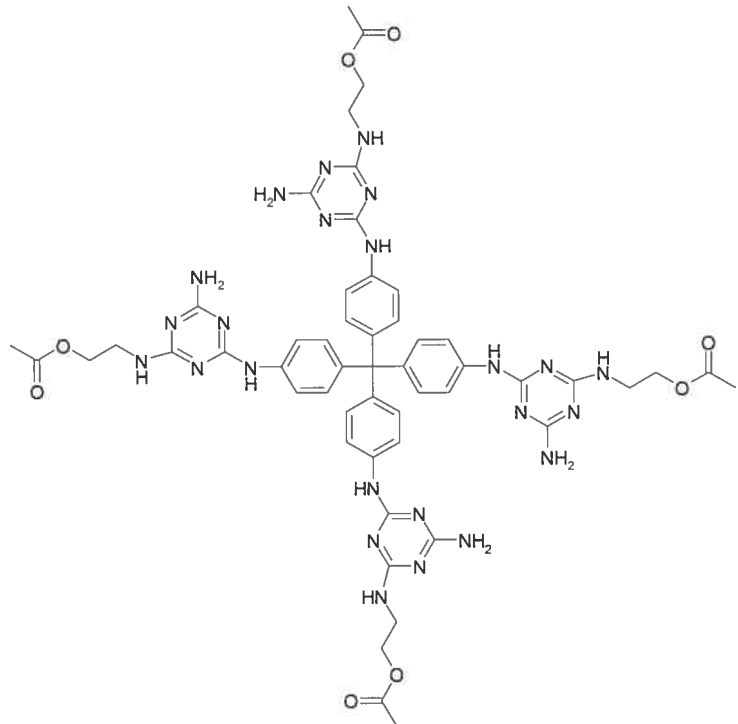
Ref : P. van der Sluis and A. L. Spek, *Acta Crystallogr.*, 1990, **A46**, 194



CRYSTAL AND MOLECULAR STRUCTURE OF
C50.60 H60.40 N24 O6.80 COMPOUND (JIW489)

Equipe WUEST

Département de chimie, Université de Montréal,
C.P. 6128, Succ. Centre-Ville, Montréal, Québec, H3C 3J7 (Canada)



Compound after hydrolysis of ≥30 % of the acetyl groups

Table 1. Crystal data and structure refinement for C₅₀.60 H₆₀.40 N₂₄ O₆.80.

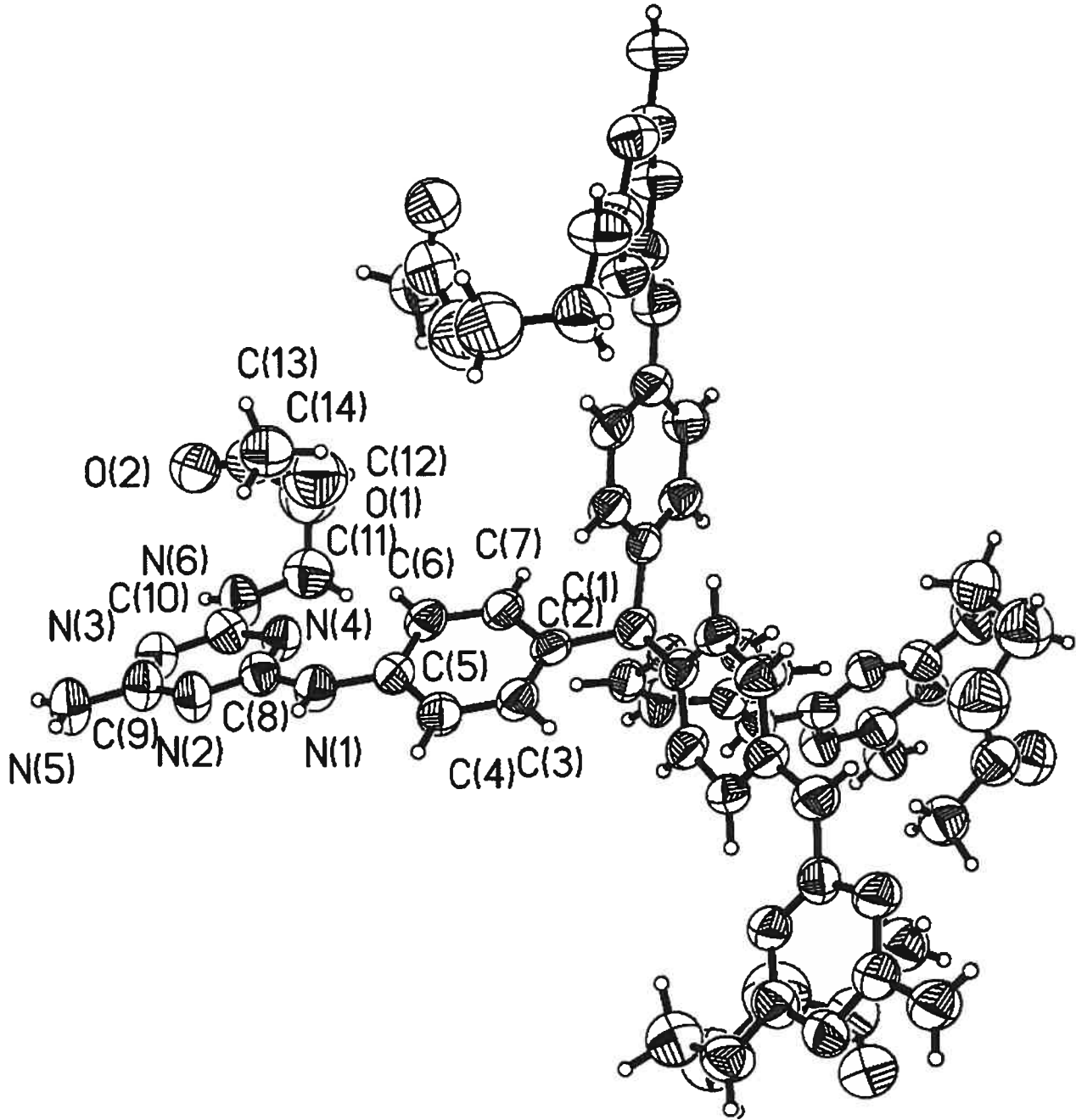
Empirical formula	C ₅₀ .60 H ₆₀ .40 N ₂₄ O ₆ .80					
Formula weight	1113.63					
Temperature	223 (2) K					
Wavelength	1.54180 Å					
Crystal system, Space group	Tetragonal, I4 ₁ /a Z = 4					
Unit cell dimensions	a = 25.6490(6) Å	α = 90°	b = 25.6490(6) Å	β = 90°	c = 11.9420(4) Å	γ = 90°
Volume	7856.3 (4) Å ³					
Density (without solvent)	0.942 g/cm ³					
Absorption coefficient	0.550 mm ⁻¹					
Crystal size	0.30 x 0.20 x 0.15 mm					
Theta range for data collection	3.45 to 59.19°					
Index ranges	-27 ≤ h ≤ 20, -25 ≤ k ≤ 25, -13 ≤ l ≤ 12					
Reflections collected	18629					
Independent reflections	2675 [R _{int} = 0.046]					
Absorption correction	Semi-empirical from equivalents					
Max. and min. transmission	1.0000 and 0.6400					
Refinement method	Full-matrix least-squares on F ²					
Data / restraints / parameters	2675 / 75 / 210					
Goodness-of-fit on F ²	1.094					
Final R indices [I>2sigma(I)]	R ₁ = 0.1196, wR ₂ = 0.3102					
R indices (all data)	R ₁ = 0.3808, wR ₂ = 0.3579					
Largest diff. peak and hole	0.346 and -0.233 e/Å ³					

Table 7. Bond lengths [\AA] and angles [°] related to the hydrogen bonding for C50.60 H60.40 N24 O6.80.

D-H	..A	d (D-H)	d (H..A)	d (D..A)	<DHA
N(1)-H(1)	N(3) #5	0.87	2.43	3.253 (12)	158.4
N(5)-H(5A)	O(20) #6	0.87	2.46	3.28 (2)	157.4
N(5)-H(5B)	N(2) #4	0.87	2.03	2.893 (12)	172.6
N(6)-H(6A)	O(2) #7	0.87	2.00	2.844 (14)	162.9

Symmetry transformations used to generate equivalent atoms:

#1 -x+1, -y+1/2, z+0	#2 -y+3/4, x-1/4, -z+3/4
#3 y+1/4, -x+3/4, -z+3/4	#4 y-1/4, -x+3/4, z-1/4
#5 -y+3/4, x+1/4, z+1/4	#6 -y+3/4, x+1/4, z-3/4
#7 -x+1/2, -y+1/2, -z-1/2	



ORTEP view of the C_{50.60} H_{60.40} N₂₄ O_{6.80} compound with the numbering scheme adopted. Ellipsoids drawn at 30% probability level. Hydrogens represented by sphere of arbitrary size.

Refinement details

X-ray crystallographic data for JIW489 were collected from a single crystal mounted on a loop fiber at 223 K. Data were collected using a Bruker Platform diffractometer, equipped with a Bruker SMART 2K charge-coupled device (CCD) area detector, using the program SMART and normal focus sealed-tube source graphite-monochromated Cu-K α radiation. The crystal-to-detector distance was 4.908 cm, and the data collection was carried out in 512 x 512 pixel mode, utilizing 4 x 4 pixel binning. The initial unit cell parameters were determined by a least-squares fit of the angular setting of strong reflections, collected by a 9.0 degree scan in 30 frames over 4 different parts of the reciprocal space (120 frames total). This sample, despite the specimen size, did not diffract well, possibly because of strain resulting from hydrolysis. The data appeared truncated at low resolution, and one complete sphere of data was collected up to 59 °. Upon completion of the data collection, the first 101 frames were recollected in order to improve the decay correction analysis.

The space group I4₁/a was determined based on systematic absences and intensity statistics. A successful direct-methods solution was calculated, which provided most non-hydrogen atoms from the E-map. Several full-matrix least-squares/difference Fourier cycles were performed, which located the remainder of the non-hydrogen atoms. In this way, the host network could easily be found and refined, but no resolved solvent molecules could be located within the cavities. Refinement of the acetyl group with an occupancy factor equal to unity did not converge and gave large anisotropic thermal parameters converging to unreasonable values. Refinement with a variable occupancy factor, with restraints on certain distances, yielded acceptable values for the thermal parameters. The solvent molecules were refined as pseudo atoms from the few significant difference peaks found by Fourier difference.

REFERENCES

International Tables for Crystallography (1992). Vol. C. Tables 4.2.6.8
and

6.1.1.4, Dordrecht: Kluwer Academic Publishers.

SAINT (1999) Release 6.06; Integration Software for Single Crystal Data.
Bruker AXS Inc., Madison, WI 53719-1173.

Sheldrick, G.M. (1996). SADABS, Bruker Area Detector Absorption
Corrections.

Bruker AXS Inc., Madison, WI 53719-1173.

Sheldrick, G.M. (1997). SHELXS97, Program for the Solution of Crystal
Structures. Univ. of Gottingen, Germany.

Sheldrick, G.M. (1997). SHELXL97, Program for the Refinement of Crystal
Structures. Univ. of Gottingen, Germany.

SHELXTL (1997) Release 5.10; The Complete Software Package for Single
Crystal Structure Determination. Bruker AXS Inc., Madison, WI 53719-
1173.

SMART (1999) Release 5.059; Bruker Molecular Analysis Research Tool.
Bruker AXS Inc., Madison, WI 53719-1173.

Spek, A.L. (2000). PLATON, Molecular Geometry Program, 2000 version.
University of Utrecht, Utrecht, Holland.

P. v.d. Sluis & A.L. Spek, (1990), Acta Cryst. A46, 194.

XPREP (1997) Release 5.10; X-ray Data Preparation and Reciprocal Space
Exploration Program. Bruker AXS Inc., Madison, WI 53719-1173.

